Investigation of microbial metal-sulfide interfacial environments under mineral bioleach simulated conditions

By

Cindy-Jade Africa

Thesis presented for the Degree of

DOCTOR OF PHILOSOPHY

In the Department of Chemical Engineering

UNIVERSITY OF CAPE TOWN

March 2017

Plagiarism Declaration

"This thesis/dissertation has been submitted to the Turnitin module (or equivalent similarity and originality checking software) and I confirm that my supervisor has seen my report and any concerns revealed by such have been resolved with my supervisor."

Name: CINDY-JADE AFRICA

Signature: Signed by candidate

Signature removed

Date: 02.03.2017

Acknowledgements

I would like to thank my supervisor Prof. S. T. L. Harrison for her help and guidance throughout the duration of my post-graduate studies. You have been an exceptional mentor and have helped mold the young professional I am today – thank you so much.

Thank you so much to Dr. Wolfgang Sand for an unforgettable exchange to Germany at the University Duisburg-Essen, thank you for accepting me into your lab, for many engaging conversations, for your support of my work.

Thanks to the members of the Centre for bioprocess engineering research for their support and friendship throughout my studies and to my colleagues in Germany at the University Duisberg-Essen. I have learned something from each and every one of you. Thank you for your friendship, assistance with academic and laboratory requirements. Special thanks to Dr. Mario Vera for assistance and support in Germany and Dr. Robert Huddy for your support and mentorship during the writing of this thesis.

For their financial support I would like to thank the Deutscher Akademischer Austauschdienst (DAAD), the Potter foundation and the Mellon Mays Foundation.

To all of those who continued to believe in me and encourage me, through the happy times and the struggles – I thank you, I will be forever grateful and I love you very much! A great many thanks to my parents James and Onetia Africa, and to my sister Melissa Africa, for your endless love and support. To an incredibly special individual, my love and my husband, Christopher Jenner - thank you so much for your unyielding patience, your kindness, your constant encouragement and belief in me – without you this would not have been possible, I love you very much.

Abstract

This research pertains to bioleaching of copper containing ores with particular reference to the copper sulfide mineral chalcopyrite ($CuFeS_2$). While it is focused on heap bioleaching, it has applications to stirred tank bioleaching operations. In the context of bioleaching, microbial extra-cellular polymeric substance (EPS) components are thought to complex chemical oxidants and extend the chemical reaction space available for mineral dissolution reactions, making the microbial-mineral-EPS interface the dominant active zone in terms of microbial oxidation and mineral dissolution. There is a limited understanding of microbial biofilm formation within a bioleach heap. The implication of various microorganisms having a set of defined or optimal conditions under which they colonise and proliferate is quite substantial. Understanding what creates favourable interfacial microenvironments enabling a sessile population to flourish (and thereby decrease lag time) has great implications for minimising costs and maximising productivity. Furthermore, limited work has been conducted on thermophilic microorganisms relevant to bioleaching. These microorganisms are pertinent to successful bioleaching at high temperatures, with work incorporating low grade ores and gangue mineralogy also being scarce. The aim of this research is to provide a thorough investigation into microbial-metal sulfide interfacial environments *in situ*, using a thermophilic archaeon *M. hakonensis*, low-grade metal-sulfide ores, a series of temperature regimes, heap-simulating conditions and an in depth extraction and analysis of the EPS produced under varied culturing conditions. This was done in three parts. The first part of the investigation involved visualising and characterising EPS, in terms of composition as well as three dimensional architecture and spatial locale, *in situ* for planktonic as well as sessile *M. hakonensis* cultured on different growth media. The second part involved development of a technique to extract, quantify and characterise the composition of EPS extracted from *M. hakonensis* cultured on three different growth mediums. In the final part of this study, the formation and development of *M. hakonensis* biofilms, using a flow through reactor system, on two massive sulphide mineral surfaces (chalcopyrite and pyrite) and a low-grade chalcopyrite bearing ore was assessed, with a borosilicate (glass) surface serving as control surface. Atomic force microscopy (AFM) in combination with fluorescent staining techniques, confocal laser scanning microscopy (CLSM) and epifluorescent microscopy (EFM) were utilised.

In the first part of the study, planktonic cells were cultured on chalcopyrite mineral grains and sulfur, 37 % of chalcopyrite grown cells observed to possess EPS, relative to only 16 % of sulfur grown cells. Lectin screening analysis was performed for cells either cultured in batch agitated flasks on chalcopyrite mineral grains, with the mineral grains containing attached cells assessed; or cultured in the biofilm reactor with the flat chalcopyrite mineral slide. For sessile *M. hakonensis* on chalcopyrite mineral grains cultured in shake flasks, three EPS architectural motifs were evident, namely; the confluent matt of EPS along the mineral surface, capsular EPS binding, and the diffuse cauliflower motif which branched outward from the mineral surface. The EPS assayed was found to contain fucose, rhamnose, glucose, mannose, galactose, sialic acids as well as N-acetyl-glucosamine (GlcNac) and N-acetyl-galactosamine (GalNac) containing residues. The aforementioned glycoconjugates were present in all three binding motifs. Cells were observed to be attached to the mineral surface and were also evident within the EPS milieu around the chalcopyrite mineral grains. The cloud-like cauliflower formations of EPS which branch outward from the mineral surface, and the creation of a confluent EPS matt across the surface, serve the sessile microbial population well in extending the surface area coverage available for entrapment of ions and increasing dissolution reaction space.

Stemming from this, the second part of the study arose. This involved extraction and characterisation of EPS from *M. hakonensis* grown on three substrates: chalcopyrite, sulphur and ferrous sulphate. An extraction method was developed to allow the recovery of colloidal EPS, EPS associated loosely with the cell and capsular EPS from the thermophilic system. The extraction of these fractions allowed quantification of the material and analysis of its composition. EPS yield varied with energy source for growth. Thus cells are able to adapt and adjust their interfacial environment through changing the chemical composition and abundance of their EPS. Following extraction using crown ether, the preferred method, EPS extracted from the chalcopyrite system yielded the most EPS, followed by sulphur and then the ferrous sulphate systems. Unlike the EPS in mesophilic leaching systems which are mainly comprised on neutral sugars and lipids, protein was the major component of the EPS extracted from *M. hakonensis*. Sugars, uronic acids, nucleic acid and iron were also present in the EPS in proportions varying with both the locale or EPS fraction and culture conditions. Sugar monomers identified in the extracted EPS by GC-MS included rhamnose, glucose, galactose, fucose and mannose. Based on the hypothesis that the EPS-mediated reaction environment allows the creation of niche reaction conditions at the mineral-microbe interface, favourable to

bioleaching, this work expanded knowledge of factors affecting EPS formation, its location and composition.

In the final study of this investigation, the formation and development of *M. hakonensis* biofilms on two massive sulphide mineral surfaces (chalcopyrite and pyrite) and a low-grade chalcopyrite bearing ore was assessed, with a borosilicate (glass) surface serving as control surface. These mono-species biofilms were grown in a specialised biofilm reactor under conditions of continuous fluid flow, mimicking fluid flow conditions found in a bioheap. The mature films were analysed through the use of fluorescent lectin and nucleic acid stains and visualised using CLSM and a combination of AFM–EFM. For biofilm formation on chalcopyrite surfaces at optimal temperatures for growth, micro-colony formation was evident after 2 days with the cell density increasing from 2.0% to 5.7% coverage of the surface after 4 days. This then decreased marginally to 4.7% after 8 days of incubation. The most prominent EPS signal was evident after 4 days of incubation at optimal temperature for growth. The greatest cell densities and extents of biofilm development, in terms of surface coverage, were observed on massive chalcopyrite at the optimal temperature for growth (5.7% coverage). The surface coverage decreased with a decrease in incubation temperature irrespective of mineral system. The mineral surface was colonised after 2 days, with cells forming a monolayer and EPS not abundantly present. Attachment was improved after 4 days incubation at room temperature, irrespective of mineral system under investigation, with EPS becoming more significant. This study provides first known insights into biofilm development of *M. hakonensis* on massive sulphide mineral surfaces, demonstrating monolayer coverage and dependence on colonisation temperature. It also provides the first study on low-grade mineral ore surfaces investigated in situ under film flow. These results suggest that introduction of high temperature organisms into the heap under conditions sub-optimal for their growth may result in their retention on the ore surface, albeit at a lower loading. Hence re-inoculation at high temperatures may not be essential. Further, the short time frame required for colonisation under ideal contacting conditions (<4 days) highlights the importance of contacting in the heap environment. Furthermore, successful attachment, colonisation and biofilm formation is essential to the proliferation of microbial life and improved heap leach efficiency. Industrial bio-heap operations are carried out using complex, low-grade (gangue containing) copper ores. An appreciation of mineralogy, microorganisms which proliferate in thermophilic temperature ranges and the interfacial environments created is fundamental to overall understanding of the bioleach process in both heap and tank scenarios.

Table of contents

LIST OF FIGURES:

LIST OF TABLES:

ABBREVIATIONS

AFM	Atomic force microscopy
B	Bacteria
BS	Irreversible attachment
[BS]*	Reversible attachment and formation of the metastable complex
CSTR	Continuous stirred tank reactor
CLSM	Confocal laser scanning microscopy
DAPI	4', 6-diamidino-2-phenylindole
EPS	Extra-cellular polymeric substance
EFM	Epifluorescent microscopy
FISH	Fluorescent *in situ* hybridisation
PCR	Polymerase chain reaction
PPL	Plane polarised light
QEMSCAN	Quantitative evaluation of minerals by scanning electron microscopy
RL	Reflected light
rRNA	ribosomal ribonucleic acid
S	Surface sites involved in the initial adhesion mechanism
SEM	Scanning electron microscopy
TL	Transmitted light
XPL	cross polarised light
XRD	X-ray diffraction
XRF	X-ray fluorescence

Chapter 1:

Introduction to bioleaching, relevance of study and major research themes investigated

1.1 INTRODUCTION

World copper production increased from 16.6 thousand metric tonnes in 2012 to 19.1 thousand metric tonnes at the end of 2015, with demand for the metal growing due to overall economic growth in developing countries[1]. One key example is the rapid and expansive development in China which has seen an annual growth rate of 9.9% between 1980 and 2010[2]. China also accounted for 45% of the global demand for copper in July 2016 according to the international study group[1]. This group showed that in the first seven months of 2016, the apparent global usage of refined copper was estimated to have increased by around 4% (565,000 t) compared with the same period of 2015 mainly due to strong Chinese apparent demand.

With respect to heap systems, oxide deposits, which are extracted using acid reactions, are becoming depleted and grades of copper are declining with available ore bodies becoming more recalcitrant (Gericke *et al.* 2005). To ensure demand does not outstrip supply there is an unremitting requirement to lower production costs associated with beneficiating low grade ores and to source innovative means of maximising copper extraction from more complex ores (Gericke *et al.* 2005, Watling 2006). Bioleaching is one such mechanism making use of microorganisms to assist in the recovery of metals from low-grade copper ores, overburden and waste materials from existing operations. Moreover, bioleaching is an economically efficient, potentially "greener" alternative for the recovery of copper from low grade ores than conventional pyrometallurgical techniques. The technology has also been applied successfully in the recovery of uranium, cobalt, nickel and zinc from sulfidic ores, as well as the pre-treatment of gold-bearing ores, both in tank and heap leach processes. The ores exploited contain metals either as oxide or as sulfide material (Gericke *et al.* 2005).

The leaching of sulfide minerals is an oxidative process, which results in the formation of ferrous iron. A more detailed discussion of leach chemistry is provided in the literature review

[1] http://www.icsg.org/index.php/component/jdownloads/finish/114/2196?Itemid; accessed 11.00, 16-11-2016

[2] http://www.aqmcopper.com/s/CopperFundamentals.asp; accessed 12.48; 06-01-2014

in Section 2.1. Ferric iron forms when ferrous iron is oxidised. At low pH and temperature, the rate of inorganic oxidation of ferrous iron by oxygen is slow. This reaction is accelerated by the metabolic activity of naturally occurring iron oxidising microorganisms. Iron and sulfur oxidizing microorganisms catalyze the oxidation of ferrous iron or reduced sulfur compounds or both, resulting in the ongoing formation of the aforementioned chemical oxidants (ferric iron and protons) which act as leach agents. These facilitate the continuity of the leach process and effectively accelerate mineral dissolution. It is this accelerated oxidation of sulfide minerals by microbial activity that has been harnessed in the minerals industry as a biotechnological tool for the recovery of metals from low-grade or waste ores. However, uncontrolled microbial activity accelerating oxidation of sulfide minerals has detrimental effects on the environment through the production of acid mine drainage (AMD).

1.2 COMMERCIAL RELEVANCE OF INVESTIGATION

Industrial biomining operations are conducted either via the construction of irrigated heaps, or with stirred tanks. Heap bioleaching involves the engineering of constructed heaps using either run-of mine (ROM) ore or crushed, agglomerated ore. Heaps may be inoculated with the microorganisms of interest through the irrigation system or during the agglomeration stage (Gericke *et al.* 2005) or allowed to colonise with naturally occurring micro-organisms. These systems are typically aerated from below using blowers and irrigated with an acidic leaching solution from the top of the heap. The collection and processing of the leachate or pregnant liquor solution (PLS) follows for the recovery of the target metals. This study focusses on heap-bioleaching of chalcopyrite bearing low grade copper ores. However, the fundamental aspects stemming from this research are expected to have applications to the leaching of other low grade sulfidic ores as well as in the tank leaching of concentrates of sulfidic minerals.

An early report of the commercial application of microorganisms for the recovery of copper from mine dumps dates back to the late 1950's (Zimmerley *et al.* 1958 in Olson *et al.* 2003). Olson *et al.* (2003) report that despite the role of microorganisms in the process being recognised, these early operations were carried out without considering the microbiology of the process. For many years bioleaching systems were operated as such - without considering or optimising the biotic component. This was, in part, due to the fact that the system worked well for the less recalcitrant ore bodies, hence there was no need to develop the microbiology of the system. It was only once process operation became more challenging in terms of leach performance predictability, and ore bodies became more difficult to treat that the focus shifted towards understanding the contribution of microorganisms to maximise production efficiency.

A particularly challenging sulphide mineral to leach, especially at low temperatures, is primary[3] chalcopyrite (Stott *et al.* 2003, Rawlings *et al.* 2003). Primary chalcopyrite is a copper sulfide mineral that comprises the bulk copper source available for metal recovery (Peters *et al.* 1966). It is proposed that the problems associated with chalcopyrite bioleaching may be due to the passivation of chalcopyrite, amongst others. Various metal sulfides have been proposed to undergo oxidative mineral dissolution via two different mechanisms, the thiosulphate[4] and polysulfide mechanisms[5] for acid insoluble and acid soluble sulphide minerals respectively (Schippers and Sand 1999). This also results in the formation of varying end products. For chalcopyrite, these may result in an increase in pH and the formation of precipitates on the mineral surface observed to hinder bioleaching (Klauber *et al.* 2003, Petersen *et al.* 2001). The microbial consortia involved are important in the regeneration of acid and ferric ions, and for the removal of sulfur precipitates on the mineral surface by sulfur oxidizers (*A. thiooxidans* and *A. caldus*), required for the dissolution to continue (Olson *et al.* 2003).

In addition to specific challenges regarding mineralogy, industrial heap bioleaching poses further operational challenges. Heap operations may undergo lag periods before effective leaching takes place, and the overall performance of the system is often unpredictable. The system allows minimal control over reaction conditions within the bioheap creating transient micro-environments as the leach progresses in terms of solution chemistry, nutrient and oxygen availability, and temperature (Brierley 2001). Internal temperature is related to the sulfide mineral content of the ore body and is difficult to control or monitor in heap systems (Dixon 2000, Olson *et al.* 2003). While heap operations may start up at ambient temperature ranges, exothermic oxidation of sulfides have been reported to increase heap temperatures up to 81 °C for systems containing just 1.2-1.8 % sulfide-sulfur (Tempel 2003 in Olson *et al.* 2003). Thus, although heap operations may be inoculated with a particular consortium of microorganisms at the start-up phase, the microbiology of the heap system will vary in response to physicochemical conditions imparted by the progression of the leach. This impacts directly on leach efficiency and predictability. One must be cognisant of the fact that difficulties related to heap leaching may be due to several contributing factors i.e. heap construction and engineering (height, irrigation and fluid-flow rates, aeration), mineralogy, and local climate (Dixon 2000, Olson *et al.* 2003, Brierley 2001). However, increasing our understanding of the active microbial consortium, and how this varies in response to changing physicochemical conditions

[3] Primary minerals refer to minerals which have not been chemically altered in any way since their time of crystallisation from molten and subsequent deposition

[4] The thiosulphate mechanism (acid insoluble sulphide metals) involves oxidation by ferric attack on the mineral surface, with thiosulphate being the main intermediate and sulphate the main end product (Schippers and Sand 1999).

[5] In the polysulfide mechanism (acid soluble sulphide metals) the dissolution is due to a combined oxidative attack of protons and ferric iron, with polysulfide as the major intermediate and elemental sulfur as the final product. The elemental sulfur can then be further oxidized to sulphate by microbial action. The dissolution of mineral via the polysulfide mechanism is acid consuming, resulting in an increase in pH. Optimal microbial leaching occurs between pH 1.4 and pH 1.6 (Rawlings 2004).

within the system, provides valuable knowledge which will inform process operation and address the abovementioned challenges. This will allow the processing of increasingly recalcitrant ores, lower capital and operating costs and improve metal recoveries (Brierley 2001).

1.3 MAJOR RESEARCH THEMES TO BE INVESTIGATED

A sedentary or surface associated microbial lifestyle may very well be the predominating form of microbial life in heap systems, with heap performance intrinsically dependent on the activity (effective distribution and size) of this mineral-associated microbial population. There is a limited understanding of microbial biofilm formation within a bioleach heap. Monitoring the microbiology in industrial bioheaps has predominantly been carried out by sampling PLS and raffinate, or through the use of indirect methods (oxygen uptake) as obtaining samples from solid particles within the heap is challenging and often unreliable (Brierley 2001). The implication of various microorganisms having a set of defined or optimal conditions under which they colonise and proliferate is quite substantial. Understanding what creates favourable interfacial microenvironments enabling a sessile population to flourish (and thereby decrease lag time) has great implications for minimising costs and maximising productivity. Furthermore, limited work has been conducted on thermophilic microorganisms relevant to bioleaching.

The aim of this research is to provide a thorough investigation into microbial-metal sulfide interfacial environments *in situ*, using a thermophilic archaeon *M. hakonensis*, low-grade metal-sulfide ores, a range of temperature regimes, heap-simulating conditions and in depth extraction and analysis of the EPS produced under varied physicochemical conditions.

Objectives of this study are:

- To investigate the mineral-microbial interfacial environment of the thermophilic archaeon *Metallosphaera hakonensis* (*M. hakonensis*) through visualising the EPS and biofilm formation *in situ*
- To investigate the spatial arrangement of the *M. hakonensis* interfacial environment and partial chemical composition of this environment through the use of lectin staining and advanced visualisation techniques using confocal laser scanning microscopy
- To investigate the mineral-microbe interfacial environment through extraction and compositional characterisation of EPS from *M. hakonensis*
- To investigate the effects of varying physicochemical conditions on spatial and compositional changes of the *M. hakonensis* interfacial microenvironment, through

extraction and compositional analysis of EPS cultured on three different growth substrates

- To investigate the transition between initial adhesion and firm attachment stages in the development of biofilms of the thermophilic archaeon *M. hakonensis*, as well as the effect of varying physicochemical conditions (temperature) on the interfacial microenvironment *in situ* through the use of advances microscopy techniques

The literature review, presented in Chapter 2, details the process of bioleaching and the factors affecting these. A review of microbial attachment to, and colonisation on, mineral surfaces; as well as trends in microbial adhesion to sulphide minerals in particular and the factors influencing this process is explored. The role of EPS, techniques to extract and analyse EPS is presented and discussed, together with mechanisms to study colonisation and biofilm formation. Following this, factors affecting the adhesion and colonisation process in bioleach systems are presented and discussed. The advantages of biofilm formation under bioleach conditions, as well as the phenomenon of detachment, are also discussed with relevance to bioleach environments. Chapter 2 is concluded by an analysis of gaps in the literature pertaining to the scope of this thesis, followed by the objectives and key questions addressed in the thesis.
Chapter 3 presents the description of, and rationale behind, the methodologies employed in this study. All analytical techniques and reactor configurations are presented. Chapter 4 presents the results and discussion of the *in situ* visualisation of EPS produced by *M. hakonensis* cultured under different methods. Visualisation was made possible through the development of an assay to rapidly screen the EPS using highly specific fluorescent labelled lectins and confocal laser scanning microscopy. Positive binding of the lectin with the EPS resulted in fluorescence and also provided an indication of the EPS composition. In Chapter 5, the results and discussion of a methodology to extract and chemically characterise EPS from *M. hakonensis* cultured on three different substrata is presented. The extent of the EPS produced and its chemical composition under each condition is compared and contrasted with literature reports. Chapter 6 presents the results and discussion of the biofilm reactor attachment study. The microbial-mineral interfacial environment is further elucidated through *in situ* visualisation of *M. hakonensis* cells colonising sulphide mineral surfaces, as well as visualisation of EPS within the resulting biofilm. Trends in attachment and colonisation of pure cultures *M. hakonensis* to a predominantly chalcopyrite containing mineral ore thin section, a predominantly pyrite containing mineral ore thin section, and a low grade chalcopyrite containing mineral ore thin section is presented. The effect of temperature on the extent of colonisation was also investigated and is presented and discussed in this chapter. In Chapter 7, a summary of conclusions drawn and recommendations made from this study in presented.

References

http://www.icsg.org/index.php/component/jdownloads/finish/114/2196?Itemid; accessed 11.00, 16-11-2016

http://www.aqmcopper.com/s/CopperFundamentals.asp; accessed 12.48; 06-01-2014

Brierley, C. L. (2001). Bacterial Succession in bioheap leaching. *Hydrometallurgy,* 59, 249-255

Dixon, D. G. (2000). Analysis of heat conservation during copper sulphide heap leaching. *Hydrometallurgy,* 58, 27-41

Gericke, M., Muller, H. H., Neale, J. W., Norton, A. E., & Crundwell, F. K. (2005). Inoculation of heap-leaching operations. *Proceedings of the 16th International Biohydrometallurgy Symposium* (pp. 255-264). Cape Town, South Africa: STL Harrison, DE Rawlings and J Petersen , Editors

Klauber, C. (2003). Fracture induced reconstruction of a chalcopyrite surface. *Surface and Interface Analysis , 35*, 415-428

Olson, G. J., Brierley, J. A., Brierley, C. L. (2003). Bioleaching review part B: Progress in bioleaching: applications of microbial processes by the mineral industries. *Applied Microbiology and Biotechnology,* 63, 249-257

Peters, W. C. (1966). Geology of the Bingham Canyon Porphyry Copper Deposits, Utha. In S. R. Titley (Ed.), *Geology of the porphyry copper deposits of Southwestern North America* (p. 167). Tuson Arizona Press

Petersen, J., Dixon, D. G., Timmins, M., & Ruitenberg, R. (2001). Batch reactor studies of the leaching of a pyrite/chalcopyrite concentrate using thermophilic bacteria. In V. S. Ciminelli, & O. Garcia (Eds.), *Biohydrometallurgy: Fundamentals, Technology and Sustainable Development Part A* (pp. 525-533). Amsterdam: Elsevier

Rawlings, D. E., Dew, D., du Plessis, C. (2003). Biomineralization of metal-containing ores and concentrates. *Trends in Biotechnology*, 21, 1, 38-44

Schippers, A., & Sand, W. (1999). Bacterial Leaching of Metal Sulfides proceeds by Two Indirect Mechanisms via Thiosulfate or via Polysulfides and Sulfur. *Applied Environmental Microbiology , 65*, 319-321

Stott, M. B., Sutton, D. C., Watling, H. R., & Franzmann, P. D. (2003). Comparative Leaching of Chalcopyrite by Selected Acidophilic Bacteria and Archaea. *Geomicrobiology Journal , 20*, 215-230

Tempel, K. (2003). Commercial biooxidation challenges at Newmont's Nevada operations. In: 2003 SME Annual Meeting, Preprint 03.067, Soc Mining, Metallurgy and Exploration, Littleton, Colo

Watling, H. R. (2006). The bioleaching of sulfide minerals with emphasis on copper sulphides – a review. *Hydrometallurgy , 84*, 81-108

Zimmerly, S. R., Wilson, D. G., Prater, J. D. (1958). Cyclic leaching process employing iron oxidising bacteria. US Patent 2, 829, 964

Chapter 2:

Literature review

2.1 AN OVERVIEW OF THE BIOLEACH PROCESS

Bioleaching is an application of biotechnology which exploits the metabolic activity of iron and sulfur oxidising microorganisms in an acidic medium for the recovery of metals from minerals. Increasingly, metals are being exploited from minerals in which they occur as metal sulfides. The mineral dissolution of metal-sulfides involves a chemical oxidant (such as ferric iron) which attacks the mineral matrix, liberating metal ions. The metabolic activity of the microorganisms involved facilitates continuity of the bioleach process through regeneration of the chemical oxidants.

2.1.1 Abiotic leach chemistry for the dissolution of sulfide minerals

The leaching of sulfide minerals is an oxidative process which results in the formation of ferrous iron shown for pyrite in Eqn 1 and 3 and chalcopyrite in Eqn 4. Ferric iron forms when oxygen oxidizes ferrous iron after it is released by pyrite (Eqn 2). At low pH, the rate of inorganic oxidation of ferrous iron by oxygen is slow.

$$FeS_2 + {}^{7}/_{2}\,O + H_2O \rightarrow Fe^{2+} + 2\,SO_4^{2-} + 2\,H^+ \quad (1)$$

$$Fe^{2+} + {}^{1}/_{4}\,O_2 + H^+ \rightarrow Fe^{3+} + {}^{1}/_{2}\,H_2O \quad (2)$$

$$FeS_2 + 14Fe^{3+} + 8\,H_2O \rightarrow 15\,Fe^{2+} + 2\,SO_4^{2-} + 16\,H^+ \quad (3)$$

$$CuFeS_2 + 4Fe^{3+} \rightarrow 5Fe^{2+} + Cu^{2+} + 2S^0 \quad (4)$$

$$CuFeS_2 + 4H^+ \rightarrow Fe^{2+} + Cu^{2+} + 2H_2S \quad (5)$$

2.1.2 Microbially assisted leaching

The leaching of sulfide minerals is accelerated by the metabolic activity of naturally occurring chemolithoautotrophic microorganisms. Chemolithoautotrophs are capable of utilising CO, CO_2 or carbonates as the sole carbon source and obtaining energy from the oxidation of reduced

inorganic compounds namely ferrous iron, reduced sulfur compounds or both[1]. Microbial oxidation of these inorganic compounds leads to the generation of ferric ions (from ferrous oxidation) and proton acidity, shown in Eqn 6 and 7 (Schippers and Sand 1999). The chemistry of microbially assisted leaching is similar to that of the abiotic chemical leaching due to the oxidation of sulfide mineral by ferric ions in acidic media, shown in Equations 2 through 5 above.

$$2Fe^{2+} + 2H^{+}\,{}^{1}/_{2}\,O_2 \rightarrow 2Fe^{3+} + H_2O \qquad (6)$$

$$2S + 3O_2 + 2H_2O \rightarrow 2H_2SO_4 \qquad (7)$$

The presence of active microorganisms effectively expedites the leaching process through regeneration of the reactants required for mineral dissolution to continue (see the indirect mechanism explaining microbial involvement in Section 2.1.3).

2.1.3 Mechanisms to describe microbial involvement in bioleaching

There are currently three schools of thought explaining the involvement of microorganisms in bioleaching with arguments supporting all three. However, some of these debates lack validity and experimental evidence. The proposed mechanisms of microbial involvement have been summarised by Crundwell (2003) and termed: the **indirect mechanism**, **the direct contact mechanism** and the **indirect contact mechanism**.

In explaining the role of bioleach microorganisms via the **indirect mechanism**, it is hypothesised that the microorganisms regenerate the reactants required for the leaching process to continue through oxidation of iron sulfides by ferric iron and sulfuric acid. No contact is made necessary between the microorganism and the mineral surface and mineral dissolution occurs by chemical reaction between the metal sulfide and the reactants (ferric ions and or protons) in solution.

According to Rawlings (2004), the **direct mechanism** of bioleaching involves microbes adhering to the mineral surface and some form of an enzymatic attack, with components of the membrane of the microbe interacting directly with the mineral surfaces. This was first proposed by Silverman and Ehrlich (1964), who hypothesised that an increased rate of pyrite dissolution by *Thiobacillus ferrooxidans* (currently classified as *Acidithiobacillus ferrooxidans*) over abiotic chemical dissolution was due to the involvement of some enzymatic oxidant (Crundwell 2003).

[1] http://serc.carleton.edu/microbelife/microbservatories/nevadahotsprings/alkchem.html ; accessed 15.51 on 16-11-2016

Thus, in the case of the direct mechanism, attachment of microorganisms to the mineral surface is essential to play an active role in the leaching process as mineral dissolution is a result of an enzymatic attack on the mineral surface. Crundwell (2003) notes that, to date, there is no evidence to support these claims, and many authors have made claims to contradict this behaviour for *Acidithiobacillus ferrooxidans* concerning pyrite dissolution.

With respect to the **indirect contact mechanism**, the dissolution of the mineral is due to the chemical attack of ferric ions or protons or both on the mineral sulfide. This reaction gives rise to the formation of ferrous iron and various forms of sulfur (Rawlings 2004). The microbes involved obtain their energy by oxidation of ferrous, sulfur and reduced-sulfur compounds (Devasia *et al.* 1993). The role of microorganisms, via this mechanism, is to catalyse the oxidation of iron sulfides to ferric iron and sulfuric acid and thus regenerate the reactants required for the leaching process to continue. For this mechanism of bioleaching, microbes need not be in direct contact with the mineral surface in order for mineral dissolution to occur, but are associated with and in proximity of the mineral surface. It is hypothesised that the extra-polymeric substance (EPS) produced by cells for attachment to surfaces and establishment of biofilms (discussed in Section 2.4), provides the reaction space for dissolution to occur (Gehrke *et al.* 1998, Harniet *et al.* 2005) in which reactants are in close proximity to the mineral surface facilitating a more effective chemical attack (Rawlings 2004). Therefore, with respect to the indirect contact mechanism, direct contact is not a requirement for bioleaching, however, attachment and biofilm formation plays an important role in bringing the microbial catalysts, the reactants and the mineral surface in close proximity, to facilitate a more effective dissolution process.

A schematic representation of the mechanisms used to explain the role of microorganisms in bioleaching is presented in Figure 2.1.

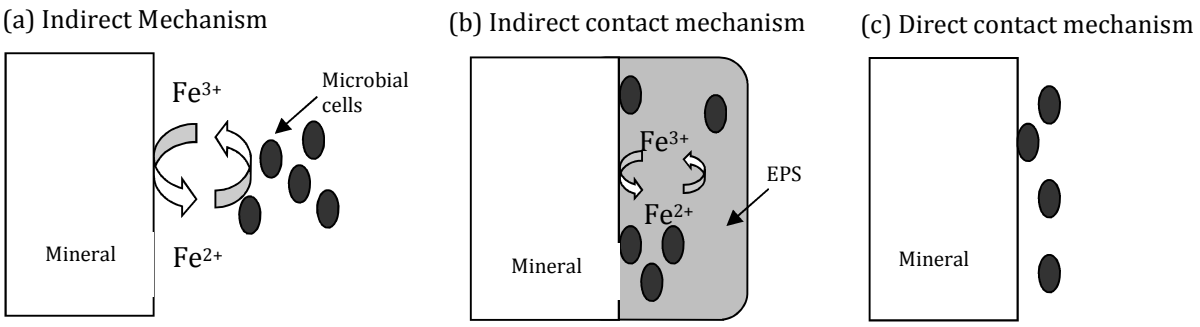

Figure 2.1: The role of microorganisms explained by the indirect mechanism **(a)**, mineral dissolution occurs due to the presence of ferric ions and or protons in solution. These reactants are regenerated by microbes via oxidation of ferrous iron and reduced sulfur compounds. In the indirect contact mechanism **(b)**, mineral dissolution is still due to the chemical attack of ferric ions and or protons in solution. The attachment and excretion of EPS by the microbes allows a more effective chemical attack by contacting of reactants, the mineral surface and the microorganisms. The direct contact mechanism **(c)** is depicted, with microbes interacting directly with the mineral surface. (Adapted from Crundwell 2003).

It is important to note that although attachment plays an essential role in both the direct and indirect contact mechanisms of bioleaching, the distinguishing difference lies in the mechanism of mineral dissolution being a result of enzymatic attack (direct) or chemical attack by ferric ions and protons (indirect).

While the activity of planktonic cells in the bioleach may not be insignificant, microbial attachment is key in the leaching process and has been demonstrated to increase leach rates (Rodriguez *et al.* 2003 **a,** Gehrke *et al.* 1998, Fowler *et al.* 1999 and Kinzler *et al.* 2003). Furthermore, most microbial life in a bioheap environment is likely to be sessile and mineral-associated through the formation of biofilms, especially owing to the greatly differing hydraulic and solids residence times and their relationship to the microbial growth rates (Govender *et al.* 2012). In appreciation of these findings, attachment and the creation of a favourable mineral-microbe-EPS interfacial environment is critical to describing microbial involvement in bioleaching.

2.2 MICROORGANISMS INVOLVED IN BIOLEACHING

The microorganisms isolated from heap leach environments are acidophilic (optimal pH for growth is typically less than pH 3) and may be mesophiles (25°C - 40°C), moderate thermophiles (40°C - 55°) and extreme thermophiles (above 65°C). Summarised in Table 2.1, are the bacteria and archaea commonly isolated from bioleach heap operations.

Metallosphaera hakonensis, first classified *Sulfolobus hakonensis* by Takayanagi *et al.* (1996), are aerobic thermoacidophilic archaea (Kurosawa, Itoh and Itoh, 2003). They thrive at an ideal temperature of 70°C and a pH of 3.0, but can tolerate temperatures between 50 and 80 °C and a pH range between 1 and 4 (Takayanagi *et al.*, 1996). They are lobed in shape or occur as irregular polyhedrons with a diameter between 0.9 and 1.1 μm. They are non-motile and lacking in flagella. The genomic DNA G + C content of *M. hakonensis* is 38.4 mol% (Kurosawa *et al.* 2003). *M. hakonensis* grows lithotrophically on elemental sulfur and reduced sulfur compounds and utilises sugars and amino acids poorly as a sole carbon source (Takayanagi *et al.* 1996). This organism has also been demonstrated to grow on ferrous sulphate, pyrite and chalcopyrite supplemented with 0.1 % yeast extract (wt. vol^{-1}).

Under mesophilic conditions *Leptospirillum ferriphilum* is proposed as the dominating iron-oxidising microbial species (Watling 2006). In continuous tank cultures, at temperatures between 40 and 45°C (moderately thermophilic conditions), *Acidithiobacillus caldus* is the dominant sulfur oxidiser in bioreactors treating arsenopyrite or copper concentrates (Rawlings *et al.* 1999, Okibe *et al.* 2003). At temperatures greater than 60°C, *Sulfolobus metallicus* and *Metallosphaera spp.* are proposed as the dominating bioleaching strains (Hallberg and Johnson, 2001).

Acidithiobacillus ferrooxidans, previously classified *Thiobacillus ferrooxidans* (Temple and Colmer, 1951), are gram negative, rod-shaped, gammaproteobacteria, 1 x 1.5 μm in magnitude. They are chemolithoautotrophs and obtain energy from the oxidation of ferrous iron, sulphur and metal sulphides (such as pyrite and chalcopyrite). *A. ferrooxidans* thrives at a pH between 1.5 and 2.5, and a temperature of 30 °C (Kelly and Wood, 2000), but can tolerate temperature between 10 °C and 40 °C (Dixon 2000). *A. ferrooxidans* is flagellated and motile (Jerez 2001).

Leptospirillum ferriphilum are gram negative vibrio- or spiral- shaped microorganisms, approximately 0.3-0.5 x 0.9-0.3 μm in magnitude. They are obligate chemolithoautotrophs and oxidize ferrous iron using oxygen as a terminal electron acceptor. They can tolerate high ferric:ferrous ratios and have a high affinity for ferrous iron (k_m = 0.25mM). They grow optimally at temperatures between 30 °C and 37 °C and at a pH range between 1.4 and 1.8, but can tolerate temperatures up to 40 °C and a pH below 1.0 (Coram and Rawlings 2002). A high temperature strain has been reported that is able to perform ferrous iron oxidation up to 49°C. *L. ferriphilum* is flagellated and motile (Jerez 2001).

Table 2.1: List of microorganisms commonly isolated from bioleach environments (From Watling 2006).

Organism	Reported growth substrates	Characteristics
Acidianus ambivalens	S oxidation and reduction	Hyperthermophiles
Acidianus brierleyi	Sulphides	pH opt 1.5–2.5
Acidianus infernus	Poor, if any, Fe oxidation	
"Acidianus tengchongensis "		
Acidimicrobium ferrooxidans	Mixotroph	Moderate thermophile pH opt 2
	Fe oxidation and reduction	
	Sulphides (poor)	
Acidiphilum spp	Obligate heterotrophs	Mesophiles
Acidiphilium SJH	S oxidation	pH opt ~ 2–3
	Fe(III) reduction	
Acidiphilium acidophilum	Facultative autotroph	Mesophile pH opt ~ 2–3
	S oxidation	
	Fe(III) reduction	
Acidithiobacillus albertensis	Autotrophs	Mesophiles
Acidithiobacillus ferrooxidans	S oxidation, sulphides	pH range 2–4
Acidithiobacillus thiooxidans	(*Af*, Fe(II) oxidation; Fe(III) reduction as a facultative anaerobe)	
Acidithiobacillus caldus	Mixotroph	Moderate thermophile
	3S oxidation, sulphides	pH opt 2–2.5
Acidolobus aceticus	Heterotroph	Hyperthermophile
	S reduction to H_2S	pH opt 3.8
Alicyclobacillus spp	S oxidation, sulphides	Mesophiles — moderate thermophiles
"Alicyclobacillus disulfidooxidans"	(*Ad*, facultative autotroph,;	pH 1.5–2.5
"Alicyclobacillus tolerans"	At, mixotroph, Fe(III) reduction)	
"Ferrimicrobium acidiphilium"	Heterotroph	Mesophile
	Fe(II) oxidation, sulphides	pH opt 1.7–1.8
	Fe(III) reduction	
Ferroglobus placidus	Fe oxidation	Thermophile
		pH neutral
"Ferroplasma acidarmanus"	Possibly autotroph	Moderate thermophiles
"Ferroplasma cyprexacervatum"	Iron oxidation	pH range < 1–2
Ferroplasma acidophilum	Pyrite oxidation poor	
Ferroplasma MT17		
Hydrogenobaculum acidophilus	S, H oxidation to produce sulphuric acid	Thermophile
		pH opt 3–4
Leptospirillum ferriphilum	Fe oxidation	Mesophiles, some thermo-tolerant strains
Leptospirilum thermoferrooxidans	Pyrite	pH range 1.6–1.9
Leptospirillum ferrooxidans	Fe oxidation, pyrite	Mesophile, pH opt 1.5–1.7
Metallosphaera sedula	S oxidation	Thermophiles
Metallosphaera prunae	Sulphides	pH 1–4
"Metallosphaera hakonensis"		
Sulfobacillus acidophilus	Fe(II) oxidation; Fe(III) reduction, Sulphides	Moderate thermophiles
Sulfobacillus thermosulfidooxidans	S oxidation	pH 1–2.5
Sulfolobus metallicus	Strict chemolithoautotroph	Hyperthermophiles
"Sulfolobus rivotincti"	S oxidation, sulphides	Various pH in range 1–4.5
Sulfolobus shibatae		
"Sulfolobus tokodaii		
Sulfolobus yangmingensis		
"Sulfolobus" JP2 and JP3		
Sulfolobus acidocaldarius	Heterotrophs	Hyperthermophiles
Sulfolobus solfataricus	Not S oxidation	pH 2–4.5
Sulfurococcus yellowstonensis	S and Fe oxidation	Hyperthermophile
Thiobacillus prosperus	S and Fe oxidation, sulphides	Mesophile, halophile, pH opt 2
Thiomonas cuprina	S oxidation, sulphides	Mesophile, pH opt 3–4

Acidithiobacillus caldus are moderately thermophilic, gram negative chemolithoautotrophs (Hallberg and Lindstromt, 1994). They grow at an optimal temperature of 45 °C and at a pH between 2 and 2.5 but can tolerate temperatures of 52 °C and a pH range of 1 to 4, exhibiting both sulfur oxidation and growth under these conditions (Hallberg and Lindstromt, 1994). They are rod-shaped and can measure between 1.2 µm x 0.7 µm to 1.8 µm x 0.8 µm. *A. caldus* are flagellated and motile, and display growth on elemental sulfur, tetrathionate and thiosulfate (Hallberg and Lindstromt, 1994).

Acidithiobacillus thiooxidans is a gram-negative, rod-shaped, sulfur oxidizing acidophilic bacterium found in many sulfur-rich environments (Travisany *et al.* 2014). *A. thiooxidans* exhibit typical dimensions of 0.5 µm x 1.0 µm, thrive at mesophilic temperatures of 28 - 30 °C , with slow growth observed at temperatures below 18 °C and above 37 °C, and temperatures above 55°C resulting in death (Waksman *et al.* 1922). It is an essential contributor to the effective copper extraction in heap systems (Pradhan *et al.* 2008). Experiments have demonstrated that mixed cultures containing *A. thiooxidans* exhibit enhanced copper extraction (Qui et al 2005).

2.3 EFFECT OF TEMPERATURE ON BIOLEACHING AND MICROBIAL ECOLOGY

The internal temperature of a bioheap is affected by the sulfide mineral content of the ore body and its reaction as well as the air and liquid flow rates through the heap. Effective monitoring and control in industrial heap bioleach systems are difficult to achieve and are noted to be affected by rate of reaction, aeration and fluid flow and distribution (Dixon 2000, Petersen and Dixon, 2002, Olson *et al.* 2003, Dew *et al.* 2011). While heap operations typically start up at ambient temperature, the exothermic oxidation of sulfides is reported to increase heap temperatures, depending on heap design and operation. Temperatures up to 81°C have been reported for systems containing just 1.2-1.8% sulfide-sulfur (Tempel 2003 in Olson *et al.* 2003). Bioleach rates are greatly influenced by temperature, with the biological processes operating within the physiological constraints of the microorganisms involved (Franzmann *et al.* 2005). The temperature progression that occurs places selective pressures on the microorganisms in the system. In heap bioleaching, a succession of microorganisms occurs from mesophiles to moderate thermophiles, and finally extreme thermophiles (Brierley 2001, Demergasso *et al.* 2005, Franzmann *et al.* 2005, Tupikina *et al.* 2014). Therefore, while heap operations may be inoculated with a particular consortium of microorganisms initially, the microbiology of the heap system changes in response to physicochemical conditions imparted by the progression of the leach, with temperature being an important contributor. A rate limiting factor in the abiotic leaching of chalcopyrite is the presence of ferric iron. Bioleaching of chalcopyrite has been demonstrated to

be more effective at temperatures between 65 and 75°C (Petersen and Dixon 2002). Thermophilic microorganisms are key in regenerating ferric iron in this operating window. Furthermore a greater understanding of microbial succession within heap environments is required with temperature being one of the key driving forces (Ascota *et al.* 2014). This underscores the value of experiments at higher temperatures and using thermophilic microorganisms (Dixon 2000, Dew *et al.* 2000, Rawlings 2002, Olson *et al.* 2003). This is of particular importance in heap bioleach systems designed for copper recovery from chalcopyrite, in order to define and improve process operations.

2.4 MINERALOGY AND ITS EFFECTS ON HEAP BIOLEACHING

Mineralogical composition, particularly of low grade ores, is complex. The mineralogy changes with geological location and includes a majority of gangue minerals, not bearing the metal of interest. The constituent minerals react at differing rates as the leach progresses, forming various products which have been observed to affect bioleaching. Therefore, mineralogy of ores and concentrates has direct impact on the efficiency of leaching and bioleaching and on the nature of the reaction products (Watling 2006). However, to date, few quantitative studies of mineralogical effects with respect to leach chemistry and leach rates have been conducted (Watling 2006). Furthermore, obtaining samples from solid particles within the heap is challenging (Remonsellez *et al.* 2009; Soto *et al.* 2013). Incorporating mineralogy in bioleach studies is becoming an increasingly important tool in facilitating feasibility studies (Watling 2006).

2.4.1 Effect of metal sulfides on heap bioleaching

Where copper is deposited as a copper sulfide mineral, primary[2] chalcopyrite most typically comprises the bulk source of copper available for metal recovery (Peters *et al.* 1966). Chalcopyrite leaching is challenging in comparison to other sulfide minerals (Stott *et al.* 2003). Chalcopyrite has also been shown to leach poorly at low temperatures (Rawlings *et al.* 2003). It is proposed that the problems associated with chalcopyrite may be due to the '*passivation of chalcopyrite*', discussed later. Minerals commonly associated with chalcopyrite include: covellite, cubanite, enargite, galena, sphalerite, and pyrite. Secondary[3] bornite and chalcocite are also common forms of recoverable copper associated with chalcopyrite (Peters *et al.* 1966).

[2] Primary minerals refer to minerals which have not been chemically altered in any way since their time of crystallisation from molten larva and subsequent deposition
[3] Secondary minerals are the result of the decomposition of a primary mineral and subsequent re-precipitation, creating a new, chemically distinct mineral

Acid soluble and acid insoluble metal sulfides undergo oxidation via two distinct mechanisms and through dissimilar intermediates, as indicated in Section 2.1. Schippers and Sand (1999) proposed that acid insoluble metal sulfides, such as pyrite, are oxidized via the *thiosulphate mechanism* and acid soluble metal sulfides such as chalcopyrite, sphalerite and galena, undergo oxidation via the *polysulfide mechanism*. In the *thiosulphate mechanism*, oxidation occurs by ferric attack on the mineral surface, with thiosulphate being the main intermediate and sulphate the main end product. In the *polysulfide mechanism* the dissolution is due to a combined oxidative attack of protons and ferric iron, with polysulfide as the major intermediate and elemental sulfur as the final product. The elemental sulfur can then be further oxidized to sulphate by microbial action of sulfur-oxidisers.

The dissolution of mineral via the *polysulfide mechanism* is acid consuming, resulting in an increase in pH (Schippers and Sand 1999). Optimal microbial leaching occurs between pH 1.4 and pH 1.6 (Rawlings 2004). Over prolonged periods of bioleaching the increase in pH will hinder microbial leaching and also lead to formation of precipitates, including ferric precipitation. With respect to chalcopyrite dissolution in particular, the formation of basic sulphates such as jarosite on the mineral surface has been implicated in hindering complete chalcopyrite dissolution (Klauber 2003, cited by Watling 2006; Petersen *et al.* 2001). Jarosite ($KFe^{3+}_3(OH)_6(SO_4)_2$) is a basic hydrous sulphate of potassium and iron formed by the oxidation of iron sulfides. The phenomenon of jarosite layers forming on the surfaces of sulfide minerals and their hindrance of leaching has been coined the '*passivation of chalcopyrite*'. This may explain the difficulties associated with chalcopyrite leaching. High redox potential (0.65 - 0.70 SHE) due to the efficiency of ferrous to ferric iron oxidation by microorganisms was also found to be less favourable for complete chalcopyrite dissolution (Watling 2006) as the high redox potential leads to the leaching of pyrite being favoured over chalcopyrite (Hiroyoshi et al. 2008). High redox potential also results in the precipitation of ferric ion to jarosite when in the vicinity of monovalent alkali cations and sulphate ions (Watling 2006). Formation of jarosite precipitates was proposed to be circumvented by operating leach conditions at pH 1.0 (Kinnunen *et al.* 2003). Fowler and Crundwell (1999) observed that oxidation of the elemental sulfur product layer by *A. ferrooxidans* increases the rate of sphalerite dissolution, thus the formation of a sulfur layer on mineral surface does not limit the sphalerite dissolution rate when sulfur oxidizing microbes are present. Dissolution kinetics is also affected by galvanic effects between various metal sulfides. The rate of sphalerite, galena and chalcopyrite dissolution was found to be slower in isolation. When leached in combination with pyrite, the rate of dissolution was 1.5, 31 and 18 times more rapid for the respective minerals (Abraitis *et al.* 2004).

In conclusion, metal sulfides undergo oxidative mineral dissolution via different mechanisms depending on whether they are acid soluble or acid insoluble. The mechanism used results in the formation of varying end products. For chalcopyrite, these may result in the formation of both an elemental sulfur layer and jarosite precipitates on the mineral surface, both observed to hinder bioleaching (Klauber *et al.* 2003, Petersen *et al.* 2001). This is known as the *passivation of chalcopyrite* and may explain incomplete leaching of chalcopyrite. High redox potentials also result in the formation of iron sulphate precipitates which impede chalcopyrite dissolution. Further pyrite leaching is given preference at high redox potential. Galvanic interactions between metal sulfides affect leach rates. Acid soluble minerals may result in the increase in pH over prolonged periods of bioleaching, depending on the acid neutralising or generating nature of the associated gangue and mineral sulfides. The microbial consortia are important in the regeneration of acid and ferric ions, and the removal of the sulfur layer and precipitates on the mineral surface, required for the dissolution to continue.

2.4.2 Effect of gangue mineralogy on bioleaching

In heap bioleaching, the ore is typically of a very low-grade such that the content of the mineral of interest is often less than 1 % in comparison to gangue (unwanted mineral). Increasingly, gangue mineralogy and leach residues are being used to predict heap leach efficiency (Helle *et al.* 2005) and economics as acid consumption by acid soluble gangue is a major cost factor (Watling 2006) in heap leaching. The formation of precipitates of the dissolved ions from gangue minerals has also been observed to be detrimental to overall bioleach efficiency (Watling 2006). Gangue mineralogy is specific to the mining region. Predominating gangue minerals are usually quartz, the silicate orthoclase, feldspars such as plagioclase and the mica biotite. The nature and rate of dissolution of constituent gangue minerals is largely dependent on the nature of the primary rock forming minerals (Wilson 2004). However, dislocation and defect structures, mineral structure and chemistry, as well as the chemistry of the external solution contribute to the overall rate of dissolution observed (Wilson 2004). Minerals that crystallize at lower temperatures are more stable. Quartz, muscovite, K-feldspar (orthoclase) are therefore particularly resistant to acid dissolution (Wilson 2004. The degree of exsolution of feldspars may affect dissolution rates (Oxburgh *et al.* 1994).

Current techniques for the quantitative analysis of mineral composition and leach residues include: X-ray Fluorescence (XRF), X-ray Diffraction (XRD) and QEMSCAN. Ore microscopy is an essential tool for the characterisation of minerals present; however, this technique provides only

a qualitative assessment. These techniques, in combination, have been successfully used in combination for the characterisation of ore and leach residues and are discussed in Chapter 3.

2.5 MICROBIAL ATTACHMENT TO SOLID SURFACES

A model to describe microbial attachment to solid surfaces was first proposed by Zobell in 1943. In this model, attachment was comprised of two stages: an initial stage of reversible adhesion and a second irreversible attachment stage. Second order irreversible rate kinetics with respect to bacterial concentration and substrate surface area in the system were used to explain the phenomenon. van Loosdrecht *et al.* (1990) reviewed the influences of interfaces on microbial activity and refined this model. They proposed that attachment consists of a four-stage sequence of events. Transport of the cell to the solid surface is followed by primary or initial attachment (described in Section 2.4.1), followed by a firm attachment stage (described in Section 2.4.2), with the final stages being colonisation and biofilm formation (described in Section 2.4.3). The model proposed by Zobell (1943) is used in combination with the attachment mechanism proposed by van Loosdrecht *et al.* (1990) to develop the most suitable representation of the adhesion process.

In Figure 1, the four stage attachment process is depicted which culminates in the formation of biofilms containing an interfacial environment primed for life under, for example, the extreme mineral bioleach conditions found in heaps.

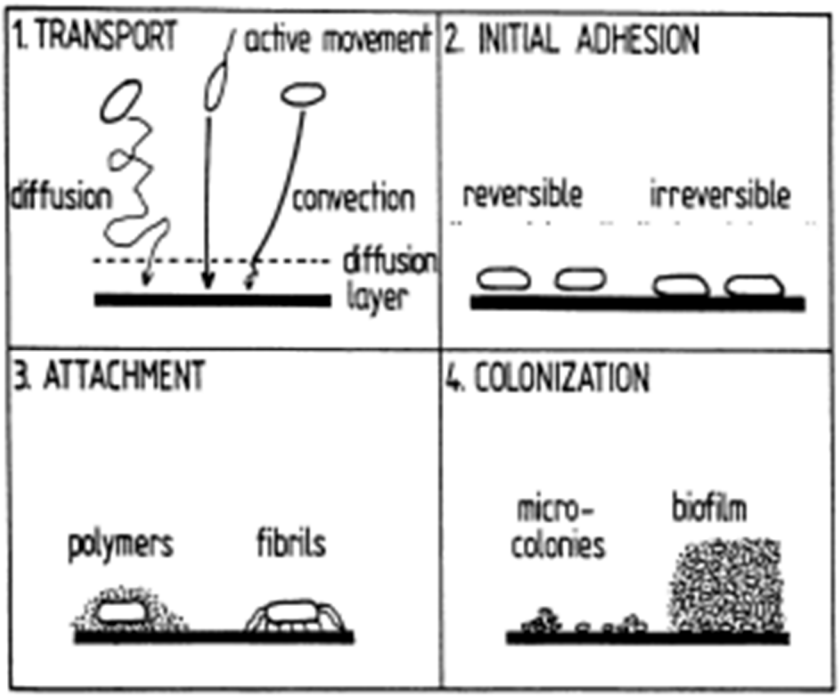

Figure 2.2: Four stages involved in attachment of microorganisms to solid surfaces, taken from van Loosdrecht *et al.* (1990)

2.5.1 Microbial transport and initial adhesion to solid surfaces

The first step of bacterial adhesion requires the transport of the microbial cell to a surface in order for contact to be made (van Loosdrecht *et al.* 1990). Three modes of transport bring the cell in close proximity to the surface, namely: **diffusive transport, convective transport** and **active movement.**

Diffusive transport involves 'non-negligible Brownian motion'. This type of transport accounts for random contacts of small bacteria with surfaces. It facilitates crossing of the diffusive layer by the microorganism, which cannot occur through convective transport alone. This process is slower than convective and active transport. **Convective transport** is due to liquid flow and may be several orders of magnitude faster than diffusive transport. However, there may be circumstances where the final path to the surface is still diffusion controlled owing to stagnant films or pores. **Active transport** occurs with motile organisms. According to Watnick and Kolter (2000), the initial microorganism-surface interaction is accelerated by force generating organelles such as flagella, responsible for active transport. *L. ferrooxidans* and *A. ferrooxidans* are both motile microorganisms possessing of flagella (Jerez 2001). *A. caldus* is also flagellated and motile (Hallberg and Lindstromt, 1994). *M. hakonensis* is non-motile (Takayanagi *et al.*, 1996).

Once the organism is in the vicinity of the surface, the next stage of adhesion can take place in which the cells become associated with the surface either via a chemotactic response or by chance. This association is known as initial or primary adhesion; it is non-specific and may be reversible. Reversible adhesion is defined as ''deposition to a surface in which bacteria can still be removed from the surface by mild shear or by the bacterium's own mobility'' (van Loosdrecht *et al.* 1990). Conversely, adhering bacteria or archaea which exhibit no Brownian motion and can only be removed by intense shear are defined as ''irreversibly attached''.

According to Zobell's model, the initial interaction between micro-organisms and surface sites requires the formation of a metastable complex between the two that is brought about by the balance of repulsive and attractive forces. This is represented in Equation 5, where B represents bacteria (or other micro-organisms), S represents surface sites involved, [BS]* represents the reversible attachment and formation of the metastable complex and BS represents irreversible attachment (adapted from Rodriguez *et al.* 2003**a**).

Eqn (8)

$$B + S \underset{K2}{\overset{K1}{\longleftrightarrow}} [BS]^* \xrightarrow{K3} BS$$

The repulsive and attractive forces governing initial adhesion of microorganisms to surfaces are primarily due to physicochemical processes explained by non-specific hydrophobic and electrostatic interactions between the cell surface and minerals (van Loosdrecht *et al.* 1990, Devasia *et al.* 1993, Arrendondo *et al.* 1994, Blake *et al.* 1994 and Harneit *et al.* 2005).

Chemotaxis refers to the response of microorganisms to a particular stimulus. The stimulus may be an 'attractant' such as a nutrient concentration gradient; in this case, motile bacteria swim towards higher concentrations of the stimulant. Conversely, the stimulus may be a repellent with motile bacteria moving away from its higher concentrations. The process makes use of signal transduction proteins containing two functional domains: a sensory domain which interacts with the stimulant at the cell surface and a signalling domain which modulates effector activities within the cell causing movement toward or away from the stimulus (Surette *et al.* 1994, Delgado *et al.* 1995; in Rojas-Chapana *et al.* 1998). This phenomenon has been well documented in *E.coli* and *Salmonella spp*. (Rojas-Chapana *et al.* 1998). Rojas-Chapana *et al.* (1998) proposed the attachment of *A. thiooxidans* and *A. ferrooxidans* to sulfur/sulfide substrates as well as pyrite was due to chemotactic behaviour as this response was suppressed by addition of the detergent Tween 80.

Jerez (2001) isolated and characterised a gene from *L. ferrooxidans*, encoding a putative chemotactic receptor (LcrI). The LcrI protein structure was similar to that of methyl-accepting chemotaxis proteins, which suggests that *L. ferrooxidans* possesses a chemotactic signal transduction mechanism similar to that of other microorganisms. The association of bioleach microbes with the surface for the onset of initial adhesion may therefore be a result of a chemotactic response.

Biofilm formation has been shown to be coordinated by diffusible signal transduction mechanisms, such as quorum sensing in *Pseudomonas* and *Vibrio fisherii.* Farah *et al.* (2005) have isolated genes which may encode for a functional type AI-1 quorum sensing system in *A. ferrooxidans*. Rivas *et al.* (2007) report the presence of an AI-1 quorum sensing system in *A. ferrooxidans* and isolated acyl-homoserine lactones (AHLs) produced by this microorganisms containing acyl chain lengths between C_8 and $C_{16,}$ with alcohols or ketones at the C_3 position (Ruiz *et al.* 2007**a**). Furthermore, the presence of AHLs was demonstrated to have an effect on the adhesion behaviour of *A. ferrooxidans*. This group also found a second AHL production system

which consisted of a cluster of 4 genes. Three genes encoded a synthase, phosphatase and acyltransferase respectively, with the fourth encoding for the production of AHLs with a C_{14} length, which was up-regulated in the presence of iron (Ruiz *et al.* 2007**b**). More recently, Gonzalez and co-workers (2013) demonstrated that long chained AHLs enhanced the adhesion of *A. ferrooxidans,* present in a mixed consortium, to pyrite mineral surfaces. This was also correlated to an increase in the production of EPS. The evidence of quorum sensing mechanisms in archaea is still to be fully established (Calderón *et al.*, 2013). There have been some implication of AHLs as quorum sensing signals in methanogenic archaea (Zhang et al., 2012), with the sulfur reducing archaeon *Sulfolobus solfataricus* reported to produce a lactonase which degrades bacterial AHLs (Ng *et al.* 2011 in Montgomery *et al.* 2013)

2.5.2 Firm attachment and the role of EPS in the attachment process

Firm attachment is the next stage of the attachment process and involves special cell surface proteins and or the excretion of polymers, which form strong links between the cell and surface (van Loosdrecht *et al.* 1990). The merits of both are discussed in this section.

Devasia *et al.* (1993) suggested the involvement of a proteinaceous cell surface appendage in adhesion of *A. ferrooxidans* to solid mineral surfaces of sulfur grown cells. More recent reports of the involvement of cell-surface proteins in the attachment of bioleach microbes to mineral surfaces were made by Arrendondo *et al.* (1994). It was suggested that partial removal of lipopolysaccharides exposed greater levels of cell surface proteins, which may increase cell hydrophobicity resulting in increased levels of adhesion. This group also reported that phosphate starved cells displayed a greater cell surface protein content and exhibited increased levels of adhesion to sulfur prills, presumably due to increased hydrophobicity (Amaro *et al.* 1993, in Arrendondo *et al.* 1994). The involvement of cell-surface proteins in attachment in these instances is restricted to hydrophobic interactions involved in initial attachment. However, the involvement of cell surface proteins in attachment cannot be completely ruled out as cell surface proteins have been shown to play an integral role in the biofilm formation of two extensively studied microorganisms, namely *E. coli spp*. and *Pseudomonas spp.* (Pratt and Kolter 1998, O'Toole *et al.* 1998 respectively). Blake *et al.* (2001) propose a model involving the cell surface protein, aporusticyanin, in the adhesion of *A. ferrooxidans*. According to this model aporusticyanin acts a mineral-specific receptor for the initial adhesion of *A. ferrooxidans* to pyrite (Blake *et al.* 2001).

As early as 1943, the presence of an excreted mucilaginous layer has been observed to enhance microbial attachment to surfaces. This was observed by Zobell (1943). This mucilaginous layer is in fact a result of the excretion of lipopolysaccharides or extra cellular polymeric substances

(EPS) (Purevdorj-Gage and Stoodley 2004, p164) and mediates attachment and biofilm formation in bioleach microbes (Savage and Fletcher 1985, in Gehrke *et al.* 1998). EPS excretion is thus important in both the firm attachment and colonization stages of attachment.

Vandevivere and Kirchman (1993) report that the presence of solid surfaces may stimulate bacteria to produce exopolymers, as the addition of sand to shake flask cultures induced exopolymer synthesis. In addition, exopolymer production by attached cells was greater than planktonic cells and when surface-grown cells were resuspended in fresh medium, exopolymer production decreased to that indicative of planktonic or unattached cells. Due to the enhanced production of exopolymers in the presence of a solid substrate it could be inferred that the production of exopolymers indeed plays a significant role in attachment. The exact nature of this putative effect of solid surfaces on exopolymer synthesis is not known.

Gehrke *et al.* (2001) report that growth of *A. ferrooxidans* on different substrata influenced the yield of EPS produced. Cells grown on ferrous sulphate produced less EPS than cells grown on a solid substrate (pyrite). This supports the claims of Vandevivere and Kirchman (1993). However, if these claims are indeed significant then the presence of solid substrata alone would enhance EPS production. The substrata used by Gehrke *et al.* (2001) provide a source of energy for the microorganism, and thus for the production of EPS. Attachment to the material would be advantageous for survival of the organism.

Arrendondo *et al.* (1994) demonstrated the involvement of excreted lipopolysaccharides in the attachment of *A. ferrooxidans* to sulfur prills, as partial removal of lipopolysaccharides diminished the attachment observed. In another study, cells containing EPS attached to covellite surfaces whereas cells without EPS where unable to attach until EPS was regenerated (Pogliani and Donati 2000).

Escobar *et al.* (1996) investigated the attachment of *A. ferrooxidans* to pyrite and chalcopyrite in shake flasks (cells enumerated using direct cell counts). Cells were treated with EDTA to remove lipopolysaccharides from the cell surface. Loss of lipopolysacharides of the outer membrane in *A. ferrooxidans* negatively influenced attachment. Therefore, it was presumed that the presence of lipopolysaccharides play a role in the adsorption of this microorganism to solid surfaces, in accordance with the findings of Arrendondo *et al.* (1994).

In a bioleach context it is proposed that complexation of ferric ions (Fe^{3+}) with glucuronic acid residues within EPS contributes to electrochemical interactions between microbial cell surfaces and negatively charged (pyrite, pH 2.0) mineral surfaces (Gehrke *et al.* 1998). In addition to mediating firm adhesion, EPS concentrates reactants (ferric ions) for mineral dissolution (Gehrke

et al. 1998) and provides a protective environment for microorganisms within the harsh bioleach environment. EPS was demonstrated to enhance attachment levels to different substrata for *A. ferrooxidans* as removal of this layer, even partially, diminished the extent of attachment observed (Arrendondo *et al.* 1994, Pogliani and Donati 2000, Escobar *et al.* 1996, Gehrke *et al.* 1998 and 2001 Harneit *et al.* 2005).

2.5.3 Microbial colonisation of solid surfaces in the context of bioleaching

The final stage of microbial adhesion is colonisation and biofilm formation. Cells within the EPS layer begin to grow and divide and new cells can become associated with the EPS layer in the development of biofilms[4]. While most of the studies reported above focused on initial attachment, limited studies investigating subsequent biofilm formation in a bioleach context have been reported by Sanhueza *et al.* (1999), Gehrke *et al.* (1998, 2001), Kinzler *et al.* (2003), Harneit *et al.* (2005 and 2006), Pradhan *et al.* (2008), Mangold *et al* (2008), Lei *et al.* (2009), Noel *et al* (2010), Florian *et al* (2011) and Gonzalez *et al.* (2012). These studies described the visualisation and qualitative investigation of colonisation and reported the subsequent formation of monolayer biofilms, but were limited to mesophilic microorganisms at ambient temperatures and were all conducted using shake flasks. This biofilm formation is recognised to involve EPS and result in a more permanent attachment, with subsequent colonisation of the surface predicted. Colonisation and biofilm formation may be dependent on the organism type involved and these processes are therefore more specific. The exact nature of this matrix may vary depending on the surrounding environment and the micro-organisms involved (Harneit *et al.* 2005). Ohmura *et al.* (1993), report that low coverage ratios of *A. ferrooxidans* to pyrite may be indicative of cells adsorbing as a single layer. Harneit *et al.* (2005) report the development of micro-colonies, covered in EPS, on the surface of pyrite by *A. ferrooxidans.* The micro-colonies subsequently developed into mono-layered biofilms as observed using atomic force microscopy. The observation of bioleach micro-organisms exhibiting an "affinity" for attachment to visible defects and dislocation sites (cracks and grain boundaries) has been reported by Rojas-Chapana *et al.* (1998), Gehrke *et al.* (1998 and 2001), Harneit *et al.* (2005) and Africa *et al.* (2010). It was postulated that sulphur atoms concentrate at grain boundaries and surface imperfections making these locations more favourable as sites of attachment (Andrews 1988). Rojas-Chapana *et al.* (1998) proposed that nutrient concentration gradients were generated at pyrite fragmentation sites, which attracted the settlement of microorganisms at these specific sites over others.

[4] A biofilm may be described as a complex sessile community of microorganisms, which is highly differentiated and enveloped in a polysaccharide matrix (Watnick and Kolter 2000).

Again these reports have been limited to pure cultures, mostly mesophiles; on pure pyrite mineral sections (Gehrke *et al.* 1998 and 2001, Kinzler *et al.* 2003, Harneit *et al.* 2005 and Lei *et al.* 2009), synthetic pyrite (Sanhueza *et al.* 1999) or sulfur (Rojas-Chapana *et al.* 1998) in shake flasks (agitated batch systems) using ambient temperature regimes. Only a limited number of papers (Sampson *et al.* 2000, Rodriguez *et al.* 2003, Mikkelsen *et al.* 2007, Gautier *et al.* 2008, Bromfield *et al.* 2011) report the use of thermophiles in the investigation of microbial adhesion to sulfide minerals, with Becker and co-workers. (2011) reporting the use of a moderate thermophile. No investigations involving colonisation and biofilm formation on low-grade ores has been reported except Africa *et al.* (2010) where adhesion of pure cultures of *A. ferrooxidans* and mixed cultures of *A. ferrooxidans* and *L. ferriphilum* to massive chalcopyrite as well as low-grade chalcopyrite containing ore were assessed using a biofilm reactor. Colonisation further influences the role of micro-organisms in the heap bioleach environment and its optimisation. No integrated studies assessing the combined effects of mineralogy as well as varying physicochemical conditions on colonisation behaviour of bioleach microorganisms have been conducted.

A comprehensive body of literature regarding factors which influence colonisation and biofilm formation and regulation in the context of bioleach microorganisms is lacking. Transition between adhesion phases as well as the regulation of these interfacial processes in bioleach microorganisms has not yet been explicitly elucidated. This highlights an exciting and highly fundamental area of research that needs to be addressed. Moreover, when considering that the microbial-mineral-EPS interface is the epicentre of activity in terms of oxidation and mineral dissolution, studies to elucidate this environment under heap bioleach conditions become increasingly important.

2.6 TRENDS IN ATTACHMENT AND FACTORS INFLUENCING THESE

2.6.1 Physical properties of mineral surfaces

Surface charge and hydrophobicity, surface tension, and mineral surface roughness have been suggested as factors which control the initial adhesion of microorganisms to mineral surfaces (Yee *et al.* 2000). The surfaces of sulfide minerals are usually negatively charged (Ohmura *et al.* 1993). For sulfide minerals under investigation, charge is determined via the oxidation state of the mineral. In this study, quartz is used as a control mineral. The potential determining ions of quartz (SiO_2) are the - OH groups present. The surface charge of oxides (quartz) is thus affected by the pH of the suspending solution. As the pH decreases, the surface becomes more positively charged. Escobar *et al.* (1996) report that quartz exhibits an isoelectric point at pH 2.0 above

which it is negatively charged. Yee *et al.* (2002) modelled surface species of quartz and predict the isoelectric point of quartz occurs at approximately pH 3.0. Measurement of contact angles can be used as an indication of the relative hydrophobicity of the mineral surface.

Certain bioleach microbes have displayed 'affinities' for attachment to visible defects and particular mineral properties. Gehrke *et al.* (1998) observed, using atomic force microscopy (AFM), that *A. ferrooxidans* attached to dislocation sites (cracks and grain boundaries) on pyrite. Some 76 % of visible cells adhered to these surface imperfections. Similar reports were made by these authors in 2001, where again using AFM, *A. ferrooxidans* was observed to be attached, specifically to dislocation sites on pyrite surfaces. Andrews (1988), cited in Gehrke *et al.* (1998 and 2001), suggests that sulfur atoms concentrate at grain boundaries and surface imperfections making these locations more favourable as energy sources and hence sites of attachment. Rojas-Chapana *et al.* (1998) also showed increased attachment at pyrite grain boundaries. Nutrient concentration gradients were proposed to be generated at pyrite fragmentation sites, which attracted the settlement of microbes at these specific sites over others. Harneit *et al.* (2005) also observed that primary attachment was restricted to surface sites with visible defects. Similar findings were reported by Africa *et al.* (2010).

Sanhueza *et al.* (1999) correlated the degree of crystallization of synthetic pyrite films to bacterial attachment behaviour. Amorphous pyrite exhibited elongated densely packed arrangements of adhered *A. ferrooxidans.* However, on highly crystallized pyrite, short, pearl-like chains were observed with a lower overall surface area coverage. Gonzalez *et al.* (1999) showed that attachment levels decrease with mineral particle size, due to the decrease in available surface area. Nemati et al. (2000) support reduced attachment below a minimum particle size in tank bioleaching studies.

2.6.2 Microbial cell surfaces

Microbial surfaces are usually negatively charged under physiological conditions (Poortinga *et al.* 2002, Blake *et al.* 1994, van Loosdrecht *et al.* 1990, Ohmura *et al.* 1993). However, this varies from species to species. Cell surface charge arises due to dissociation or protonation of the carboxyl (-COOH), phosphate, hydroxyl (-OH) and amino groups ($-NH_2$) which constitute the cell wall. This dissociation and protonation is dependent on pH (Sampson *et al.* 2000, Poortinga *et al.* 2002, Sharma *et al.* 2003). Various components of the microbial cell wall contribute to the overall surface charge and hydrophobicity. The charge and hydrophobicity of these components may be affected by growth conditions and solution chemistry. The mesophilic microorganisms used in this research are Gram negative. The components of Gram negative bacteria include a

peptidoglycan layer (1 - 2 nm thick), flanked by phospholipids bilayer membranes, namely the cytoplasmic and outer membranes, separated by a periplasmic space as depicted in Figure 2.4(**c**).

The outer membrane contains membrane-associated proteins which have been reported to contribute to surface charge (Poortinga *et al.* 2002) and hydrophobicity (van Loosdrecht *et al.* 1987, Arrendondo *et al.* 1994). The outer membrane of Gram negative bacteria may also contain lipopolysaccharide chains which confer a negative charge and are hydrophilic in nature. Some Gram negative cell envelopes also contain a capsule or S-layer linked to the lipopolysaccharide layer. This S-layer may vary in thickness, is usually anionic and may render the cell surface hydrophobic by partially masking the hydrophilic lipopolysaccharide surface (Sleytr *et al.* 2001). Many bacterial species produce EPS which contribute to cell surface charge and hydrophobicity. The archaeal species used in this study, *M. hakonensis*, is a crenarchaeote containing a glycoprotein S-layer cell wall (Kandler and Konig 1998). The S-layer contains glycoprotein subunits with P3 symmetry and a centre to centre distance of 21 nm (Fuchs *et al.* 1995, Albers and Meyer 2011). Figure 2.4 (**a**) and (**b**) depicts a schematic representation of the *M. hakonensis* S-layers.

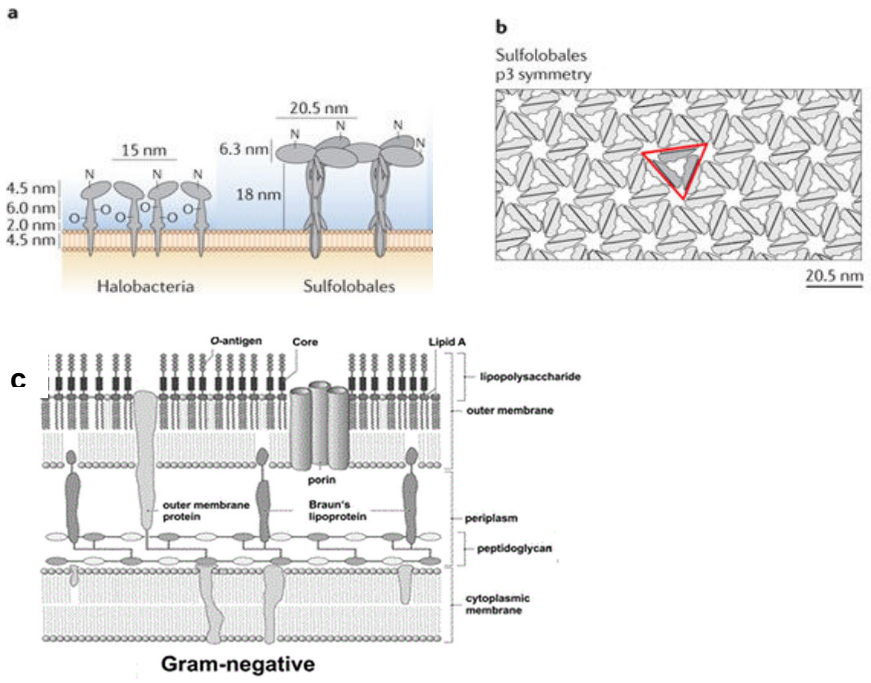

Figure 2.3: (**a**) A side view of the assembly of the surface layers of members of the order *Sulfolobales*, (**b**) a schematic depiction of the repeating glycoprotein units have P3 symmetry, (**c**) schematic representation of a gram negative microbial cell wall. (Images **a** and **b** taken from Albers and Meyer 2011, and **c** from Fuchs *et al.* 2007).

2.6.3 Effect of varying growth conditions on cell surface properties and attachment

A liquid medium that is rich in nutrients primes many bacteria for attachment to any local surface (Prigent-Combaret *et al.* 1999, in Watnick and Kolter 2000, O'Toole *et al.* 1998, and Pratt and Kolter 1998). In addition to this, surface chemistry determining adhesion is influenced by growth conditions (van Loosdrecht *et al.* 1987**b**). Gehrke *et al.* (1998 and 2001) correlated the influence of growth history of *A. ferrooxidans* to changes in cell surface properties, EPS yield and composition, and subsequent attachment ability. Growth on solid pyrite enhanced the yield of EPS relative to ferrous grown cells. This in turn altered the cell surface properties as the complexation of ferric ions with gluco-uronic residues in the EPS layer rendered the cell surface positively charged allowing microorganisms to adhere to both hydrophobic and negatively charged surfaces. Similarly, Harneit *et al.* (2005) observed this dependence of EPS composition on growth medium and subsequent attachment ability imposed on cells.

Amaro *et al.* (1993 in Arrendondo *et al.* 1994), also observed that attachment could be affected by growth conditions. This group demonstrated that phosphate starved *A. ferrooxidans* cells have greater cell surface protein content and display increased degrees of hydrophobicity, which affected attachment behaviour. Arrendondo *et al.* (1994) also reported that EPS production enhances attachment levels.

Porro *et al.* (1997) investigated the relationship between growth conditions, cell surface hydrophobicity and adhesion behaviour. *A. ferrooxidans* cells were grown on sulfur or on ferrous iron and then subsequently grown on wurtzite (Zn, Fe,)S). Sulfur grown cells were most hydrophobic (using bi-phasic partitioning). However, greater attachment efficiencies were achieved with mineral grown cells over ferrous grown cells, despite these cells having lower hydrophobicities.

Sampson *et al.* (2000) observed a correlation between growth history, cell surface hydrophobicity and subsequent adhesion behaviour using the theoretical energy of adhesion of cells grown on the various substrates (sulfur, chalcopyrite and ferrous iron). Sulfur grown cells were predicted to have the greatest free energy of adhesion and thus should be more likely to adhere to hydrophobic surfaces.

Devasia *et al.* (1993) observed that sulfur, pyrite and chalcopyrite grown *A. ferrooxidans* exhibit greater hydrophobicity than ferrous iron grown cells. In addition, cells cultured on solid media exhibited an isoelectric point at a higher pH than ferrous grown cells. The growth substrate therefore also affected surface charge of the microorganism. Sharma *et al.* (2003) characterised

A. ferrooxidans cell surface groups using diffuse and reflectance FT-IR and FT-Raman spectroscopies. Cells were cultured with ferrous ion, sulfur or pyrite mineral as sole energy source. The cell surface charge of iron-grown cells (isoelectric point at pH 2.0) was different to that of cells grown on solid substrata (pyrite) (isoelectric point pH 3.0 – 3.5). Therefore, surface charge was dependent on growth medium of the microorganism. Similarly, Blake *et al.* (1994) observed a dependence of surface charge on the growth history of the *A. ferrooxidans* cultured on ferrous sulphate, pyrite and sulfur.

Several other authors have noted the influence of the activity of the microorganism on the attachment efficiencies observed (Zobell 1943, van Loosdrecht *et al.*1990 and Rijnaarts *et al.* 1993). Zobell (1943) observed that more cells attach during early logarithmic growth than during late log or lag phase i.e. when the activity of the cells was not optimum. van Loosdrecht *et al.* (1987) related the growth rate and activity level of microorganisms to attachment levels (higher dilution rates related to higher attachment levels). Similarly, Elwood *et al.* (1982, cited in van Loosdrecht *et al.*1990) and Rijnaarts *et al.* (1993) report that the adhesion of microbes may be increased during exponential growth. Elwood postulated this to be due to increased cell wall hydrophobicity during this phase.

Bromfield *et al.* (2011) demonstrated a correlation between the extent of attachment observed to sulphide minerals for *M. hakonensis* after growth on four different substrates (sulfur, ferrous sulfate, chalcopyrite mineral concentrate and pyrite mineral concentrate) in a batch agitated, shake flask system. The highest extents of attachment were observed for attachment to chalcopyrite after growth on sulfur. Authors suggest growth on sulfur resulted in an alteration of surface associated EPS, making cells more hydrophobic which improved interactions with the hydrophobic sulfide mineral surface relative to other surfaces. However, attempts to assay the relative hydrophobicity of sulfur cultured cells were inconclusive.

2.6.5 Selective attachment of microorganisms to sulfide minerals

Several authors (Ohmura *et al.* 1993, Nagaoka *et al.* 1999, Gonzalez *et al.* 1999, Sampson *et al.* 2000, Rodriguez *et al.* 2003 and Harneit *et al.* 2005, Bromfield *et al.* 2011) have demonstrated the prevalence of selective attachment to sulfide minerals over other minerals. Solari *et al.* (1992, cited by Watling 2006), observed increased levels of adhesion of *A. ferrooxidans* to sulfide minerals per unit area over quartz. This was attributed to hydrophobic interactions between cells and sulfide mineral surfaces, as both cell and sulfide mineral whereas quartz is more hydrophilic. Ohmura *et al.* (1993) demonstrated selective adhesion of *A. ferrooxidans* to sulfide minerals over other minerals in shake flask experiments using *E. coli* as a control organism. *A. ferrooxidans* was

shown to attach preferentially to pyrite, followed by chalcopyrite, with little attachment to quartz and galena. The attachment was shown to be selective by using hydrophobicity as well as cell and mineral surface charge measurements. For selective attachment to occur, these forces must be overcome as both the cell and mineral surface have negative charges and display varying degrees of hydrophobicity. Attachment levels were shown to increase with an increase in cell concentration. This increase in the level of attachment continued until a certain threshold concentration was reached, beyond which no further increase in attachment could be seen. The maximum level of attachment could be due to spatial distribution of microbes due to repulsive forces of cell surfaces.

Similarly, Nagaoka *et al.* (1999) and Gonzalez *et al.* (1999) showed selective adhesion of *A. ferrooxidans* to pyrite over other minerals using a range of cell concentrations. Attachment increased with cell concentration, and in addition to this, an increase in adhesion with mineral (pyrite) concentration was also shown (Nagaoka *et al.* 1999). Gonzalez *et al.* (1999) showed that attachment occurs rapidly. The level of attachment achieved was influenced by the liquid environment. Maximum concentration of attached cells increased with the addition of ferric ions.

Sampson *et al.* (2000) demonstrated that non-specific hydrophobic interactions do not control attachment of the mesophile *A. ferrooxidans* which attaches selectively to arsenopyrite, followed by pyrite and chalcopyrite. Similarly, selective attachment of various thermophilic bioleach micro-organisms exhibited increased levels of attachment to pyrite, followed by arsenopyrite and chalcopyrite (Sampson *et al.* 2000). These results are in agreement with Rodriguez *et al.* (2003**a**) who demonstrated selective attachment of mesophiles and thermophiles to sulfide minerals using mixed cultures. The mesophiles, *Acidithiobacillus spp*. and *Leptospirillum spp*., exhibited higher levels of attachment to pyrite followed by chalcopyrite and sphalerite. The affinity of the thermophile, *Sulfolobus spp.*, differed with preferential attachment to chalcopyrite and sphalerite followed by pyrite. Higher overall attachment efficiencies were achieved by thermophiles. Presence of ferrous iron resulted in detachment, corroborating that the liquid environment influences the degree of attachment achieved (Gonzalez *et al.*1999). Supplying excess ferrous iron in solution decreases adhesion of *A. ferrooxidans* to mineral surfaces as the chemotactic benefit is removed. The results for selective attachment of thermophiles contradict claims made by Sampson *et al.* (2000) who report preferential attachment of thermophiles to pyrite over chalcopyrite. Harneit *et al.* (2005) demonstrated rapid selective attachment of *A. ferrooxidans* to pyrite, with slower rates of attachment to chalcopyrite, sphalerite and galena. This is in agreement with Gonzalez *et al.* (1999) that attachment occurs rapidly; and with Rodriguez *et al.* (2003) that *A. ferrooxidans* attaches selectively to sulfide minerals. The current body of literature provides evidence which suggests that bioleach microorganisms attach preferentially to sulfide

minerals. The attachment to the sulfide minerals is rapid and increases with cell concentration until a threshold concentration is attained; above this no further increase in attachment levels can be seen.

Bromfield *et al.* (2011) investigated the extent of attachment of *M. hakonensis* cultured on different growth substrates (sulphur, ferrous sulphate, pyrite and chalcopyrite) to a chalcopyrite mineral concentrate, pyrite mineral concentrate and a low-grade chalcopyrite containing mineral ore. The study compared two approaches; one mimicked the hydrodynamic fluid flow as it would occur in a heap bioleach system through the use of continuous flow through column reactors. The other system utilised shake flasks in a batch agitated system, typical of all earlier research reported. For the batch agitated system, the greatest extents of attachment were observed for the chalcopyrite mineral system, followed by pyrite and the low-grade ore system. This trend of preferential attachment to chalcopyrite is in agreement with reports by Rodriguez *et al.* (2003**b)**. The overall extents of attachment were marginally lower. For the column reactor approach, greater levels of attachment were observed to the chalcopyrite mineral concentrate over the low-grade ore. This finding was consistent irrespective of the culture growth substrate. Overall maximum attachment levels obtained using this approach were substantially lower than batch agitated results, and previous reports for thermophilic attachment made by Rodriguez *et al.* (2003**b)** which also made use of a batch agitated approach. Similarly Africa et al. (2013) report a greater attachment levels to sulphide minerals over low-grade ores in the continuous flow through column reactor for mesophilic microorganisms, with the extents of the attachment being less than that observed in the shake flask systems reported in literature. Africa and Bromfield et al. argue that the mineral loading in the column system, seeing continuous fluid flow and having finite length, allowed only half the surface to be exposed and available for attachment (the remainder being attached to the support beads) when compared to the batch agitated system. Africa and Bromfield et al. postulated that the level of attachment would increase with an increase in reactor length or residence time in the reactor (decrease in flow rate). However, the residence time of the columns exceeded the time necessary for maximum attachment in the shake flask studies. Batch agitated systems are believed to overestimate the extents of attachment achieved in heap leach systems in which continuous fluid flow occurs, hence the data from the column experiment may be better suited for validating attachment models in heap systems.

2.7 EPS AND BIOLEACH INTERFACIAL ENVIRONMENTS

2.7.1 The role of EPS interfacial environments and the advantages of a surface associated lifestyle

The most predominant form of microbial life exists in aggregations in the form of biofilms or flocs[5] (Wingender *et al.* 1999, p2). Biofilms can be defined as communities of sessile microorganisms which aggregate at the gas-liquid or solid-liquid interface and are enveloped in a matrix composed of an extracellular polymeric substance (EPS). These communities have been found to form highly complex, hydrated and often charged, three dimensional structures (Neu and Lawrence 1997), contain mixed populations of microorganisms and are ubiquitously distributed in natural soil and aquatic environments (Wingender *et al.* 1999, p2). The EPS are, in essence, the "building-blocks" of the microbial biofilm, conveying and maintaining structural integrity and stability to the biofilm. EPS also serve as boundary structures, mediating contact with biotic and abiotic environments (Wingender *et al.* 1999, p7).

EPS play a major role in both adhesion (attachment of cells to a substratum) and cohesion (attachment of cells with other cells or particulate matter) of microorganisms. The EPS is also considered a major determinant of the physicochemical and biological properties of the microbial biofilm. EPS effectively terraform the microenvironment of the biofilm thereby creating ideal conditions the proliferation of microorganisms in harsh environments (Watnick and Kolter 2000). In the case of medically relevant bacteria such as *Pseudomonas*, bacteria are particularly resistant to conventional antimicrobials as the EPS matrix physically restricts diffusion of these agents effectively shielding bacteria within (Bhinu 2005).

EPS provides protection against hydrodynamic shear. Purevdorj-Gage and Stoodley (2004) demonstrated that biofilms grown in high shear conditions had a stronger EPS matrix and were subsequently more strongly adhered cells than those grown under low shear. In a bioleach heap environment where channelling and hence hydrodynamic shear may vary, the production of EPS may be beneficial in protection against these forces. EPS has also been shown to provide significant protection against reactive oxygen species and heavy metals (Starkey *et al.* 2004). This would be beneficial in a bioleach environment where reactive oxygen species have been shown to form in association with pyrite (Jones et al. 2011).

[5] Flocs may be described as "planktonic biofilms" (Wingender et al p1 Ch2)

In addition to the advantage of creating a favorable niche and a means of protection within the harsh environment of the bioleach heap, attachment and biofilm formation by bioleach microorganisms is expected to convey an added advantage. In some instances, EPS is also believed to serve as a nutrient reserve (Wolfaardt *et al.* 1999, p178). This is thought to occur via two means. In the first, EPS is directly produced and utilized as a nutrient reserve. In the second, EPS serves as a nutrient reserve indirectly through sorption and/or chelation of compounds for metabolism. Christensen and Characklis (1990) note that "*most EPS have cation exchange properties which may enable bacteria to use EPS as nutrient trap under oligotrophic conditions*". In the context of bioleaching, the second mechanism is used to explain the role of microbial EPS in the mineral dissolution process via the indirect contact mechanism. The complexation of ferric ions through uronic acid and other residues within the EPS (Gehrke *et al.* 1998), concentrates reactants required for mineral dissolution. Further the energy generation through oxidation of ferrous iron is in close proximity for iron oxidizing microbes within the EPS layer. In a bioleach environment where ferrous iron availability may be low, it is advantageous to be situated in close proximity to the source of the ferrous ions (Watling 2006).

From an ecological standpoint, the formation of stable aggregates of cells with different metabolic abilities allows for consortial or commensal microbial behaviour. One consequence of these co-operative interactions is the sequential degradation or uptake of substances not readily degraded or metabolised by a singles species (Wingender *et al.* 1999, p15; Wolfaardt *et al.* 1999, p173). The interactions of microorganisms in consortium are responsible for optimization of nutrient utilization and waste cycling for the proliferation of the entire biofilm community. Such relationships have been suggested in a bioleach context, for example, the presence of sulfur oxidizers for the removal of the passivation layer on chalcopyrite surfaces which allows access to the mineral surface for the survival of iron oxidizers, and the presence of heterotrophs which also assists the growth of iron oxidising microorganisms (Rawlings 2005). Another advantage is that the formation of biofilms allows an increased probability for the acquisition of new environmental survival factors via horizontal gene transfer. This beneficial aspect of biofilm formation has not been fully explored in bioleach microorganisms (Watnick and Kolter 2000). In summary, microorganisms derive benefits from the production of EPS through its modification of their macro-and micro- environments (Wolfaardt *et al.* 1999, p194). Some of the proposed functional benefits of EPS production have been reviewed and summarised by Wingender *et al.* (1999) and are presented in Table 2.2.

Table 2.2: A summary of the proposed functions of microbial EPS (adapted from Wingender *et al.* 1999)

Function	Ecological relevance/advantage
Adhesion to surfaces	Mediates initial adhesion as well as colonization of surfaces, accumulation of bacteria on nutrient rich surfaces in oligotrophic environments
Cohesion (aggregation of bacterial cells, formation of flocs and biofilm)	Bridging between cells, inorganic particles and mineral surface active sites, immobilisation of mixed bacterial populations, basis for development of high cell densities, generation of a medium for communication processes, cause biofouling and biocorrosion events, provide a reactive space for mineral dissolution reactions, aid sediment stability, terraforming micro and macro-environment
Cell-cell recognition and associations	Symbiotic relationships with plants, animals or other microorganisms, initiation of pathogenesis, EPS concentrate cells and or signaling molecules enabling these associations
Structural elements of biofilm	Mediation of mechanical stability of biofilms, often in conjunction with multivalent cations, governs EPS architecture
Protective barrier	Resistance to host defenses (compliment – mediated killing, phagocytosis, antibody response, free radical generation), resistance to certain biocides (disinfectants, antibiotics), resistance to extreme pH, elevated temperature, dehydration, freezing, biocides and heavy metals and detergents
Retention of water	Hydrodynamic/hygroscopic stability (cell walls need to remain hydrated to maintain selective permeability; exo-enzymes need hydrated environments in which to be active (Wolfaardt *et al.* 1999), prevention of desiccation
Sorption of exogenous organic compounds	Scavenging and accumulation of nutrients from the environment, sorption of xenobiotics (detoxification) terraforming macro-environment
Sorption of inorganic compounds	Accumulation of toxic metal ions (detoxification), promotion of polysaccharide gel formation, mineral formation, terraforming macro-environment
Enzymatic activities	Digestion of exogenous macromolecules for nutrient acquisition, release of biofilm cells by degradation of structural EPS of the biofilm. Excretion of bacteriolytic enzymes (Wolfaardt *et al.* 1999)
Interaction of polysaccharides with enzymes	Accumulation/retention and stabilization of secreted enzymes

2.7.2 EPS composition and proposed component functions

The chemical composition of the EPS is considered to be important for the activity of the microorganisms encased by it (Nielsen and Jahn 1999). EPS may constitute between 50% - 90% of the total biofilm organic matter (Christensen and Characklis 1990 in Wingender *et al.* 1999) and are essentially biopolymers extruded by the microorganisms, by definition located at or outside the cell surface (Wingender *et al.* 1999). It was first believed that EPS consisted mainly of polysaccharides (Costerton *et al.* 1981). However, the exact nature of this matrix may vary depending on the surrounding environment and the micro-organisms involved (Harneit *et al.*

2005). Proteins, nucleic acids, uronic acids, humic substances, lipids and heavy metals have in recent years been found to be common constituents of microbial EPS in acidic environments (Gehrke *et al.* 1998 and 2001, Aguilera *et al.* 2008; Tapia *et al.* 2009; Michel *et al.* 2009 and Jiao *et al.* 2010). When regarding the constituents of EPS, production of EPS must involve a significant investment of carbon and energy (Wolfaardt *et al.* 1999, p172). Harder and Dijkhuizen (1983) report as much as 70% of the total microbial energy may be invested in the production of EPS. Underwood *et al.* (1995) calculated that for a single *Azotobacter* cell, enough EPS can be produced to coat 500 particles with a 0.4 μm diameter per day! Intuitively, one may surmise that the energetic costs of producing EPS, and especially exo-enzymes, outweigh the reward. However, a study by Wetzel in 1991 suggests that as long as the hydrolysis product is within 500 μm of the cell, the energy of synthesising and exporting enzymes is justified. In this section, a discussion of the role of each of the constituents of the EPS is presented.

As previously mentioned, a primary function of EPS is to convey structural and mechanical stability to the biofilm. This is believed to be mediated by non-covalent interactions (Flemming 1996, Mayer *et al.* 1999) either directly between **polysaccharide chains** or indirectly via multivalent cation bridges (Wingender *et al.* 1999, p11). Higgins and Novak (1997) report the contribution of lectin-like **proteins** in the formation of the three-dimensional network of biofilm matrix through direct cross-linkages with polysaccharides or indirect multivalent cation bridges. Dignac *et al.* (1998) suggest that negatively charged proteins are more influential than sugars in activated sludge systems, in the determination of the floc or biofilm structure through electrostatic bonds with multivalent cations. However, a more universal role of **proteins** in EPS is their role as **exo-enzymes** for the degradation of exogenous macromolecules and particulates (Wingender *et al.* 1999, p11). This results in the formation of low-molecular weight nutrients in the immediate vicinity of the cell which can be metabolised readily. Some exo-enzymes are also believed to be involved in the degradation of the EPS matrix, resulting in the re-mobilisation of entrained cells and migration of the constituents to new microenvironments (Allison *et al.* 2004).

Binding and accumulation of cations such as Ca^{2+} and Mg^{2+} affect the stability, rheology and diffusivity of the film (Wingender *et al.* 1999, p14). **Uronic acids** and proteins sequester these cations. Uronic acids also play a role in microbial attachment to negatively charged sulfide minerals. The sequestration of Fe^{3+} by uronic acids (1 Fe^{3+} : 2 uronic acid molecules; the Fe^{3+} - uronic acid complex has a net positive charge of 1+) renders a net positive charge in the cell surface environment (Gehrke *et al.* 1998), which is favourable for initial adhesion interactions with negatively charged sulfide mineral surfaces. Cells deficient of EPS were unable to sequester Fe^{3+} and mineral oxidation of pyrite did not occur in their presence - it was comparable to the abiotic control (Gehrke *et al.* 1998). In addition, this same study showed that dead cells are unable

to catalyse oxidation of pyrite. A further proposed function of uronic acids present in EPS is to provide protection from shear forces. Dade *et al.* (1990) demonstrated that *Altermonas atlantica* grown in fine sands yielded increased amounts of acidic EPS containing high uronic acid content, which was correlated to sediment resistance to shear stress. The authors infer that acidic EPS aids permanent adhesion to sedimentary surfaces and also leads to grain-to-grain adhesion which increases sediment stability (Wolfaardt *et al.* 1999, p190).

Less is known about the contribution of **nucleic acids** and **lipids** to EPS. However, it is expected that these components influence the rheology and thus aid stability of the film. Extra-cellular lipids of the microorganism *Serratia marcescens* have been proposed to help bacteria in surface environments to overcome the strong surface tension of surrounding water, thus facilitating growth on solid surfaces (Matsuyama and Nakagawa 1996). Extracellular lipids are generally postulated to be involved in the interaction between bacteria and surfaces (Neu 1996 in Sand and Gehrke 1999). Exopolymer lipid components may, in part, be considered surface active compounds (biosurfactants) (Sand and Gehrke 1999). These biosurfactants have potential to increase the solubility of hydrophobic compounds and/or create a conditioning film at the interface. Furthermore, they may serve as an anchor for the hydrophilic compounds of the EPS in the hydrophobic part of the outer membrane (Neu 1996 in Sand and Gehrke 1999). These compounds may also be involved in the initial stages of attachment to hydrophobic substrates (Sand and Gehrke 1999). Lorenz and Wackernagel (1994) report the adsorption or complexation of DNA onto clay minerals, quartz, feldspars, humic substances, minerals in soil environments, as well as suspended material in water. According to Lorenz and Wackernagel, sorption of extra-cellular nucleic material to these surfaces provides some means of protection against DNases. Lebaron *et al.* (1997) report that bacterial adhesion may promote or favour horizontal gene transfer as the EPS interface concentrates cells and allows for a greater probability of cell-cell contact and thus horizontal DNA or plasmid exchange. However, this particular role of EPS is yet to be extensively studied.

In a bioleach context, Gehrke *et al.* (1998 and 2001) analysed the chemical composition of partially purified EPS. EPS excreted from *A. ferrooxidans* was comprised predominantly of neutral sugars and lipids with the composition dependent on growth medium. Similar findings were observed by Kinzler *et al.* (2003) and Harneit *et al.* (2005). Enhanced production of exopolymers in the presence of a solid substrate has been demonstrated by Vandevivere and Kirchman (1993). However, the exact nature of this putative effect of solid surfaces on exopolymer synthesis is not known. Gehrke *et al.* (2001) report that growth of *A. ferrooxidans* on different substrata influenced the yield of EPS produced. Limited studies have been conducted on archaeal biofilms in the context of bioleaching.

Koerdt *et al.* (2010) investigated crenarchaeal biofilms in terms of their diversity, architecture and EPS composition, as well as the effect of pH and temperature on these factors. Three crenarchaeal species were investigated, namely; *Sulfolobus solfataricus* DSM 1617 and DSM 1616, *Sulfolobus acidocaldarius* DSM 639 and *Sulfolobus tokodaii* DSM 16993, in batch microtitre plates after incubation periods of two to three days. Koerdt *et al.* (2010) report the presence of the following glycoconjugates within the EPS: glucose and mannose, galactose and N-acetyl-glucosamine in the biofilms of all three microorganisms. The presence of glucose, mannose, galactose and N-acetyl-glucosamine in the EPS of *Sulfolobus sulfotaricus* was also demonstrated by Zolghadr *et al.* (2010). Koerdt et al. challenged the three microorganisms with low temperatures and near neutral pH, only *Sulfolobus acidocaldarius* exhibited an increase in biofilm thickness.

2.7.3 Factors influencing EPS composition

Type and amount of EPS produced is influenced by environmental conditions (Wolfaardt *et al.* 1999, p189). Wang and McNeil *et al.* (1995) and Lee *et al.* (1997) demonstrate the influence of pH on the type and amount of EPS produced by *Sclerotium glucanicum* and *Bacillus polymyxa* respectively. Martinez-Chenca *et al.* (1996), Lee *et al.* (1997) and Taverneiera *et al.* (1997) demonstrated the influence of growth medium on EPS composition type and quantity for *Volcaniella eurihalina*, *Bacillus polymyxa* and *Rhizobium meliloti* respectively.

Becker *et al.* (2011) investigated the influence of pH on EPS thickness of a moderate thermophile *Sulfobacillus thermosulfidooxidans in situ* and report an increase in EPS thickness with a decrease in pH. Studies have focussed on growth history and solution chemistry, the effect on capsular EPS has also already been discussed in Section 2.6.3. Other factors influencing EPS composition, type and quantity include microbial growth stage (Bhosle *et al.* 1995, Taverneiera *et al.* 1997) and specific growth rate (Evans *et al.* 1994). The amount of attachment surface, where sessile cells are concerned, has been demonstrated to affect EPS production (Beech *et al.* 1991). A summary of these influences is provided in Table 2.3.

Table 2.3: A summary of the factors influencing EPS production and the nature of EPS produced.

Condition	Microorganism/system	Author
pH	*A. ferrooxidans* (pH influenced charge of capsular EPS)	Solari *et al.* 1992 Porro *et al.* 1993, Blake *et al.* 1994, Sharma *et al.* 2003, Valinska and Rao 2008
	Sulfobacillus thermosulfidooxidans	Becker *et al.* 2011
	Sclerotium glucanicum	Wang and McNeil *et al.* 1995
	Bacillus polymyxa	Lee *et al.* 1997
Growth Stage	Diatom: *Navicula subinflata* *Rhizobium meliloti*	Bhosle *et al.* 1995, Taverneiera *et al.* 1997
Microbial species	*A. ferrooxidans, A. thiooxidans, L. ferrooxidans, Sulfobacillus thermosulfidooxidans, Sulfobacillus acidophilus*	Ghauri and Johnson 2007
Growth history influences surface properties of cells, (capsular EPS)	*A. ferrooxidans*	Porro *et al.* 1993, Blake *et al.* 1994, Gehrke *et al.* 1998, Kinzler *et al.* 2003, Sharma *et al.* 2003, Harneit *et al.* 2005, Tan and Chen *et al.* 2012 Valinska and Rao 2008
	Volcaniella eurihalina *Bacillus polymyxa* *Rhizobium meliloti* *Mixed biofilm dominated by Bacillus coagulans* *Polianthes tuberosa*	Martinez-Chenca *et al.* 1996; Lee *et al.* 1997, Taverneiera *et al.* 1997 Wolfaardt *et al.* 1998 Otsuji *et al.* 1994
Specific growth rate	*Staphylococcus epidermidis*	Evans *et al.* 1994
Hydrodynamic conditions/shear	*Pseudomonas spp.*	Rijnaardts *et al.* 1993

2.7.4 Techniques available for the analysis of EPS

2.7.4.1 Destructive techniques for analysis of EPS

Investigations into microbial EPS can be carried out via **destructive methodologies** and **non-destructive methodologies** (Neu and Lawrence 1999). **Destructive methodologies** include electron microscopy and scanning probe techniques, as well as chemical extraction techniques. Traditionally, studies which investigate microbial biofilms utilised electron microscopy. These techniques require preparation of the sample prior to visualisation (Woldring *et al.* 1977 in Neu and Lawrence 1997), which typically involves a fixation step. However, fixation of the sample may induce morphological changes or shrinkage of the specimen or both, thus not providing an adequate representation of the biofilm structure *in situ*. Similarly, scanning electron microscopy (SEM) also contains a fixation step which dehydrates the sample. Due to this, EPS may manifest as strands of polymeric material between microorganisms and the surface (Costerson *et al.* 1986,

Richards and Turner 1984 in Neu and Lawrence 1999, p25). Transmission electron microscopy (TEM), in addition to fixation and dehydration of the sample, requires embedding and sectioning of the sample in order to prepare it for microscopic examination (Neu and Lawrence 1999, p25). Work conducted by Costerson *et al.* (1986) reports the visualisation of "fibrils" of EPS between cells in the biofilm after utilisation of this technique. The underlying point of caution for use of these techniques is the interpretation of artefacts generated through sample preparation. Although useful in order to either visualise the microbial content or EPS or both within the biofilm, these techniques do not account for biofilm chemical composition and may mask architectural intricacies as they would occur *in situ*.

Other **destructive methodologies** to investigate biofilm communities involve scraping a sample of the biofilm, isolation of the innate microorganisms in solid or liquid media, followed by plate counts (Costerson *et al.* 1987, Wardell *et al.* 1988 in Neu and Lawrence 1997). EPS is analysed through extraction of the substance from the media via centrifugation followed by extraction of tightly bound EPS from the cell pellet.

2.7.4.2 Non-destructive techniques for EPS analysis

In the last two decades, more modern approaches have been utilised which allowed for investigation of the biofilm structure *in situ*, without the need for culturing or altering dynamic morphological components. These included the use of biomarkers, microelectrodes and gene probes in combination with advanced microscopy techniques (Neu and Lawrence 1999). New scanning probe microscopy techniques require less sample preparation and are less disruptive e.g. **atomic force microscopy, scanning tunnelling microscopy and scanning ion conductance microscopy** (Beech 1996, Drake *et al.* 1989, Hansma *et al.* 1989a, 1989b, Martin *et al.* 1988). **Atomic force microscopy** has been utilised for the study of attachment and biofilm formation of bioleach relevant microorganisms (Gehrke *et al* 1998, Liu *et al.* 2003, Sand and Gehrke 2006, Mangold *et al.* 2008, Lara *et al.* 2010, Noel *et al.* 2010, Florian *et al.* 2010 and 2011, Becker *et al.* 2011, Africa *et al.* 2012, Zhang *et al.* 2013). Again these studies have been limited to the investigation of mesophilic microorganisms, with the exception of Zhang *et al.* and Becker *et al.* who investigated *Ferroplasma acidiphilum* and *Sulfobacillus thermosulfidooxidans* respectively, both moderate thermophiles. The technique reveals structural surface information regarding the EPS coverage and spatial distribution around cells and over the surface, and the use of a unique shuttle stage and coupling of the AFM with epi-fluorescent microscopy allows *in situ* visualisation of the attached biofilm with high resolution (Gehrke *et al.* 1998, Sand and Gehrke 2006, Mangold

et al. 2008, Noel *et al.* 2010, Florian *et al.* 2010 and 2011, Africa *et al.* 2012, Zhang *et al.* 2013). This experimental setup is discussed in more detail in Chapter 3 and Chapter 6.

Attenuated total reflection or fourier transform-infrared spectroscopy (**FT-IR spectroscopy**) and **Raman spectroscopy** have been utilised as a non-destructive, online technique for studying bacterial adhesion, surface properties, biofilms and properties of exposed EPS. The technique allows one to track major chemical groups present on surfaces and thus provides a chemical characterisation of the surface. No sample preparation or staining is required, which also reduces any risks of introducing artefacts (Wagner *et al*., 2009). The method has been used to characterise cell surfaces of the bioleach relevant mesophilic microorganism *A. ferrooxidans* (Devasia *et al.* 1993; Edwards *et al.* 2000; Sharma *et al.* 2003; Pradhan *et al.* 2008; Pisapia *et al.* 2008) and moderately thermophilic *Sulfidobacillus thermosulfidooxidans* (Becker *et al*., 2011) This technique is also being used in combination with AFM for high resolution investigation of microorganisms and EPS surfaces (Vu *et al.*, 2009). Magnetic resonance spectroscopy (NMR) has been used for the non-destructive characterisation of polysaccharides from EPS for many years (Ravenscroft *et al.* 1991). The technique has also been employed to study intact biofilms (Clark 1990 in Neu and Lawrence 1999, p29).

Confocal laser scanning microscopy has been used routinely for the study of biofilms (Vu *et al.* 2009) and has been successfully utilised in combination with fluorescent labelled markers in numerous studies involving fully hydrated biofilms (Neu and Lawrence 1997; Neu *et al.* 2001; Koerdt *et al.* 2010; Africa *et al.* 2013).

Table 2.4: Summary of the fluorescent probes used in conjunction with CLSM to study biofilms and EPS

Specific binding	Probe	Information	Authors
Polysaccharides	Lectins	Carbohydrate binding proteins. Used to study glycoconjugate distribution and provide information on EPS composition (extensive list of lectins provided in Chapter 4)	Koerdt *et al.* 2010 Neu *et al.* Lawrence *et al.* Bellenberg *et al.* 2012 Boretska *et al.* 2013 Zhang *et a.l* 2013
	Calcofluorwhite M2R Congo Red	(1 → 4) and (1 → 3)β-D-glucan (1 → 4) and (1 → 3)β-D-glucan (1 → 4) and (1 → 3)β-D-glucan	Allison and Sutherland 1984, Wood 1980
	Alcian Blue	Copper containing cationic phthalocyanin dye which binds to anionic molecules e.g. glycosaminoglycan. Used as an indirect measure of EPS.	Wetzel *et al.* 1997
Proteins	Antibodies	Raised in animals or cell cultures against an isolated protein or polysaccharide. Provides very specific binding. Antibodies against whole cell surfaces have successfully employed. The use of this technique for bioleach microorganisms and related biofilms is non-existent.	Neu and Lawrence 1999, p31 Ch 2
Nucleic acids	4'6-diamidino-2-phenylindole (DAPI) Acridine orange (AO) SYTO9 Hoescht	General presence and distribution of nucleic material. Cells permeate stains; can be used in fully hydrated systems.	
	FISH	Binds predetermined sequence of DNA or RNA. Allows detection of particular species within the biofilm.	Africa *et al.* 2010 Africa *et al.* 2013 Florian *et al.* 2010 Florian *et al.* 2011

The technique provides three dimensional structural information of the biofilm, as well as identification and distribution of various different components within the film (Vu *et al.* 2009), highlighting the structural complexity and heterogeneity within these interfacial environments. Furthermore, information on the chemical composition can also be gained *in situ*. Fluorescent probes commonly used alongside the CLSM technique are specific for polysaccharides, proteins and nucleic acids (Neu and Lawrence 1999, p30). A summary of fluorescent probes commonly used in conjunction with CLSM to study biofilms is presented in Table 2.4.

2.7.4.3 Extraction of EPS

EPS extraction for quantitative analysis is a destructive approach that involves separation of the EPS from the cellular mass and should cause minimal damage to the cell or cell lysis. It should not disrupt or alter biopolymers and should release all biopolymers (Nielsen and Jahn 1999, p50). A universal method for the extraction of EPS is yet to be established. Typically, a sample is taken, either from the environment or a bioreactor, and may or may not undergo a pre-treatment step. The pre-treatment step generally involves a wash step using a medium with similar ionic strength to the sample to limit any disruption of the EPS, or sub-lytic homogenisation or both in the case of a thick slime or pellicle[6] biofilm (cell lysis needs to be monitored). EPS components are then extracted from the cell suspension and from the cell pellet. A purification step follows using various methods of filtration and dialysis (Nielsen and Jahn 1999). Once purified, the EPS is ready for chemical analysis of its macromolecular composition.

An important factor to be aware of is that the type of extraction or separation method used will yield different fractions of the EPS. These fractions are categorised into two groups, namely: bound EPS and soluble EPS (Fig 2.4). Soluble EPS refers to colloids[7], slimes[8] and any soluble macromolecules in the cellular suspension. This fraction can be recovered with a centrifugation step with polymers separated into the supernatant. Bound EPS refers to sheaths, capsules, condensed gels, loosely bound polymers and any attached organic molecules. Bound EPS is usually tightly associated with the cell and cell pellet and requires further mechanical or chemical treatment in order to be recovered for analysis.

[6] Pellicle biofilms refer to biofilms proliferating as dense microbial mats at the liquid-air interface

[7] Colloids can be defined as dissolved polymers (Nielsen and Jahn 1999, p51)

[8] "*Slimes are used to describe looser binding to the bio-aggregate than capsular polymers, but they are not dissolved*" (Nielsen and Jahn 1999, p51)

Table 2.5: Summary of chemical methods used to extract bound or capsular EPS

Method	Information	Microbial system	Author
Alkaline hydrolysis (NaOH pH 9 – 13)	NaOH used causes charged groups (carboxylic groups in proteins and polysaccharides) to be ionized since isoelectric points are below pH 4 – 6. Results in repulsion within the EPS matrix and improves water solubility of constituent compounds for removal. Also disrupts covalent disulphide bindings of glycoproteins at pH above 9.	Sludge Aerobic flocs and granular sludge	Liu and Fang 2002 Mcswain *et al.* 2005
	Disruption of disulphide bridges using β-mercaptoethanol		Emerson and Ghiorse 1993 in Nielsen and Jahn 1999
Dowex, EDTA, EGTA, Crown Ether	Removal of divalent cations (mainly Ca^{2+} and Mg^{2+}) disrupts crosslinking of charged compounds, essentially destabilising the matrix	*A. ferrooxidans* *Natural eukaryotic acidophilic biofilm* *Acidiphilium spp.* Mixed (*A. caldus, L. ferriphilum, S. benefaciens)* Mixed (*A. caldus, L. ferriphilum)*	Gehrke *et al.* 1998 Aguilera *et al.* 2008 Tapia *et al.* 2009 Michel *et al.* 2009 Zeng *et al.* 2010
High saline concentrations	Principle of using high salt concentration is also to remove divalent cations through cation exchange and thereby disrupt the EPS matrix.	Intertidal sediments	Perkins *et al.* 2004
Enzymatic digestion	Enzyme used to de-flocculate cells before further treatment	*Pseudomonas sp.* Isolated from activated sludge	Tago and Aida 1977 in Nielsen and Jahn 1999
Detergents	Used to isolate capsular antigens	*E. coli*	Jann *et al.* 1980, Schmidt and Jann 1982
	Used to purify EPS	*Klebsiella pneumoniae*	Dominico *et al.* 1989
Ethanol	Used to extract lipids from activated sludge. No differentiation was made between lipids originating from the cell versus that solely from EPS.	Activated sludge	Forster and Clark 1983 in Neilsen and Jahn 1999, p61

Figure 2.4 depicts the categories of EPS for a pure microbial culture. It is important to note that with this categorisation of EPS into soluble and bound EPS, any polymers outside the cell wall and not directly anchored to the outer membrane or murein protein layer are considered part of the EPS (Nielsen and Jahn 1999, p51). Thus, any products of cell lysis, adsorbed macromolecules i.e. hydrolysis products and or humic substances which surround the cells and are assimilated into the EPS matrix, contribute to the physico-chemical properties of the matrix, and are considered part of the EPS composition.

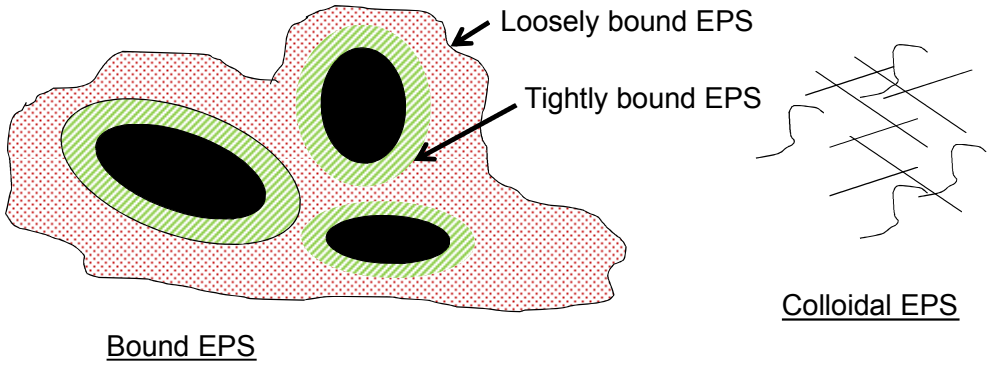

Figure 2.4: Schematic representation of the categories of EPS for a pure microbial culture.

As previously mentioned, quantitative extraction of bound EPS requires treatment of the cell pellet using either physical or chemical methods. Chemical methods usually act through disruption of the chemical interactions of the EPS components. These include van der waals forces, electrostatic interactions, hydrogen bonds and hydrophobic interactions (Christensen and Characklis 1990), as well as covalent bonds and disulphide bonds in glycoproteins (Emerson and Ghiorse 1993). Reported chemical methods are summarised in Table 2.5.

Physical methods of bound EPS extraction rely on shear stress applied to the cell pellet to enable separation and removal of the closely associated bound layer. This may include mixing, shaking, sonication or heat treatment. These techniques are not as efficient as their chemical counterparts and result in lower yields of EPS recovered (Nielsen and Jahn 1999, p55). In addition, these techniques often result in high levels of cell lysis which is problematic for quantitative analysis.

A combination of both physical and chemical methods may be used in order to maximise EPS recovery and extraction efficiency. This is typically done through combining a defined shear (heat, stirring or agitation) force with a chemical treatment. EPS yield was demonstrated to be dependent on extraction time, shear rate, temperature and chemical used (Frolund *et al.* 1996).

Extraction efficiency is defined by Nielsen and Jahn 1999 as the total amount of EPS extracted from all organic matter in a certain sample. This can be calculated indirectly through quantification of the biovolume, i.e. the number of bacteria present, the total organic carbon present or the total protein present. The amount of organic matter varies depending on the method employed to extract EPS, as well as source of EPS being analysed (Nielsen and Jahn 1999, p66- 67). For a quantitative analysis of EPS extracted and its macromolecular composition, cell lysis must be minimised. Kara-ppanagiotis et al. (1989) report that boiling and alkaline treatment above pH 9 have been demonstrated to cause high levels of cell lysis. Alkaline treatment was also observed to alter polymer composition (Hancock and Poxton 1988), and degrade uronic acids (Haug *et al.* 1967). Use of EDTA was demonstrated to cause a certain degree of cell lysis as well, postulated to be a result of the removal of divalent cations from the cell wall leading to its degradation (Johnson and Perry 1976). Dowex combined with stirring, agitation or sub-lytic sonication under defined conditions does not seem to yield high levels of cell breakage although the yield on EPS recovered is lower that alternate methodologies (Rudd *et al.* 1983, Kara-ppanagiotis *et al.* 1989).

In the context of bioleaching, there is no defined EPS extraction protocol. However, some authors have made use of a combination of physical and chemical treatments, namely the use of centrifugation combined with ethylenediaminetetraacetic acid (EDTA) or ethylene glycol-bis(β-aminoethyl ether)-N,N,N',N'-tetraacetic acid EGTA in the extraction of EPS from acidophilic systems (Gehrke *et al.* 1998, Aguilera *et al.* 2008, Zeng *et al.* 2010, Michel *et al.* 2009, Tapia *et al.* 2009). EDTA and EGTA facilitate the removal of EPS from the capsular region through removal of divalent cations (mainly Ca^{2+} and Mg^{2+}) which disrupt crosslinking of charged compounds, essentially destabilising the EPS matrix. Aguilera *et al.* (2008) investigated the efficiency of four different chemical treatments (Water, NaCl, EDTA, Dowex and Crown ether) for the recovery of EPS from an acidophilic eukaryotic biofilm isolated from nature. This group succeeded in characterizing both colloidal and capsular fractions of the EPS recovered and compared the efficiencies of the treatments assessed. The yield and composition of the EPS varied with the treatment method used, as did the extent of cell lysis. Treatment with salt recovered the highest proportion of EPS. However, the salt treatment also caused the greatest extent of cell damage and lysis. Crown ether yielded the second highest levels of EPS, followed by treatment with EDTA, Dowex and water. The level of cell damage caused by Crown ether, EDTA and Dowex were comparable and were substantially lower than that caused by salt treatment. Due to this fact, Crown ether and EDTA were utilised in this study for the recovery of capsular or bound EPS.

2.8 DETACHMENT OF BIOLEACH MICROORGANISMS

While detachment is known to occur and plays an important role in the life-cycle of biofilms, little is known regarding the mechanisms underlying the detachment process. It is of particular interest in heap bioleaching where changing temperatures and physicochemical conditions demand the requirement for a microbial succession. Detachment of microbes from biofilms could be attributed to physical forces such as hydrodynamic shear either via erosion of single cells or sloughing off of large aggregates of biomass (Bryers *et al.* 2004, Purevdorj-Gage and Stoodley 2004), as well as various other stresses. Detachment may also result from biological action such as enzymatic dissolution of the polysaccharide matrix (Allison *et al.* 2004). The phenomenon of 'hollowing out' of biofilms is also cited in terms of detachment. This refers to microorganisms actively vacating the interiors of the biofilm. However, it may also result from lysis of cells within the interior of the colony (Purevdorj-Gage and Stoodley 2004), possibly due to nutrient limitation or byproduct build-up. Rojas-Chapana *et al.* (1998) demonstrated that Tween 80 disrupted adhesion of *A. ferrooxidans* to sulfur prills.

2.9 SUMMARY

It is currently postulated that the major contribution of microorganisms to bioleaching is via the indirect contact mechanism (Tributsch 2001, Crundwell 2003), discussed in Section 2.1.3. According to the indirect contact mechanism, attachment of microbes to mineral surfaces and excretion of an EPS layer is important in the bioleaching process. The EPS layer provides a reaction space for mineral dissolution to occur (Gehrke *et al.* 1998) and brings the reactants for mineral dissolution in close proximity to the mineral surface and the microbial cells (Rawlings 2004). Consequently, the microbial-EPS-mineral interface becomes the major site of both microbial oxidation and mineral dissolution reactions, thus the location of cells, i.e. attached or planktonic, would have an effect on the observed bioleach rate. Several authors have correlated attachment of *A. ferrooxidans* to various sulfide mineral surfaces with an increase in bioleach rate (Gehrke *et al.* 1998; Fowler *et al.* 1999; Kinzler *et al.* 2003) with the presence of EPS also demonstrated to have a positive effect on bioleach rates (Gehrke *et al.* 1998 and 2001, Sand and Gehrke 2006).

Early literature regarding attachment of bioleach microbes to facilitate mineral interfacial interactions was centred on developing a proposal of a mechanism of attachment and its understanding, discussed in Section 2.5 (Zobell 1943; van Loosdrecht *et al.* 1990). Studies into cell surface as well as mineral surface chemistry were conducted to explain the observed attachment (Sections 2.5 and 2.6). In the context of bioleaching, the focus of a large proportion of

the available literature is to identify trends in microbial adhesion behaviour during the initial adhesion stage (discussed in Section 2.6). Rapid and high levels of attachment of *A. ferrooxidans* to sulfide mineral concentrates were observed, with the attachment equilibrium predominantly established within two hours (Rodriguez *et al.* 2003, Gonzalez *et al.* 1999, Escobar *et al.* 1996, Harneit *et al.* 2005, Bromfield *et al.* 2011, Africa et al. 2013). Attachment of microorganisms was observed to be selective for, or preferential to sulfide minerals over quartz (Solari *et al.* 1992, Ohmura *et al.* 1993; Gehrke *et al.* 1998, 2001; Nagaoka *et al.* 1999; Gonzalez *et al.* 1999; Sampson *et al.* 2000; Rodriguez *et al.* 2003a, b; Kinzler *et al.* 2003; Harneit *et al.* 2005 and Bromfield *et al.* 2011).

The aforementioned researchers have investigated relative attachment through the use of agitated batch systems, with the quantitative results not expected to represent attachment dynamics adequately in a heap environment for a number of reasons. Hydrodynamic conditions experienced in agitated batch systems differ from those encountered in a heap, an important factor which has been overlooked when interpreting the results of attachment in agitated batch systems. Shake flask systems present a well-mixed environment which facilitates more effective particle transport but does not simulate heap-like fluid dynamics with less efficient microbial-mineral contacting. This was demonstrated effectively by Bromfield *et al.* (2011). There is a requirement for studies which take into consideration heap-like fluid-flow dynamics, generating results which are more representative of the microbial-mineral interfacial processes as they would occur in industry. Furthermore, the work predominantly pertains to pure culture investigations and microbial interactions with sulphide mineral concentrates. Successful industrial heap bioleaching requires a microbial consortium (Brierly 2001, Olson *et al.* 2003, Demergasso *et al.* 2005, Walting 2006) with the content of the mineral of interest in the ore leached seldom more than 1% in comparison to gangue minerals (Helle *et al.* 2005, Watling 2006). Integrated studies, incorporating the use of mixed consortia and interactions with low-grade ores and gangue mineralogy will also assist in the generation of industrially relevant data.

Investigations into microbial-mineral-interfacial interactions have become increasingly geared toward visualising the transition from initial to firm attachment and colonisation on mineral surfaces. Several research groups have utilised high powered microscopy techniques in order to visualise biofilms in an attempt to better understand this interfacial environment. Early-stage, mono-layered biofilm formation has been reported by Sanhueza *et al.* (1999), Gehrke *et al.* (1998, 2001), Kinzler *et al.* (2003), Harneit *et al.* (2005 and 2006), Pradhan *et al.* (2008), Mangold et al (2008), Lei *et al.* (2009), Noel *et al.* (2010), Florian *et al.* (2010 and 2011), Becker *et al.* 2011, Zhang *et al.* (2013) and Gonzalez *et al.* (2012.). This work predominantly pertains to mesophilic and moderately thermophilic microorganisms. Bioleaching of chalcopyrite is more successful at

high temperatures of 65°C and above (Dixon 2000, Dew *et al.* 2000, Rawlings 2002, Olson *et al.* 2003), warranting studies making use of elevated temperatures and thermophilic microorganisms. Furthermore, a greater understanding of microbial succession within heap environments is required, with temperature being one of the key driving forces. Quantification of microbial population compositions and elucidation of strain-specific activities in response to changes within a bioleach environment are expected to add greatly to current understanding of microbial interactions in heap systems.

As previously mentioned, the microbial-EPS-mineral interface is the major site of both microbial oxidation and mineral dissolution reactions. Attempts to further elucidate the microbial-mineral-interfacial environment and interfacial processes have been carried out through visualisation of the microbial biofilm (Bellenberg *et al.* 2012, Boretska *et al.* 2013 and Zhang *et al.* 2013), extraction and characterisation of the EPS (Gehrke *et al.* 1998 and 2001, Aguilera *et al.* 2008, Michel *et al.* 2009, Tapia *et al.* 2009, Zeng *et al.* 2010, Jiao *et al.* 2010). EPS extracted from acidic environments, or from bioleach relevant microorganisms and biofilms, contained proteins, nucleic acids, uronic acids, humic substances, lipids and heavy metals (Gehrke *et al.* 1998 and 2001, Aguilera *et al.* 2008; Tapia *et al.* 2009; Michel *et al.* 2009 and Jiao *et al.* 2010). There is no clear consensus on a universal methodology for extraction of EPS hence comparison of EPS yields across published work is difficult. Combinations of physical and chemical methods, mostly involving cation exchange techniques, have been used for the extraction of colloidal and capsular EPS. Work in this field is limited, especially with respect to moderate and extreme thermophiles.

Fundamental to the understanding of microbial adhesion and the establishment of interfacial environments through production of EPS, is an appreciation for the factors influencing interface chemistry. In a bioleach context, studies have focussed on factors which affect surface properties or composition, namely growth history and solution chemistry. Culture growth history has been correlated to changes in the surface properties of *A. ferrooxidans* (Porro *et al.* 1993, Blake *et al.* 1994, Gehrke *et al.* 1998, Kinzler *et al.* 2003, Sharma *et al.* 2003, Harneit *et al.* 2005, Chen *et al.* 2008 and Valinska and Rao 2008) and composition of the EPS (Gehrke *et al.* 1998, Harneit *et al.* 2005, Kinzler *et al.* 2003). Again, this work is limited to mesophilic microorganisms, mainly *A. ferrooxidans*. Knowledge on the regulation of EPS production and the formation of biofilm is limited with respect to bioleach relevant microorganisms. Chemotaxis is under investigation (Rojas-Chapana *et al.* 1998, Jerez *et al.* 2001) with quorum sensing N-acylhomoserine lactones (AHLs) demonstrated to play an essential role in modulating biofilm formation (Gonzalez *et al.* 2013). Furthermore, the involvement of quorum sensing is also yet to be fully elucidated in bioleach microorganisms, with work predominantly being conducted on microorganisms in the mesophilic and moderately thermophilic temperature range (Farah 2005, Ruiz *et al.* 2007**b**,

González *et al.*, 2013, Calderón *et al.*, 2013, Zhang *et al.*, 2012 and Ng *et al.* 2011 cited by Montgomery *et al.* 2013).

There is insufficient knowledge available on the detachment of bioleach microorganisms and the factors that influence this occurrence in the context of bioleaching.

The limitations of the current body of literature and requirement for its extension can be summarised as follows:

- Studies using mixed consortia are limited. Further, the limited studies on thermophiles show contradictory findings in terms of microbial-mineral affinity as well as extent of attachment and colonisation to sulfide minerals.
- Integrated studies of colonisation as a function of process parameters (physicochemical conditions) which influence mineral-microbial interface chemistry, colonisation and microbial succession are required.
- There is a requirement for knowledge on colonisation of thermophiles in heap environments as well as thermophilic temperature regimes
- Since gangue mineralogy comprises the bulk of the ore body processed in heap operations, studies on microbial colonisation to low-grade ore are required.
- To date, approaches used to study microbial adhesion to mineral surfaces in the field of biohydrometallurgy may not adequately represent the attachment dynamics in a bioheap in terms of mineral-microbial contacting and fluid-flow.
- Knowledge regarding the microbial-EPS-mineral interfacial environments and biofilm formation in heap bioleach systems is limited, despite the fact that this sedentary life-style may be the predominating form of microbial life in a heap environment
- Limited studies on EPS production, quantification and composition are available in literature, with limited available on thermophiles
- There is limited knowledge regarding the regulation of EPS production and biofilm formation in bioleach relevant microorganisms
- The current body of literature on factors that influence attachment behaviour of bioleach microorganisms is limited, while studies investigating detachment in the context of bioleaching are non-existent

2.10 OBJECTIVES, RESEARCH APPROACH AND KEY QUESTIONS

2.10.1 Objectives

Based on the gaps in the literature presented, the aim of this research is to provide an investigation into microbial-metal sulfide interfacial environments of the thermophilic archaeon *M. hakonensis* under heap bioleach-like conditions, including its application to low grade ores.

Objectives of this study are:

1. To investigate and visualise the mineral-microbial interfacial environment through visualising the EPS and *in situ* biofilm formation on contacting the thermophilic archaeon *Metallosphaera hakonensis* (*M. hakonensis*) with metal sulfide concentrates and low grade ores
2. To investigate the mineral-microbe interfacial environment through extraction and compositional characterisation of EPS from *M. hakonensis* cultured on three substrata (ferrous sulphate, sulfur and chalcopyrite mineral concentrate)
3. To investigate the transition between initial adhesion and firm attachment stages in the development of biofilms of the thermophilic archaeon *M. hakonensis*, as well as the effect of temperature on the interfacial microenvironment *in situ*

2.10.2 HYPOTHESES

In light of the literature reviewed and the research approach outlined above, the following hypotheses are put forward:

Hypothesis 1:

M. hakonensis produces EPS to enable development of a favourable microenvironment. This microenvironment varies depending on the contacting mechanism and the need to nurture surface colonisation. Differing levels and locality of EPS production occur in an unsaturated ore bed relative to that in fully agitated slurry reactors, the extent of which is described in this study.

Hypothesis 2:

Mineralogy, surface topography and temperature influence spatial colonisation of *M. hakonensis* under heap simulated conditions. Mineral type, composition and presence of surface defects are expected to affect colonisation trends. Microorganisms preferentially attach to and colonise sulfide mineral surface over other mineral surfaces with these microbial-mineral associations evident on low-grade ore sections. Colonisation is expected to be more extensive at temperatures for optimal growth.

2.10.3 Research approach and key questions

2.10.3.1 *In situ* visualisation and characterisation of the EPS and EPS interfacial environments produced by *M. hakonensis*

To meet objective (1) of this study, a combination of fluorescent labelled lectin probes and CLSM was used to elucidate the microbial-EPS-mineral interfacial environment *in situ*. Investigations were carried out to establish the presence of EPS produced by the thermophilic archaeon *M. hakonensis,* and to elucidate the structure, architecture and composition of microbial-EPS-mineral interfacial environments created under bioleach simulated conditions.

The key questions to be addressed through this investigation can be summarised as follows:

- Does *M. hakonensis* produce EPS, and if so, what is the architecture thereof and how can this be characterised?
- How does the EPS architecture vary with changes in experimental conditions?
- Where is the EPS localised and how does this vary with changes in experimental conditions?
- Which lectins give rise to strong positive binding with EPS produced by *M. hakonensis*, and conversely what is the composition of the EPS produced by *M. hakonensis* as indicated through strong positive binding with specific lectins?
- What are the implications of these findings for bioleach systems?

2.10.3.2 Extraction and chemical compositional analysis of EPS produced by *M. hakonensis* cultured on different growth substrata

To meet objective (2) of this study, and to provide a more fundamental understanding of the building blocks of the EPS interfacial environments produced by *M. hakonensis*, a methodology to extract EPS from *M. hakonensis* cultured on three growth substrata (sulphur, ferrous sulphate and chalcopyrite mineral concentrate) was established. The EPS was then chemically characterised to determine its composition under each respective growth condition.

The key questions to be addressed through this investigation can be summarised as follows:

- Which methodology is most suited for extraction of EPS from *M.* hakonensis?
- What is the composition of EPS produced by *M. hakonensis*?
- How does the growth substrate affect the quantity and composition of EPS produced?
- What are the implications of these findings for the bioleach process operation?

2.10.3.3 *In situ* investigation and visualisation of the effect of temperature on *M. hakonensis* biofilm formation and EPS-mineral interfacial environments

A novel, integrated *in situ* biofilm reactor (design and methodology presented in Chapter 3.3) was used for the investigation and visualisation of microbial-mineral association in the context of objective (3) and to gain a greater understanding of the biofilm formation and EPS interfacial environments created by *M. hakonensis*. Visualisation of EPS production and spatial distribution is also possible. The investigations focused on pure cultures of *M. hakonensis*, massive sections of sulphide minerals (pyrite, chalcopyrite) and low-grade chalcopyrite containing mineral ore (Escondida CH2-Type B). The effect of varying temperature on the extent of colonisation and formation of EPS interfacial environments is assessed. Confocal microscopy (CLSM) provides 3-dimensional imaging of microbial biofilms *in situ,* a quantitative assessment of the extent of attachment and a qualitative assessment of the EPS present. Combined Atomic Force Microscopy (AFM) and epi-fluorescent microscopy (EFM) are used to provide a more detailed analysis of mineral-microbial interactions.

The following key questions are addressed through this investigation:

- How long does it take before the onset of colonisation and biofilm formation and how does this vary across the microbial species used?
- What trends are observed for the architecture of a pure *M. hakonensis* biofilm?
- What is the spatial locale and distribution of cells and EPS on the mineral surfaces?
- How do temperature and mineral substrata affect colonisation and biofilm formation trends?
- What is the impact of these findings on process operation?

2.10.3.5 Schematic outline of research approach

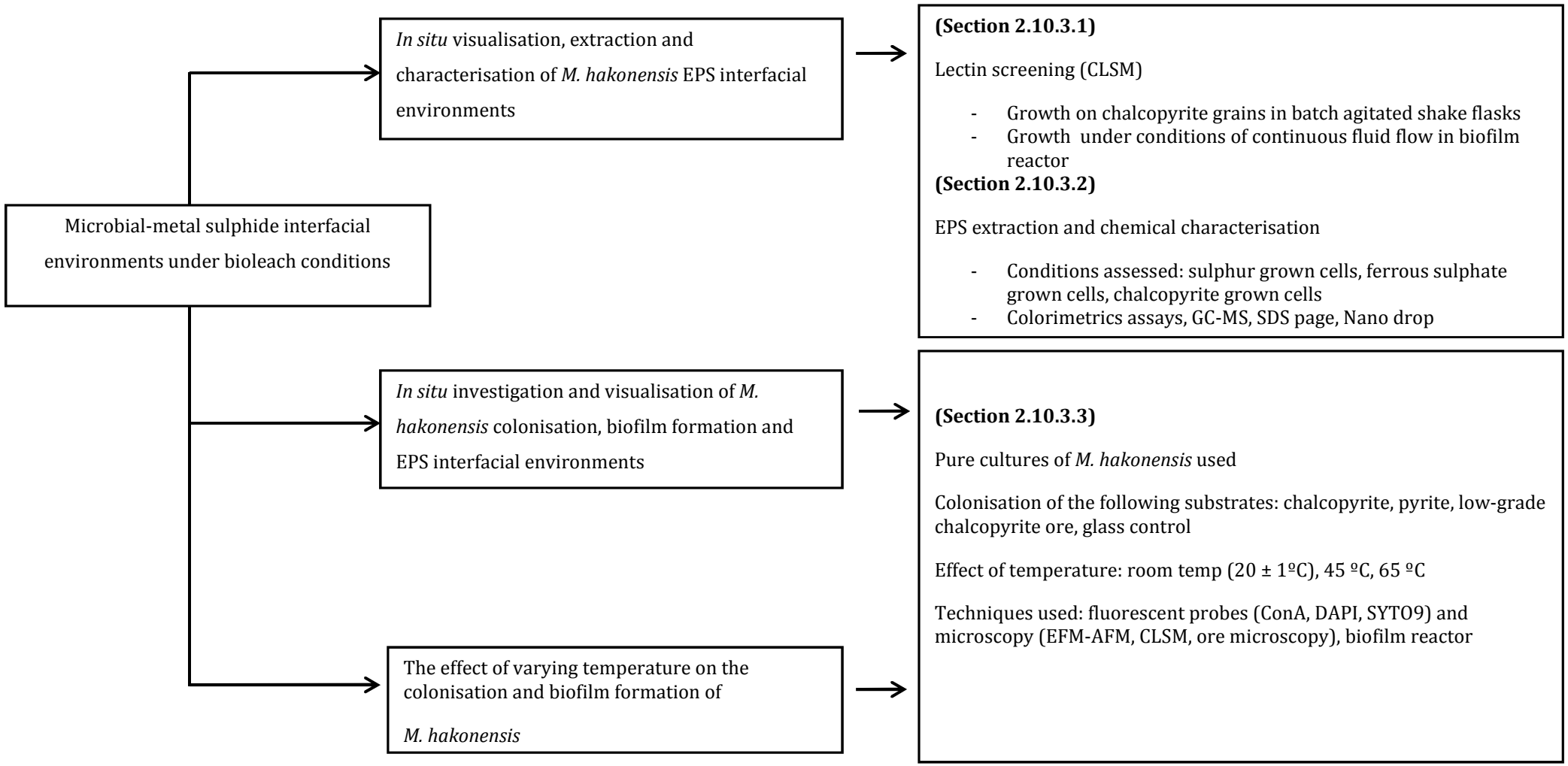

References

Africa, C. J., Harrison, S. T. L., Becker, M., & Hille, R. P. van. (2010). In situ investigation and visualisation of microbial attachment and colonisation in a heap bioleach environment: The novel biofilm reactor. *Minerals Engineering*, *23*(6), 486–491.

Africa, C. J., Van Hille, R. P., Sand, W., & Harrison, S. T. L. (2013). Investigation and in situ visualisation of interfacial interactions of thermophilic microorganisms with metal-sulphides in a simulated heap environment. *Minerals Engineering*, *48*, 100–107.

Aguilera, A., Souza-Egipsy, V., San Martín-Úriz, P., & Amils, R. (2008). Extraction of extracellular polymeric substances from extreme acidic microbial biofilms. *Applied Microbiology and Biotechnology*, *78*(6), 1079–1088.

Acota M., Galleguillos P., Ghorbani Y., Tapia P., Contador Y., Velasquez C., Espoz C., Pinilla C. and Dermergasso C., (2014) Variation in microbial Community from predominantly mesophilic to termotolerant and moderately thermophilic species in an industrial copper heap bioleaching operation.*Hydrometallurgy*, 150, 281-289

Becker, T., Gorham, N., Shiers, D. W., & Watling, H. R. (2011). In situ imaging of Sulfobacillus thermosulfidooxidans on pyrite under conditions of variable pH using tapping mode atomic force microscopy. *Process Biochemistry*, *46*(4), 966–976.

Bellenberg, S., Leon-Morales, C. F., Sand, W., & Vera, M. (2012). Visualization of capsular polysaccharide induction in Acidithiobacillus ferrooxidans. *Hydrometallurgy*, *129–130*, 82–89.

Boretska, M., Bellenberg, S., Moshynets, O., Pokholenko, I., & Sand, W. (2013). Microbial & Biochemical Technology Change of Extracellular Polymeric Substances Composition of *Thiobacillus thioparus* in Presence of Sulfur and Steel, *5*(3), 68–73.

Brierley, C. . (2001). Bacterial succession in bioheap leaching. *Hydrometallurgy*, *59*(2–3), 249–255.

Calderón, K., González-Martínez, A., Gómez-Silván, C., Osorio, F., Rodelas, B., & González-López, J. (2013). Archaeal diversity in biofilm technologies applied to treat urban and industrial wastewater: Recent advances and future prospects. *International Journal of Molecular Sciences*, *14*(9), 18572–18598.

Coram, N. J., & Rawlings, D. E. (2002). Molecular Relationship between Two Groups of the Genus Leptospirillum and the Finding that *Leptospirillum ferriphilum* sp . nov . Dominates South African Commercial Biooxidation Tanks That Operate at 40 ° C, *68*(2), 838–845.

Demergasso, C. S., Galleguillos P., P. A., Escudero G., L. V., Zepeda A., V. J., Castillo, D., & Casamayor, E. O. (2005). Molecular characterization of microbial populations in a low-grade copper ore bioleaching test heap. *Hydrometallurgy*, *80*(4), 241–253.

Devasia, P., Natarajan, K. A., Sathyanarayana, D. N., & Rao, G. R. (1993). Surface chemistry of *Thiobacillus ferrooxidans* relevant to adhesion on mineral surfaces. *Applied and Environmental Microbiology*, *59*(12), 4051–4055.

Dixon, D. G. (2000). Analysis of heat conservation during copper sulphide heap leaching. *Hydrometallurgy*, *58*(1), 27–41.

Edwards, K. J., Bond, P. L., & Banfield, J. F. (2000). Characteristics of attachment and growth of *Thiobacillus caldus* on sulphide minerals: A chemotactic response to sulphur minerals? *Environmental Microbiology*, *2*(3), 324–332.

Franzmann, P. D., Haddad, C. M., Hawkes, R. B., Robertson, W. J., & Plumb, J. J. (2005). Effects of temperature on the rates of iron and sulfur oxidation by selected bioleaching Bacteria and Archaea: Application of the Ratkowsky equation. *Minerals Engineering*, *18*(13–14), 1304–1314.

Fuchs, T., Huber, H., Teiner, K., Burggraf, S., & Stetter, K. O. (1995). *Metallosphaera prunae*, sp. nov., a Novel Metal-mobilizing, Thermoacidophilic Archaeum, Isolated from a Uranium Mine in Germany. *Systematic and Applied Microbiology*, *18*(4), 560–566.

Gehrke, T., Telegdi, J., Thierry, D., & Sand, W., 1998. Importance of extracellular polymeric substances from Thiobacillus ferrooxidants for bioleaching. *Applied and Environmental Microbiology*, 64, 2743-2747.

Gehrke, T., Hallman, R., Kinzler, K., & Sand, W., 2001. The EPS of *Acidithiobacillus ferrooxidans* – a model for structure-function relationsips of attached bacteria and their physiology. *Water Science and Technology*, 43, 159-167.

Hallberg, K. B., & Lindstromt, E. B. (1994). Characterization of *Thiobacillus caldus*. *Microbiology*, (140), 3451–3456.

Hiroyoshi N., Kitagawa H. and Tsunekawa M., (2008) Effect of solution composition on the optimum redox potential for chalcopyrite leaching in sulfuric acid solutions. *Hydrometallurgy*. 91, 144-149.

Jiao, Y., Cody, G. D., Harding, A. K., Wilmes, P., Schrenk, M., Wheeler, K. E., … Thelen, M. P. (2010). Characterization of extracellular polymeric substances from acidophilic microbial biofilms. *Applied and Environmental Microbiology*, *76*(9), 2916–2922.

Jones G., Corin K.C., van Hille R.P., Harrison S.T.L., (2011) The generation of toxic reactive oxygen species (ROS) from mechanically activated sulphide concentrates and its effect on thermophilic bioleaching. *Minerals Engineering.* 24(11), 1198-1208.

Kelly, D. P., & Wood, A. P. (2000). Reclassification of some species of Thiobacillus Acidithiobacillus gen . nov ., Halothiobacillus, International Journal of of systematic and Evolutionay Microbiology, 50, 511–516.

Koerdt, A., Gödeke, J., Berger, J., Thormann, K. M., & Albers, S. V. (2010). Crenarchaeal Biofilm Formation under Extreme Conditions. *PLoS ONE*, *5*(11).

Kurosawa, N., Itoh, Y. H., & Itoh, T. (2003). Reclassification of Sulfolobus hakonensis Takayanagi et al. 1996 as Metallosphaera hakonensis comb. nov. based on phylogenetic evidence and DNA G+C content. *International Journal of Systematic and Evolutionary Microbiology*, *53*(5), 1607–1608.

Liu, H., & Fang, H. H. P. (2002). Extraction of extracellular polymeric substances (EPS) of sludges. *Journal of Biotechnology*, *95*(3), 249–256.

Liu, H. L., Chen, B. Y., Lan, Y. W., & Cheng, Y. C. (2003). SEM and AFM images of pyrite surfaces after bioleaching by the indigenous Thiobacillus thiooxidans. *Applied Microbiology and Biotechnology*, *62*(4), 414–420.

McSwain, B. S., Irvine, R. L., Hausner, M., & Wilderer, P. A. (2005). Composition and Distribution of Extracellular Polymeric Substances in Aerobic Flocs and Granular Sludge Composition and Distribution of Extracellular Polymeric Substances in Aerobic Flocs and Granular Sludge. *Applied and Environmental Microbiology*, *71*(2) 1051-1057.

Michel, C., Bény, C., Delorme, F., Poirier, L., Spolaore, P., Morin, D., & D'Hugues, P. (2009). New protocol for the rapid quantification of exopolysaccharides in continuous culture

systems of acidophilic bioleaching bacteria. *Applied Microbiology and Biotechnology*, *82*(2), 371–378.

Montgomery, K., Charlesworth, J. C., LeBard, R., Visscher, P. T., & Burns, B. P. (2013). Quorum sensing in extreme environments. *Life (Basel, Switzerland)*, *3*(1), 131–48.

Neu, T. R., & Lawrence, J. R. (1997). Neu and Lawrence 1997 Development and structure of microbial bioflms in river water using CLSM FEMS 24,p 11 -25.pdf. *FEMS Microbiology Ecology*, *24*, 11–25.

Neu, T., Swerhone, G. D., & Lawrence, J. R. (2001). Assessment of lectin-binding analysis for in situ detection of glycoconjugates in biofilm systems. *Microbiology (Reading, England)*, *147*(Pt 2), 299–313.

Ng, F. S. W., Wright, D. M., & Seah, S. Y. K. (2011). Characterization of a phosphotriesterase-like lactonase from Sulfolobus solfataricus and its immobilization for disruption of quorum sensing. *Applied and Environmental Microbiology*, *77*(4), 1181–1186.

Perkins, R. G., Paterson, D. M., Sun, H., Watson, J., & Player, M. A. (2004). Extracellular polymeric substances: Quantification and use in erosion experiments. *Continental Shelf Research*, *24*(15), 1623–1635.

Petersen, J., & Dixon, D. G. (2002). Thermophilic heap leaching of a chalcopyrite concentrate. *Minerals Engineering*, *15*(11), 777–785.

Pisapia, C., Humbert, B., Chaussidon, M., & Mustin, C. (2008). Perforative Corrosion of Pyrite Enhanced by Direct Attachment of Acidithiobacillus ferrooxidans. *Geomicrobiology Journal*, *25*(6), 261–273.

Pradhan, N., Pradhan, S. K., Nayak, B. B., Mukherjee, P. S., Sukla, L. B., & Mishra, B. K. (2008). Micro-Raman analysis and AFM imaging of Acidithiobacillus ferrooxidans biofilm grown on uranium ore. *Research in Microbiology*, *159*(7–8), 557–561.

Qiu, M.q., Xiong, S., Zhangb, W., Wang, G., 2005. A comparison of bioleaching of chalcopyrite using pure culture or a mixed culture. *Minerals Engineering*. 18, 987–990.

Remonsellez F., Galleguillos F., Moreno-Paz M., Parro V., Acosta M. and Dermergasso C.,(2009) Dynamic of active microorganisms inhabiting a bioleaching industrial heap of low-grade copper sulfide ores monitored by real-time PCR and oligonucleaotide prokaryotic acidophilic microarray. *Microbial Biotechnology*. 2, 613 - 624

Rodriguez, Y., Ballester, A., Blazquez, M. L., Gonzalez, F., & Munoz, J. A., 2003. New information on the chalcopyrite bioleaching mechanism at low and high temperature. *Hydrometallurgy.* 71: 47-56

Ravenscroft, N., Walker, S. G., Dutton, G. G., & Smit, J. (1991). Identification, isolation, and structural studies of extracellular polysaccharides produced by Caulobacter crescentus. *Journal of Bacteriology*, *173*(18), 5677–84.

Richards S.R., Turner R.J., (1984) A comparative study of techniques for the examination of biofilms by scanning electron microscopy. Wat. Res. 18: 767 - 773

Sharma, P. (2003). Surface characterization of Acidithiobacillus ferrooxidans cells grown under different conditions. *Hydrometallurgy*, *71*(1–2), 285–292.

Schippers, A., Sand, W., (1999) Bacterial leaching of metal sulfides proceeds by two indirect mechanisms via thiosulfate or via polysulfides and sulfur. *Applied and Environmental Microbiology.* 65 (1), 319 -321.

Soto P. E., Galleguillos P.A., Seron M.A., Zepeda V.J., Dermergasso C.S., Pinilla C., 2013 Parameters influencing the microbial oxidation activity in the industrial bioleaching heap at Escondida mine, Chile. *Hydrometallurgy*. 157, 107 - 115

Takayanagi, S., Kawasaki, H., Sugimori, K., Yamada, T., Sugai, a, Ito, T., … Shioda, M. (1996). Sulfolobus hakonensis sp. nov., a novel species of acidothermophilic archaeon. *International Journal of Systematic Bacteriology*, *46*(2), 377–382.

Tapia, J. M., Muñoz, J. A., González, F., Blázquez, M. L., Malki, M., & Ballester, A. (2009). Extraction of extracellular polymeric substances from the acidophilic bacterium Acidiphilium 3.2Sup(5). *Water Science and Technology*, *59*(10), 1959–1967.

Temple, K. L., & Colmer, A. R. (1951). The autotrophic oxidation of iron by a new bacterium: *Thiobacillus ferroxidans*. *Journal of Bacteriology*, 605–611.

Tupikina, O.V.; Ngoma, I.E.; Minnaar, S.; Harrison, S.T.L. Some aspects of the effect of pH and acid stress in heap bioleaching. *Minerals Engineering.* 2011, 24, 1209–1214.

Travisany D., Cortes M. P., Latorre M., Genova A. D., Budinich M., Bobadilla-Fazzini R. A., Parada P., Gonzalez M., Maass A., (2014) A novel genome of Acidithiobacillus thiooxidans provide novel insights into adaptation to a bioleaching environment. *Research in Microbiology.* 165(9) 742-752.

Vu, B., Chen, M., Crawford, R. J., & Ivanova, E. P. (2009). Bacterial extracellular polysaccharides involved in biofilm formation. *Molecules*, *14*(7), 2535–2554.

Wagner, M., Ivleva, N. P., Haisch, C., Niessner, R., & Horn, H. (2009). Combined use of confocal laser scanning microscopy (CLSM) and Raman microscopy (RM): Investigations on EPS - Matrix. *Water Research*, *43*(1), 63–76.

Waksman S. A. and Joffe J.S., (1922). "Microorganisms concerned in the oxidation of sulfur in the soil: II. *Thiobacillus thiooxidans*, a new sulfur-oxidizing organism isolated from the soil." *Journal of bacteriology* **7** (2): 239-256

Watling H.R., (2006) The bioleaching of sulphide minerals with emphasis on copper sulphides - A review. *Hydrometallurgy*. 84(1-2), 81-108

Zhang, G., Zhang, F., Ding, G., Li, J., Guo, X., Zhu, J., Zhou L., Cai S., Liu X., Luo Y., Zhang G., Shi W., Dong, X. (2012). Acyl homoserine lactone-based quorum sensing in a methanogenic archaeon. *The ISME Journal*, *6*(7), 1336–44.

Zhang, R. Y., Vera, M., Bellenberg, S., & Sand, W. (2013). Attachment to Minerals and Biofilm Development of Extremely Acidophilic Archaea. *Advanced Materials Research*, *825*, 103–106.

Zolghadr, B., Kling, A., Koerdt, A., Driessen, A. J. M., Rachel, R., & Albers, S. V. (2010). Appendage-mediated surface adherence of Sulfolobus solfataricus. *Journal of Bacteriology*, *192*(1), 104–110

Chapter 3:

Methodology

In this chapter, a description of protocols and techniques employed to investigate the attachment of *M. hakonensis* to mineral surfaces is presented with special regard to experimental set-up and reactor configuration. Mineralogical information of the substratum used is provided in Section 3.1. The microbial species used and their respective growth conditions are presented in Section 3.2. Descriptions of the reactor configurations are provided in Section 3.3. Analytical and molecular techniques employed are provided in Sections 3.4 through 3.9. Finally, descriptions of the experimental design used to study attachment are given in Section 3.10.

3.1 SUBSTRATA USED TO INVESTIGATE ATTACHMENT

3.1.1 Sulfide mineral substratum

A chalcopyrite mineral concentrate (courtesy of Goldfields) was used as the primary sulfide mineral substrate. A summary of the major elemental composition of the concentrates, determined by X-ray fluorescence (XRF) analysis (analysis performed as uncalibrated samples courtesy of Miss Zulpha Le Riche, Department of Chemical Engineering, University of Cape Town) is presented in Table 3.1. Particle size distribution was performed by laser diffraction using a Malvern Mastersizer (Malvern Instruments) particle size analyser. The results showed that a final size fraction of less than 10 µm was achieved (Appendix C).

Table 3.1: Major elemental composition of the Goldfields chalcopyrite concentrate.

Mineral concentrate	Copper (%)	Iron (%)	Sulfur (%)
Chalcopyrite	19.39	21.08	38.2

3.1.2 Preparation of sulfide mineral thin sections for biofilm development investigation

Massive sulfide mineral samples (Ward's Natural Science), consisting of either predominantly chalcopyrite or pyrite were also used for experimental studies. The samples were cut into thin sections (1 mm thick) and mounted onto glass slides using an epoxy resin (Department of Geology, University of Cape Town).

3.1.3 Preparation and mineralogical mapping of mineral thin sections for biofilm attachment study

A low grade chalcopyrite mineral containing ore sample (CH-32 Type B, Escondida, Chile) was used. The predominant sulfide minerals present were pyrite and chalcopyrite (4.0 and 0.5 % wt, respectively), with the predominating gangue minerals present being quartz and muscovite (44.8 and 28.6 % wt, respectively). The full mineralogical composition of the CH-32 Type B ore is presented in Appendix (C).

Samples were cut into 60 and 100 µm thin sections, and mounted onto glass slides using an epoxy resin (Department of Geology, University of Cape Town). The 60 µm sections were polished for the purposes of generating a mineralogical map, while the 100 µm sections left unpolished to investigate the prevalence of microbial attachment under conditions mimicking that of a heap bioleach.

Important properties which guide the identification of specific minerals include the physical properties of the mineral as well as optical properties. The physical properties which are commonly used for mineral identification include properties such as hardness, tenacity, streak, lustre, density and specific gravity, cleavage, parting, fracture and associated minerals (Rogers 1937). Hardness refers to the resistance offered by the smooth surface of a mineral to scratching. The property is dependent on the strength and atomic bonding in the mineral. Tenacity refers to 'the resistance offered by a mineral to breaking crushing, bending or tearing' also referred to as its 'cohesiveness'. Streak refers to the colour of finely powdered mineral. Cleavage refers to the tendency of certain minerals to break smoothly, parallel to particular planes of atoms in the crystal structure. The presence of cleavage therefore indicates weak bond strength in the crystal along those planes. Parting is a description of the tendency of a mineral to break along discrete

surfaces of structural weakness. Of the physical properties presented for mineral identification, only mineral associations were considered. Other factors were less important since the basis of the mineral identification technique employed relied on classification of minerals through characteristic optical properties via ore microscopy.

Optical properties refer to properties such as refractive index, luminescence and colour, as well as pleochroism, isotropism or anisotropism, birefringence, internal reflectance and twinning, all of which may be determined using ore microscopy (Rogers 1937). Colour pleochroism refers to a change in the colour exhibited by anisotropic minerals due to differing degrees of absorption of light in different crystallographic orientations in plane polarized light. Isotropic crystals allow light to move in all directions with equal velocity and have a single refractive index. In cross polarised light, these appear dark in all directions. In the case of anisotropic crystals, the velocity varies with crystallographic direction resulting in more than one refractive index. In cross polarised light these show interference colours (associated with birefringence) with characteristic extinction. Birefringence refers to the difference in refractive index. Minerals will exhibit a range of colours due to strong birefringence under transmitted, cross polarized light. The Michel-Levy chart is used as a standardized means to reveal the characteristic colours exhibited by a mineral according to its birefringence index (Appendix C). Twinning refers to the occurrence of two separate crystals sharing the same crystal lattice points in an asymmetrical manner, which results in an intergrowth of the crystals in a variety of specific configurations.

Ore microscopy exploits the optical properties of various minerals under reflected and transmitted light in polarised and cross polarised planes in order to identify minerals present. Ore microscopy, together with mineralogical information provided by BHP Billiton Escondida mine, was used to characterise ore samples and identify minerals present. Using this technique, together with photographic analysis, a data base was compiled for the generation of a detailed mineralogical map of the surface of each thin section studied. Minerals present were identified, labelled and mapped in order to identify the type, spatial arrangement, and relative abundance. Table E.3 in Appendix C shows the predominant sulfide and gangue minerals contained in the ore sample with their corresponding optical properties used for mineral identification via this technique.

The thin section surface micrographs were captured using a Zeiss polarising geology microscope attached to a Canon camera. Images were managed using Zoombrowser-X

Canon imaging software. Photographs were taken in transmitted and reflected light, in polarised and cross-polarised planes, using various magnifications (5 x, 10 x and 50 x objectives).

3.2 MICROBIAL CULTURES

Metallosphaera hakonensis (DSMZ7519) was investigated. Microorganisms were cultivated in defined media (DSMZ, Appendix A) in Erlenmeyer flasks on orbital shakers operating at 180 rpm. *M. hakonensis* was cultured on Mackintosh basal salts medium (Appendix A) with ferrous sulphate (20 g L^{-1}) at pH 2.5. *M. hakonensis* was also maintained on elemental sulfur (1.6 % wt vol^{-1}) serving as an energy source at 65°C.

Sub-culturing of microorganisms grown under shake flask conditions took place twice weekly with 30% of the liquid volume in the flask, removed and replace with fresh media. Sub-culturing was done under sterile conditions, by flaming the mouth of all feed and culture containing vessels at each sub-culturing event, in a fume hood. Morphology of microorganisms was routinely monitored using an Olympus microscope and 1000 times magnification. Due to the frequency of sub-culturing, it was assumed that microorganisms remained in an actively growing state.

The ferrous grown *M. hakonensis* was weaned onto a suspension of 0K media at pH 2.5 containing 0.67% (wt vol^{-1}) chalcopyrite mineral concentrate (Goldfields). The weaning procedure involved the addition of 2 g of a chalcopyrite concentrate to an actively growing ore free microbial culture having a final liquid volume of 300 ml. This culture was then sub-cultured twice a week for one month with 30% of the actively growing culture removed and the volume of the solution made up by the addition of basal salts medium at pH 2.5. A mass of 0.5 g of a chalcopyrite concentrate was added at each sub-culturing event to account for any loss of mineral during the sub-culturing procedure. Mineral adapted cultures were maintained through sub-culturing twice weekly.

3.3 REACTOR CONFIGURATION

3.3.1 Biofilm reactor configuration

The biofilm reactor consisted of sealed rectangular vessel, connected to a peristaltic pump. The reactor housed 4 chambers (each 78 x 26 mm) in which the mineral thin sections were mounted at a slight decline to allow unidirectional fluid-flow. Feed was distributed evenly as a thin film over the surface of the mineral thin section (at a rate of 60 µl min^{-1}), simulating the trickling fluid-flow of the leach liquor percolating through an industrial heap. A schematic representation of the biofilm reactor is presented in Figure 3.1.

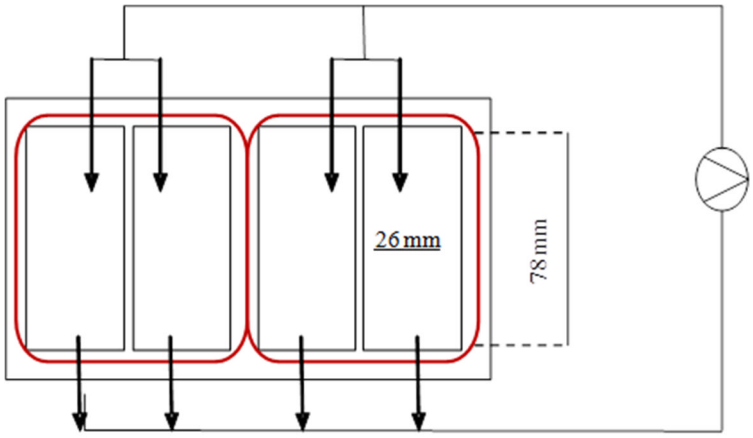

Figure 3.1: Schematic representation of the biofilm reactor configuration (left) and fluid flow operation (right).

3.3.2 Biofilm reactor operating conditions

The biofilm reactor was housed in an incubator, allowing temperature control at 20 ± 1°C, 45°C and 65°C. The reactor chambers were continuously charged with humidified air to minimise evaporative losses and ensure aerobic growth conditions. The reactor was inoculated with the microorganisms under investigation and operated mono-septically as a closed recycle for the duration of the inoculation period. Post inoculation it was run as a continuous flow through system, with fresh basal salts medium (pH 2.0) introduced continuously for 2, 4 or 8 days at the temperature under investigation. Biofilm formation on chalcopyrite, pyrite, and a low-grade chalcopyritic ore was assessed. A borosilicate (glass) slide was used as a control surface to assess non-specific attachment. After the

specified incubation time, the chambers were drained, the mineral sections removed carefully and the surface gently washed with basal salts medium (pH 2.0) followed by milliQ water and subjected to fluorescent staining and various forms of microscopy. The residence time was calculated to be 5.6 hours. The linear velocity was calculated to be 7.69E-05 m s^{-1} which is in the same order of magnitude experienced in commercial heap systems. (Appendix D).

3.4 ANALYTICAL TECHNIQUES

3.4.1 Determination of pH

All pH measurements were performed using a Metrohm 704 pH metre and probe, which was calibrated at pH 7.0, pH 4.0 and pH 1.0 before each use.

3.4.2 Iron assay

The methodology for the determination of ferrous and ferric iron content in samples utilised 1-10-phenanthroline as an indicator for the presence of iron (Harris 2003).

3.4.3 EPS chemical characterisation

As discussed in Section 2.7, microbial EPS is commonly comprised of a combination of polysaccharides, DNA, uronic acids, lipids and proteins. Standard biochemical colorimetric assays were used to quantify EPS components. These were carried out in triplicate with DNA was measured using a Nanodrop 2000 spectrophotometer (Thermo Scientific).

3.4.3.1 EPS sugar content analysis

Neutral hexose sugar content of the EPS was determined using a combination of the Dubois assay (Dubois *et al.* 1956), using glucose as a standard, and an assay modified by Michel *et al.* (2009) which incorporated ferric iron into the glucose standard to correct for any inference caused by the presence of iron. The Dubois assay only provides a quantitative indication of sugar content. In order to gain more detailed information on the

sugar monomers present in the polysaccharides extracted, samples were sent to the Centre for Analytical (CAF; Stellenbosch University) for analysis using gas chromatography mass spectroscopy (GSMS).

3.4.3.2 EPS protein content analysis

Protein content was determined using the Bradford assay (Bradford 1976). Bovine serum albumin (BSA) serum was used as a standard (standard curve for concentrations 0 – 300 $\mu g ml^{-1}$ created) together with Bradford reagent (Bio-Rad). The protein from EPS was further analysed through the use of SDS-Polyacrylamide Gel Electrophoresis (PAGE) gel electrophoresis, according to Laemmli (1970), to determine whether similar sized proteins were present in all samples or if any visual differences could be observed between the samples due to the culture growth substrate history.

3.4.3.3 EPS Uronic acids content analysis

Uronic acids were measured using the methodology described by Blumenkrantz and Asboe-Hansen (1973).

3.4.3.4 EPS DNA content analysis

An aliquot of 15 µl of each of the extracted, purified *M. hakonensis* EPS samples (colloidal, loosely bound and bound EPS) was treated with 2.7 µl of an EcoR1 restriction enzyme at 37ºC for two hours. Subsequently, DNA gel-electrophoresis (0.9 % agarose and 0.05, $\mu g nl^{-1}$ ethidium bromide, 80 mV, 1 x Tris-borate-EDTA buffer pH 8.0) was performed in order to visualise the presence of DNA. Lambda phage DNA was used as a marker. Where the presence of DNA was evident, the DNA content was measured using a Nanodrop 2000 spectrophotometer (Thermo Scientific). An aliquot of 2 µl of purified EPS sample was placed on the Nanodrop and the concentration measured and recorded.

3.4.3.5 Cell integrity assay for EPS extraction investigation

In order to evaluate whether the composition of the EPS was a true representation of EPS components and not due to contamination caused by cell lysis during the extraction

process, the glucose-6-phosphate-dehydrogenase (G6PDH) activity (Sigma) was measured in extracted EPS samples. The percentage cell lysis caused by the extraction procedure was measured as a percentage of the G6PDH activity observed for complete cell lysis according to Platt et al. (1985) and Rashid et al. (2002).

3.4.3.6 Chemical oxygen demand analysis to determine the presence of organic matter in the EPS samples extracted

The chemical oxygen demand of (cell free) EPS samples extracted from *M. hakonensis* were assayed using the potassium dichromate method (Rice *et al.* 2012) and spectrophotometry (optical density reading at 620 nm) to verify presence of organic matter in the extracted EPS samples.

3.5 ENUMERATION OF CELL CONCENTRATION

The concentration of the inoculum (cells ml^{-1}) was determined microscopically using a Thoma counting chamber and an Olympus epifluorescent microscope using 1000x magnification (under oil emersion). The formula used for calculating cell concentration per ml using microscopy and a Thoma counting chamber was as follows:

$$Volume\ of\ one\ small\ square = depth * area$$
$$= \frac{0.02x(0.05x0.05)}{1000}$$
$$= 5x10^{-8}\ cm^3 \qquad \text{(Eqn 6)}$$

$$Concentration\ totall\ (cells\ ml^{-1}) = dilution\ factor\ x\ \frac{(cell\ count\ x\frac{N}{n})}{volume\ one\ square\ x\ total\ number\ of\ small\ squares} \qquad \text{(Eqn7)}$$

Where N = total number of big squares (16)
n = number of squares counted (4).

3.6 INOCULUM PREPARATION

For colonisation studies, microbial cultures used were subjected to low speed centrifugation (2000 rpm at 20 °C; Beckmann) to remove precipitates. Cells were subsequently harvested by centrifugation (10000 rpm at 4 °C; Beckmann) and the cell pellet re-suspended in basal salts medium (pH 2.0). The cell concentration was then

determined microscopically, as described in Section 3.5. The inoculum was then diluted, if necessary, with basal salts medium in order to achieve the desired cell concentration. For EPS production and extraction, 5L Schott bottle reactors were inoculated with a 10% (vol^{-1}) of an actively growing *M. hakonensis* culture ($1x10^8$ cells ml^{-1}) and cultured until the onset of early stationary phase.

3.7 FLUORESCENT PROBES

3.7.1 Fluorescence techniques for visualising attached cells

Samples were counter stained for 10 minutes using 10 µl of a 1µg ml^{-1} 4', 6-diamidodino-2-phenlyindole solution (DAPI, Sigma Chemical Co) or SYTO9™ (Invitrogen©) per 1 cm^2 of sample area in order to visualised attached cells. Samples were then rinsed with distilled water and dried using compressed air in the dark. The surface of the sample was then embedded using and antifade containing mounting medium VECTASHIELD® (Vector laboratories, CA, U.S.A.) or Citifluor™. The fluorescence was visualised using an *Olympus* epifluorescent microscope and a confocal laser scanning microscope. For visualisation with the *Olympus* epifluorescent microscope, ultraviolet (UV) and interference blue (IB) filters were used, allowing visualisation of DAPI (excitation λ 372 nm and emission λ 456 nm) and SYTO9™ (excitation λ 483 nm and emission λ 503 nm) fluorescence respectively (Appendix C, Table E3). Images were captured and managed using the AxioVision (Carl Zeiss, Germany) and ImageJ (Abramoff *et al.* 2001).

3.7.2 Fluorescent labelled lectin probes for EPS visualisation

Lectins are defined as carbohydrate binding proteins, isolated from a variety of plant and microbial sources, with defined binding specificities and which bind without enzymatic or antibody activity (Barondes *et al.,* 1988). Within the context of this study, fluorescently labeled lectins were used as a positive indicator for the presence of EPS and thus development of the *M. hakonensis* biofilm. A total of 77 lectins (EY Laboratories Inc., Vector Laboratories Inc., Sigma) labelled with either fluorescein isothiocyanate (FITC), tetramethyl rhodamine isothiocyanate (TRITC) or Alexa568 were used for EPS screening, summarised in Table 3.4. These were prepared at a concentration of 100 µg mL^{-1}, in sterile milliQ water. The staining procedure involved gently pipetting 1 ml of individual lectin-staining solutions over the mineral surface of interest and incubating at room temperature in the dark for 20 minutes. The surface was then rinsed gently three times with sterile milliQ water to remove excess stain.

A nucleic acid counter stain was added to the mineral surface and incubated for 10 minutes at room temperature in the dark, before being washed off with sterile milliQ water.

3.8 MICROSCOPY

3.8.1 Confocal laser scanning microscopy (CLSM)

A laser scanning module (LSM 510 Carl Zeiss® Jena) coupled to an inverted Axiovert 100 M BP microscope (Zeiss®) was used and operated using the ZEN LSM 510 Release 3.2 (Zeiss®) software. The appropriate laser excitation wavelengths and optical filters for detection of the fluorophores of interest were used (Argon laser: 488 nm, 505 – 550 nm bandpass filter; Helium neon laser: 543 nm, > 560 nm long pass filter) with constant laser excitation energies and detector settings. All micrographs were attained using a Plan-Neofluar® 100 x 1.3 oil immersion objective. For CLSM work, samples were mounted in an anti-fading agent VECTASHIELD® (Vector laboratories, CA, U.S.A.) prior to visualisation. Images were analysed and surface area covered by cells quantified using ImageJ software (Abramoff *et al.* 2004).

The lectin screening assays made use of a TCS SP5X (Leica, Germany) equipped with upright microscope. An acusto optical beam splitter, and a supercontinuum light source was used (470 -670 nm) together with the appropriate filter settings for detection of fluorophores. The system was controlled by the LAS AF software version 2.6.1. Samples were examined by the 63 × 1.2 NA (high resolution) objective lens.

3.8.2 Combined atomic force&epi-fluorescent microscopy (AFM-EFM)

Intimate and specific associations between the mineral and microbial surfaces were visualised using a Nano Wizard II atomic force microscope (JPK Instruments Germany) aligned to an upright Epifluorescence microscope (AxioImager A1m; Zeiss, Germany) using a BioMaterialWorkstation (JPK Instruments) as described by Mangold *et al.* (2008). The shuttle stage of the BioMaterialWorkstation allowed the mineral section to be transferred between the EFM and the AFM maintaining the position of the sample area under investigation. Thus, the same region could be visualised under both microscopes with an approximate error of only 3-5 µm (Mangold *et al*. 2008) enabling a high level of precision. A CS37/8 silicon cantilever (Mirkomasch, Estonia) was employed for AFM

surface imaging and was operated in intermittent contact mode in air. Attached cells were visualised by staining with DAPI or SYTO9® for 10 minutes prior to AFM/EFM analysis of the surface. In addition, EPS was visualised through staining with the TRITC- or FITC-labelled lectin, ConA (50 µg ml^{-1}), for 20 minutes prior to AFM/EFM analysis. The fluorescence was visualised at 1000 fold magnification using the appropriate filters.

3.9 DATA ANALYSIS

The following section presents a description of the method used to quantify the attachment per surface area available (Section 3.9.1) and the approach for quantifying total EPS extracted (Section 3.9.2).

3.9.1 Quantification of maximum attachment per unit surface area

Quantification of the attachment per available surface area was performed by taking the following into consideration:

- Repulsive forces between cells and minerals were ignored
- Attachment was assumed to be mono-layered with cells orientated such that the major axis was parallel to the surface of the mineral
- Dimensions of a *M. hakonensis* cell, along its longest axis, is approximately 1.1 x 0.9 µm (Kurosawa *et al.* 2003)

The total surface area made available by the mineral thin sections ($75x10^{-3}$ m X $25x10^{-3}$ m) housed in the reactor was calculated to be $1.875x10^{-3}$ m^2. Therefore, the maximum number of *M. hakonensis* cells that could be accommodated by the available surface area in the reactor was calculated to be 1.9 x 10^9 cells. This was done by dividing the total surface area made available for attachment by the mineral, by the surface area per microbial cell in terms of its longest axis. This number will be subsequently referred to as the saturation cell number. Attachment efficiency per unit surface area was estimated by dividing the surface area covered by the cells attached to the mineral surface at the end of the experimental run by the total surface area available for attachment as shown. ImageJ software was used to determine the number of cells attached to the mineral surface at the end of the experimental run. An explanation of this methodology is detailed in Appendix B.

3.9.2 Quantification of extracted EPS

Duplicate 1 ml samples of extracted EPS were taken and lyophilised to determine the dry weight per ml. The total mass of EPS extracted was then extrapolated and quoted as a mass extracted per $1x10^{10}$ cells. Normalising the EPS extracted as a mass per $1x10^{10}$ cells allowed comparisons to be drawn across the experimental runs and known literature values for EPS extracted using the same methodologies and for EPS extracted acidophilic microorganisms relevant to the bioleaching field.

3.10 EXPERIMENTAL DESIGN AND RATIONALE

3.10.1 The use of lectins for EPS visualisation and characterisation

Lectins are carbohydrate binding proteins and are very specific in their interaction with carbohydrate moieties. In this study, lectins were employed in combination with CLSM to enable the *in situ* visualisation and chemical characterization of EPS from planktonic (Section 3.10.1.1) and sessile (mineral-associated) communities (Section 3.10.1.2).

3.10.1.1 Visualisation of EPS from planktonic cells

A 10 ml aliquot of planktonic *M. hakonensis* cells, grown on either sulfur or chalcopyrite mineral grains until stationery phase and having a final cell concentration of ± 1 x 10^8 cells ml^{-1} was harvested on to 0.22 µm filter paper using a vacuum filter apparatus (Figure 3.2). No centrifugation step was included in the extraction protocol in order to maintain the colloidal EPS fraction. Subsequently, 10 ml of sterile Mackintosh basal salts medium (Mackintosh 1978), as used in the growth medium, was passed through the filter paper once to wash the surface gently. The nucleic acid stain, SYTO9™ was used as a counter stain to visualise cells within the EPS. Therefore, the surface of the filter was stained with 100 µl SYTO9™ (working solution 100 $\mu g ml^{-1}$) for 30 minutes in the dark, at room temperature, and then rinsed with milliQ water. A suite of five fluorescently-labelled lectins (Table 3.3) were then assayed to determine the presence of any EPS carbohydrate bearing components.

Table 3.3: A list of the 5 fluorescently labelled lectins used to detect the presence of EPS. EPS is detected through binding of lectins with carbohydrates associated with EPS resulting in positive fluorescence. Lectins used were labelled with either TRITC or FITC.

Lectin	Abbreviation	Binding specificity
Canavalia ensiformis (concanavalin A)	ConA	α-glucose, α-mannose

Griffonia (Bandeiraea) *simplicifolia*	GS-I	α-galactose, α-galNac
Arachis hypogaea (peanut agglutinin)	PNA	Galactose, β-D-Glc(1-3)-D-galNAc
*Triticum vulgaris (*wheat germ agglutinin)	WGA	Chitobiose containing molecules, GlcNac
Phaseolus vulgaris	PHAE	Terminal galactose; N acetylglucosamine

Briefly, the surface of the filter was stained with the fluorescently labelled lectins (working concentration of 50 µg ml^{-1}), for 30 minutes in the dark at room temperature. The lectin stain was then removed by rinsing the surface of the filter with sterile milliQ water. VECTASHIELD® was used as a mounting medium and the resulting fluorescence, indicating the presence of carbohydrate components found in EPS and thus the presence of EPS, was then visualised using CLSM (see Section 3.8).

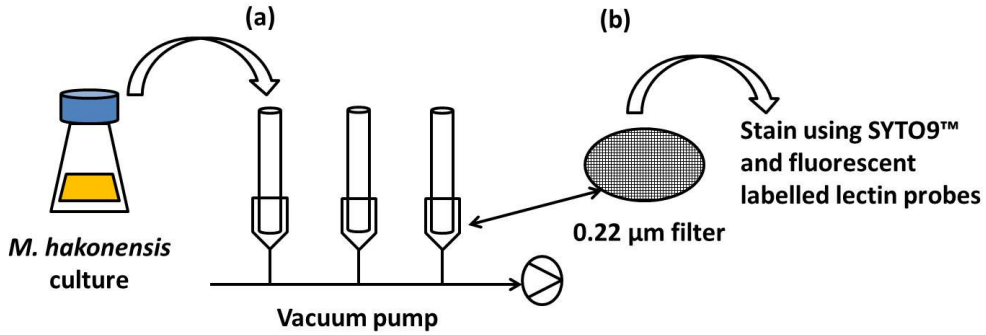

Figure 3.2: Schematic representation of the lectin staining procedure to determine the presence of EPS produced by *M. hakonensis* grown in batch agitated systems on sulfur or chalcopyrite. (**a**) A total volume of 10 ml of culture (±1x10^{8} cells ml^{-1}) was filtered onto sterile 0.22 µm vacuum filters using a vacuum pump, which was followed by a wash step (10 ml of basal salts medium pH 2.0 filtered through the system); (**b**) the sample was then stained using SYTO9™, washed, stained with an appropriate fluorescently-labelled lectin before visualising using CLSM.

3.10.1.2 Lectin screening approach

Lectins are carbohydrate binding proteins and are specific in their interaction. In this investigation, lectins were employed to characterise EPS from sessile (mineral-associated) *M. hakonensis* communities *in situ*. Two culturing techniques were employed which allowed us to assess the effect of differences in hydrodynamics and mineral contacting during cultivation and cell growth to be assessed. In the first approach, *M. hakonensis* was cultured on chalcopyrite grains (2 % wt.vol^{-1}) suspended in Mackintosh media at pH 2.5, in shake flasks at 65 ºC and agitated at 160rpm until stationery phase (Figure 3.3 A). The chalcopyrite grains, together with some of the spent media, were removed and stored in sterile 50 ml falcon tubes and transported to the Helmholtz Centre for Environmental Research (Magdeburg, Germany) for analysis. For lectin screening, the chalcopyrite

grains were fractioned into 2 ml Eppendorf tubes and washed three times with 1 ml sterile milliQ water via aspiration with a pipette and exchange of the liquid suspending medium. The water was removed and a 100 µl aliquot of lectin probe (working solution of 100µgml^{-1}) added. A total of 77 lectins (Table 3.4) were assessed. Samples were incubated for 20 minutes in the dark after which the lectin probe was rinsed off with 2 ml of water using repeated pipette aspiration.

Table 3.4: List of lectins used for screening of the EPS from *M. hakonensis* cultured on chalcopyrite mineral grains. Lectins were labelled with either FITC or TRITC.

Lectin abbreviation	Organism isolated	Specific binding affinity
AAA	*Anguilla anguilla*	α-fucose
ABA	*Agaricus bisporus*	β-gal, gal(β1,3)galNAc
ACA	*Amaranthus caudatus*	gal(β1,3)galNAc, gal(β1,3)Neu5Ac
AIA	*Artocarpus integrifolia*	α -gal, gal(β1,3)galNAc
AMA	*Arum maculatum*	
APP	*Aegopodium podagraria*	α-galNAc, β-galNAc
ASA	*Allium sativum*	
BDA	*Bryonia diocia*	α-galNAc, β-galNAc
BPA	*Bauhinia purpurea*	α-galNAc, β-galNAc, gal(β1,3)
CA	*Colchicum autumnale*	lac, gal, galNAc
CAA	*Caragana aborescens*	α-gal, β-gal, galNAc
Calsepa	*Calystegia sepium*	mannose
ConA	*Concanavalin A*	α-man,α-glc,α-glcNAc, branched mannoses
CPA	*Cicer arietinum*	
CSA	*Cytisus scoparius*	β-gal, galNac, lac
DBA	*Dolichos biflorus*	terminalα-galNAc,galNAc(α 1,3)galNAc
DGL	*Dioclea grandiflora*	
DSA	*Datura stramonium*	glcNAc(β1,4)glcNAc oligomers, gal(β1,4)
ECA	*Erythrina cristagalli*	gal(β1,4)glcNAc, galNAc gal
EEA	*Euonymus europaeus*	gal(α 1,3)gal, gal(α1,3)Fuc(α 1,2)gal
GHA	*Glechoma lederacea*	
GNA	*Galanthus nivalis*	α-man, man(α 1,3)man5
GS-1	*Griffonia (Bandeiraea) simplicifolia*	α-gal, α-galNAc
HAA	*Helix aspersa*	galNAc, glcNAc
HHA	*Amaryllis*	α-man, polymannose structures
HMA	*Humarus americanus*	
HPA	*Helix pomatia*	α-galNAc
IRA	*Iris hybrid*	
LAA	*Laburnum alpinum*	β-glcNAc, glcNAc(β1,4)glcNAc
LAL	*Laburnum anagyroides*	
LBA	*Phaseolus lunatus*	galNAc(α 1,3)[L-fuc(α1,2)gal], galNAc
LcH	*Lens culinaris*	α-man, fucose, α-glc, α-glcNAc
LEA	*Lycropersicon esculentum*	glcNAc(β1,4)glcNAc oligomers
LFA	*Limax flavus*	
Lotus	*Tetragonolobus purpurea*	terminal α-fucose
LPA	*Limulus polyphemus*	NeuAc
MAA	*Maackia amurensis*	NANA(α 2,3)gal, sialic acid
MNA-G	*Morus nigra agglutinin*	galactose
MOA	*Marasmium oreades*	

MPA	*Maclura pomifera*	α-gal, α-galNAc, gal(β1,3)galNAc
NPA	*Narcissus pseudonarcissus*	binds internal and terminal α-man groups
PHA-E	*Phaseolus vulgaris*	galNAc
PHA-L	*Phaseolus vulgaris*	galNAc
PMA	*Polygonatum*	
PNA	*Arachis hypogaea*	β-gal, gal(β1,3)galNAc
PSA	*Pisum sativum*	α-man, α-glc, α-glcNAc
PSL	*Polyporus squamosus*	
PTA	*Psophocarpus tetragonolobus*	β-gal, galNAc
PWA	*Phytolacca americana*	glcNAc(β1,4)glcNAc oligomers,
RPA	*Robinia pseudoaccacia*	NI
SBA	*Glycine max*	terminal α- or β-linked galNAc
SJA	*Sophora japonica*	β-galNAc
SNA	*Sambucus nigra*	β-gal, sialic acid
STA	*Solanum tub*	β-glcNAc, glcNAc(β1,4)oligomers
TKA	*Trichosanthes kirilowii*	gal, β-gal oligosaccharides
TL	*Tulipa sp.*	galNAc
UDA	*Uritica dioicia*	glcNAc(β1,4)glcNAc oligomers
UEA	*Ulex europaeus*	Fucose
VFA	*Vicia faba*	man, glc
VGA	*Vicia graminea*	NI
VRA	*Vigna radiata*	α-gal
VVA	*Vicia villosa*	galNAc, α-galNAc, galNAc(α 1,3)gal
WFA	*Wisteria floribunda*	terminal galNAc(β1,4) and galNAc(β1,3)
WGA	*Triticum vulgaris*	Chitobiose containing molecules
AAL - Alexa	*Aleuria aurantia*	Fucose and rhamnose specific
CCA	*Cancer antennarius crude*	NeuAc, 9-O-Ac-NeuAc, 4-O-Ac-NeuAc
Co	*Codium fragile*	galNAc
Ecor	*Erythrina corallodendron*	gal(β1,4)glcNAc, galNAc, lac gal
HMA	*Homarus americanus crude*	Sialic acid
IAA	*Iberis amara*	GlcNac
MIA	*Mangifera indica crude*	NI
PAA	*Perseau americana crude*	
PA-1	*Psuedomonas aeroginosa*	galactose
PPA	*Ptilota plumosa*	terminal α-gal
RTA	*Trifolia repens crude*	2-deoxyglucose
TML	*Tritichomonas mobilensis*	sialic acid
VGA	*Vicia graminea*	NI

Results were visualised using CLSM (Section 3.8.2). The second approach utilised the cultivation of *M. hakonensis* biofilms on chalcopyrite mineral sections within the biofilm reactor (Sections 3.3 and 3.11; Figure 3.3 B). The slides were removed after 4 days and placed in sterile falcon tubes containing 1 – 2 ml Mackintosh basal salts media. Lectins which resulted in positive fluorescence from the screening of the chalcopyrite mineral grains, were then used to stain the surface of the chalcopyrite mineral section and the results visualised using CLSM (Section 3.8.2).

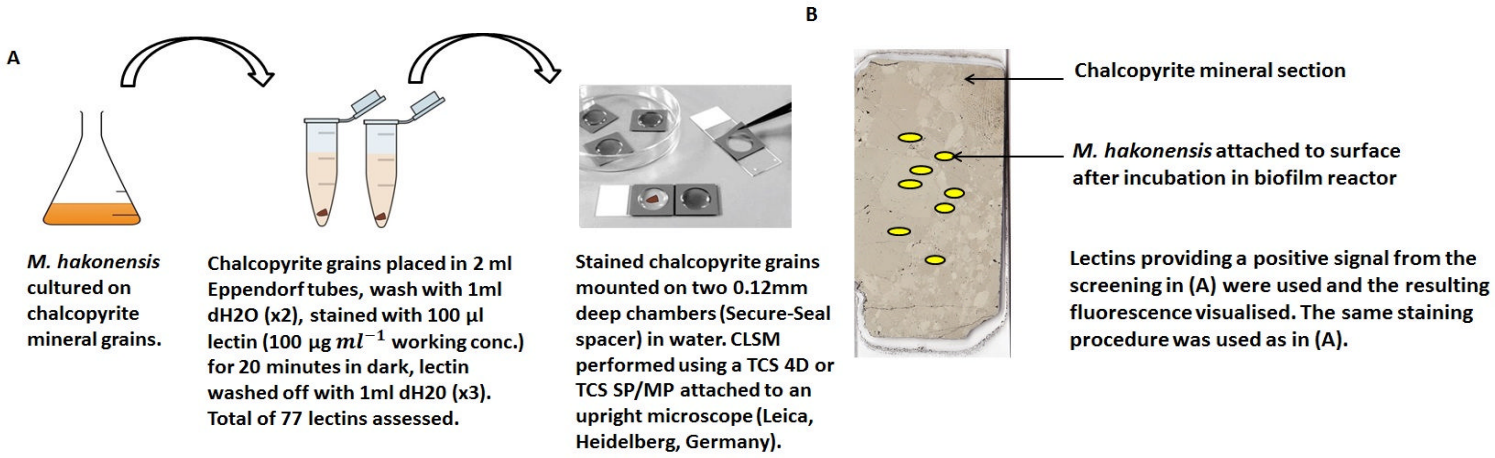

Figure 3.3: Schematic representation of the approach used for visualising planktonic *M. hakonensis* cells (**A**) and sessile cells contacted with chalcopyrite under two varying conditions of mineral contacting and fluid flow (**B**).

3.10.2 EPS cultivation and extraction methodology

The effect of culture history and growth substrate on the quantity and composition of EPS produced by *M. hakonensis* DSMZ7519 was investigated in a series of experiments. Briefly, the experiments were conducted in duplicate and EPS extractions, from each reactor, were carried out in parallel to minimize variances introduced by culture or growth conditions or both. *M. hakonensis* DSMZ7519, was grown in Erlenmeyer flasks as previously described, in DSMZ 88 medium containing sulfur (1.6 % wtvol^{-1}), ferrous sulphate (20 g L^{-1}) or chalcopyrite mineral grains (2 % wtvol^{-1}) as an energy source. The actively growing culture was then used as a 10% vol^{-1} inoculum to achieve a cell concentration following inoculation of approximately 1 x 10^7 cell mL^{-1}, for duplicate 5 litre (L) Schott bottle reactors to increase the volume of the culture on the corresponding substrate. Reactors were vigorously aerated making provision for mixing and aerobic growth until early stationary phase. Each Schott bottle reactor had a working volume of 5L and a final cell concentration of approximately 1 x 10^8 cells mL^{-1}. Colloidal EPS was then recovered and capsular or bound EPS extracted in a step-wise manner, as described below.

The colloidal EPS fraction was recovered by centrifugation (7,500 rpm for 20 min at 4°C; Beckman Avanti Centrifuge) of the 5L culture volume. The efficiency of cell recovery to the pellet was calculated to be 98%. Samples of the supernatant, containing the colloidal EPS fraction, were collected and stored at 4ºC for further processing. The harvested cell pellet, which was assumed to contain all of the cell biomass in the culture ± 2%, was washed by gentle re-suspension in 40 mL of Mackintosh basal salts medium (pH 2.5) followed by centrifugation as described above. The supernatant fraction, containing loosely bound or associated EPS, was retained and stored at 4ºC for further processing. The bound or capsular EPS fraction was recovered from the cell pellet using 10 mL of 10 mM EDTA based on Gehrke *et al.* (1998), Tapia *et al.* (2009) and Michel *et al.* (2009), or 30 mM dicyclohexyl-18-crown-6-ether (CE) in Tris buffer as per Aguilera *et al.* (2008), followed by gentle agitation for 2 hours at 4ºC. A sample was taken from each bound EPS extraction and the presence of the intracellular enzyme glucose-6-phosphate-dehydrogenase (G6PDH) measured, according to Platt *et al.* (1985), to determine the extent of cell lysis during the extraction process. The bound EPS fractions, from the two extraction processes, were subsequently harvested by centrifugation, as previously described, and stored for further processing. A second extraction was then performed on the respective supernatant fractions, by the addition of a further 10 mM EDTA or 30 mM CE, and the samples were agitated for a further 2 hours at 4ºC. As before, the supernatant fractions were harvested by centrifugation and retained for further processing. All the samples were then filtered twice through a 0.22 µm filter (Merck Millipore), before being dialysed (Pur-A-lyzer Mega 20 ml dialysis kit, Sigma Aldrich, 3.5 kDa cut-off) against sterile milliQ water (water volume was always greater than 25 times the total sample volume to be dialysed) for 12 hours with water exchanged twice. Samples were subsequently stored at 4ºC until quantitative chemical characterisation was carried out. The EPS dry weight was determined, in duplicate, following lyophilisation of 1 mL fractions of the stored samples. A schematic of the EPS cultivation and extraction approach can be found in Figure 3.2.

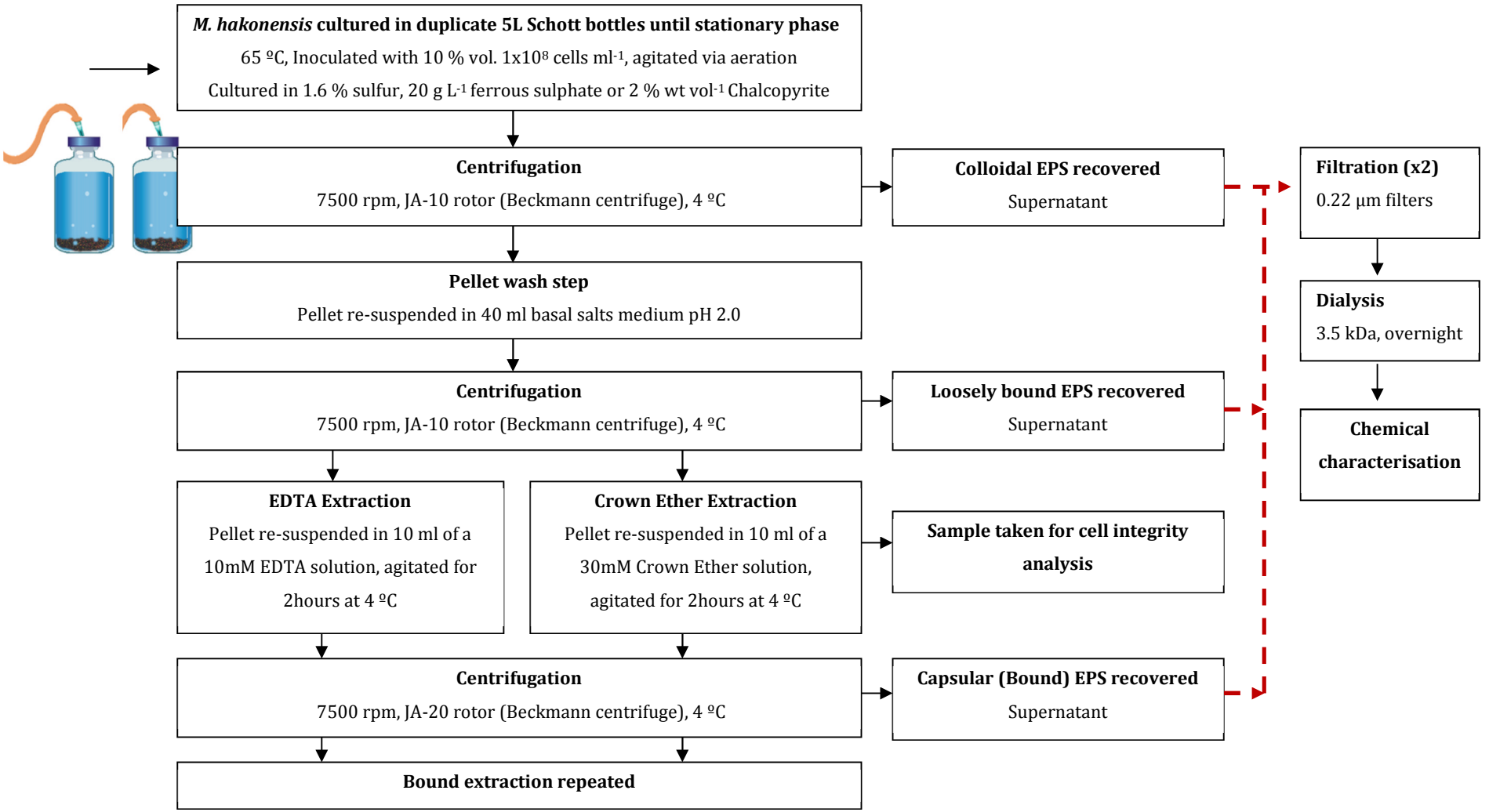

Figure 3.4: Schematic representation of the EPS cultivation and extraction approach utilised.

3.10.3 Biofilm reactor approach for *in situ* visualisation of colonisation and biofilm formation

The aim of this study was to develop a novel, integrated *in situ* approach for the investigation of mineral-microbe interactions. This made use of low grade chalcopyrite ores and mixed microbial consortia under conditions which simulated heap attachment dynamics. This enabled spatial attachment of microorganisms to mineral surfaces to be studied; including the establishment of more permanent microbe-mineral interactions and the development and structure of microbial communities. Thinly sectioned massive or low grade chalcopyrite containing mineral ore (100 µm and 1 mm thick for low-grade and massive sections respectively) mounted onto glass slides (7.5 x 2.5 cm) were used. These sections were mapped mineralogically using ore microscopy and photographic analysis (explained earlier in Section 3.1.3). The surface of the sections were gently wiped clean with acetone followed by acidified water (H_2SO_4 pH 1.8), before being rinsed with distilled water. Following this, the sections were placed in a biofilm reactor and subsequently inoculated with a pure culture of *M. hakonensis*. The inoculum was prepared as described previously. The design of the reactor allowed feed to be distributed evenly as a thin film over the surface of the mineral thin section. This simulated the trickling fluid flow of the leach liquor percolating through an industrial heap.

Inoculum concentrations used in column studies conducted at the Centre for Bioprocess Engineering Research ranged from 10^5 to 10^9 cells kg^{-1}. The biofilm reactor was operated using an inoculum with a final concentration of 1 x 10^8 cells ml^{-1} suspended in 40 ml of basal salts medium. The reactor was operated as a closed recycle for the inoculation period (12 hours), allowing a contact period of the microorganisms with the mineral surface. Subsequently it was operated as a continuous flow-through system with fresh basal salts medium, continually passing through the system. The duration of the experiment ranged from 2 to 8 days. A flow rate of 60 µl min^{-1} was used which equates to a linear velocity of 7.8 x10^{-5} m s^{-1}. This linear velocity is comparable to that typically found in heap environments, where linear velocities of 1.4 x 10^{-6} m s^{-1} are reported (Information used for industrial heap linear velocity calculation was supplied courtesy of BHP Billiton. Calculations are found in Appendix D). Assumptions made include perfect plug, laminar flow, negligible friction and a constant flow rate of 60 µl min^{-1}. Once colonised, the thin section was removed from the reactor and the attached cells visualised through the use of fluorescent stains (FISH) explained in Section 3.7.2, and a combination of epifluorescent, confocal and atomic force microscopy techniques explained in Section 3.8.

The results of the FISH procedure were compared to the mineralogical maps compiled and the spatial locale, distribution and relative abundance of the attached microorganisms assessed. The effect of temperature on colonisation and biofilm formation of *M. hakonensis* on massive and low-grade sulfide mineral bearing ores was also assessed. Experiments were conducted at room temperature (20 ± 1 °C), 45 °C and 65 °C and the extent of colonisation and EPS production assessed using *in situ* using fluorescent staining and microscopy (CLSM, AFM and EFM).

References

Abramoff M. D., Magelhaes P.J., Ram S.J., 2001 Image processing with ImageJ. *Biophotonics International*. 11, 36 - 42

Anon. "Sigma Modified Lowry Protein Assay," Sigma Procedure No. P 5656

Blumenkrantz and Asboe-Hansen 1973, A New method for quantitative determination of uronic acids. *Anal. Biochem.* 54 (2):484-9

Bradford, M. 1976 "A Rapid and Sensitive Method for the Quantitation of Microgram Quantities of Protein Utilizing the Principle of Protein-Dye Binding" *Anal. Biochem*. **72:**248-254.

Dubois M., Gilles K. A., Hamilton J. K., Rebers P. A., Smith F. (1956) Colorimetric method for determination of sugars and related substances. *Anal. Chem.* 28: 350-356

Gehrke, T., Telegdi, J., Thierry, D., & Sand, W. (1998). Importance of extracellular polymeric substances from *Thiobacillus ferrooxidans* for bioleaching. *Applied and Environmental Microbiology* , **64:** 2743-2747.

Harris, C. D. (2003). Quantitative Chemical Analysis 6th Ed. 18-8, 18-9.

Kurosawa N., Itoh Y., Itoh T. (2003). Reclassification of *Sulfolobus hakonensis* Takayanagi *et al.* 1966 as *Metallospheara hakonensis* comb. Nov. based on phylogenetic evidence and DNA G+C content. *International Journal of Systematic and Evolutionary Microbiology.* **53**: 1607 – 1608

Laemmli U.K., (1970) Cleavage of structural proteins during the assembly of the head of bacteriophage T4. *Nature* 227 (5259): 680-5

Platt R.M., Geesey G.G., Davis J.D., White D.C., 1985. Isolation and partial chemical analysis of firmly bound exopolysaccharide from adherent cells of a freshwater sediment bacterium. *Canadian Journal of Microbiology* 31, 675-680.

Rice, E.W. et al. *Standard Methods For The Examination Of Water And Wastewater, 22Nd Edition ISBN: 9780875530130 Author: E.W. Rice, R.B. Baird, A.D. Eaton, L.S. Clesceri, Editors Publisher: American Public Health Association, American Water Works Association, Water Environment Federation*. 22nd ed. American Public Health Association, American Water Works Association, Water, 2012. Print.

Rashid N., Imnaka H., Kanai T., Fukui T., Atomi H., Imnaka T. (2002). A novel candidate for the true Fructose-1,6-bisphosphatase in archaea. *The Journal of Biological Chemistry.* 277(34) 30649-30655.

Schrenk, M.O., Edwards, K.J., Goodman, R.M., Hamers, R.J., Banfield, J.F., (1998) Distribution of *Thiobacillus ferrooxidans* and *Leptospirillum ferrooxidans*: implications for generation of acid mine drainage. *Science,* 287 (1998), 1519–1522

Chapter 4:

Visualisation of the *Metallosphaera hakonensis*-EPS interfacial environment

4.1 INTRODUCTION

Microbial biofilms may be the predominant form of microbial life and can be defined as communities of sessile microorganisms which aggregate at the gas-liquid or solid-liquid interface and are enveloped in a matrix composed of an extracellular polymeric substance (EPS). In spite of the fact that the microbial-mineral-EPS interface is likely the major active site of both microbial oxidation and mineral dissolution activity (Schippers and Sand 1999, Tributsch 2001, Crundwell 2003, indirect contact mechanism discussed in Chapter 2.1.3); little is known of these interfacial environments in heap bioleach systems. Studies involving microbial-mineral interfacial interactions reported to date for mineral systems have been limited to mesophilic microorganisms, ambient temperature regimes and largely investigated initial adhesion interactions under conditions which were not representative of microbe-mineral contacting or fluid flow in the heap (Chapter 2.9).

This chapter presents studies which demonstrate the presence of EPS produced by the thermophilic archaeon *M. hakonensis*, an industrially relevant thermophile (Bromfield *et al.* 2011). Furthermore, the structure, architecture and composition of microbial-EPS-mineral interfacial environments created under bioleach simulated conditions were investigated using variations in fluid flow and mineral contacting. The study employed non–destructive *in situ* techniques, combining fluorescent labelled lectins and CLSM microscopy. Results providing visual evidence of EPS from *M. hakonensis* cultured on sulphur and chalcopyrite mineral grains are presented in Section 4.2. This is followed by the presentation and discussion of findings of a lectin screening study. The lectin screening study allowed 3 dimensional EPS architectures of *M. hakonensis* grown under two mineral contacting conditions to be visualised: namely, growth on chalcopyrite mineral grains in batch agitated shake flasks, and growth on a mineral section in a biofilm reactor under conditions simulating a heap bioleach (Section 4.3). Furthermore, the sugar composition of *M. hakonensis* EPS formed under the growth conditions imposed could be elucidated through positive binding with lectins used in the screening process. A summary with conclusions drawn from this chapter is presented in Section 4.5.

4.2 DETECTION AND VISUALISATION OF EPS PRODUCED BY *M. hakonensis*

M. hakonensis was cultured in shake flasks on sulphur or chalcopyrite, the cells harvested and assessed for the presence of EPS using fluorescently labelled lectin stains combined with CLSM. The methodology is outlined in Section 3.10.1.1. Results and discussion are presented in terms of EPS localisation and architecture, the effect of growth substrate on EPS and the use of lectins to characterise EPS glycoconjugate composition.

4.2.1 CLSM analysis of EPS produced by planktonic *M. hakonensis* cells

The relationship of Con-A-binding EPS with respect to *M. hakonensis* was first investigated to ascertain the presence of any EPS production by this microorganism when grown under the conditions of this experiment. Micrographs in Figure 4.1 represent the overlays of planktonic *M. hakonensis* cells cultured on sulphur (Figure 4.1 row A) or chalcopyrite (Figure 4.1 row B) in agitated shake flasks and harvested onto 0.22µm filters. The harvested cells were stained using tetramethyl rhodamine (TRITC) labelled ConA (red) with fluorescein isothiocynate (FITC) labelled Syto9™ as a nucleic acid counter stain (green). ConA fluorescence, in the red channel, is localised in regions immediately around the cell, indicative of capsular EPS. Cells exhibiting positive interaction with the ConA probe could be found disseminated throughout the sample. However, only a certain fraction of cells exhibited positive ConA probe uptake with associated positive red fluorescence. ConA has been demonstrated to bind glucose- and mannose-containing glycogonjugates within the EPS (Neu et al. 2000), thus, the presence of capsular EPS containing glucose and mannose residues in planktonic *M. hakonensis* was not ubiquitous. This trend was observed for both sulphur and chalcopyrite cultured cells.

Of the total number of cells visualised per image, the proportion of cells exhibiting positive interaction with the ConA lectin appeared greater for cells cultured on chalcopyrite relative to cells cultured on sulphur. This significance was quantified using ImageJ software (see Appendix E for method). This allowed statistical evaluation of microbial counts performed in the FITC-SYTO9™ channel, measuring total cells present, in comparison to the proportion of cells which gave positive fluorescence in the TRITC-ConA channel, representing cells with EPS containing glucose and mannose residues.

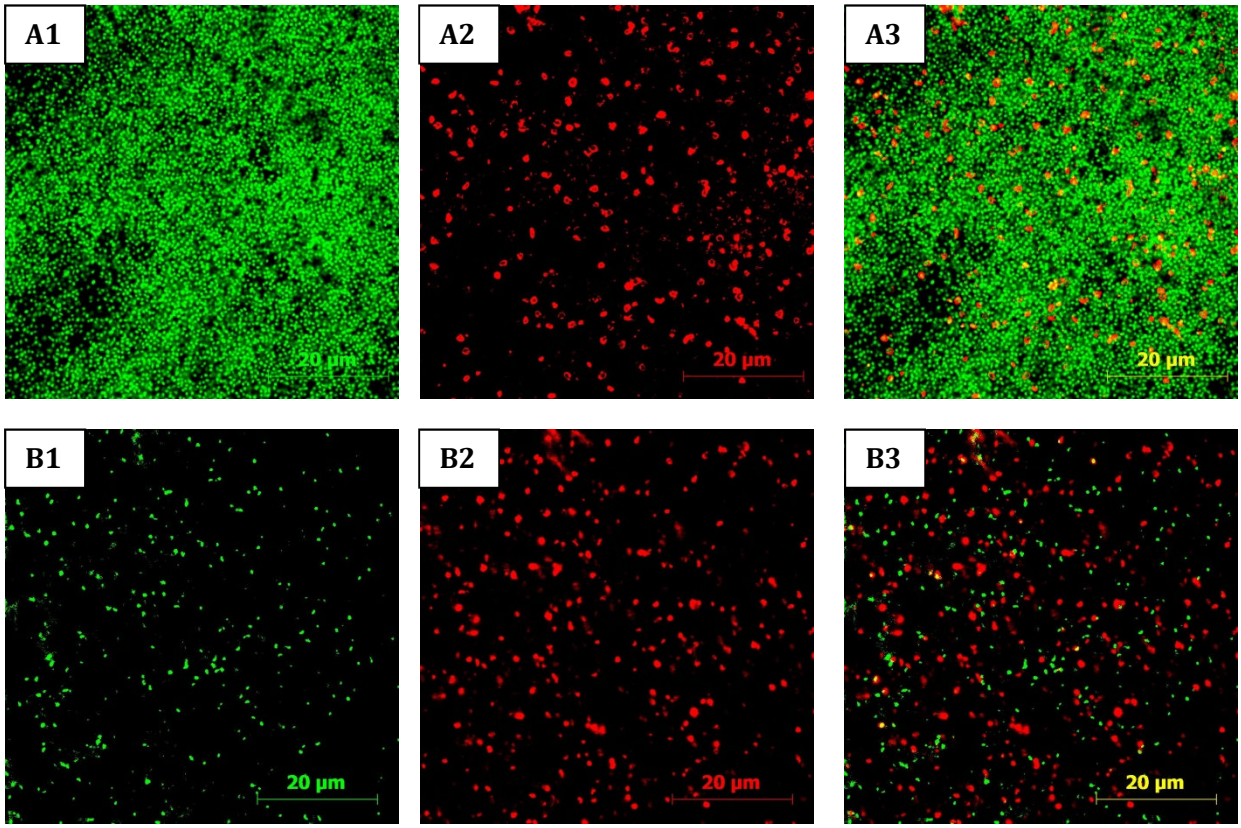

Figure 4.1: Micrographs depict *M. hakonensis* harvested onto 0.22µm filters: (row **A**) sulfur cultured cells; (row **B)** chalcopyrite cultured cells). Images in column (**1**) depict fluorescence of nucleic material due to staining with FITC-labelled Syto9™ visualised using CLSM (LSM 510 Carl Zeiss® Jena). All micrographs were attained using a Plan-Neofluar® 100 x 1.3 oil objective. In column (**2**) red fluorescence due to positive binding of EPS glycoconjugates with TRITC-labelled ConA can be seen. Overlays of the two channels are seen in column (**3**) indicative of EPS glycoconjugates being co-localised to regions immediately around the cell, namely the capsular EPS region.

Cells were assumed to follow a Poisson distribution. They were counted in randomly selected fields until either 20 fields or 400 bacteria were counted, as per Schallenberg *et al.* (1989). Since the lectin probes are specific for different glycoconjugates, positive binding with a particular lectin provided insight into the EPS composition for the planktonic cells grown under the conditions investigated. To further this analysis, a suite of four additional lectins were used to assess the EPS produced by the planktonic *M. hakonensis* cells. This provided insight into the composition of the EPS residues present under various planktonic growth conditions. The results of this analysis are presented in Table 4.1 and provide a qualitative assessment of the extent of the interaction of each lectin with the *M. hakonensis* cells.

Table 4.1: Summary of lectin staining results for *M. hakonensis* grown on various culture media.

Lectin		Binding specificity	Result sulfur grown cells	(%) Cells exhibiting lectin binding	Result chalcopyrite grown cells	(%) Cells exhibiting lectin binding
Canavalia ensiformis, concanavalin A	ConA	α-glucose, α-mannose	**+++**	16	**+++**	**37**
Griffonia (Bandeiraea) *simplicifolia*	GS-I	α-galactose, α-galNac	**-**	-	**+**	**-**
Arachis hypogaea, Peanut agglutinin	PNA	Galactose β-D-Glc(1-3)-D-galNAc	**-**	-	**+**	**-**
Triticum vulgaris, Wheat germ agglutinin	WGA	chitobiose containing molecules, GlcNac	**-**	-	**-**	**-**
Phaseolus vulgaris	PHAE	Terminal galactose; Nacetylglucosamine	**-**	-	**-**	**-**

(+++) very good stain uptake; (-) no visible stain uptake

For planktonic cells cultured on chalcopyrite, 37 % of the cells detected (Table 4.1) exhibited positive interactions with ConA resulting in red fluorescence and thus contained EPS comprised of glucose and mannose. Cells cultured on chalcopyrite thus display enhanced production of EPS relative to planktonic cells cultured on sulfur, as only 16 % (Table 4.1) of cells displayed positive fluorescence with the ConA lectin. The strongest fluorescent signal, under both culture conditions, was observed for the mannose and glucose specific ConA lectin. The micrographs in Figure 4.2 represents overlays of *M. hakonensis* cells harvested onto filters, stained with the various TRITC-labelled lectins (red) and counter stained with FITC-SYTO9™ (green). From the micrographs presented in Figure 4.2 and the tabulated results in Table 4.1, it is evident that limited fluorescence was observed for the galactose specific PNA and GS-I lectins (Figure 4.3, B1 and B2) with no definitive binding patterns evident. No binding or subsequent fluorescence was observed for chitobiose or GlcNac specific WGA, and galactose and GlcNac- specific PHAE lectins for cells grown on chalcopyrite. No positive fluorescence was observed for sulphur cultured cells stained with the GS-I, PNA, WGA or PHAE TRITC-labelled lectin probes in this study.

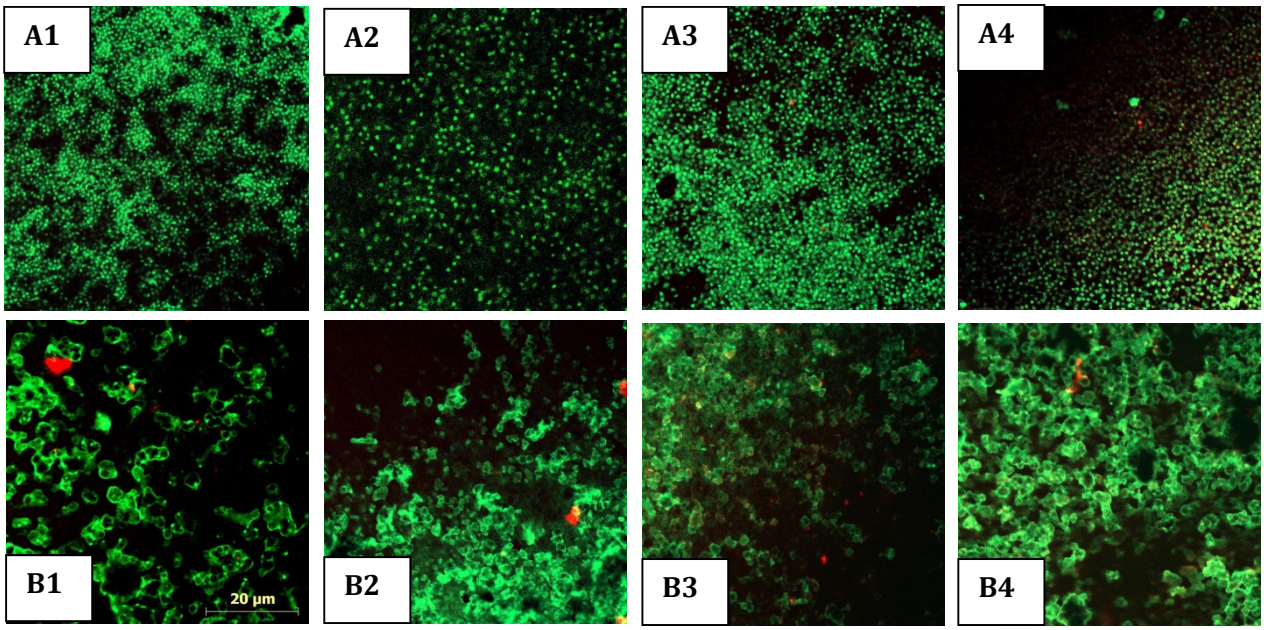

Figure 4.2: Micrographs (A1) - (A4) represent overlays of sulfur cultured *M. hakonensis* harvested onto a 0.22 µm filter, stained with TRITC-labelled GS-I (A1), PNA (A2), WGA (A3), and PHAE (A4), counter stained with FITC-SYTO9™ (green) and then visualised using CLSM (LSM 510 Carl Zeiss® Jena). All micrographs were attained using a Plan-Neofluar® 100 x 1.3 oil objective. Micrographs (B1) – (B4) depict chalcopyrite cultured cells, harvested and stained with the same suite of TRITC-lectins and FITC labelled counter stain. Limited fluorescence in the red channel using TRITC-lectin probes is evident.

M. hakonensis cells cultured on sulphur and chalcopyrite produce EPS which was visualised using fluorescent labelled lectin probes. Positive binding with ConA lectin was evident with typical binding patterns demonstrating the co-localization of the glycoconjugates and cells, i.e. glycoconjugates are observed in the immediate vicinity of the cells indicative that the EPS of cells grown under these conditions is bound to the cell. The observation of planktonic cells producing EPS which is bound to cells, or localised to the capsular region, has been demonstrated by Bellenberg *et al.* (2012) for *A. ferrooxidans*, Zhang *et al.* (2013) for *Ferroplasma acidiphilum*. Koerdt *et al.* (2010) and Zolghadr *et al.* (2010) report co-localisation of ConA lectin signals with DAPI signals for biofilms formed by *Sulfolobus spp.* with confluent binding patterns of ConA evident as the biofilm aged.

Limited fluorescence was observed for the use of galactose specific PNA and GS-I lectins in this study. The localisation and binding patterns observed for staining with these lectins did not yield any distinct formations or associations with the cells and appeared to be scattered sparingly throughout the sample. Furthermore, the fluorescence observed was always much more intense for these TRITC-labelled lectins than that given off by the FITC-labelled SYTO9™ stain. Neu *et al.* (2001) made use of the PNA lectin probe for analysis of EPS from a mixed lotic river biofilm growing on polycarbonate slides in a rotating annular reactor. Although the system for growth

and the microorganisms used differ from the approach in this study, the group reports characteristic cell-associated binding and diffuse cloud like binding patterns when using PNA. Positive binding with PNA in this study would thus be expected to yield systematic patterns in terms of its localisation. It is likely that concentrated globules of TRITC-labelled lectin observed for PNA and GS-I may be the result of excess lectin stain left over on the filter after the wash step, or lectin which has precipitated and gave rise to a false positive in this study.

From the binding interactions observed, namely, positive lectin uptake of ConA, it can be deduced that the capsular EPS composition of sulphur and chalcopyrite grown *M. hakonensis* contain, at least in part, glucose and mannose residues. Positive binding of the ConA lectin with the capsular EPS fraction of *A. ferrooxidans* ATCC23270 and *Ferroplasma acidiphilum* BRGM4 was observed by Bellenberg *et al.* (2012) and Zhang *et al.* (2013) respectively. The microorganisms used by the aforementioned groups are commonly found in bioleach environments and were cultured on either ferrous sulphate or sulfide mineral grains (pyrite) at low pH. Koerdt *et al.* (2010) visualised EPS of biofilms formed by *Sulfolobus spp* grown on Brock Medium in standing petri dishes at a pH of 3 and a temperature of 76 °C. EPS was visualised using ConA in addition to other lectins. Positive strong binding was observed for early stage biofilms with ConA for *Sulfolobus spp*. In this study, *M. hakonensis* displays similar characteristics in terms of EPS composition and lectin binding affinity to the *Sulfolobus spp.* reported by Koerdt *et al.*

The effect of growth substrate on EPS composition has been demonstrated by several groups (Gehrke *et al.* 2001, Bellenberg *et al.* 2012, Boretska *et al.* 2013, Zhang *et al.* 2013). In this study, within the confines of the range of lectins used, the growth substrate does not seem to have an effect on the composition of the EPS. For the range of lectins used in this study, the composition of capsular EPS for planktonic sulphur and chalcopyrite grown cells contain glucose and mannose residues due to positive uptake of the ConA lectin.

There is limited information regarding the regulation of EPS production, especially for thermophilic microorganisms involved in bioleaching. The phenomenon of induction of EPS production upon contact with solid substrate, namely sand, was reported by Vandevivere and Kirchman in 1993. The presence of sulfide mineral grains has been demonstrated to enhance EPS production in *A. ferrooxidans* (Gehrke *et al.* 2001 and Bellenberg *et al.* 2012). In this study, the growth substrate affected the proportion of cells observed to possess EPS. More than a twofold enhancement of cells exhibiting positive uptake of ConA was observed for chalcopyrite grown cells (37 %) relative to sulphur grown cells (16 %). Gehrke *et al.* (2001) report more than a twofold enhancement in EPS produced by *A. ferrooxidans* (R1) cells cultured on sulfide mineral grains (pyrite) relative to cells cultured on sulphur, with the amounts of EPS increasing from

1155±94 µg per 10^{10} cells to 2760±01 µg per 10^{10} cells. Furthermore, Bellenberg *et al.* (2012) used TRITC-labelled ConA to visualise capsular EPS produced by planktonic and sessile *A. ferrooxidans* (ATCC23270) and report an enhancement (measured as a threefold increase in the ConA fluorescent signal intensity) for cells cultured on sulphide mineral grains (pyrite) relative to those cultured on ferrous sulphate. The finding of chalcopyrite grown cells exhibiting enhanced proportions of cells containing EPS is in agreement with Gehrke *et al.* (2001) and Bellenberg *et al.* (2012).

It is noteworthy that despite the level of cells exhibiting positive uptake of ConA being markedly enhanced, not all cells exhibited positive uptake of ConA on contact with chalcopyrite. A similar finding was made in Bellenberg *et al.* (2012). However, no quantitative efforts were made by other groups to differentiate between the fraction of cells exhibiting positive uptake of ConA, and thus containing EPS, and those which did not.

4.3 LECTIN SCREENING OF EPS PRODUCED BY SESSILE *M. hakonensis* CULTURED ON CHALCOPYRITE MINERAL GRAINS

Section 4.1 represented a base line study which provided evidence of EPS production by *M. hakonensis in situ*. The investigation demonstrates the potential of single-lectin binding analysis for the visualisation of glycoconjugate distribution in planktonic cells contacted with elemental sulphur or chalcopyrite mineral grains in well mixed environments with good substrate-microbial contacting. From this, it was deduced that capsular glycoconjugates of *M. hakonensis* cells are comprised, at least in part, of glucose and mannose residues when cultured on either sulphur or chalcopyrite mineral grains. While the composition of the capsular fraction was similar for growth on both substrata, the levels of cells observed to be producing EPS were more than doubled when cells are cultured on chalcopyrite mineral substrata relative to sulphur. In light of this, and its importance in heap leaching for copper extraction and recovery, chalcopyrite was selected as the focal point of the investigation in Section 4.3, in which a more detailed study on the nature of the microbial-EPS-mineral interface created for sessile *M. hakonensis* cells attached to chalcopyrite mineral grains after incubation in shake flasks was conducted; as well as visualisation of EPS formed by *M. hakonensis* grown in the biofilm reactor on a chalcopyrite mineral surface. *M. hakonensis* was cultured on chalcopyrite grains (2 % wt.vol^{-1}) suspended in Mackintosh media at pH 2.5, in shake flasks at 65 ºC and agitated at 160rpm until stationery phase. The chalcopyrite grains, together with some of the spent media, were removed and stored

in sterile 50 ml falcon tubes and transported to the Helmholtz Centre for Environmental Research (Magdeburg, Germany) for analysis. For lectin screening the chalcopyrite grains were fractioned into 2 ml Eppendorf tubes and washed three times with 1 ml sterile milliQ water via aspiration with a pipette and exchange of the liquid suspending medium. The water was removed and a 100 µl aliquot of lectin probe (working solution of 100µgml^{-1}) added. A total of 77 lectins were assessed. The second approach utilised the cultivation of *M. hakonensis* biofilms on chalcopyrite mineral sections within the biofilm reactor (Sections 3.3 and 3.11; Figure 3.3 B). The slides were removed after 4 days and placed in sterile falcon tubes containing 1 – 2 ml Mackintosh basal salts media. Lectins which resulted in positive fluorescence from the screening of the chalcopyrite mineral grains were then used to stain the surface of the chalcopyrite mineral section and the results visualised using CLSM (Section 3.8.2).

4.3.1 CLSM analysis of sessile *M. hakonensis* EPS topography

Micrographs in Figure 4.3 depict the results of the lectin screening conducted on sessile *M. hakonensis* cells attached to chalcopyrite mineral grains. Results of the strongest binding patterns are presented. Three distinct architectural motifs were observed. The first motif observed was indicative of binding with the capsular EPS fraction as lectin fluorescence was localised to regions immediately around the cell surface. Evidence of binding with capsular EPS is shown in Figure 4.3 (A1 – A3), where samples were stained with FITC-labelled *Aleuria aurantia* (Orange peel fungus) lectin (1b-AAL). The 1b-AAL lectin specifically binds fucose and rhamnose residues.

The second definitive binding pattern observed, revealed a close association of the EPS with the mineral surface. The lectin fluorescence appeared as a confluent mat which was disseminated across the mineral surface, in some instances EPS covered the entire grain and in others, lichen-like patches of EPS were evident (Figure 4.3 D1 and D2). Evidence of this architectural motif is presented in Figure 4.3 (B1 – B3). The following FITC-labelled lectins gave rise to this particular motif; *Pisum sativum* (Garden peas, PSA) and *Helix pomatia* (Burgundy snail, HPA). These lectins are specific for mannose, glucose, and N-acetylgalactosamine (GalNac) residues respectively.

In the third structural arrangement of EPS observed, lectin fluorescence appeared as cloud-like clusters resembling cauliflower which branched outward from the mineral surface, as seen in Figure 4.3 (C1-C3 and D1-D3).

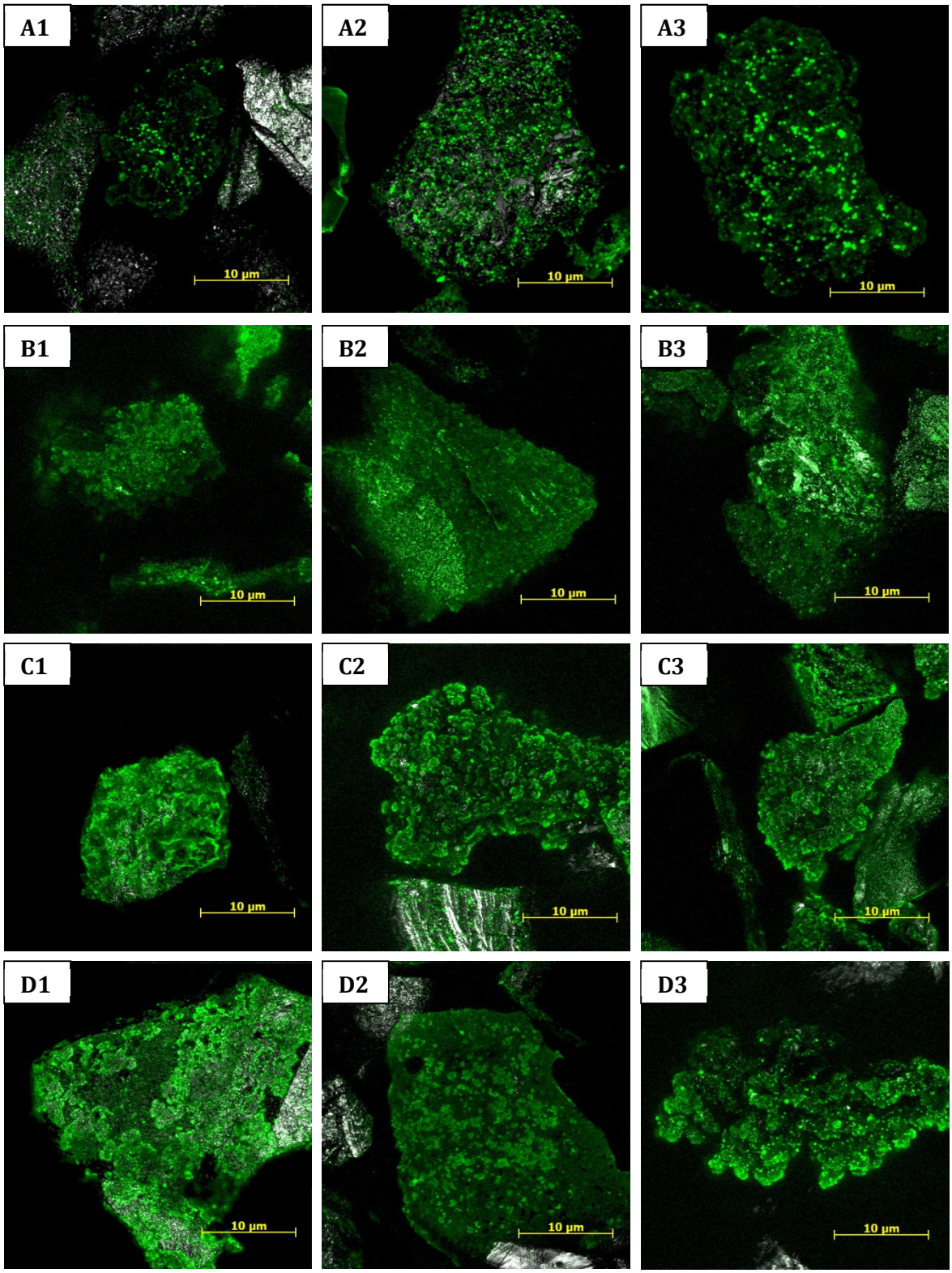

Figure 4.3: Micrographs depicting the results using lectin screening conducted on sessile *M. hakonensis* cells attached to chalcopyrite mineral grains after growth in batch agitated flasks. Three lectin-EPS glycoconjugates binding motifs were observed, the first depicts positive binding of capsular EPS with FITC labelled lectin 1b-AAL in (**A1**) **–** (**A3**). The second motif depicts EPS disseminated across the surface as a confluent mat in images (**B1**) – (**B3**). Lectins which gave rise to these motifs include the (**B1**) and (B2) PSA lectin and (B3) HPA lectin. In the final motif observed, EPS exhibits "diffuse" or cloud-like architecture seen in micrographs (C1 – D3). Lectins which resulted in this motif included: (**C1**) GNA, (**C2**) MNA-G, (**C3**) ECA (**D1**) 1b AAL, (**D2**) MPA and (**D3**) 6b-1AA. Images were taken using a TCS SP5X (Leica, Germany) equipped with upright microscope. The system was controlled by the LAS AF software version 2.6.1. Samples were examined by the 63 × 1.2 NA (high resolution) objective lens. All lectins in these micrographs were FITC labelled.

The following FITC labelled lectins exhibited this motif: *Galanthus nivalis* (Snowdrop plant) GNA, *Morus nigra* (Black Mulberry tree) a.k.a. morniga G lectin MNA-G, *Erythrina cristagalli* ECA, 1b-AAL, *Maclura pomifera* MPA, *Iberis amara* 6b-1AA. The GNA lectin is specific for mannose; 1b-AAL is specific for mannose and rhamnose, MNA-G, ECA and MPA are specific for galactose, GlcNac and GalNac residues, and 6b-1AA is specific for GalNac residues. In some instances combinations of the motifs were observed. Examples of this can be seen in Figure 4.3 (C1), (D1) and (D2) where combinations of the cauliflower motif together with the confluent mat surface coverage with the EPS is evident. These were observed with mannose specific GNA, fucose and rhamnose specific 1b-AAL and galactose specific MPA lectins in Figure (C1), (D1) and (D2) respectively.

Micrographs in Figure 4.4 depict the results of the lectin screening conducted on sessile *M. hakonensis* cells attached to chalcopyrite mineral grains. In Figure 4.4, overlays of two channels can be seen. Lectin probes were labelled with either Alexa568™ or TRITC and are depicted in red, with SYTO9™ used as a counter stain to visualise attached cells depicted in the green channel. A combination of all three motifs can be seen. The confluent mat EPS motif which is disseminated across the mineral grain surface is evident in micrographs (A) – (E), as well as co-localisation of EPS to the capsular region, demarcated by white arrows. Cloud like EPS architecture is evident in micrographs Figure 4.4 (A), (B), (C) and (E), with attached cells embedded in this milieu. A control was performed to verify the presence of an attached microbial population. Any EPS present at the mineral liquid interface was therefore derived from this sessile population.

Cells attached to the surfaces of chalcopyrite mineral grains visualised using a Syto9™ nucleic acid stain only can be observed in micrographs (F) and (G). The morphology of the attached cells observed in (F) and (G) is identical to that of FITC-labelled lectins which exhibit binding with the capsular EPS fraction.

The images in micrographs (A) - (G) verify the presence of *M. hakonensis* cells attached to the mineral surface grains. EPS present at the mineral interfacial environment is therefore derived from the sessile population clearly present at the surface. A further control was performed where unstained mineral grains were visualised. These results are presented in Figure 4.5 (H) and (I). No fluorescence is observed, thus that any fluorescence observed was not a result of mineral auto fluorescence or artefacts introduced during sample preparation. The fluorescence observed is due to the presence of sessile cells and the EPS produced by this population.

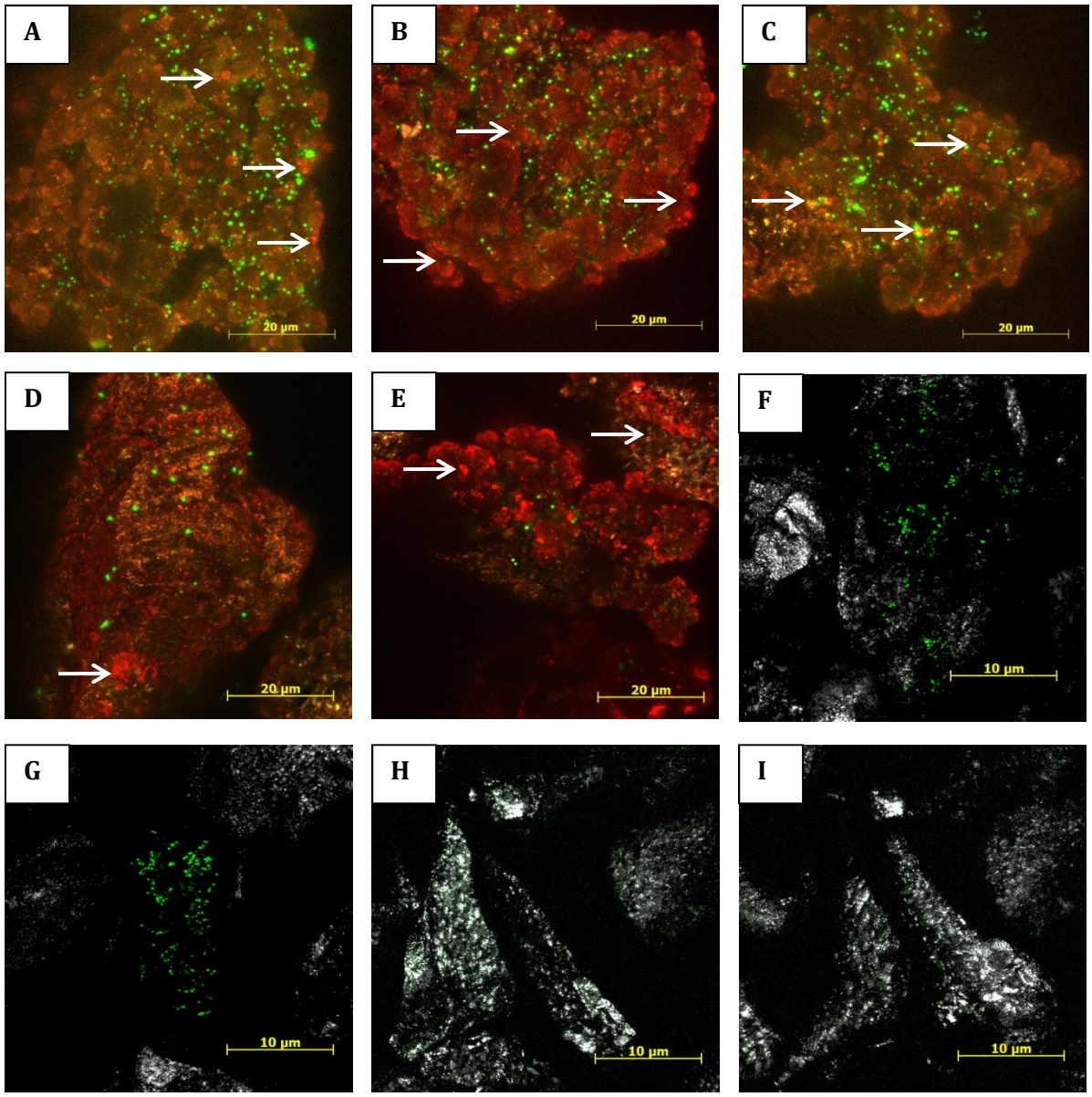

Figure 4.4: Micrographs depicting results of lectin screening conducted on sessile *M. hakonensis* cells attached to chalcopyrite mineral grains after growth in batch agitated flasks. Micrographs depict overlays of two channels; lectin probes were labelled with either Alexa568™ or TRITC are depicted in red, with SYTO9™ used as a counter stain to visualise attached cells depicted in the green channel. A combination of all three motifs can be seen. The confluent mat EPS motif which is disseminated across the mineral grain surface is evident in micrographs (A) – (E), as well as co-localisation of EPS to the capsular region (white demarcations). Cloud like EPS architecture is evident in micrographs (**A**), (**B**), (**C**) and (**E**) with attached cells embedded in this milieu. The lectins used in the micrographs presented as follows: (**A**) Alexa568-PSA, (**B**) TRITC-GSI, (**C**) Alexa568-HMA, (**D**) Alexa568-PSA and (**E**) TRITC-HPA. Cells attached to the surfaces of chalcopyrite mineral grains are visualised using a Syto9 nucleic acid stain only are presented in micrographs (**F**) and (**G**). Results of the control using no stain are presented in (**H**) and (**I**)4.

4.3.2. Characterisation of sessile *M. hakonensis* EPS glycoconjugates

In Table 4.2, the results of the lectin screening assay are presented for sessile *M. hakonensis* cells cultured on chalcopyrite mineral grains in shake flasks. The lectin used, along with its particular specificity and a qualitative ranking of the strength of the interaction between the EPS and the lectin (visual inspection of resulting fluorescence) is given. Fluorescence which was visible but not extensive was given an arbitrary ranking of (+) for the binding interaction of lectin with EPS. Visible fluorescence which was more extensive was given a ranking of (++), and the strongest positive fluorescence as seen in the micrographs presented in Figures 4.3 and 4.4 were given the highest ranking (+++), with no fluorescence demarked (-) in Table 4.2.

Table 4.2: Results of lectin screening of the EPS from sessile *M. hakonensis* attached to chalcopyrite mineral grains after growth in batch agitated flasks.

Lectin abbreviation	Organism isolated	Specific binding affinity	Result
AAA - FITC	*Anguilla anguilla*	α-fucose	-
ABA	*Agaricus bisporus*	β-gal, gal(β1,3)galNAc	-
ACA	*Amaranthus caudatus*	gal(β1,3)galNAc, gal(β1,3)Neu5Ac	+
AIA	*Artocarpus integrifolia*	α -gal, gal(β1,3)galNAc	+
AMA	*Arum maculatum*		-
APP	*Aegopodium podagraria*	α-galNAc, β-galNAc	-
ASA	*Allium sativum*		-
BDA	*Bryonia diocia*	α-galNAc, β-galNAc	-
BPA	*Bauhinia purpurea*	α-galNAc, β-galNAc, gal(β1,3)	-
CA	*Colchicum autumnale*	lac, gal, galNAc	-
CAA	*Caragana aborescens*	α-gal, β-gal, galNAc	-
Calsepa	*Calystegia sepium*	mannose	+++
ConA	*Concanavalin A*	α-man, α-glc, α-glcNAc, branched mannoses	+ +
CPA	*Cicer arietinum*		-
CSA	*Cytisus scoparius*	β-gal, galNac, lac	-
DBA	*Dolichos biflorus*	terminal α-galNAc, galNAc(α 1,3)galNAc	+
DGL	*Dioclea grandiflora*		-
DSA	*Datura stramonium*	glcNAc(β1,4)glcNAc oligomers, gal(β1,4)	+
ECA	*Erythrina cristagalli*	gal(β1,4)glcNAc, galNAc gal	+
EEA	*Euonymus europaeus*	gal(α 1,3)gal, gal(α1,3)Fuc(α 1,2)gal	-
GHA	*Glechoma lederacea*		-
GNA	*Galanthus nivalis*	α-man, man(α 1,3)man5	+++
GS-1	*Griffonia (Bandeiraea) simplicifolia*	α-gal, α-galNAc	+++
HAA	*Helix aspersa*	galNAc, glcNAc	-
HHA	*Amaryllis*	α-man, polymannose structures	-
HMA	*Humarus americanus*		-
HPA	*Helix pomatia*	α-galNAc	+++
IRA	*Iris hybrid*		-
LAA	*Laburnum alpinum*	β-glcNAc, glcNAc (β1,4) glcNAc	-
LAL	*Laburnum anagyroides*		-
LBA	*Phaseolus lunatus*	galNAc(α 1,3)[L-fuc(α 1,2)gal], galNAc	-
LcH	*Lens culinaris*	α-man, fucose, α-glc, α-glcNAc	-
LEA	*Lycropersicon esculentum*	glcNAc(β1,4)glcNAc oligomers	-
LFA	*Limax flavus*		-
Lotus	*Tetragonolobus purpurea*	terminal α-fucose	-
LPA	*Limulus polyphemus*	NeuAc	-
MAA	*Maackia amurensis*	NANA(α 2,3)gal, sialic acid	-
MNA-G	*Morus nigra agglutinin*	galactose	+++
MOA	*Marasmium oreades*		-
MPA	*Maclura pomifera*	α-gal, α-galNAc, gal(β1,3)galNAc	+++
NPA	*Narcissus pseudonarcissus*	binds internal and terminal α-man groups	-
PHA-E	*Phaseolus vulgaris*	galNAc	+++
PHA-L	*Phaseolus vulgaris*	galNAc	-
PMA	*Polygonatum*		-
PNA	*Arachis hypogaea*	β-gal, gal(β1,3)galNAc	+
PSA	*Pisum sativum*	α-man, α-glc, α-glcNAc	+++
PSL	*Polyporus squamosus*		-
PTA	*Psophocarpus tetragonolobus*	β-gal, galNAc	+
PWA	*Phytolacca americana*	glcNAc(β1,4)glcNAc oligomers,	-
RPA	*Robinia pseudoaccacia*	NI	-
SBA	*Glycine max*	terminal α- or β-linked galNAc	++
SJA	*Sophora japonica*	β-galNAc	++

SNA	*Sambucus nigra*	β-gal, sialic acid	+
STA	*Solanum tub*	β-glcNAc, glcNAc(β1,4)oligomers	-
TKA	*Trichosanthes kirilowii*	gal, β-gal oligosaccharides	-
TL	*Tulipa sp.*	galNAc	+
UDA	*Uritica dioicia*	glcNAc(β1,4)glcNAc oligomers	-
UEA	*Ulex europaeus*	Fucose	++
VFA	*Vicia faba*	man, glc	+
VGA	*Vicia graminea*	NI	-
VRA	*Vigna radiata*	α-gal	-
VVA	*Vicia villosa*	galNAc, α-galNAc, galNAc(α 1,3)gal	++
WFA	*Wisteria floribunda*	terminal galNAc(β1,4) and galNAc(β1,3)	++
WGA	*Triticum vulgaris*	Chitobiose containing molecules	+
AAL - Alexa	*Aleuria aurantia*	Fucose and rhamnose specific	+++
CCA	*Cancer antennarius crude*	NeuAc, 9-O-Ac-NeuAc, 4-O-Ac-NeuAc	-
Co	*Codium fragile*	galNAc	+
Ecor	*Erythrina corallodendron*	gal(β1,4)glcNAc, galNAc, lac gal	+++
HMA	*Homarus americanus crude*	Sialic acid	+++
IAA	*Iberis amara*	GlcNac	++
MIA	*Mangifera indica crude*	NI	+
PAA	*Perseau americana crude*		+
PA-1	*Psuedomonas aeroginosa*	galactose	+++
PPA	*Ptilota plumosa*	terminal α-gal	+
RTA	*Trifolia repens crude*	2-deoxyglucose	-
TML	*Tritichomonas mobilensis*	sialic acid	+
VGA	*Vicia graminea*	NI	+

(+++)strong positive binding, (++) moderate binding, (+)some fluorescence but not excessive,(-)no binding

From these results, a summary of the lectins which gave rise to moderate and strong positive interactions with EPS from sessile *M. hakonensis* was drawn. This is presented in Table 4.3 in terms of the lectin, its binding specificity and also notes the resultant EPS locale and architecture observed for binding with said lectin. This information allows one to piece together the glycoconjugates composition of EPS produced by sessile *M. hakonensis* at the various locales to uncover the nature of this mineral-EPS-microbial interface *in situ*.

Table 4.3: Summary of positive binding lectins and their binding motifs

No.	Lectin		Specific binding	Binding motif
Strongest binding lectins (+++)				
1	1b-AAL	*Aleuria aurantia*	fucose and rhamnose specific	Capsular, surface, cauliflower
2	Calsepa	*Calystegia sepium*	mannose	Cauliflower
3	PSA	*Pisum sativum*	α-man, a-glc, α-glcNAc	Surface
4	HPA	*Helix pomatia*	α-galNAc	Surface, cauliflower
5	GNA	*Galanthus nivalis*	α-man, man(α 1,3)man5	Surface
6	MNA-G	*Moringa G (Moringa Oleifera)*	galactose/N-acetylgalactosamine	Cauliflower
7	MPA	*Maclura pomifera*	α-gal, α -galNAc, gal(b1,3)galNAc	Cauliflower
8	GSI	*Griffonia (Bandeiraea) simplicifolia*	α-gal, α -galNAc	Cauliflower
9	HMA	*Humarus americanus*	sialic acid-specific, GalNAc-specific	Cauliflower
10	Ecor	*Erythrina corallodendron*	gal(b1,4)glcNAc, galNAc, lac gal	Cauliflower
11	PA1	*Psuedomonas aeroginosa*	fucose	Cauliflower
Moderate binding lectins (++)				
1	SBA	*Glycine max*	Terminal α - and β- GalNac	Capsular
2	ConA	*Concanavalin A*	Glucose, mannose	Capsular, surface
3	SJA	*Sophora japonica*	β-GalNac	Cauliflower(geometric branches)
4	UEA	*Ulex europaeus*	Fucose	Cauliflower
5	VVA	*Vicia villosa*	α-GalNac	Cauliflower, surface (lichen)
6	WFA	*Wisteria floribunda*	Terminal GalNac	Capsular
7	IAA	*Iberis amara*	GlcNac	Cauliflower

From the summary presented in Table 4.3, the lectins which gave rise to strong positive binding were specific for the following glycoconjugates: mannose, glucose, galactose, fucose, rhamnose and sialic acid residues. Lectins which gave to moderate binding were specific to glucose, mannose and galactose residues. Thus the EPS produced by sessile *M. hakonensis* on chalcopyrite grains is characterised by the presence of these glycoconjugate components. No definitive trends were evident in terms of the glycoconjugate composition and binding motif. All binding motifs contained combinations of the glycoconjugates listed in Table 4.3. However, a greater proportion of galactose and fucose specific lectins resulted in the cauliflower binding motif over the other glycoconjugates listed in Table 4.3.

4.4 DISCUSSION

Traditional methods to study EPS environments involve culturing bacteria in pure cultures, in liquid media, to produce EPS. The EPS is then isolated from the system and characterised (supernatant and cell pellet or a combination of both) using methods which destroy the natural architecture of the EPS *in situ*. Few attempts have been made to examine true adhesive or biofilm EPS (Neu *et al.* 2001). One mechanism which has proven valuable in the *in situ* examination of sessile microorganisms and biofilms is the use of lectins coupled with CLSM. Lectin staining provides information on the nature and structure of the EPS interfacial environment and demonstrates spatial heterogeneity. Furthermore, chemical heterogeneities within the extracellular biofilm locations can be identified and characterised (Neu *et al*. 2001). The resulting information sheds light on the role of EPS and the associated interfacial environment in various niches.

In this study, the glycoconjugate composition of EPS produced by sessile *M. hakonensis* cultured on chalcopyrite mineral grains in shake flasks was screened using a suite of 77 lectins. The EPS assayed was found to contain fucose, rhamnose, glucose, mannose, galactose, sailic acids as well as N-acetyl-glucosamine (GlcNac) and N-acetyl-galactosamine (GalNac) containing residues. Three binding motifs were observed; namely, the confluent matt of EPS along the mineral surface, capsular EPS binding, and the diffuse cauliflower motif which branched outward from the mineral surface. The aforementioned glycoconjugates were present in all three binding motifs. However, more lectins specific for galactose and fucose resulted in the cauliflower type EPS architecture. From this, one can surmise that the glycoconjugates composition of *M. hakonensis* cultured on chalcopyrite mineral grains is largely homogenous i.e. it does not vary greatly with spatial locale, although the presence of certain glycoconjugate residues may be more prevalent than others in particular EPS architectural motifs. Cells were observed to be attached to the mineral surface and were also evident within the EPS milieu around the chalcopyrite mineral grains. Controls verify the fluorescence visualised was a result of EPS present on and around the mineral-microbial-interfacial environment as no auto-fluorescence or false positive fluorescence was observed for unstained chalcopyrite mineral grains.

Table 4.4 presents a summary of archaeal, as well as bioleach relevant, microbial species assessed for their ability to form attached biofilms or multicellular structures that have been visualised using lectins and CLSM. From the list of lectins in Table 4.4, EPS from microorganisms growing in acidophilic conditions contain the following commonly occurring glycoconjugates: glucose, mannose, galactose, N-acetylglucosamine, N-acetylgalactosamine, fucose and galacturonic acids

(Mayberry-Carson *et al*. 1978, Gliboa-Garber *et al.* 1998, Fife *et al.* 2000, Neu 2000, Koerdt *et al*. 2010, Zolghadr *et al.* 2010, Gonzalez-Toril *et al.* 2011, Bellenberg *et al.* 2012 and Zhang *et al.* 2013). Glycoconjugates constituents evident in EPS from *M. hakonensis* were in accord with the reports made by the abovementioned authors. However, due to the more extensive list of lectins utilised in this study, a greater range of glycoconjugates could be identified. Thus, EPS produced by *M. hakonensis*, in addition to containing glucose, mannose, fucose, galactose, N-acetyl-galactosamine and N-acetyl-glucosamine, was demonstrated to contain rhamnose and sialic acid residues as well.

Koerdt *et al.* (2010) investigated crenarchaeal biofilms in terms of their diversity, architecture and EPS composition, as well as the effect of pH and temperature on these factors. Three crenarchaeal species were investigated, namely; *Sulfolobus solfataricus* DSM 1617 and DSM 1616, *Sulfolobus acidocaldarius* DSM 639 and *Sulfolobus tokodaii* DSM 16993, in batch microtitre plates after incubation periods of two to three days. These species were reported to form surface-attached biofilms or multicellular structures which followed two architectural motifs as per visual inspection using lectin probes and CLSM (Koerdt *et al.* 2010, Fröls 2013). The first motif was characterised by biofilms as flat, patched films of cells embedded in EPS which were associated with tower like aggregates of cells in an EPS milieu. The second consisted of biofilms visible as confluent carpet-like films with surface associated aggregates of cells within the EPS layer. Koerdt *et al.* (2010) report the presence of the following glycoconjugates within the EPS of the crenarchaeotes used in their study due to positive binding with ConA, IB4 and GS-II lectins: glucose and mannose, galactose and N-acetyl-glucosamine. Co-localisation of cells with the EPS was observed when ConA lectin was used. The presence of glucose, mannose, galactose and N-acetyl-glucosamine in the EPS of *Sulfolobus sulfotaricus* was also demonstrated by Zolghadr *et al.* (2010). The architectural motifs and EPS glycoconjugates composition observed in this study for sessile *M. hakonensis* cultured on mineral chalcopyrite grains are in accordance with that described by Koerdt *et al.* (2010) and Zolghadr *et al.* (2010) for creanarchaeotes. The use of ConA for the visualisation of EPS produced by mineral bioleaching relevant *A. ferrooxidans* and *F. acidiphilum* have been reported by Bellenberg *et al.* (2012) and Zhang *et al*. (2013) respectively. Both these authors report EPS binding motifs associated with the capsular region using this lectin. The findings in this study are in agreement with Bellenberg *et al.* (2012) and Zhang *et al*. (2013), as positive capsular EPS binding were also evident.

Table 4.4: Summary of lectins used to investigate biofilms and showed positive binding with EPS in archaea and or acidophilic environments

Author	Microorganism	Lectin	Abbr.	Specific binding	Staining pH
Mayberry-Carson *et al.* 1978	*Thermoplasma acidophilum*	concanavalin A	ConA	α-glucose, α-mannose	5
Gilboa-Garber *et al.* 1998 (Varied salt concentration, 0.15 – 3.0 M, to optimise protocol for halophilic archaea)	*Halobacterium salinarium R1,* *Halobacterium salinarium Strain 5,* *Haloferax. volcanii ATCC 29605^T,* *Haloferax mediterranei ATCC 35300^T,* *Haloarcula marismortui ATCC 43049^T,* *Haloarcula vallismortis ATCC 29715^T,* *Halorubrum sodomense ATCC 33755^T,* *Natronomonas pharaonis SP1 (NCBIMB 2191)*	concanavalin A *Triticum vulgaris* *Arachis hypogaea* *Ulex europaeus* *Maclura pomifera* soy bean agglutinin *Erythrina corallodendron* *Psuedomonas aeruginosa* *Aplysia* gonad	ConA WGA PNA UEA-I MPA SBA ECorL PA-I, PA-II AGL	α-glucose, α-mannose chitobiose containing molecules galactose L-fucose Galactose Galactose Galactose L-fucose, D-mannose Galacturonic acid, D-galactose	7.4
Fife *et al.* 2000 (G + biomining microorganisms)	*Sulfolobus acidophilus* *Sulfolobus acidocaldarius* *Sulfolobus shibatae* *Acidimicrobium ferrooxidans* *Ferromicrobium acidophilus*	*Triticum vulgaris*	WGA	N-acetylglucosamine; N-acetylneuraminic acid	7.2
Neu 2000 (EPS staining using lectins and CLSM Observed 2 morphologies: cell-surface associated and diffuse, cloud like with A. hypogea lectin)	*Mixed Lothic river biofilm grown in rotating annular reactor on polycarbonate slides*	*concanavalin A* *Arachnis hypogea* *Trticum vulgaris* *Tetragonolobus purpurea* *Limulus polyphemus* *Ulex europaeus*	ConA PNA WGA LOTUS LPA UEA	α-glucose, α-mannose galactose chitobiose containing molecules terminal fucose NeuAc L-fucose	7
Koerdt *et al*. 2010 (3 day biofilms, 70 ºC, ph 2-3)	*Sulfolobus solfataricus* *Sulfolobus acidocaldarius* *Sulfolobus tokodaii*	concanavalin A *Griffonia simplicifolia* Iso - *Griffonia simplicifolia*	ConA GS-II GS-IB4	α-glucose, α-mannose terminal α-D-galactosyl residues with a secondary affinity for terminal GalNac	5
Zolghadr *et al*. 2010	*Sulfolobus solfataricus*	concanavalin A *Griffonia simplicifolia* Iso - *Griffonia simplicifolia*	ConA GS-II GS-IB4	α-glucose, α-mannose terminal α-D-galactosyl residues with a secondary affinity for terminal GalNac	5
González-Toril *et al*. 2011	*Acidithiobacillus thiooxidans*	concavalin A nile red	ConA	α-glucopyranosyl, α-mannopyranosyl lipids and hydrophobic domains	<2
Bellenberg *et al.* 2012 Zhang *et al.* 2013	*A. ferrooxidans* *F. acidiphilum*	Concanavalin A	ConA	α-glucose, α-mannose	2

4.5 SUMMARY AND CONCLUSIONS

In the context of bioleaching, microbial EPS components are thought to complex chemical oxidants and extend the chemical reaction space available for mineral dissolution reactions, making the microbial-mineral-EPS interface the dominant active zone in terms of microbial oxidation and mineral dissolution (indirect contact mechanism, discussed in Chapter 2.1.3). In this study, the microbial-mineral-EPS interface was successfully visualised and characterised *in situ* in terms of its glycoconjugates constituents and architectural traits using fluorescent lectin probes and CLSM.

In the first part of this study, EPS was successfully visualised. The effect of varying culture growth substrate on the extent of EPS present, as well as on the resulting EPS architecture, and spatial distribution was assessed. For planktonic cells cultured on chalcopyrite mineral grains and sulfur, glucose and mannose specific lectin ConA resulted in positive binding, the locale of which was restricted to the area immediately around the cell surface. This is indicative of the presence of capsular EPS. Growth on chalcopyrite was correlated to an enhanced presence of cells which exhibited positive binding with the ConA lectin relative to sulphur grown cells, with 37 % of planktonic cells grown in the presence of chalcopyrite observed to possess EPS, relative to only 16 % of sulfur grown cells.

For the second part of this study, a more robust lectin screening process was incorporated with a focus on EPS produced by sessile cells cultured on chalcopyrite surfaces. Cells were either cultured in batch agitated flasks on chalcopyrite mineral grains, and the mineral grains containing attached cells assessed; or cultured in the biofilm reactor with the flat chalcopyrite mineral slide assessed using the lectin staining. Thus, the effect of varying culture growth conditions, in terms of mineral-microbe contacting, fluid flow and attrition, could also be investigated. For sessile *M. hakonensis* on chalcopyrite mineral grains cultured in shake flasks, three EPS architectural motifs were evident, namely; the confluent matt of EPS along the mineral surface, capsular EPS binding, and the diffuse cauliflower motif which branched outward from the mineral surface. The EPS assayed was found to contain fucose, rhamnose, glucose, mannose, galactose, sialic acids as well as N-acetyl-glucosamine (GlcNac) and N-acetyl-galactosamine (GalNac) containing residues. The aforementioned glycoconjugates were present in all three binding motifs. Cells were observed to be attached to the mineral surface and were also evident within the EPS milieu around the chalcopyrite mineral grains.

The EPS architecture observed under these conditions support the hypothesis proposed by both Tribusch et al. (2001) and by Sand and Gehrke (2006); namely, that EPS extends the reaction space available for dissolution reactions. The cloud-like cauliflower formations of EPS which

branch outward from the mineral surface, and the creation of a confluent EPS matt across the surface, serve the sessile microbial population well in extending the surface area coverage available for entrapment of ions and increasing dissolution reaction space. Further investigation on the chemical composition *M. hakonensis* EPS is required to uncover the potential contribution of thermophiles in creation and proliferation of the microbial-mineral-EPS interfacial environment in the context of bioleaching. Stemming from this, an investigation which involved extraction and characterisation of EPS from *M. hakonensis* was carried out and is presented in the next chapter.

References

Bellenberg, S., Leon-Morales, C. F., Sand, W., & Vera, M. (2012). Visualization of capsular polysaccharide induction in *Acidithiobacillus ferrooxidans*. *Hydrometallurgy*, *129–130*, 82–89.

Boretska, M., Bellenberg, S., Moshynets, O., Pokholenko, I., & Sand, W. (2013). Microbial & Biochemical Technology Change of Extracellular Polymeric Substances Composition of *Thiobacillus thioparus* in Presence of Sulfur and Steel, *5*(3), 68–73.

Fife, D. J., Bruhn, D. F., Miller, K. S., Daphne, L., Fife, D. E. E. J. a Y., & Stoner, D. L. (2000). Evaluation of a Fluorescent Lectin-Based Staining Technique for Some Acidophilic Mining Bacteria *Applied Environmental Microbiology. 66*(5), 2208–2210.

Fröls, S. (2013). Archaeal biofilms: widespread and complex. *Biochemical Society Transactions*, *41*(1), 393–8.

Gehrke, T., Hallmann, R., Kinzler, K., & Sand, W. (2001). The EPS of Acidithiobacillus ferrooxidans - A model for structure-function relationships of attached bacteria and their physiology. *Water Science and Technology*, *43*(6), 159–167.

Gilboa-Garber, N., Mymon, H., & Oren, a. (1998). Typing of halophilic Archaea and characterization of their cell surface carbohydrates by use of lectins. *FEMS Microbiology Letters*, *163*(1), 91–7.

González-Toril, E., Águilera, Á., Souza-Egipsy, V., Pamo, E. L., España, J. S., & Amils, R. (2011). Geomicrobiology of La Zarza-Perrunal acid mine effluent (Iberian Pyritic Belt, Spain). *Applied and Environmental Microbiology*, *77*(8), 2685–2694.

Koerdt, A., Gödeke, J., Berger, J., Thormann, K. M., & Albers, S. V. (2010). Crenarchaeal Biofilm Formation under Extreme Conditions. *PLoS ONE*, *5*(11) e14104.

Mayberry-Carson, K. J., Jewell, M. J., & Smith, P. F. (1978). Ultrastructural localization of Thermoplasma acidophilum surface carbohydrate by using concanavalin A. *Journal of Bacteriology*, *133*(3), 1510–1513.

Neu, T. R. (2000). In situ cell and glycoconjugate distribution in river snow studied by confocal laser scanning microscopy. *Aquatic Microbial Ecology*, *21*(1), 85–95.

Schallenberg, M., Kalff, J., & Rasmussen, J. B. (1989). Solutions to Problems in Enumerating Sediment Bacteria by Direct Counts Solutions to Problems in Enumerating Sediment Bacteria by Direct Countst, *Applied Environmental Microbiology*.55(5) 1214-1220.

Zhang, R. Y., Vera, M., Bellenberg, S., & Sand, W. (2013). Attachment to Minerals and Biofilm Development of Extremely Acidophilic Archaea. *Advanced Materials Research*, *825*, 103–106.

Zolghadr, B., Kling, A., Koerdt, A., Driessen, A. J. M., Rachel, R., & Albers, S. V. (2010). Appendage-mediated surface adherence of *Sulfolobus solfataricus*. *Journal of Bacteriology*, *192*(1), 104–110.

Chapter 5:
Extraction and compositional analysis of EPS from planktonic and sessile *M. hakonensis*

5.1 INTRODUCTION

Microbial life in the natural environment exists predominantly in biofilms and bioaggregation (Wingender *et al.,* 1999), allowing the environment to be tailored for the microbial community. In microbially-mediated bioleaching, colonisation of the mineral surface and the associated formation of a biofilm on colonisation enables good delivery of leach agents with the generation of a niche leaching environment (Tributsch, 2001; Sand and Gehrke 2006; Crundwell, 2003; Rawlings, 2004). Hence, biofilm formation can play a key role in mineral bioleaching.

EPS and its primary components are, in essence, the "building-blocks" of the microbial biofilm and provide its structural integrity and stability. EPS may also serve as a boundary, mediating contact between biotic and abiotic environments (Wingender *et al.,* 1999). It facilitates the transformation of the microenvironment within the biofilm, allowing niche and ideal conditions for the proliferation of the biofilm-associated microbial community in harsh environments (Watnick and Kolter, 2000). The nature and composition of EPS is considered a major determinant of the physicochemical and biological properties of the microbial biofilm and are important for the activity of the microorganisms encased by it (Nielsen and Jahn, 1999). This is especially true in bioleach systems where the EPS interfacial environment is the major active site for both microbial activity and mineral dissolution, according to the indirect contact mechanism (Schippers and Sand, 1999; Tributsch, 2001; Crundwell, 2003).

Knowledge on EPS production, composition and the factors give insight into the establishment and longevity of "ideal" interfacial environments (biofilms) for effective bioleaching. In particular, challenges around effective inoculation and proliferation of suitable microflora, as well as reduction of lag times before effective leaching (Gericke et al. 2005) can be addressed. Microbial culturing and inoculation regimes are needed to reduce costs and turn-around times in bioleach systems, by promoting ideal microbial-mineral interfacial environments.

In work completed by Nielsen and Jahn (1999), EPS is categorised into the soluble or colloidal EPS fraction, the loosely-cell associated EPS fraction and the bound EPS fractions, the latter being tightly associated with the cell surface (discussed in literature review Section 2.7.4.2). In Chapter

4, lectin binding was used to visualise EPS and gain insight into the spatial arrangement of the microbial-mineral interfacial environment *in situ* on the ore surface. Furthermore, the presence of specific EPS components of *M. hakonensis* was identified. To date, limited application of this methodology, developed for environmental applications, has been reported for mineral bioleaching. In this Chapter, an extraction method was developed to allow the recovery of colloidal EPS, EPS associated loosely with the cell as well as capsular EPS from three planktonically grown *M. hakonensis* systems. The three systems studied were: *M. hakonensis* cultured on ferrous sulphate, *M. hakonensis* cultured on sulphur and *M. hakonensis* cultured on chalcopyrite mineral grains. In addition, EPS was also extracted from chalcopyrite mineral grains, representative of EPS produced by an attached population, hereafter referred to as mineral bound EPS. Mineral bound and capsular EPS was extracted using either crown-6-ether or EDTA with experiments performed across duplicate reactor systems and all analysis carried out in triplicate (methodology detailed in Section 3.10.2). The EPS yield was quantified and its composition characterised. The effect of varying culture growth history or energy source on these parameters was also assessed.

5.2 EXTRACTION AND CHARACTERISATION OF *M. hakonensis* EPS

5.2.1 Approach to extraction of EPS

EPS was extracted from planktonically grown *M. hakonensis,* cultured on three different substrates, namely chalcopyrite minerals, ferrous sulphate and sulphur. EPS was also extracted from chalcopyrite mineral grains, representative of EPS associated with an attached population (mineral bound EPS). To generate enough EPS for effective extraction and compositional analysis, *M. hakonensis* DSMZ7519 was grown planktonically in 5 litre (L) Schott bottles on the corresponding substrate. Experiments were carried out in duplicate. The growth medium consisted of DSMZ88 media containing sulphur (1.6 % wt vol^{-1}), ferrous sulphate (20 g L^{-1}) or chalcopyrite mineral grains (2 % wt vol^{-1}) as an energy source. Reactors were vigorously aerated making provision for mixing and aerobic growth until stationary phase. Each Schott bottle reactor had a working volume of 5 L and a final cell concentration of approximately 1 x 10^8 cells mL^{-1}. Colloidal EPS was then recovered, with capsular and mineral bound EPS extracted in a step-wise manner, as described in Section 3.10.2 and outlined in Figure 5.1.

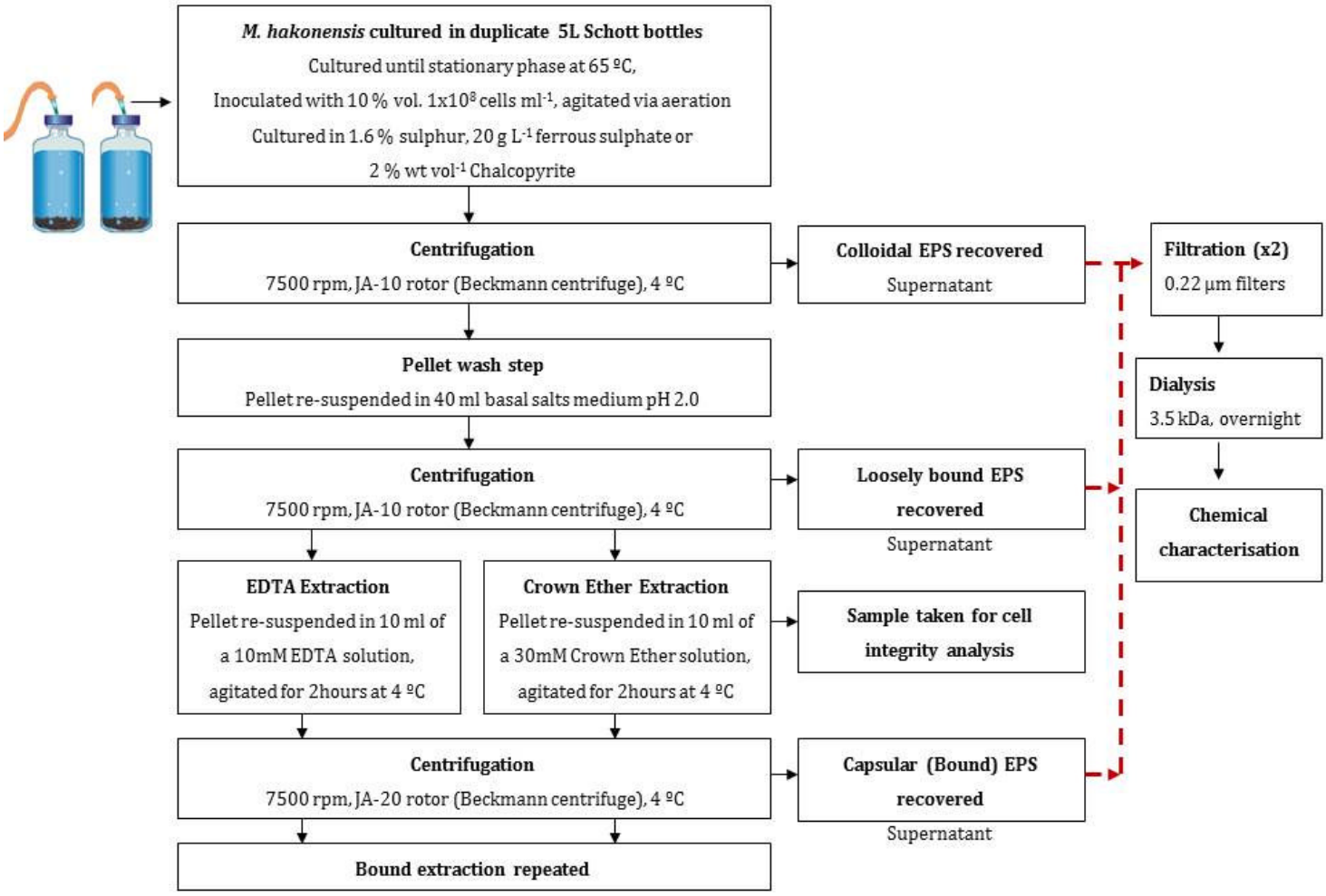

Figure 5.1: Schematic representation of methodology used for culturing *M. hakonensis* on three energy source systems, namely: ferrous sulphate, sulphur and chalcopyrite mineral grains and subsequent extraction of resultant EPS.

The efficiency of cell recovery to the pellet was calculated to be 98%. Samples of the supernatant, containing the colloidal EPS fraction, were collected and stored at 4ºC for further processing. The harvested cell pellet, assumed to contain all of the cell biomass in the culture ± 2%, was washed by gentle re-suspension in 40 mL Mackintosh basal salts medium (pH 2.5) followed by centrifugation. The supernatant fraction, containing loosely bound or associated EPS, was retained and stored at 4ºC for further processing. The cell pellet, containing the capsular EPS fraction was split into two with capsular EPS recovered through the addition of either 10 mL 10 mM EDTA based on Gehrke *et al.* (1998), Tapia *et al.* (2009) and Michel *et al.* (2009) or 30 mM dicyclohexyl-18-crown-6-ether (CE) in Tris buffer as per Aguilera *et al.* (2008), followed by gentle agitation for 2 hours at 4° C. A measure of 2 grams of chalcopyrite mineral grains was harvested

from the chalcopyrite reactor systems. These were then treated with EDTA and crown ether as explained above, in order to extract the mineral bound EPS portion. This fraction is associated with an attached *M. hakonensis* population.

A sample was taken from each capsular EPS extraction and the presence of the intracellular enzyme glucose-6-phosphate-dehydrogenase (G6PDH) measured according to Platt *et al.* (1985) to determine the extent of cell lysis during the extraction process. The chemical oxygen demand of the extracted sample was also analysed, providing validation for the presence of organic matter in the extracted EPS fractions.

All the samples were then filtered twice through a 0.22 µm filter (Merck Millipore), before being dialysed (Pur-A-lyzer Mega 20 ml dialysis kit, Sigma Aldrich, 3.5 kDa cut-off) against sterile milliQ water (water volume was greater than 25 times the total sample volume to be dialysed) for 12 hours with water exchanged twice. Samples were subsequently stored at 4°C until quantitative chemical characterisation was carried out. The EPS dry weight was determined, in duplicate, following lyophilisation of 1 mL fractions of the stored samples (detailed in Section 3.9.2). The dry weights of a control sample containing lyophilised extraction medium (crown ether or EDTA) as well as a control containing lyophilised growth media were determined. These dry weights were subtracted from the dry weights of the EPS samples in order to determine the dry weight of EPS only.

The EPS dry weight presented was normalised as a mass per $1x10^{10}$ cells to allow for comparisons to be drawn across experimental runs and known literature values presented in discussion of the results.

5.2.2 Interrogation of the degree of cell disruption of extraction protocol

An optimised EPS extraction protocol should minimise cell lysis in order to ensure that the biochemical components measured are only constituents of the EPS and do not originate from the cytoplasm. In this study an assay for the intracellular enzyme, glucose-6-phosphate-dehydrogenase (G6PDH), was employed following the EPS extraction process to determine the extent of *M. hakonensis* cell lysis and intracellular contamination (Platt *et al.,* 1985). The extent of cell lysis due to extraction with either EDTA or crown ether is represented graphically in Figure 5.2. Light microscopy of the same samples was carried out for visual confirmation of intact *M. hakonensis* cells.

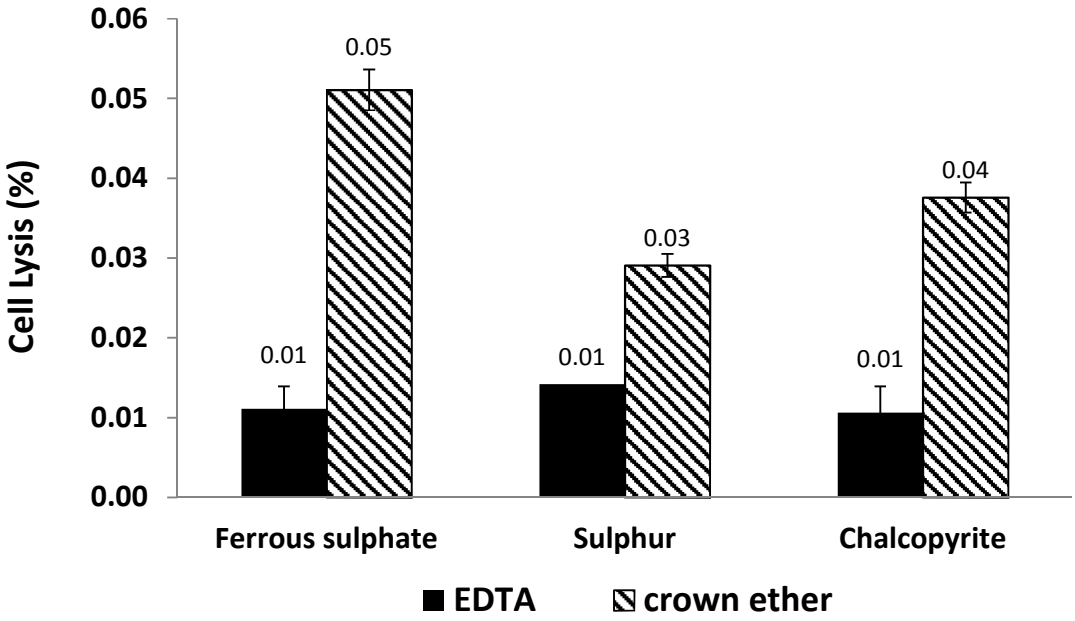

Figure 5.2: Extent of cell lysis given as a percentage observed relative to complete cell lysis by measuring G6PDH activity.

Crown ether resulted in higher levels of cell lysis over EDTA for EPS extraction across all three energy sources. However, overall negligible G6PDH activity was detected from samples taken through the extraction process. Thus the extraction protocols employed did not result in significant lysis of *M. hakonensis.*

5.2.3 Chemical oxygen demand of EPS extraction from *M. hakonensis* cultured on three energy sources

To verify the presence of organic matter in extracted EPS fractions, the chemical oxygen demand of the samples was assayed using the potassium dichromate method (Chapter 3.4.3.6). All samples investigated contained cell free capsular EPS extracted from *M. hakonensis* cultured on either ferrous sulphate, sulphur or a chalcopyrite mineral concentrate. Analyses were conducted in duplicate with the average across the two samples assayed and the associated standard deviation presented in Table 5.1. Since numerous washing steps were involved in preparation of the EPS samples, the interference of inorganic compounds is thought to be negligible in the COD

analysis. Cell free spent media from the chalcopyrite mineral system, which contained both the colloidal and loosely bound EPS fractions, was also assayed to confirm the presence of organic matter in these fractions.

Table 5.1: Chemical oxygen demand measured to verify presence of organic matter after EPS extraction.

Sample	COD (mg L^{-1})
Extraction sample, Chalcopyrite mineral conc. grown	399.6 ± 14.0
Extraction sample, Sulphur grown	72.7 ± 9.3
Extraction sample, Ferrous sulphate grown	19.8 ± 0.0
Cell free, spent chalcopyrite media (colloidal and loosely bound EPS)	6.6 ± 0.0
Reference and Negative control (distilled water)	0.0 ± 0.0

Extracts recovered from chalcopyrite grown cells yielded the highest COD (see Table 5.2), followed by extracts from sulphur grown cells, with ferrous sulphate grown cells yielding the lowest COD. The spent media sample yielded a COD of 6.6 mg L^{-1}. Thus the data presented confirms that organic material was indeed present in the samples extracted from cells grown on the three energy sources. This, together with minimal cell lysis observed, indicates the presence of EPS successfully extracted from *M. hakonensis* cells cultured on the three energy systems.

5.3 YIELD AND EXTRACTION EFFICIENCY OF EPS FROM PLANKTONICALLY GROWN *M. hakonensis*

EPS yield was demonstrated to be dependent on extraction time, shear rate, temperature and chemical used (Frolund *et al.* 1996). In the context of bioleaching, there is no defined EPS extraction protocol. However, some authors have made use of a combination of physical and chemical treatments, namely the use of centrifugation combined with ethylenediaminetetraacetic acid (EDTA) or ethylene glycol-bis(β-aminoethyl ether)-N,N,N',N'-tetraacetic acid EGTA in the extraction of EPS from acidophilic systems (Gehrke *et al.* 1998, Aguilera *et al.* 2008, Zeng *et al.* 2010, Michel *et al.* 2009, Tapia *et al.* 2009). Use of EDTA was demonstrated to cause a certain degree of cell lysis as well, believed to be a result of the removal of divalent cations from the cell wall leading to its degradation (Johnson and Perry 1976). Aguilera *et al.* (2008) investigated the

efficiency of four different chemical treatments (Water, NaCl, EDTA, Dowex and dichlorohexyl-18-crown-6-ether) for the recovery of EPS from an acidophilic eukaryotic biofilm isolated from nature. This group succeeded in characterizing both colloidal and capsular fractions of the EPS recovered and compared the efficiencies of the treatments assessed. The yield and composition of the EPS varied with the treatment method used, as did the extent of cell lysis. Crown ether yielded the second highest levels of EPS, followed by treatment with EDTA, Dowex and water. The level of cell damage caused by Crown ether, EDTA and Dowex were comparable and were substantially lower than that caused by other treatments. Due to this fact, Crown ether and EDTA were utilised in this study for the recovery of capsular EPS.

Table 5.2 presents a summary of the EPS yields recovered from planktonic *M. hakonensis* grown on three substrates, namely chalcopyrite, ferrous sulphate and sulphur. The experiment was performed in duplicate. In each experimental run, the cell pellet was split and the capsular fraction extracted using EDTA and crown ether, the results of which were compared. The greatest yields of EPS were recovered from *M. hakonensis* cultured on chalcopyrite mineral grains, followed by those grown on sulphur and ferrous sulphate when crown ether was used as an extraction reagent (Table 5.2). Overall, enhanced recoveries of EPS are yielded using crown ether as an extraction reagent relative to EDTA. When EDTA was used as an EPS extraction reagent, the highest recoveries of EPS were observed from the chalcopyrite system relative to the ferrous sulphate and sulphur systems. However, greater amounts of EPS were recovered from ferrous sulphate system relative to the sulphur system using EDTA.

Table 5.2: A summary of the total EPS yields recovered from *M. hakonensis* grown on three substrates

Fraction of EPS recovered	**Energy source**					
	Chalcopyrite		Ferrous sulphate		Sulphur	
	(mg /1x10^{10} cells)	% total dry weight EPS	(mg /1x10^{10} cells)	% total dry weight	(mg /1x10^{10} cells)	% total dry weight
Colloidal	2.9 ± 0.2	17	3.6 ± 0.5	48	1.3± 0.06	14
Loosely Bound	2.3 ± 0.2	13	1.5 ± 0.9	20	1.0 ± 0.2	10
Capsular (CE)	12.1 ± 1.8	70	2.4 ± 0.5	32	7.3 ± 0.3	76
Total	17.4 ± 1.8	100	7.6 ± 1.2	100	9.6 ± 0.4	100
Fraction of EPS recovered	**Energy source**					
	Chalcopyrite		Ferrous sulphate		Sulphur	
	(mg /1x10^{10} cells)	% total dry weight EPS	(mg /1x10^{10} cells)	% total dry weight	(mg /1x10^{10} cells)	% total dry weight
Colloidal	2.9 ± 0.2	19	3.6 ± 0.5	53	1.3± 0.06	33
Loosely Bound	2.3 ± 0.2	15	1.5 ± 0.9	22	1.0 ± 0.2	25
Capsular (EDTA)	10.3 ± 1.8	66	1.7 ± 0.3	25	1.7 ± 0.2	42

Total	15.5 ± 1.8	100	6.9 ± 1.1	100	4 .0 ± 0.3	100

Since the highest levels of EPS were extracted from cells grown on chalcopyrite than on sulphur and ferrous sulphate, irrespective of which extraction reagent was used, it may be inferred that the presence of chalcopyrite mineral enhances EPS production. Similar findings were observed by Gehrke et al. (2001) who demonstrated the effect of growth substrate and subsequent EPS yield for *A. ferrooxidans*, with highest levels of EPS obtained for cells grown on pyrite, followed by sulphur and then ferrous sulphate. EPS production has been demonstrated to increase when a solid substrate is introduced (Vandevivere and Kirchman 1993). Usher *et al.* (2010) observed enhanced production of exopolymers in the presence of a solid mineral (pyrite) substrate for *M. hakonensis* using TEM visualisation of cells. This group reported negligible EPS for ferrous and sulphur grown *M. hakonensis* under the conditions of their experiment.

Gerhke et al. (2001) harvested EPS using centrifugation for cells in liquid suspension which is the equivalent of only the colloidal fraction in this study. They report yields of 0.215 ± 0.03; 2.76 ± 0.001 and 1.155 ± 0.094 mg EPS/1x10^{10}cells for colloidal EPS extracted from *A. ferrooxidans* cultivated on ferrous sulphate, pyrite and sulphur respectively. This is the same order of magnitude, but in some cases a two to four fold difference is seen relative to the colloidal and loosely bound EPS values in this study. This trend is observed across all three growth systems, with the exception of ferrous sulphate grown *M. hakonensis* which yielded enhanced levels of EPS relative to *A. ferrooxidans*. A graphical representation of the results presented in Table 5.2 is provided in Figure 5.3. This allows for the localisation of the EPS fractions to be further interrogated.

The effect of extraction methodology on the yield of EPS attained was observed by Aguilera *et al.* (2008) and Tapia *et al.* (2009) for acidophilic biofilms. Aguilera et al. (2008) also report superior levels of EPS extraction using crown ether relative to EDTA for the recovery of EPS from eukaryotic biofilms isolated from extreme acidic environments. This same trend is observed in this investigation. Both crown ether and EDTA act by way of cation exchange in order to recover and concentrate EPS from the environment. EDTA acts as a hexadentate ligand and chelating agent. It can sequester metal ions through cation exchange. EDTA and EGTA facilitate the removal of EPS from the capsular region through removal of divalent cations (mainly Ca^{2+} and Mg^{2+}) which disrupt crosslinking of charged compounds, essentially destabilising the EPS matrix. Crown ether strongly binds certain cations, and form complexes. Oxygen atoms are well situated to coordinate with a cation located at the interior of the ring, whereas the exterior of the ring is hydrophobic. The resulting cations often form salts that are soluble in nonpolar solvents. EPS from different

spatial locales were purified and quantified. The amount of EPS recovered from each locale varied depending on the growth medium used. For the chalcopyrite growth system, most of the EPS mass extracted was closely associated with the cells, with 66 - 70 % of the EPS mass attributed to the bound fraction extracted (Figure 5.4).

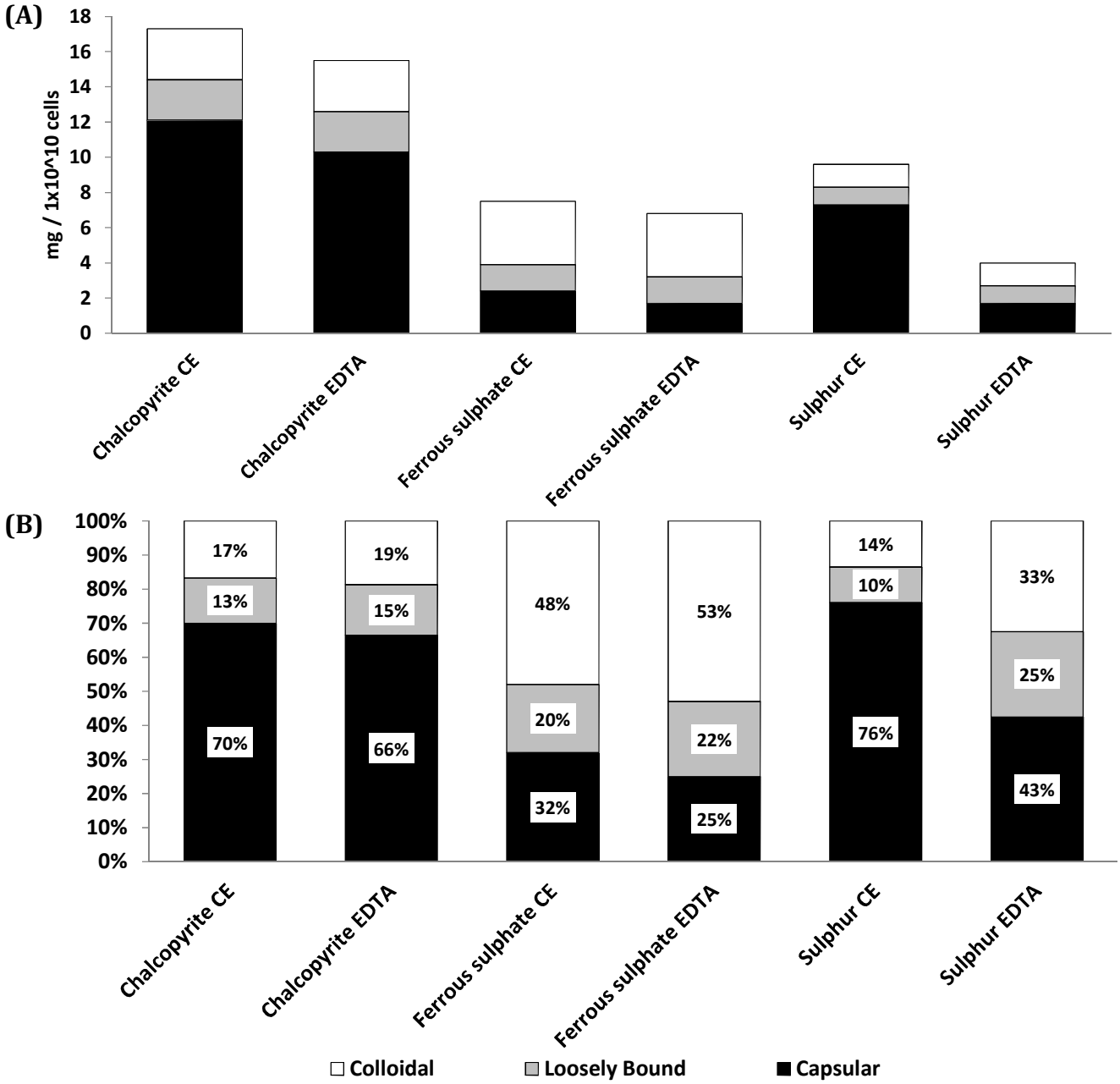

Figure 5.3: The yield of EPS, separated into three distinct fractions, extracted from *M. hakonensis*, grown on three substrates, namely chalcopyrite, sulphur and ferrous sulphate. The three fractions were colloidal, loosely bound and capsular EPS. Capsular EPS was extracted using chemical treatment with either EDTA or Crown Ether (CE). EPS yield is reported as mg EPS dry weight associated with 1 x 10^{10} cells (A) and each fraction recovered as a percentage of the total EPS dry weight recovered (B).

This was followed by colloidal EPS, contributing 17 - 19 % to the total EPS mass extracted, with loosely bound EPS yielding 13 - 15 % of the total mass of EPS recovered from the chalcopyrite growth system. A similar trend is observed for EPS recovered from the sulphur growth system. The greatest yield of EPS is recovered from the bound fractions, with this fraction contributing up to 76 % of the total EPS mass recovered when extracted using crown ether. Colloidal and loosely bound EPS contribute lesser amounts 14 – 33 and 10 – 25 % respectively for EPS recovered from the sulphur growth system. There is a general trend of EPS predominantly localised to the immediate vicinity of the cells, namely the capsular region, for cells grown on chalcopyrite or sulphur as a substrate. From this it can be inferred that EPS potentially plays a role in metabolism or offers a protective and stabilising function due to its locale.

For the ferrous sulphate growth system, the greatest yield of EPS was recovered from the colloidal 48 – 53 % of the total EPS mass recovered. This was followed by the capsular EPS fraction contributing 20 - 32% of the total EPS mass; with only 20 – 22 % of the total EPS mass attributed to the loosely bound fraction (Figure 5.3, Table 5.2). The proportion of the total EPS mass made up by the colloidal fraction in the ferrous sulphate system was two to three times greater than that observed for colloidal fractions of the chalcopyrite and sulphur grown systems. Thus, for ferrous sulphate grown cells, there is trend toward the excretion of greater quantities of EPS into the environment, with a lesser abundance of EPS located in the immediate vicinity of the cells (capsular EPS) relative to chalcopyrite and sulphur grown cells.

5.4 EXTRACTION OF CHALCOPYRITE MINERAL BOUND EPS

Thus far, EPS under investigation has been cell associated, or excreted into the liquid environment by cells cultured in a planktonic system. In a heap bioleach environment, the EPS form would be largely associated with the mineral surface in the formation of active biofilms. In Chapter 4, clouds of EPS branching out from the mineral grains were evident (represented again in Figure 5.4). Cells attached to the mineral surface and associated with the EPS were also observed. The results presented in Figure 5.4, and discussed in Chapter 4, provided evidence of *M. hakonensis* cells attached to the surface of chalcopyrite mineral grains, embedded in a milieu of cloud-like EPS. For the section of the investigation reported in this section, EPS was extracted from the surfaces of chalcopyrite mineral grains. The chalcopyrite mineral grains were sourced from the 5L Schott bottle reactors used for *M. hakonensis* EPS cultivation, described in Section 5.2.1.

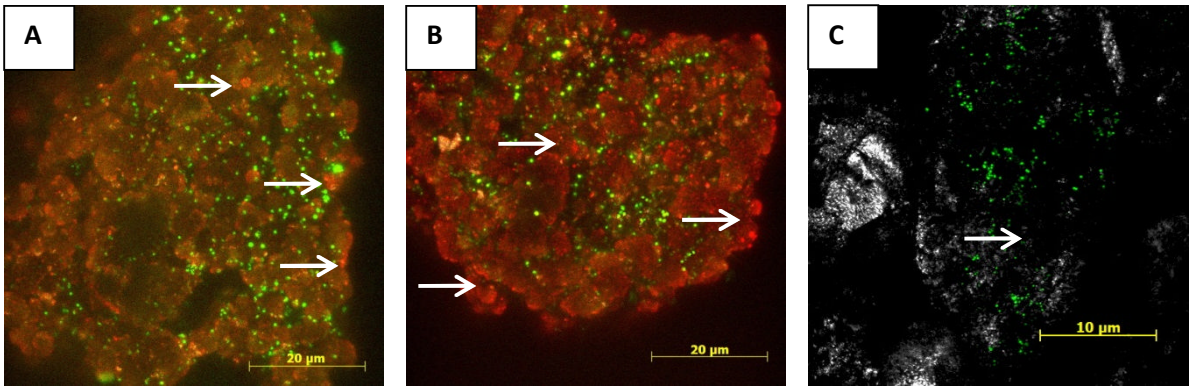

Figure 5.4: Micrographs depicting results of lectin screening conducted on sessile *M. hakonensis* cells attached to chalcopyrite mineral grains after batch agitated incubation in a shake flask. Micrographs depict overlays of two channels; lectin probes were labelled with either Alexa568™ or TRITC are depicted in red, with SYTO9™ used as a counter stain to visualise attached cells depicted in the green channel. The confluent mat EPS motif, as well as the cloud-like EPS motif can be seen in micrographs (A) and (B). The lectins used in the micrographs presented as follows: (**A**) Alexa568-PSA, (**B**) TRITC-GSI. Cells attached to the surfaces of chalcopyrite mineral grains are visualised using a Syto9 nucleic acid stain only are presented in micrograph (**C**).

Crown ether or EDTA was used to recover EPS which was tightly associated with the chalcopyrite mineral grains and the associated sessile cells, hereafter referred to as mineral bound EPS. The mineral bound EPS was then quantified and its composition analysed. The results are presented in Table 5.5.

A trend of greater levels of EPS is observed to be recovered from the mineral grains when EDTA is used relative to CE. Also, the amount of EPS recovered from the mineral surface is similar to that recovered from the colloidal and loosely bound environments. The increased amount of capsular EPS could be due to the fact that the environment was continuously well agitated throughout the EPS cultivation.

Table 5.3: Mass of mineral bound EPS, produced by *M. hakonensis* cultured on chalcopyrite, recovered using either crown ether (CE) or EDTA

Mineral bound EPS – CE extracted	(mg /1x10^{10} cells)	% total mineral bound EPS
Total recovered	1.45 ± 0.07	100
Mass of measurable components	1.29	89
Unaccounted mass	0.16	11

Mineral bound EPS – EDTA extracted	(mg /1x10^{10} cells)	% total mineral bound EPS
Total recovered	1.94 ± 0.21	100
Mass of measurable components	1.11	57
Unaccounted mass	0.83	43

Since the environment is continuously mixed, the majority of the EPS is located in the immediate vicinity around the cells – i.e. the capsular fraction, as opposed to around the mineral surface. Production of capsular EPS may have benefits in bioleach environments as it would offer more protection in harsh microenvironments and allow for bioleach reactions to take place in close proximity to the cell as per the indirect contact mechanism.

Yildiz *et al.* (2014) demonstrated increased production of EPS in the thermophile *Brevibacillus thermoruber* led to increased chelation of cations in the biofilm matrix which led to enhanced biofilm matrix stability. This characteristic would be beneficial in the continuously well agitated tank reactors as used in this investigation and in a bioleaching environment.

Kreft and Wimpenny (2001) modelled biofilm formation in a nitrifying biofilm and demonstrated that production of capsular EPS gave rise to more uniform well-spaced biofilms with increased porosity. Furthermore, EPS production has been said to aid biofilm dispersion (Yildiz et al. 2014). Thus the production of EPS may be a means of controlling the microbial population in the immediate vicinity, which will enable the archaea to dominate larger areas of mineral surface while keeping the overall population size under control.

5.5 BIOCHEMICAL COMPOSITION OF *M. hakonensis* EPS

5.5.1 Identification of predominating components of EPS from planktonic *M. hakonensis* cultures

As shown in Table 5.6 and Fig. 5.5, the main components present in the EPS extracted from *M. hakonensis* grown on three different substrates included carbohydrates (sugars), proteins, uronic acids, small amounts of iron, as well as nucleic material. The abundance of each component varied depending on the growth substrate and the chemical reagent used for capsular EPS extraction.

The following trends were observed for EPS extracted using crown ether: EPS extracted from chalcopyrite-grown systems contained predominantly protein, comprising 38% of the total EPS dry weight extracted from the system, followed by sugars (10%) uronic acids (7%) and iron (6%), as detailed in Figure 5.5. The nucleic components measured were less than 1 % of the total EPS dry weight for this system.

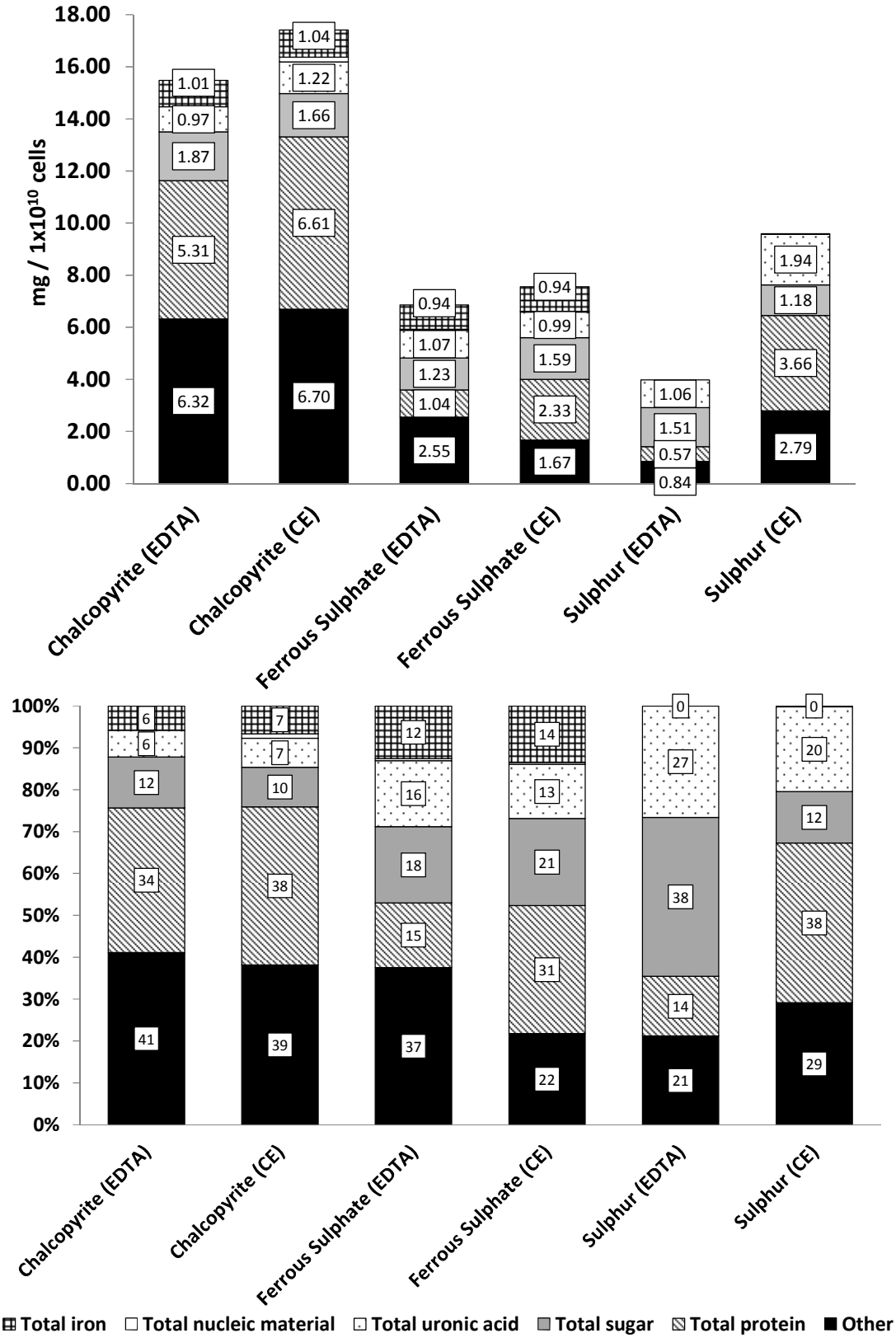

Figure 5.5: The biochemical composition of EPS extracted from planktonic *M. hakonensis* grown on three different substrates, namely chalcopyrite, sulphur and ferrous iron (A). The main components identified were DNA, sugars, uronic acids, proteins and iron. The biochemical composition of each EPS fraction extracted from *M. hakonensis* grown on three different substrates is reported as a percentage of the total EPS dry weight recovered (B).

For the crown ether extracted sulphur system, a similar trend is observed with the protein component contributing most of the total mass (31%). However, the sugar and uronic acid components were higher than that observed for the chalcopyrite system, uronic acids contributing 20% and sugars contributing 12% and of the total EPS dry weight recovered. Interestingly, no measurable nucleic acid material was recovered from the sulphur system. For the ferrous sulphate system, proteins still accounted for a third of the total EPS mass recovered. However, greater levels of sugars were present, with sugars accounting for 21% of the total EPS mass and uronic acids contributing 13%.

In Section 5.3, the chemical reagent used for EPS extraction from planktonic cells was shown to affect the yield of EPS attained. The results of this section indicate that the chemical reagent used for EPS extraction also impacts on the proportions of the chemical compounds recovered in the EPS. For the ferrous sulphate and sulphur systems, EPS recovered using crown ether were observed to be enriched with protein, whereas extraction of these systems using EDTA correlated to enhanced levels of sugars and uronic acids. The chalcopyrite system presented an exception in which the proportions of components recovered using crown ether were similar to that recovered using EDTA. However, in all cases the overall recovery of EPS yielded greater amounts using crown ether relative to EDTA.

A mass balance of the chemical components and the total EPS isolated was performed. In each fraction of EPS recovered and analysed, an unaccounted mass was observed. This mass is demarcated as "Other" in Figure 5.5. To date, EPS composition has been said to be comprised of polysaccharides, heavy metals, uronic acids, amino sugars, proteins, humic substances, nucleic acids and phospholipids (Nielsen and Jahn 1999, Chapter 1, p4). EPS can also be comprised of components which are sequestered from the local environment; these include heavy metals (Aguilera et al. 2008). The works of several authors regarding chemical compositions of EPS isolated from acidic environments or from microorganisms relevant to bioleaching is summarised in Table 5.4.

Gehrke et al. (1998 and 2001) analysed the chemical composition of partially purified *A. ferrooxidans* EPS, and demonstrated that it was predominantly comprised of neutral sugars and lipids with the relative composition dependent on the growth medium. EPS from this microorganism contained 52.2% sugars and 36.9% lipids when grown on ferrous sulphate, 48.5% sugars and 39.4% lipids when grown on pyrite mineral grains, and 40.9% sugars and 53.8% lipids when cultured on sulphur (Table 5.4). Gehrke do not report the presence of any proteins or nucleic material. The EPS extraction technique differed to that used here as it made use of centrifugation of the liquid medium only – which is equivalent to the colloidal fraction of EPS in this study. When comparing the colloidal fraction of EPS isolated from chalcopyrite grown *M. hakonensis*, the EPS fraction contains 16% sugars 19% uronic acids. No proteins were observed.

This is in line with the reports of Gehrke et al., who do not report the presence of proteins. Methodology of extraction affects the composition of the EPS isolated. Method used by Gehrke et al. may have excluded proteins and nucleic materials.

Zeng et al (2010) extracted EPS from sessile cells in a mixed moderately thermophilic culture containing *Acidithiobacillus caldus, Leptospirillum ferriphilum* cultured in a CSTR with a 6-8% chalcopyrite mineral loading at 48 ºC for three days. The chalcopyrite loading used by Zeng et al. is significantly higher than the 1.6% used in this thesis. Zeng et al. reported total sugars to comprise 54% of the total EPS dry weight with fatty acids making up 38%, proteins 7% and uronic acids 6%. EPS was extracted using EDTA. The level of proteins and uronic acids reported by Zeng et al. are in line with those observed in this study for EDTA extracted EPS cultured on chalcopyrite, where 9% and 6% for proteins and uronic acids were observed respectively (Figure 5.5). However, a mass balance across results reported by Zeng et al. indicate an over estimation in one of the components as individual components identified summed to more than the total mass of EPS extracted.

Jiao et al. (2010) extracted EPS using sulphuric acid, from two pellicle biofilms growing on acid mine drainage solutions. These biofilms were dominated by *Leptospirillum group* II, *Leptospirillum* group III and archaea. This group reports an EPS composition comprising of carbohydrates (52 and 43%), heavy metals (31 and 23%), proteins (9 and 23%) and DNA (2 and 5%). Lipids were also found to be present. However, quantitative results for lipids were not reported. Also, there was no assay for cell integrity performed after the use of concentrated sulphuric acid for the EPS extraction. Thus, the potential for results to be contaminated by intracellular components exists.

Tapia et al. (2009) extracted EPS from planktonically grown *Acidiphilium* cultures in the presence and absence of carbon fibre supports using EDTA, NaOH, heat treatment and centrifugation as EPS extraction reagents. IR and UV spectroscopy was used to identify EPS chemical components, with carbohydrates, proteins and lipid material observed to be present. Tapia et al. and Gehrke et al. (2001) observed the presence of fatty acids in the make-up of the EPS recovered from acidophilic systems using EDTA as an extraction reagent. A portion of the unaccounted mass in this study may be attributed to the presence of lipid material. The presence of lipid material in EPS samples arising from this study were analysed using NMR spectroscopy (see Appendix D). The results depict the presence of a methyl group which could be associated with fatty acids or lipid material. However, NMR results were inconclusive in this study due to the presence of a contaminant in unit at the time of analysis.

Table 5.4: Summary of EPS composition extracted from acidophilic microenvironments

Author	Microorganism	Method	Concentration components	pH
Gerhke et al 2001	*A. ferrooxidans* strain 1 Sulphur, ferrous sulphate and pyrite grown	Cells grown on pyrite grains <100µm, sulphur or ferrous sulphate media. EPS extracted from sessile cells using homogenization and centrifugation	Ferrous sulphate grown: 0.215 ±0.03mg EPS/1 x10^{10} cells EPS composition: 52.2% w/w sugars, 36.9% lipids negligible protein and DNA Pyrite grown:2.76 ±0.001mgEPS / x10^{10} cells EPS composition: 48.5.% w/w sugars, 39.4% lipids negligible protein and DNA Sulphur grown:1.155 ±0.094mg EPS x10^{10} cells EPS composition: 40.9% w/w sugars, 53.8% lipids negligible protein and DNA	2.0
Aguilera *et al.* 2008;	EPS extracted from three benthic eukaryotic acidic biofilms from riotinto. Biofilm consisted of predominantly diatoms, green algae	Crown ether EDTA Dowex exchange resin NaCl Water	Colloidal EPS more abundant than capsular in these biofilms. CE yielded greater amounts relative to EDTA, close to 300mg/g versus close to 200mg/g biofilm. Mostly hexose sugars Protein: Lowry method only accounted for 2% of total EPS mass recovered. 3.9 – 4 mg/gDW Smaller quantities of heavy metals, nucleic material, humic substances observed	0.9-2.5
Tapia *et al.* 2009	*Acidiphilium 3.2Sup(5)* *Final cell concentrations 1.28 – 1.5x10^{9} cells/ml*	EPS extraction using EDTA, exchange resin, centrifugation, NaOH in presence and absence of solid support	Amount and composition of EPS recovered varied depending on extraction method used. EDTA resulted in best yields of EPS with minimum lysis of cells. Proteins measured using FT-IR, ranged from 97 – 2278mg /g cell DW for EPS extracted from cells in liquid suspension EPS protein levels were highest for EPS extracted from carbon fiber surfaces	2.5
Jiao *et al.* 2010	2 pellicle biofilms (floating biofilms) predominantly comprised of *Leptospirillum* group II (43%) and III (28%) as well as archaea (29%)	*150 – 350 mg EPS extracted per g DW biofilm* *Sulphuric acid and centrifugation to extract EPS*	Carbohydrates 52 – 43% Metals 34% - 23% Protein 9 – 23% DNA 2 – 5% Lipids present but not quantified	1.1
Zeng *et al.* 2010	Mixed moderately thermophilic culture (dominant *Acidithiobacillus caldus, Leptospirillum ferriphilum*) 2x10^{9}cells/ml final cell concentration EPS extracted from sessile cells attached to mineral chalcopyrite mineral surface	3L CSTR 6 – 8% pulp density chalcopyrite; 48 ºC, Bradford assay for protein analysis EPS extracted using EDTA and centrifugation KDO cell integrity assay done	Proteins 7 -12 % Sugars 54 – 52% Uronic acids 6% Fatty acids 38 – 40% After 3 and 8 days	2.0
Usher *et al.*2010	*A. ferrooxidans* *L. ferriphilum* *M. hakonensis* *Grown in shake flasks*	No EPS was detected using visualisation methods employed by Usher for *M. hakonensis* for growth on sulphur or ferrous sulphate. (TEM) EPS only detected for *M. hakonensis* grown on chalcopyrite.	Not applicable Visualised presence of EPS using TEM	2.0

Aguilera et al. (2009) extracted EPS from biofilms growing in the Rio Tinto River under very acidic conditions. The biofilms consisted of predominantly green algae and diatoms. Interestingly, the EPS extracted from these biofilms consisted largely of colloidal EPS, rather than capsular EPS. The colloidal fractions contained high levels of hexose sugars, with proteins only comprising 2 % of the total EPS mass. Smaller quantities of heavy metals, humic substances and nucleic material were also observed. As observed in this study, Aguilera et al. also report that the EPS extraction methodology used affects the biochemical characteristics of the isolated EPS. The group used a variety of methods to extract EPS, with crown ether being superior in extraction efficiency, relative to EDTA. However, the use of EDTA for EPS extraction was also correlated to enhanced recoveries of heavy metals (up to 10 % of the EPS dry weight recovered) and hexose sugars from the system. In this study, iron analysis was performed on samples isolated from the chalcopyrite and ferrous sulphate systems. However, the presence of other metals which could have been released during the culturing phase was not assayed for in the chalcopyrite mineral system. These could have contributed a small fraction of the unaccounted mass in this system.

5.5.2 Distribution of biochemical components in EPS from planktonically grown *M. hakonensis*

The biochemical composition of each EPS fraction was determined, namely composition of the colloidal, loosely bound and capsular fractions. Each fraction was observed to contain varying proportions of the chemical compounds assayed for. A trend of sugars and uronic acids being localised to the colloidal EPS fraction was evident (Figure 5.6, Table 5.5). This trend was observed across all three growth substrates investigated. The colloidal and loosely bound fractions isolated from both the ferrous sulphate and chalcopyrite systems also contained the highest levels of iron present relative to the capsular fractions. A greater proportion of uronic acids, in comparison to sugars was observed for the colloidal EPS fraction from chalcopyrite and sulphur grown cells, with comparable proportions of sugars and uronic acids exhibited in the ferrous sulphate system (Table 5.5, Figure 5.6).

For loosely bound EPS fractions, the composition varied depending on the growth medium. Loosely bound EPS samples from chalcopyrite and ferrous sulphate systems contained sugars and uronic acids at 0.11 and 0.12 mg per $1x10^{10}$ cells respectively. However, both these systems contained, most dominantly, proteins, with 1.71 and 1.04 mg per $1x10^{10}$ cells for EPS from chalcopyrite and ferrous grown cells respectively. In contrast, loosely bound EPS isolated from sulphur grown cells contained only small amounts of sugars and uronic acids.

Table 5.5: A summary of the chemical compositional analysis of EPS extracted from *M. hakonensis* grown on chalcopyrite, ferrous sulphate and sulphur is presented. Results presented and analysed per recovered EPS fraction.

Chemical compositional analysis per EPS fraction recovered						
Colloidal (Coll.) EPS Fraction						
	Chalcopyrite		**Ferrous sulphate**		**Sulfur**	
Component	**mg 1x10^{10} cells^{-1}**	**% dry wt**	**mg 1x10^{10} cells^{-1}**	**% dry wt**	**mg 1x10^{10} cells^{-1}**	**% dry wt**
Protein	BD	0	BD	0	BD	-
Sugar	0.46±0.00	16	0.27±0.02	7	0.47±0.01	36
Uronic acid	0.54±0.04	19	0.29±0.09	8	0.54±0.26	42
Nucleic matter	BD	0	BD	0	BD	-
Total Iron	0.9 ± 0.004	31	0.73 ± 0.01	21	-	-
Other	1.0	34	2.31	64	0.29	22
Total Coll. EPS	2.9±0.2	100	3.6±0.5	100	1.30±0.06	100
Loosely Bound (LB) EPS Fraction						
	Chalcopyrite		**Ferrous sulphate**		**Sulfur**	
Component	**mg 1x10^{10} cells^{-1}**	**% dry wt**	**mg 1x10^{10} cells^{-1}**	**% dry wt**	**mg 1x10^{10} cells^{-1}**	**% dry wt**
Protein	1.71±0.39	73	1.04±0.02	65	-	-
Sugar	0.11±0.00	5	0.12±0.01	7	0.034±0.10	3
Uronic acid	0.15±0.004	7	0.25±0.04	16	0.052±0.10	5
Nucleic matter	BD	0	BD	0	BD	-
Total Iron	0.20±0.03	9	0.10±0.03	12	-	-
Other	0.33	6	0.0	0	0.91	91
Total LB EPS	2.3 ± 0.2	100	1.5±0.9	100	1.0±0.2	100
Capsular EPS Fraction – crown ether extracted						
	Chalcopyrite		**Ferrous sulphate**		**Sulfur**	
Component	**mg 1x10^{10} cells^{-1}**	**% dry wt**	**mg 1x10^{10} cells^{-1}**	**% dry wt**	**mg 1x10^{10} cells^{-1}**	**% dry wt**
Protein	4.90±0.06	41	BD	0	3.66±0.18	50
Sugar	1.09±0.00	9	1.20±0.17	50	0.36±0.024	5
Uronic acid	0.53±0.03	4	0.44±0.14	20	0.88±0.07	12
Nucleic matter	0.19 ±0.00	2	0.03 ±0.002	<1	0.02±0.001	0
Total Iron	0.01±0.00	0	0.01±0.00	0	-	-
Other	5.39	44	0.72	30	2.38	33
Total Bound - CE	12.10 ± 1.8	100	2.4±0.5	100	7.3±0.3	100
Capsular EPS Fraction – EDTA extracted						
	Chalcopyrite		**Ferrous sulphate**		**Sulfur**	
Component	**mg 1x10^{10} cells^{-1}**	**% dry wt**	**mg 1x10^{10} cells^{-1}**	**% dry wt**	**mg 1x10^{10} cells^{-1}**	**% dry wt**
Protein	3.60±0.00	35	BD	0	0.57±0.09	31
Sugar	1.3 ±0.01	13	0.84±0.33	49	0.69±0.21	40
Uronic acid	0.28±0.01	3	0.56±0.12	31	0.52±0.07	29
Nucleic matter	BD	0	BD	2	BD	-
Total Iron	0.04 ±0.002	0	0.01±0.00	<1	-	-
Other	6.3	49	0.3	18	0	-
Total Bound EDTA	10.3±1.8	100	1.7±0.3	100	1.7±0.2	100

*Results normalised as mg per 1x10^{-10} cells, standard deviation of totals calculated using square root of mean variance, "Other" refers to mass unaccounted relative to the total dry weight recovered ***BD –** below detection limit

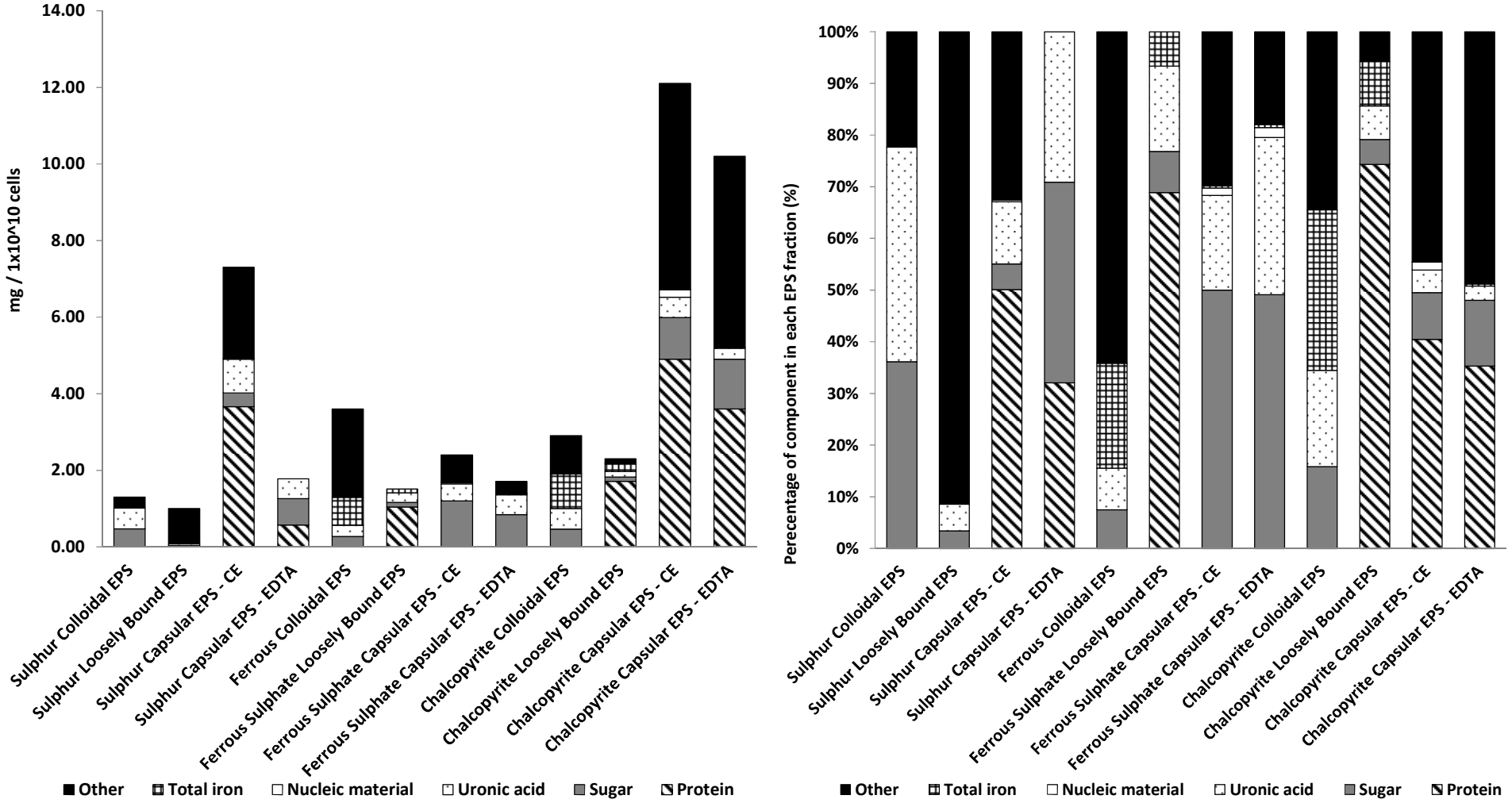

Figure 5.6: The biochemical composition of EPS extracted from *M. hakonensis* grown on sulphur, ferrous sulphate or chalcopyrite mineral grains. The components found in each EPS fraction, namely colloidal EPS, loosely bound EPS and capsular EPS extracted using crown ether (CE) and capsular EPS extracted using EDTA, are reported as mg component measured per 1 x 10^{10} cells (A). The main components identified were DNA, sugars, uronic acid, proteins with some iron detected in

chalcopyrite and ferrous sulphate samples. The biochemical composition of each EPS fraction extracted from *M. hakonensis* grown on three different substrates is reported as a percentage of the total EPS recovered (B).

For capsular EPS, all constituents were found to be present. However, the amount of constituents measured varied with the extraction method employed. EPS extracted from chalcopyrite grown cells using crown ether contained higher levels of proteins and uronic acids (4.90 mg.($1x10^{10}$)cells^{-1} and 0.53 mg.($1x10^{10}$)cells^{-1} respectively) than EPS extracted using EDTA (3.61 mg.($1x10^{10}$)cells^{-1} and 0.28 mg.($1x10^{10}$)cells^{-1} respectively). Furthermore, EPS extracted using crown ether contained small amounts of nucleic acid in the bound EPS fraction, while no nucleic acid was detected in the bound EPS extracted with EDTA.

To date, the distribution of biochemical components of EPS has not been investigated in this much detail for archaeal thermophilic bioleach microorganisms. Michel et al. (2009) extracted and analysed the chemical composition of three separate fractions EPS from a CSTR containing mixed acidophilic consortium. The consortium contained *Leptospirilim ferriphilum, Acidithiobacillus caldus* and *Sulfobacillus benefaciens.* EPS from this culture contained largely sugars. Free sugars were identified using ATR-FTIR. The colloidal EPS fraction contained the highest proportion of sugars with 86 – 91.9% of the total sugars isolated from this fraction. The capsular EPS component only contained 4 – 11 % of the total sugars isolated. Similar results are reported by Aguilera et al. (2009), where greater proportions of sugars are localised in the colloidal fractions relative to the capsular fractions, which are comparable to the trends observed in this study (Figure 5.6).

5.5.3 Biochemical components of mineral bound EPS

For the EPS extracted from the chalcopyrite mineral grains, the yield and composition was affected by the extraction method employed. For crown ether extracted EPS, the most abundant component was protein, contributing 47% to the total EPS mass recovered (Table 5.6). This was followed by sugars contributing 12%, uronic acids contributing 9%, with nucleic acids and iron contributing 11% and 10 % respectively. The EDTA extracted EPS yielded higher amounts of EPS than the CE extracted EPS for mineral bound EPS. However, a significant proportion of this could not be attributed to any of the components analysed for, with 43% of the mass attributed to components not identified by the assays in this investigation. EDTA extracted mineral bound EPS contained a substantial amount of iron which contributed 31% of the total mass isolated. Proteins, uronic acids, sugars and nucleic materials were observed as 9%, 5%, 5% and 7 % of total EPS weight recovered respectively. Greater quantities of nucleic material were recovered from the chalcopyrite mineral grains than that observed for EPS recovered from the planktonic system.

Table 5.6: A summary of the chemical compositional analysis of EPS extracted from chalcopyrite mineral grains in duplicate Schott bottle reactors where *M. hakonensis* was cultured. EPS was extracted using either crown ether (CE) or EDTA, with results presented as mg EPS recovered per $1x10^{10}$cells. Results are also given as a percentage of the total EPS dry weight recovered from the mineral grains.

Chalcopyrite Mineral bound EPS - CE	**mg / $1x10^{10}$ cells**	**stdev**	**% Mineral bound EPS dry wt**
protein	0.68	0.003	47
sugar	0.18	0.098	12
uronic acid	0.13	0.020	9
nucleic material	0.16	0.120	11
Fe total	0.14	0.003	10
Other	0.16		11
Total dry weight EPS recovered	1.45	0.07	100%
Chalcopyrite Mineral bound EPS - EDTA			
protein	0.17	0.01	9
sugar	0.10	0.005	5
uronic acid	0.10	0.008	5
nucleic material	0.14	0.1	7
Fe total	0.6	0.07	31
Other	0.83		43
Total dry weight EPS recovered	1.94	0.21	100

5.5.4 Analysis of *M. hakonensis* EPS proteins, uronic and nucleic acids

The results of SDS-PAGE electrophoresis performed on EPS extracted from *M. hakonensis* cultured on ferrous sulphate, sulphur and chalcopyrite mineral grains is depicted in Figure 5.7. SDS page results indicate the presence of proteins in the extracted EPS samples, particularly for samples containing tightly bound EPS extracted with crown ether. This is in agreement with the aforementioned results depicted in Figure 5.6, where the highest proportion of proteins were observed for tightly bound EPS samples recovered using chemical methods with either crown ether or EDTA.

In lane 4 of gel A, a high density of proteins evident with large range of sizes containing more than 10 distinct bands. The largest band observed in lane 4, which is between 80 – 90 KDa, is also observed in lane 3. This particular band is quite indistinct which could be indicative of the presence of multi-pass transmembrane proteins, proteins containing hydrophobic regions or proteins containing non-protein constituents[1]. Subsequent lanes are slightly more distinct which

[1] http://www.ruf.rice.edu/~bioslabs/studies/sds-page/gellab3.html

could be indicative of the presence of soluble proteins. A doublet can be observed in lane 4. This may be due to the presence of proteins which have migrated together due to them being of a similar size and structure. Lanes 3 and 4 contained crown ether extracted, bound EPS from sulphur grown *M. hakonensis*.

Lane 14 and 15, which contained bound EPS extracted using crown ether from cells grown on ferrous sulphate. The banding pattern is comparable to that observed in lane 4. However, it is quite feint, likely due to insufficient protein concentration present in the sample. In lanes 23 and 24, containing bound EPS samples extracted using crown ether from cells grown on chalcopyrite mineral, the same banding pattern is observed as seen in lanes 4, 14 and 15.

In lanes 19, 20, 25, 26, extremely feint banding patterns can be observed. Lanes 19 and 20 contain loosely bound EPS samples, lanes 25 and 26 contain capsular EPS extracted using EDTA from cells grown on chalcopyrite mineral. Again, insufficient protein concentration in the sample would result in the very feint banding patterns observed. Although these bands are feint, they are similar in pattern to that observed for crown ether extracted samples. This is indicative of the EPS containing similar types of proteins. However, the concentration of proteins varied depending on the growth medium deployed.

Proteins have been observed to be common constituents of EPS in activated sludge flocs (Frølund *et al*., 1996 Bala et al. 2007), EPS of biofilms associated with microbially induced metal corrosion (Beech et al. 2005), as well as archaeal biofilms (Orell et al. 2013) and microbial EPS in acidic environments (Gehrke *et al.* 2001, Aguilera *et al.* 2008; Tapia *et al.* 2009 and Jiao *et al.* 2010). A primary function of EPS is to convey structural and mechanical stability to the biofilm. This is believed to be mediated by non-covalent interactions (Flemming, 1996; Mayer *et al.,* 1999) either directly between polysaccharide chains or indirectly via multivalent cation bridges (Wingender *et al.,* 1999). Higgins and Novak (1997) report the contribution of lectin-like proteins in the formation of the three-dimensional network of biofilm matrix through direct cross-linkages with polysaccharides or indirect multivalent cation bridges. Dignac *et al.* (1998) suggest that negatively charged proteins are more influential than sugars in activated sludge systems, in the determination of the floc or biofilm structure through electrostatic bonds with multivalent cations.

A more universal role of proteins in EPS is their role as exo-enzymes for the degradation of exogenous macromolecules and particulates (Wingender *et al.,* 1999). This results in the formation of low-molecular weight nutrients in the immediate vicinity of the cell which can be readily metabolised.

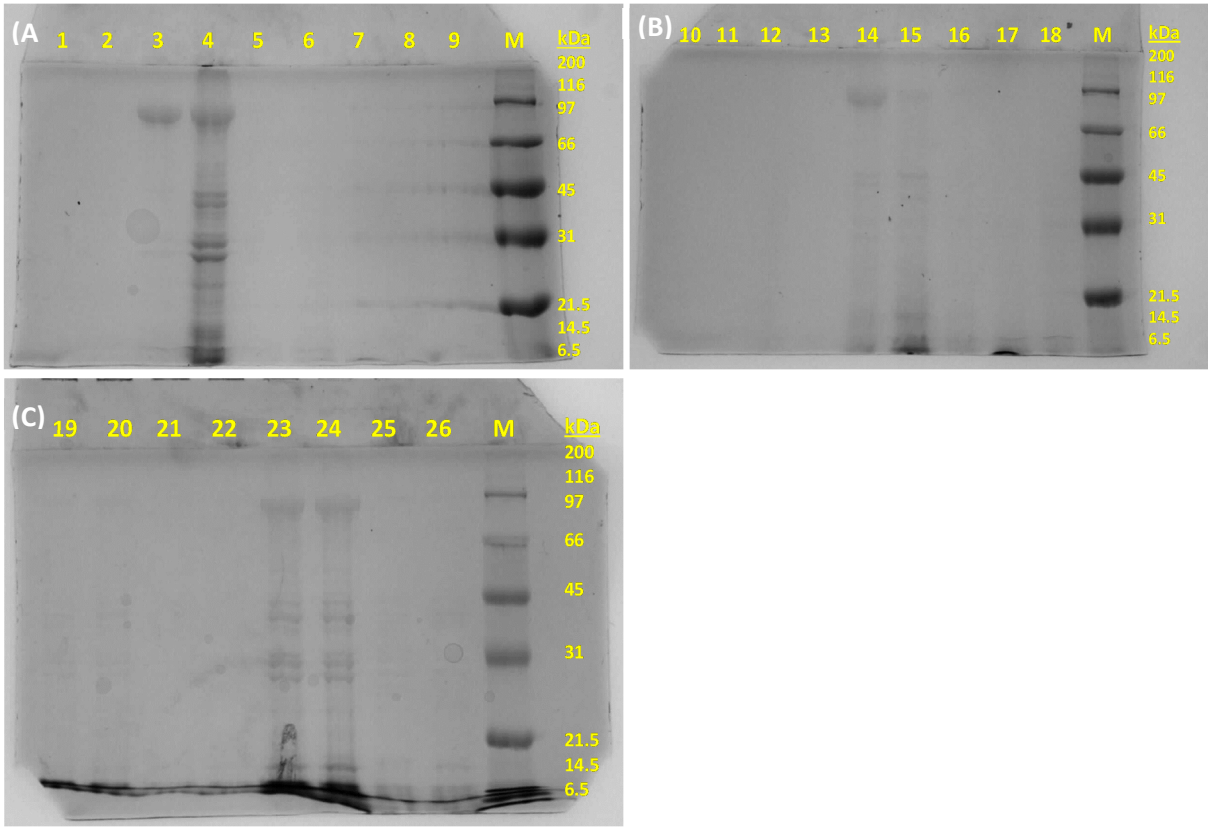

Figure 5.7: SDS-PAGE gel electrophoresis results of EPS from *M. hakonensis* cultured on: (**A) sulphur grown cells:** Lane 1 and 2 - colloidal EPS, Lane 3 and 4 CE capsular EPS, Lane 5 and 6 – loosely bound EPS, Lane 7 and 8 - EDTA capsular EPS; **(B) ferrous sulphate grown cells:** Lane 11 - EDTA capsular EPS, Lane 12 and 13 – colloidal EPS, Lane 14 and 15 – CE capsular EPS, Lane 16 and 17 – loosely bound EPS, Lane 18 – EDTA capsular EPS; **(C) chalcopyrite mineral concentrate:** Lane 19 and 20 – loosely bound EPS, Lane 21 and 22– colloidal EPS, Lane 23 and 24 – CE capsular EPS, Lane 25 and 26 – EDTA capsular EPS.

Some exo-enzymes are also believed to be involved in the degradation of the EPS matrix, resulting in the remobilisation of entrained cells and migration of the constituents to new microenvironments (Allison *et al.,* 1987). Binding and accumulation of cations, such as Ca^{2+} and Mg^{2+}, affect the stability, rheology and diffusivity of the biofilm, proteins sequester these cations (Wingender *et al.,* 1999). Beech et al (2005) also report the presence of ectoenzymes which are associated with the microbial cell but expressed outside the cytoplasmic membrane. These may include polysaccharidases, pro- teases, lipases, esterases, peptidases, glycosidases, phospha- tases, and oxidoreductases. The presence of these enzymes could account for the larger proportion of proteins observed in this study. Redfield et al. (2002) suggests that expression of secreted proteins are induced in the presence of autoinducing signals not because of the bacteria have evolved to work cooperatively, but because the benefits of secreted proteins are realized by an individual bacterial cell when local conditions limit diffusion and mixing. The secretion of

protease is used to degrade exogenous proteins so that the bacteria can assimilate amino acids (Jeferson 2004).

Uronic acids also sequester Ca^{2+} and Mg^{2+}, which affect the stability, rheology and diffusivity of the biofilm (Wingender *et al.,* 1999). In addition, uronic acids play a role in attachment to negatively charged sulfide minerals as well as the dissolution of sulfide minerals. The sequestration of ferric ions by uronic acids renders the cell surface environment with a net positive charge (Gehrke *et al.,* 1998), which is favourable for initial adhesion interactions with negatively charged sulfide mineral surfaces. Gehrke *et al.* showed that cells deficient of EPS were unable to sequester Fe^{3+} and mineral oxidation of pyrite did not occur in their presence, with performance comparable to their abiotic control (Gehrke *et al.,* 1998). In addition, this same study showed that dead cells are unable to oxidize pyrite. The presence of uronic acids in the EPS of bioleach microorganisms has thus been proposed to serve as a prerequisite for initial mineral-microbe adhesion interactions and to facilitate the oxidation of pyrite. A further proposed function of uronic acids present in EPS is to provide protection from shear forces. Dade *et al.* (1990) demonstrated that *Altermonas atlantica* grown in fine sands yielded increased amounts of acidic EPS containing high uronic acid content, which was correlated to resistance to shear stress. The authors inferred that acidic EPS aids in permanent adhesion to sedimentary surfaces and also leads to grain-to-grain adhesion which increases sediment stability (Wolfaardt *et al.,* 1999).

EPS extracted using crown ether contained small amounts of nucleic acid in the bound EPS fraction, while no nucleic acid was detected in the bound EPS extracted with EDTA. Very little is known about the role of extracellular nucleic acids within biofilms associated with mineral leaching to the successful proliferation of the biofilm and its constituent cells. Lorenz and Wackernagel (1994) proposed that extracellular nucleic material within EPS may contribute some means of protection for biofilm-associated cells against DNases. Lebaron *et al.*(1997) suggested that the EPS interface within a biofilm concentrates cells and allows for a greater probability of cell-to-cell contact and DNA or plasmid exchange, leading to enhanced horizontal gene transfer.

5.5.5 Analysis of *M. hakonensis* EPS carbohydrates

Five sugar monomers, namely rhamnose, fucose, mannose, galactose and glucose within *M. hakonensis* EPS were detected using GC-MS (Figure 5.8). The proportions of the sugar monomers

varied with growth substrate. EPS extracted from the chalcopyrite system contained 0.5% rhamnose, 0.7% fucose, 11.5% mannose, 7.0% galactose and 80.3% glucose. The ferrous sulphate system contained 0.8% rhamnose, 0.8% fucose, 16.5% mannose, 0.8% galactose and 82% glucose. The sulphur system contained 5.7% rhamnose, 6.0% fucose, 50.3% mannose, 8.2% galactose and 29.8% glucose. Chalcopyrite and ferrous sulphate grown cells contain enhanced proportions of glucose monomers relative to sulphur grown cells.

The following groups report the same component sugar monomers of EPS extracted from mesophilic bioleach microorganisms. Gehrke et al. (2001) report the following sugar monomers present in EPS extracted *A. ferrooxidans* grown on pyrite, sulphur and ferrous sulphate: pyrite grown cells contained 10.8% rhamnose, 17.1% fucose, 0.8% xylose, 0.7% mannose, 15.2% glucose and 3.3% glucuronic acid; ferrous sulphate grown cells contained 13.9% rhamnose, 20.5% fucose, 0.9% xylose, 0.4% mannose, 11.4% glucose and 4.4% glucuronic acid. Sulphur grown cells only contained glucose with a small quantity of glucuronic acid. Zeng et al (2010) extracted EPS from a mixed moderately thermophilic culture containing *Acidithiobacillus caldus, Leptospirillum ferriphilum* cultured in a CSTR with a 6-8% chalcopyrite mineral loading at 48 ºC. The following sugars were reported: rhamnose (10.6%), fucose (18.2%), xylose (3.3 %), mannose (3%) and glucose (18.5%). Jiao et al. (2010) report the presence of glucose (20.1 and 17.2%), galactose (12.1 and 5.6%), rhamnose (13.0 and 17.7%), mannose (11.8 and 21.9%), hexose (25.5 and 12.0%), heptose (28.4 and 19.5%) and arabinose (1.0 – 4.2%) for EPS extracted from two pellicle biofilms (floating biofilms) predominantly comprised of *Leptospirillum* group II (43%) and III (28%) as well as archaea (29%).

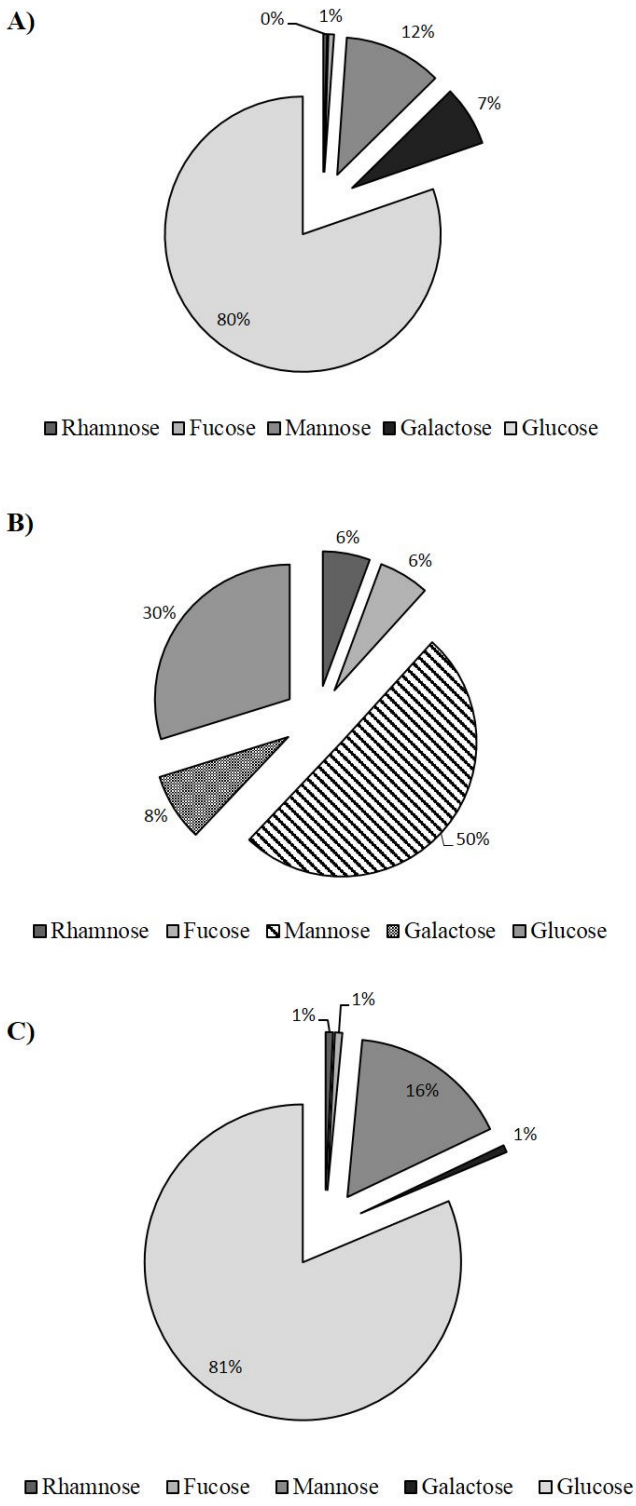

Figure 5.8: The relative proportions of sugar monomers present in EPS extracted from *M. hakonensis* cultured on chalcopyrite (A), sulphur (B) or ferrous sulphate (C) substrates. Five sugar monomers were detected, namely, rhamnose, fucose, mannose, galactose and glucose, in varying relative proportions (%) depending on the growth substrate.

It is apparent that the sugar components of EPS from bioleach microorganisms consist of the same monomers. However, the proportions of those monomers may differ depending on the microorganism in question and the growth culture medium used. To date, this paper presents the first in depth analysis of EPS sugar components for *M. hakonensis,* a thermophilic archaea relevant to bioleaching.

The detection of the five sugar monomers, namely rhamnose, fucose, mannose, galactose and glucose within *M. hakonensis* EPS were detected using GC-MS, was consistent with results obtained using lectin screening where positive binding was observed for lectins specific for mannose, glucose, fucose and galactose (Table 5.7).

Table 5.7: Summary of positive binding lectins and specific sugar binding partners

Strongest binding lectins (+++)			
No.	**Lectin**		**Specific binding**
1	1b-AAL	*Aleuria aurantia*	fucose and rhamnose specific
2	Calsepa	*Calystegia sepium*	mannose
3	PSA	*Pisum sativum*	α-man, a-glc, α-glcNAc
4	HPA	*Helix pomatia*	α-galNAc
5	GNA	*Galanthus nivalis*	α-man, man(α 1,3)man5
6	MNA-G	*Moringa G (Moringa Oleifera)*	galactose/N-acetylgalactosamine
7	MPA	*Maclura pomifera*	α-gal, α -galNAc, gal(b1,3)galNAc
8	GSI	*Griffonia (Bandeiraea) simplicifolia*	α-gal, α -galNAc
9	HMA	*Humarus americanus*	sialic acid-specific, GalNAc-specific
10	Ecor	*Erythrina corallodendron*	gal(b1,4)glcNAc, galNAc, lac gal
11	PA1	*Psuedomonas aeroginosa*	fucose
Moderate binding lectins (++)			
1	SBA	*Glycine max*	Terminal α - and β- GalNac
2	ConA	*Concanavalin A*	Glucose, mannose
3	SJA	*Sophora japonica*	β-GalNac
4	UEA	*Ulex europaeus*	Fucose
5	VVA	*Vicia villosa*	α-GalNac
6	WFA	*Wisteria floribunda*	Terminal GalNac
7	IAA	*Iberis amara*	GlcNac

As previously mentioned, a primary function of EPS is to convey structural and mechanical stability to the biofilm. Polysaccharides hydrate very quickly in contact with water and link the cells to form these gel-like structures (Wotton, 2007). This is believed to be mediated by non-covalent interactions (Flemming 1996, Mayer *et al.* 1999) either directly between polysaccharide chains or indirectly via multivalent cation bridges (Wingender *et al.* 1999, p11). Higgins and

Novak (1997) report the contribution of lectin-like proteins in the formation of the three-dimensional network of biofilm matrix through direct cross-linkages with polysaccharides or indirect multivalent cation bridges. They also serve as protection against heavy metals through chelation of metals present (Gehrke et al. 1998).

5.6 SUMMARY AND CONCLUSIONS

An extraction method was developed to allow the recovery of colloidal EPS, EPS associated loosely to the cell and capsular EPS from the thermophilic system. The extraction of these fractions allowed quantification of the material and analysis of its composition. These approaches were used in the study of the formation and location of EPS by *M. hakonensis* grown on three substrates and represent the first detailed description of EPS in thermophilic mineral leaching environments.

The effect of varying culture growth history on the resulting EPS yield and composition was assessed. EPS yield varied with energy source for growth: chalcopyrite, sulphur and ferrous sulphate. Thus cells are able to adapt and adjust their interfacial environment through changing the chemical composition and abundance of their EPS. Following extraction using crown ether, the preferred method, EPS extracted from the chalcopyrite system yielded the most EPS, followed by sulphur and then the ferrous sulphate systems. Unlike the EPS in mesophilic leaching systems which are mainly comprised on neutral sugars and lipids, protein was the major component of the EPS extracted from *M. hakonensis*. Sugars, uronic acids, nucleic acid and iron were also present in the EPS in proportions varying with both the locale or EPS fraction and culture conditions. Sugar monomers identified in the extracted EPS by GC-MS included rhamnose, glucose, galactose, fucose and mannose. This was consistent with results obtained using lectin screening where positive binding was observed for lectins specific for mannose, glucose, fucose and galactose. Based on the hypothesis that the EPS-mediated reaction environment allows the creation of niche reaction conditions at the mineral-microbe interface, favourable to bioleaching, this work expanded knowledge of factors affecting EPS formation, its location and composition.

References

http://www.ruf.rice.edu/~bioslabs/studies/sds-page/gellab3.html

Africa C J, Harrison S T L, Becker M and van Hille R P, 2010. *In situ* investigation and visualisation of microbial attachment and colonisation in a heap bioleach environment: the novel biofilm reactor. *Minerals Engineering* 23, 486-491.

Africa C. J., van Hille R. P., Harrison S. T. L., 2013a. Attachment of *A. ferrooxidans* and *L. ferriphilum* cultured under varying conditions to pyrite, chalcopyrite, low-grade ore and quartz in a packed column reactor. *Applied Microbiology and Biotechnology* **97**(3), 1317-1324.

Africa C.-J., van Hille R.P., Sand W. and Harrison S.T.L., 2013b. Investigation and in situ visualisation of thermophilic microbial interfacial interactions with mineral sulphides in a heap simulated environment. *Minerals Engineering* **48**, 100-107

Aguilera, A., Souza-Egipsy, V., San Martín-Uriz, P., & Amils, R., 2008. Extraction of extracellular polymeric substances from extreme acidic microbial biofilms. *Applied Microbiology and Biotechnology* 78(6), 1079–88.

Allison D.G., Sutherland I.W., 1987 The role of exopolysaccharides in adhesion of freshwater bacteria. *J Gen Microbiol* 133:1319 – 1327

Bala Subramanian, S. et al., 2007. Characterization of Extracellular Polymeric Substances (EPS) Extracted from both Sludge and Pure Bacterial Strains Isolated from Wastewater Sludge for Sludge Dewatering. *Water research*, 12, pp.157–164.

Beech, I.B., Sunner, J.A. & Hiraoka, K., 2005. Microbe-surface interactions in biofouling and biocorrosion processes. *International Microbiology*, 8(3), pp.157–168.

Bellenberg, S., Leon-Morales, C.-F., Sand, W., & Vera, M., 2012. Visualization of capsular polysaccharide induction in *Acidithiobacillus ferrooxidans. Hydrometallurgy* 129-130, 82–89.

Bromfield L, Africa C-J, Harrison S T L and van Hille R P., 2011. The effect of temperature and culture history on the attachment of *Metallosphaera hakonensis* to mineral sulphides with application to heap bioleaching. *Minerals Engineering* 24 (11), 1157-1165.

Crundwell, F. K., 2003. How do bacteria interact with minerals? *Hydrometallurgy,* 71, 75-81

Dade W.B., Davis J.D., Nichols P.D., Nowell A.R.M., Thistle D., Trexler M.R., White D.C., 1990 Effects of bacterial exopolymer adhesion on the entrainment of sand. *Geomicrobiol J.* 8:1-16

Dignac M.F. Urbain V., Rybacki D., Bruchet A., Snidaro D. and Scribe P., 1998. Chemical description of extracellular polymers: implication on activated sludge floc structure. Water Science and Technology 38, 45-53.

Dubois M., Gilles K.A., Hamilton J.K., Rebers P.A. and Smith F., 1956. Colorimetric method for determination of sugars and related substances. *Analytical Chemistry* 28(3), 350-356.

Fife, D. J., Bruhn, D. F., Miller, K. S., Daphne, L., Fife, D. E. E. J. a Y., & Stoner, D. L. (2000). Evaluation of a Fluorescent Lectin-Based Staining Technique for Some Acidophilic Mining Bacteria *Applied Environmental Microbiology. 66*(5), 2208–2210.

Flemming, H.C., 1996. The forces that keep biofilms together. In: Sand W. (ed.), Biodeterioration and Biodegradation, Dechema Monographs 133, VCH, Weinheim, pp311-316.

Florian B., Noel N., Thyssen C., Felshau I., Sand W., 2011. Some quantitative data on bacterial attachment to pyrite. *Minerals Engineering* 24,1132-1138.

Fowler T.A., Holmes P.R. and Crundwell F.K., 1999. Mechanism of pyrite dissolution in the presence of *Thiobacillus ferrooxidans*. *Applied and Environmental Microbiology* 65(7), 2987-2993.

Fröls, S., 2013. Archaeal biofilms: widespread and complex. *Biochemical Society Transactions*, *41*(1), 393–8.

Gautier V., Escobar B., Vargas T., 2008. Cooperative action of attached and planktonic cells during bioleaching of chalcopyrite with *Sulfolobus metallicus* at 70°C. *Hydrometallurgy* 94, 121-126

Gehrke, T., Telegdi, J., Thierry, D., & Sand, W., 1998. Importance of extracellular polymeric substances from Thiobacillus ferrooxidants for bioleaching. *Applied and Environmental Microbiology*, 64, 2743-2747.

Gehrke, T., Hallman, R., Kinzler, K., & Sand, W., 2001. The EPS of *Acidithiobacillus ferrooxidans* – a model for structure-function relationsips of attached bacteria and their physiology. *Water Science and Technology*, 43, 159-167.

Gericke M., Muller H.H., Neale J. W., Norton A.E. and Crundwell F.K., Inoculation of heap-leaching operations. Proceedings of the 16th International Biohydrometallurgy Symposium. Harrison, S.T.L., Rawlings, D.E. and Petersen, J. (eds.). Cape Town, Compress, 2005. pp. 255–264.

Gilboa-Garber, N., Mymon, H., & Oren, A., 1998. Typing of halophilic Archaea and characterization of their cell surface carbohydrates by use of lectins. *FEMS Microbiology Letters*, 163(1), 91–7.

González-Toril, E., Aguilera, A., Souza-Egipsy, V., López Pamo, E., Sánchez España, J., & Amils, R., 2011. Geomicrobiology of La Zarza-Perrunal acid mine effluent (Iberian Pyritic Belt, Spain). *Applied and Environmental Microbiology*, *77*(8), 2685–94.

Gonzalez D. M., Lara R. H., Alvarado K. N., Valdez-Perez D., Navarro-Contreras H. R., Cruz R. & Garcia-Meza J. V., 2012. *Appl. Microbiol. Biotechnol*. 93: 763-775

Harneit K., Goksel A., Kock D., Klock H.J., Gehrke T., Sand W., 2005. Adhesion to metal sulfide surfaces by cells of *Acidithiobacillus ferrooxidans, Acidithiobacillus thiooxidans* and *Leptospirillum ferrooxidans*. In: Harrison S.T.L., Rawlings D.E., Petersen J., (Eds.), Proceedings of the 16th International Biohydrometallurgy Symposium, Cape Town, South Africa.

Harneit K., Goksel A., Kock D., Klock J.-H., Gehrke T., & Sand W., 2006. Adhesion to metal sulfide surfaces by cells of *Acidithiobacillus ferrooxidans*, *Acidithiobacillus thiooxidans*, and *Leptospirillum ferrooxidans*. *Hydrometallurgy* 83, 245 – 254

Higgins M.J. and Novak J.T., 1997. Characterisation of exocellular protein and its role in bioflocculation. *Journal of Environmental Engineering* 123, 479-485.

Jiao, Y., Cody, G. D., Harding, A. K., Wilmes, P., Schrenk, M., Wheeler, K. E., Thelen, M. P., 2010. Characterization of extracellular polymeric substances from acidophilic microbial biofilms. *Applied and Environmental Microbiology*, *76*(9), 2916–22.

Kinzler, K., Gehrke, T., Telegdi, J., & Sand, W., 2003. Bioleaching – a result of interfacial processes caused by extracellular polymeric substances (EPS). *Hydrometallurgy*, 71: 82-88.

Koerdt, A., Gödeke, J., Berger, J., Thormann, K. M., & Albers, S.-V., 2010. Crenarchaeal biofilm formation under extreme conditions. *PloS One*, 5(11), e14104

Kreft J., Wimpenney J., 2001, Effect of EPS on biofilm structure and function as revealed by an individual-based model of biofilm growth. *Water Science and Technology*, 43 (6), 135-141

Lee J., Acar S., Doerr D.L. and Brierley J.A., 2011. Comparative bioleaching and mineralogy of composited sulphide ores containing enargite, covellite and chalcocite by mesophilic and thermophilic microorganisms. *Hydrometallurgy* 105, 213-221.

Lebaron P., Baude, P., Lett, M.C., Duval-Iflah, Y., Simonet P., Jacq E., Frank, N., et al., 1997. Recombinant plasmid mobilisation between *E.coli* strains in seven sterile microcosms. *Canadian Journal of Microbiology* 43, 534-540.

Lei, J., Huaiyang, Z., Xiaotong P. and Zhonghao, D., 2009. The use of microscopy techniques to analyze microbial biofilm to the bio-oxidized chalcopyrite surface, *Minerals Engineering,* **22**: 37–42.

Lorenz M.G. and Wackernagel W. 1994. Bacterial gene transfer by natural genetic transformation in the environment. *Microbiological Reviews* 58, 563-602.

Mangold S., Laxander M., Harneit K., Rohwerder T., Claus G., Sand W., 2008. Visualisation of *Acidithiobacillus ferrooxidans* biofilms on pyrite by atomic force and epifluorescent microscopy under various experimental conditions. *Hydrometallurgy* 94, 127 – 132

Mayberry-Carson, K. J., Jewell, M. J., & Smith, P. F., 1978. Ultrastructural Localization of Thermoplasma acidophilum Surface Carbohydrate by Using Concanavalin A. *Journal of Bacteriology*, *133*(3), 1510–1513

Mayer C., Moritz R., Kirschner, C., Borchard, W., Maibaum R., Wingender J. and Flemming H.-C., 1999. The role of intermolecular interactions: studies on model systems for bacterial biofilms.

Michel, C., Bény, C., Delorme, F., Poirier, L., Spolaore, P., Morin, D., & d'Hugues, P., 2009. New protocol for the rapid quantification of exopolysaccharides in continuous culture systems of acidophilic bioleaching bacteria. *Applied Microbiology and Biotechnology*, 82(2), 371–8.

Mikkelsen, D., Kappler, U., Webb, R.J., Rasch, R. McEwan, A.G., Sly, L.I., 2007. Validation of pyrite leaching by selected thermophilic archae: nature of microorganism-ore interactions during bioleaching. *Hydrometallurgy* 88, 143-153.

Morillo Pérez, J.A., García-Ribera, R., Quesada, T. & Monteolivia-Sanchez M. 2008. Biosorption of heavy metals by the exopolysaccharide produced by *Paenibacillus jamilae. World J Microbiol Biotechnol* (2008) 24 (11) 2699-2704.

Neu T.R. and Lawrence J.R., 1997. Development and structure of microbial biofilms in river water studied by confocal laser scanning microscopy. *FEMS Microbiol. Ecol.* 24, 11-25.

Neu, T. R., 2000. In situ cell and glycoconjugate distribution in river snow studied by confocal laser scanning microscopy. *Aquat Microb Ecol,* 21.

Neu T.R., Swerhone G.D.W., and Lawrence J.R. 2001. Assessment of lectin binding analysis for in situ detection of glycoconjugates in biofilm systems. *Microbiology* 147, 299-313.

Nielsen, P.H., and Jahn, A., 1999. Extraction of EPS In *Microbial Extracellular Polymeric Substances*, ed. Wingender, J.E., Neu, T.R., and Flemming, H.-C. Springer, Berlin, 1999, pp. 49-72

Noel N., Florian B., Sand W., 2010. AFM & EFM study on attachment of acidophilic leaching organisms. *Hydrometallurgy* 104: 370 – 375

Platt R.M., Geesey G.G., Davis J.D., White D.C., 1985. Isolation and partial chemical analysis of firmly bound exopolysaccharide from adherent cells of a freshwater sediment bacterium. *Canadian Journal of Microbiology* 31, 675-680.

Pradhan N., Nathsarma, K.C., Srinivasa Rao, K., Sukla L.B., Mishra B.K., 2008. Heap bioleaching of chalcopyrite: a review. *Minerals Engineering* 21 (5), 355-365.

Rawlings D. E., 2004 Microbially assisted dissolution of minerals and its use in the mining industry. *Pure Appl. Chem.* 76: 37 -46

Redfield R., 2002. Is quorum sensing a side effect of diffusion sensing? *Trends in Microbiology.* 10(8) 365-370.

Rodriguez, Y., Ballester, A., Blazquez, M. L., Gonzalez, F., & Munoz, J. A., 2003. New information on the chalcopyrite bioleaching mechanism at low and high temperature. *Hydrometallurgy*. 71: 47-56

Rohwerder, T., Gehrke, T., Kinzler, K., Sand, W., 2003. Bioleaching Review Part A: progress in bioleaching: fundamentals and mechanisms of bacterial metal sulphide oxidation. *Applied Microbiology and Biotechnology* 63, 239-248.

Sampson, M. I., Phillips, C. V., & Blake II, R. C., 2000. Influence of the attachment of acidiphilic bacteria during the oxidation of mineral sulfides. *Minerals Engineering*. 13, 373-389.

Sand W., Gehrke T., 2006. Extracellular polymeric substances mediate bioleaching/biocorrosion via interfacial processes involving iron (III) ions and acidophilic bacteria. *Res. Microbiol*. 157, 49 – 56.

Sanhueza, A, Ferrer I.J, Vargas T., Amils R and Sanchez C. 1999. Attachment of *Thiobacillus ferrooxidans* on synthetic pyrite of varying structural and electronic properties. *Hydrometallurgy* 51, 115-129.

Schippers A., Sand W., 1999. Bacterial leaching of metal sulfides proceeds by two indirect mechanisms via thiosulfate or via polysulfides and sulfur. *Appl. Environ. Microbiol*. 65, 319 – 321

Stoodley P., Hall-Stoodley L. and Lappin-Scott H.M., 2001. Detachment, surface migration and other dynamic behaviour in bacterial biofilms revealed by digital time-lapsed imaging. *Methods in Enzymology* 337, 306-319.

Tapia, J. M., Muñoz, J. a, González, F., Blázquez, M. L., Malki, M., & Ballester, A., 2009. Extraction of extracellular polymeric substances from the acidophilic bacterium *Acidiphilium* 3.2Sup(5). *Water Science and Technology* 59(10), 1959–67.

Tributsch H., 2001. Direct versus indirect bioleaching. *Hydrometallurgy* 59, 177 – 185.

Usher K.M., Shaw J.A., Kaksonen A. H. and Saunders M., 2010 Elemental analysis of extracellular polymeric substances and granules in chalcopyrite bioleaching microbes. *Hydrometallurgy*, 104, 376 – 381.

Vandevivere P. and Kirchman D.L., 1993. Attachment stimulates exopolysaccharide synthesis by a bacterium. *Applied and Environmental Microbiology* 59, 3280-3286.

Watnick P. and Kolter R., 2000. Biofilm, city for microbes. *Journal of Bacteriology* 182, 2675-2679.

Wingender J., Neu T.R. and Flemming H-C., 1999. What are bacterial extracellular polymeric substances? In: Microbial Extracellular Polymeric Substances (ed. J. Wingender, T.R. Neu, and H.-C. Flemming), Ch 1, Springer-Verlag, Berlin.

Wolfaardt G., Lawrence J.R. and Korber D.R., 1999. Function of EPS. In: Microbial Extracellular Polymeric Substances (ed. J. Wingender, T.R. Neu, and H.-C. Flemming), pp171-200, Springer-Verlag, Berlin.

Yildiz, S. Y., Anzelmo, G., Ozer, T., Radchenkova, N., Genc, S., Di Donato, P., Nicolaus, B., Toksoy Oner, E. and Kambourova, M., 2014, *Brevibacillus themoruber*: A promising microbial cell factory for exopolysaccharide production. *Journal of Applied Microbiology*, 166(2), 314 - 324

Chapter 6:
Colonisation and biofilm development of *Metallosphaera hakonensis* on sulphide mineral surfaces

6.1. INTRODUCTION

In Chapter 4, the microbial-EPS-mineral interface was successfully visualised for planktonic *M. hakonensis* cells as well as for sessile *M. hakonensis* cells. This interfacial environment was characterised in terms of the architectural elements and spatial distribution in relation to the microbial cells and mineral surfaces, as well as its glycoconjugate composition *in situ.* The EPS from *M. hakonensis* cultured on three substrates was extracted and its chemical composition characterised, presented in Chapter 5. Fundamental knowledge on the nature and composition of the EPS interfacial environment was attained. These studies were conducted using cells cultivated in batch agitated systems, which provide valuable information regarding the EPS interfacial environment in tank systems, as well as that created during inoculum preparation which primes cells for attachment during inoculation of heap bioleaching systems. However, some key questions regarding the behaviour of *M. hakonensis* under heap bioleach simulated conditions remained.

This chapter describes the attachment, colonisation and biofilm formation on massive and low-grade sulphide–mineral bearing ores of *M. hakonensis*. This work was done *in situ* using the biofilm reactor described in Section 3.10. It made use of state of the art visualisation techniques (AFM–EFM and CLSM) to provide three dimensional topographical details of the association of the microbes with the mineral surface, as well as confirmation of the presence of EPS and cells (nucleic material) within the biofilm.

Operating conditions in the biofilm reactor simulated those of a bioheap in terms of fluid-flow and mineralogy, where the low-grade chalcopyrite ore sections were used. Pure cultures of *M. hakonensis* were used to inoculate the mineral sections in the biofilm reactors to enable the attachment and subsequent biofilm development to be visualised *in situ.* The AFM–EFM technique enhanced the level of detail at which site specific associations of microorganisms with mineral surfaces could be assessed. Insights into biofilm structure and architecture could therefore be revealed. Spatial orientation and density of attached micro-colonies were noted. This revealed insights into biofilm structure and architecture. The effect of varying temperature on the extent of attachment and biofilm development was also assessed between 20 and 65 ºC.

The biofilm reactor consisted of a sealed rectangular vessel, connected to a peristaltic pump. The reactor housed four chambers (each 78 x 26 mm) in which the mineral thin sections were mounted at a slight decline to allow unidirectional fluid-flow. Feed was distributed evenly as a thin film over the surface of the mineral thin section (at a rate of 120 µl min^{-1} with a linear velocity of 1.6 $x10^{-4}$ m s^{-1}), simulating the trickling fluid-flow of the leach liquor percolating through an industrial heap. The biofilm reactor was housed in an incubator, allowing temperature control at ambient (20 ± 1 °C); 45 °C and 65 °C. The reactor chambers were continuously charged with humidified air to minimise evaporative losses and ensure aerobic growth conditions. The reactor was inoculated and operated aseptically as a closed recycle for the duration of the inoculation period, after which it was run as a continuous flow through system, with fresh 0 K medium (pH 2.0) introduced continuously for 2, 4 or 8 days at the temperature under investigation. To achieve inoculation and initial colonisation, the reactor was run as a closed recycle for 20 hours, whereafter it was operated as a continuous flow through system. Attached cells were visualised by staining with DAPI (4,6-diamidino-2-phenylindole) or SYTO9, dissolved in water to a concentration of 100 µg ml^{-1} for 10 min. DAPI complexes with AT-rich sequences in the minor groove of double stranded DNA and is taken up by all microbial species present. EPS was visualised by staining with TRITC- or FITC-labelled Concanavalin A (50 µg ml_{-1}, Sigma) for 20 min. Colonising cells were visualised using either a combination of atomic force and epifluorescence microscopy (AFM–EFM) or via confocal laser scanning microscopy (CLSM). Biofilm formation on chalcopyrite, pyrite, and a low-grade chalcopyritic ore was assessed.

6.2. BIOFILM ESTABLISHMENT ON MASSIVE SULPHIDE MINERALS

6.2.1 Establishment of *M. hakonensis* biofilms on chalcopyrite surfaces

The development of an *M. hakonensis* biofilm on massive chalcopyrite after 2 days is presented as CLSM micrographs in Figure 6.1. *M. hakonensis* is a lobed, non-motile thermophilic archeon, approximately 0.9–1.0 µm in diameter. It grows optimally between 50 and 80 °C on sulphur, iron sulphate (Takayanagi et al., 1996; Kurosawa et al., 2003), pyrite and chalcopyrite. Individual lobed cells, approximately 1 µm in diameter are evident after 2 days on staining with DAPI and visualisation with CLSM. The cells were distributed across the mineral surface in a capacious manner. However, some regions contained denser expanses of cells, forming more defined microcolonies. These are observed in the bottom three micrographs of Figure 6.1.

EPS was visualised by staining with the lectin stain ConA, which specifically binds glucopyranosyl and α-mannopyranosyl (Chazotte, 2011). The fields of view were chosen in a representative manner, with a minimum of 40 images taken per mineral section under investigation in order to calculate surface area colonised. After 2 days, the ConA signal was evident in the region immediately surrounding individual cells, indicative of capsular EPS. Not all sessile cells were observed to exhibit the presence of EPS. In areas which were more saturated with cells where microcolonies formed, the ConA signal was more pronounced at the mineral surface, indicative of EPS localised at the base of the film.

In Figure 6.2, the results of biofilm development of *M. hakonensis* on chalcopyrite mineral thin sections after 4 days incubation in the biofilm reactor are presented. After 4 days, vast expanses of compactly attached cells are evident. The ConA signal remained localised to the region a few microns above the mineral surface and encapsulating individual cells. The amount of EPS present after 4 days was substantially greater than after 2 days, and appeared most dense after 4 days. Mono-layered films of sessile cells were evident after 4 days.

In Figure 6.3, the results after 8 days incubation are presented. The mineral surface contained varying motifs of cellular attachment. Small clusters of sessile cells were evident on the surface, forming microcolony islets of just 4 to 8 cells. Individual sessile cells sparsely scattered across the surface were also evident. In addition to this, expanses of more densely clustered cells were observed. The ConA signal observed after 8 days was weaker, relative to the 4 day experiment, but still more pronounced than after 2 days. Furthermore, the ConA signal was also localised to the area around the cell surface and the immediate region above the mineral surface.

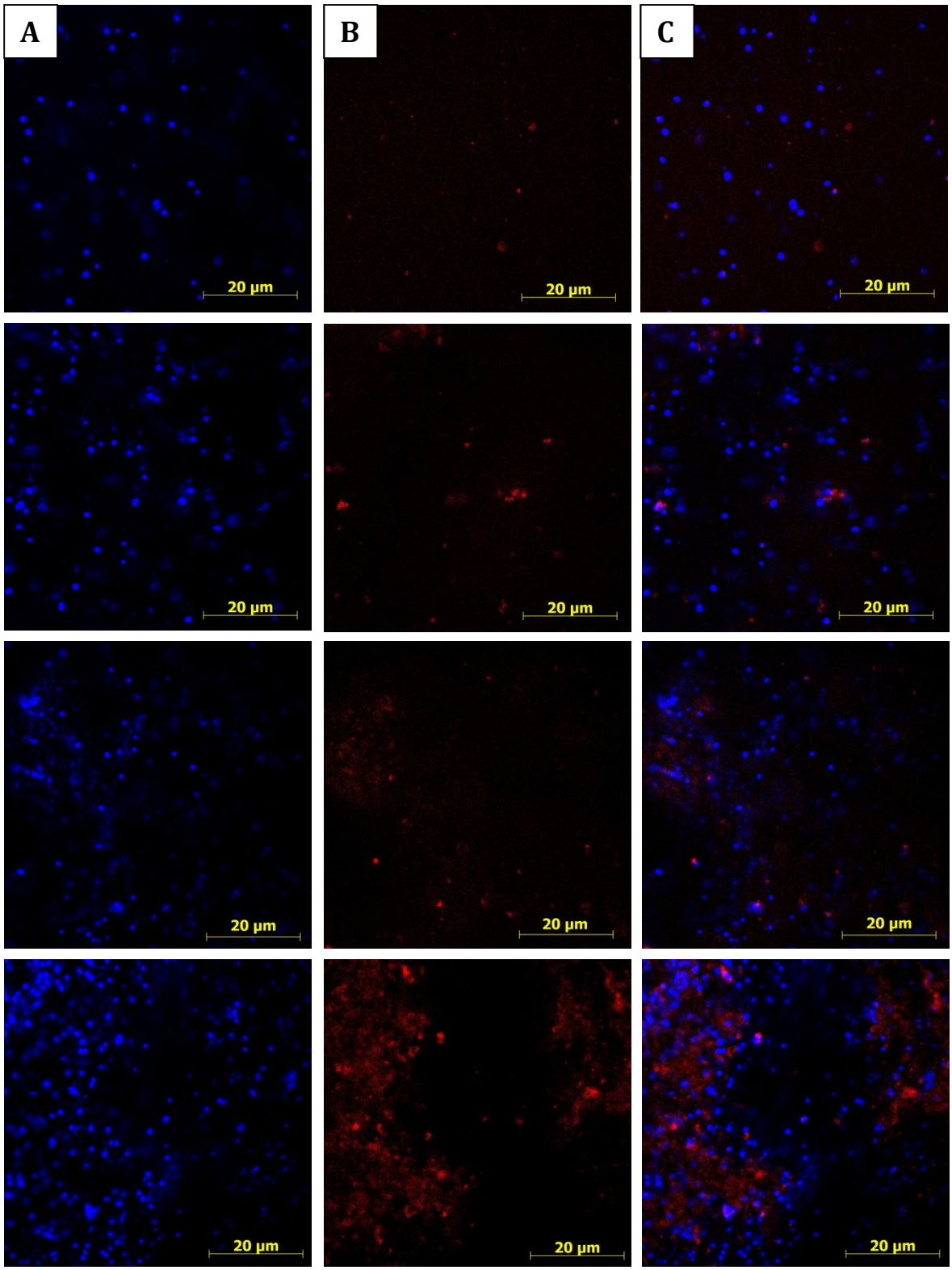

Figure 6.1: Micrographs depict colonisation of a chalcopyrite mineral thin section by *M. hakonensis* after 2 days incubation in the biofilm reactor operated as a continuous flow through system at 65 ºC. Images represent different fields across the same mineral surface used in this experiment. Samples were stained with DAPI (A) and TRITC-labelled ConA (B). Micrographs in (A) depict sessile cells on the surface exhibiting positive staining with DAPI, (B) depicts the same region showing the presence of EPS due to positive staining with ConA. Images in (C) depict overlays of the two channels in (A) and (B). A laser scanning module (LSM 510 Carl Zeiss® Jena) coupled to an inverted Axiovert 100 M BP microscope (Zeiss®) was used and operated using the ZEN LSM 510 Release 3.2 (Zeiss®) software. All micrographs were attained using a Plan-Neofluar® 100 x 1.3 oil objective.

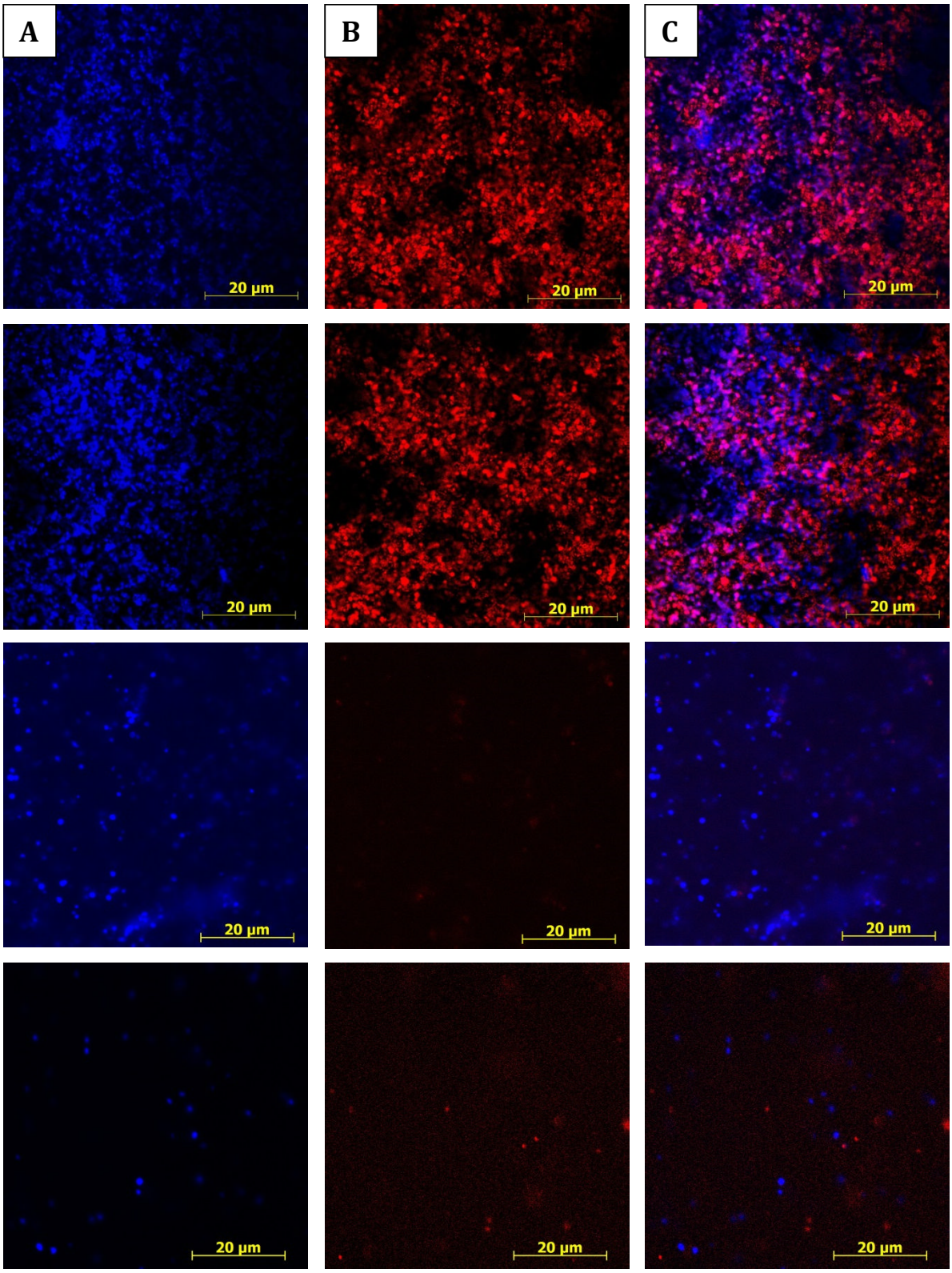

Figure 6.2: Micrographs depict colonisation of a chalcopyrite mineral thin section by *M. hakonensis* after 4 days incubation in the biofilm reactor operated as a continuous flow through system at 65 ºC. Images represent different fields across the same mineral surface used in this experiment. Samples were stained with DAPI (A) and TRITC-labelled ConA (B). Micrographs in (A) depict sessile cells on the surface exhibiting positive staining with DAPI, (B) depicts the same region showing the presence of EPS due to positive staining with ConA. Images in (C) depict overlays of the two channels in (A) and (B). A laser scanning module (LSM 510 Carl Zeiss® Jena) coupled to an inverted Axiovert 100 M BP microscope (Zeiss®) was used and operated using the ZEN LSM 510 Release 3.2 (Zeiss®) software. All micrographs were attained using a Plan-Neofluar® 100 x 1.3 oil objective.

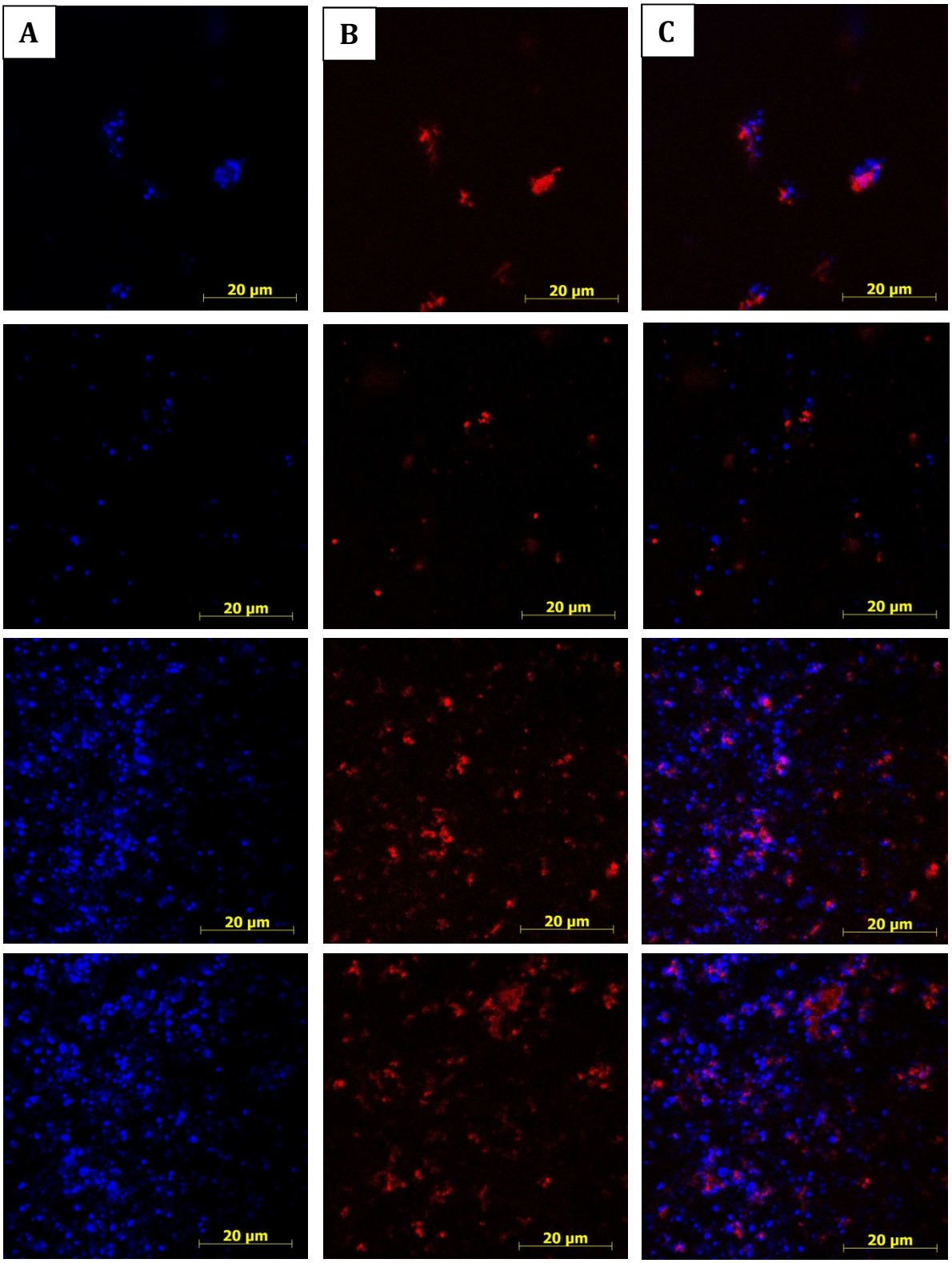

Figure 6.3: Micrographs depict colonisation of a chalcopyrite mineral thin section by *M. hakonensis* after 8 days incubation in the biofilm reactor operated as a continuous flow through system at 65 ºC. Images represent different fields across the same mineral surface used in this experiment. Samples were stained with DAPI (A) and TRITC-labelled ConA (B). Micrographs in (A) depict sessile cells on the surface exhibiting positive staining with DAPI, (B) depicts the same region showing the presence of EPS due to positive staining with ConA. Images in (C) depict overlays of the two channels in (A) and (B). A laser scanning module (LSM 510 Carl Zeiss® Jena) coupled to an inverted Axiovert 100 M BP microscope (Zeiss®) was used and operated using the ZEN LSM 510 Release 3.2 (Zeiss®) software. All micrographs were attained using a Plan-Neofluar® 100 x 1.3 oil

The extent of the surface area covered by sessile cells after 2, 4 and 8 days was assessed using ImageJ software (Appendix B). A minimum of 40 fields of view were assessed per investigation. Table 6.1 presents the results of this analysis in terms of the surface area covered by sessile cells as a percentage of the total surface area available for attachment.

Table 6.1: Summary of the extent of attachment and colonisation of bioleach microorganisms to the chalcopyrite mineral system at optimal temperature for growth (65 °C), expressed as a percentage surface area covered, calculated using fluorescence of cells positively stained with DAPI. A borosilicate surface served as a control for non-specific attachment.

Mineral system	Temperature (° C)	Age biofilm (days)	Surface area coverage (%)
Chalcopyrite	65	2	2.0
	65	4	5.7
	65	8	4.2
Glass	65	4	0.1

The mineral surface area covered by colonising cells after 2 days was relatively low, with only 2% coverage of the mineral surface area available for attachment. Microcolonies appeared to be fairly evenly disseminated across the surface, and were not restricted to dislocation sites or regions with a high density of surface defects. After 4 days, the microcolonies present were markedly denser than after 2 days. The surface area covered by cell aggregates increased to 5.7%. A similar trend was observed after 8 days, although the surface area covered by cells decreased marginally to 4.2%.

Figure 6.4 presents CLSM micrographs of *M. hakonensis* attaching to massive chalcopyrite after 2, 4 days and 8 days in the biofilm reactor operated at 65ºC under conditions of continuous fluid flow. Attached cells subjected to staining with DAPI are shown in rows A1–C1 (cyan) and EPS visualised using ConA in rows A2–C2 (magenta) with overlay of the two channels in rows A3–C3. Images are stacks approximately 10 µm thick. The thickness of the biofilm present varied across the mineral surface within one sample and typically ranged between 4 and 8 µm, with a maximum of 10 µm observed after 4 days. Interestingly, the film thickness did not vary greatly temporally under the conditions of this experiment following its initial establishment, with similar film thicknesses and mono-layered biofilms observed after 8 days relative to that observed after 4 days.

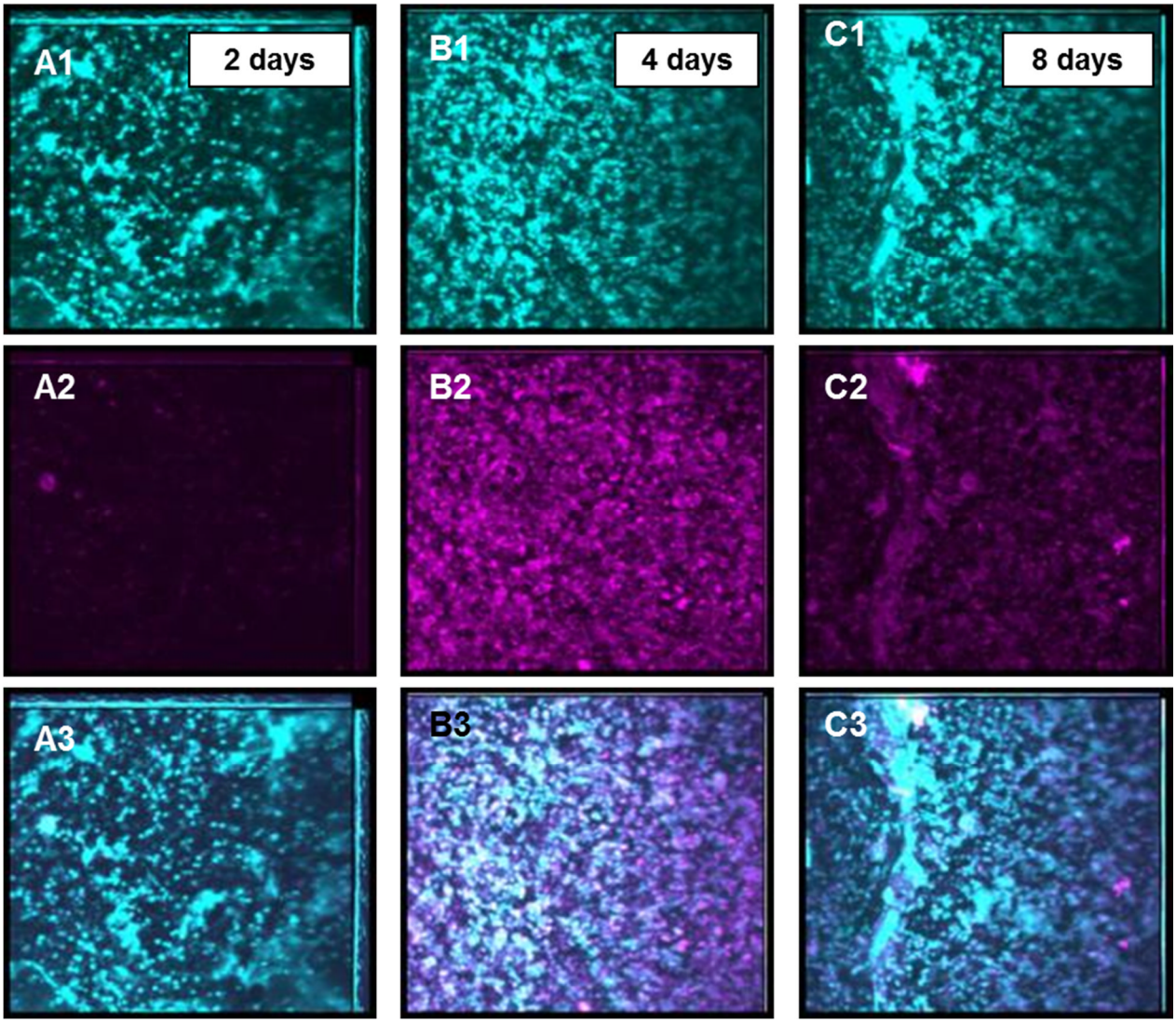

Figure 6.4: CLSM micrographs of *M. hakonensis* attaching to massive chalcopyrite after 2, 4 days and 8 days in the biofilm reactor operated at 65 ºC under conditions of continuous fluid flow. Attached cells subjected to staining with DAPI in rows A1–C1 (cyan) and EPS visualised using ConA in rows A2–C2 (magenta) with overlay of the two channels in rows A3–C3. Images are stacks approximately 10 µm thick.

6.2.2 Analysis of biofilm topography using combined AFM-EFM techniques

AFM is a powerful imaging device allowing spatial and three-dimensional visualisation of samples with sub-nanometre resolution capabilities (Mangold *et al.* 2008). The AFM is essentially a "blind-microscope" making use of scanning probe (known as a cantilever) with a sharp tip, which "sweeps" or taps across the surface of the sample and gathers information regarding size, shape, texture and hardness (Flores and Toca-Herrera 2009). The cantilever is controlled by a piezo-driven device which expands and contracts proportionally to the voltage

applied and moves the cantilever over the sample in three dimensions (X, Y and Z movement). The AFM operates in two modes, it either "sweeps" across the surface, known as contact mode, or taps across the surface, known as non-contact or intermittent contact mode.

When the cantilever is brought in close contact with the surface, forces between the tip and the sample (e.g. van der Waals, capillary and electrostatic forces) lead to deflection of the cantilever according to Hooke's law. This deflection is measured by a laser focused on, and reflected from, the top of the cantilever onto an array of photodiodes, the output signal of which is collected by a differential amplifier, is processed by a computer and presented as an image. AFM has been demonstrated a useful tool for the investigation of biological samples as no sample preparation is required which would alter the nature of the sample thus allowing for *in situ* studies. Furthermore, it can be used on samples containing liquid and can be combined with epifluorescent and or confocal laser scanning microscopy.

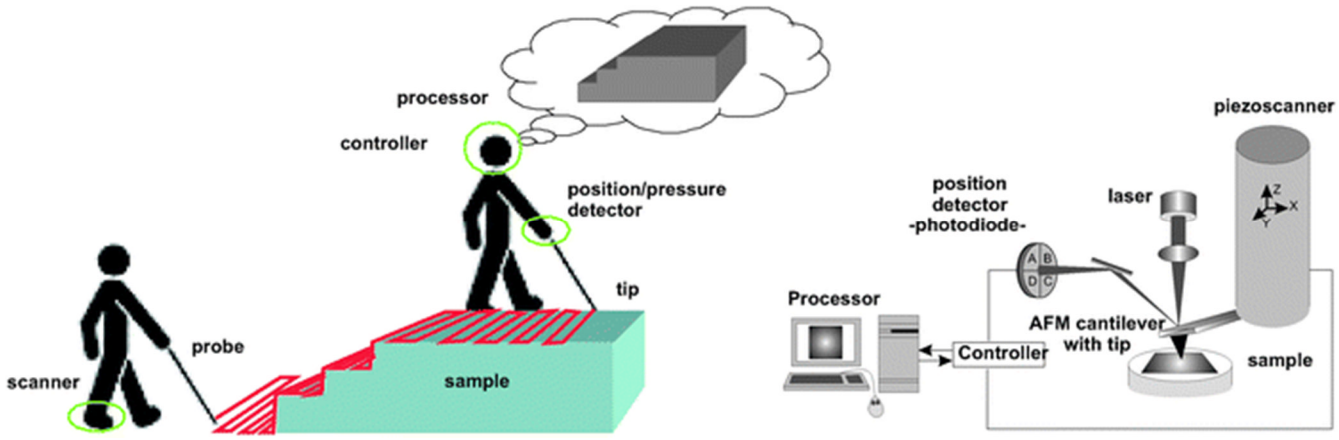

Figure 6.5: (a) Schematic diagram illustrating the functioning of an AFM as a "blind microscope" either sweeping across the surface of tapping over the surface in order to gain information regarding size, shape, texture and hardness. (b) Schematic representation of the operation of an AFM, the piezo controlled cantilever, the deflection of which is detected by a laser coupled to a photodiode. The information is then processed and converted into a three dimensional image. Images (a) and (b) are taken from Flores and Toca-Herrera (2009).

In this study, the AFM was combined with epifluorescence microscopy (EFM) and a custom shuttle stage. Use of the shuttle stage allowed the sample to be transferred between the two microscopes while being able to view the same region within an error margin of only 3-5 µm (Mangold *et al*. 2008). The colonisation of *M. hakonensis* on massive chalcopyrite mineral surfaces was assessed using this technique with results of chalcopyrite surface colonisation after 4 days incubation in the biofilm reactor being presented in Figure 6.7.

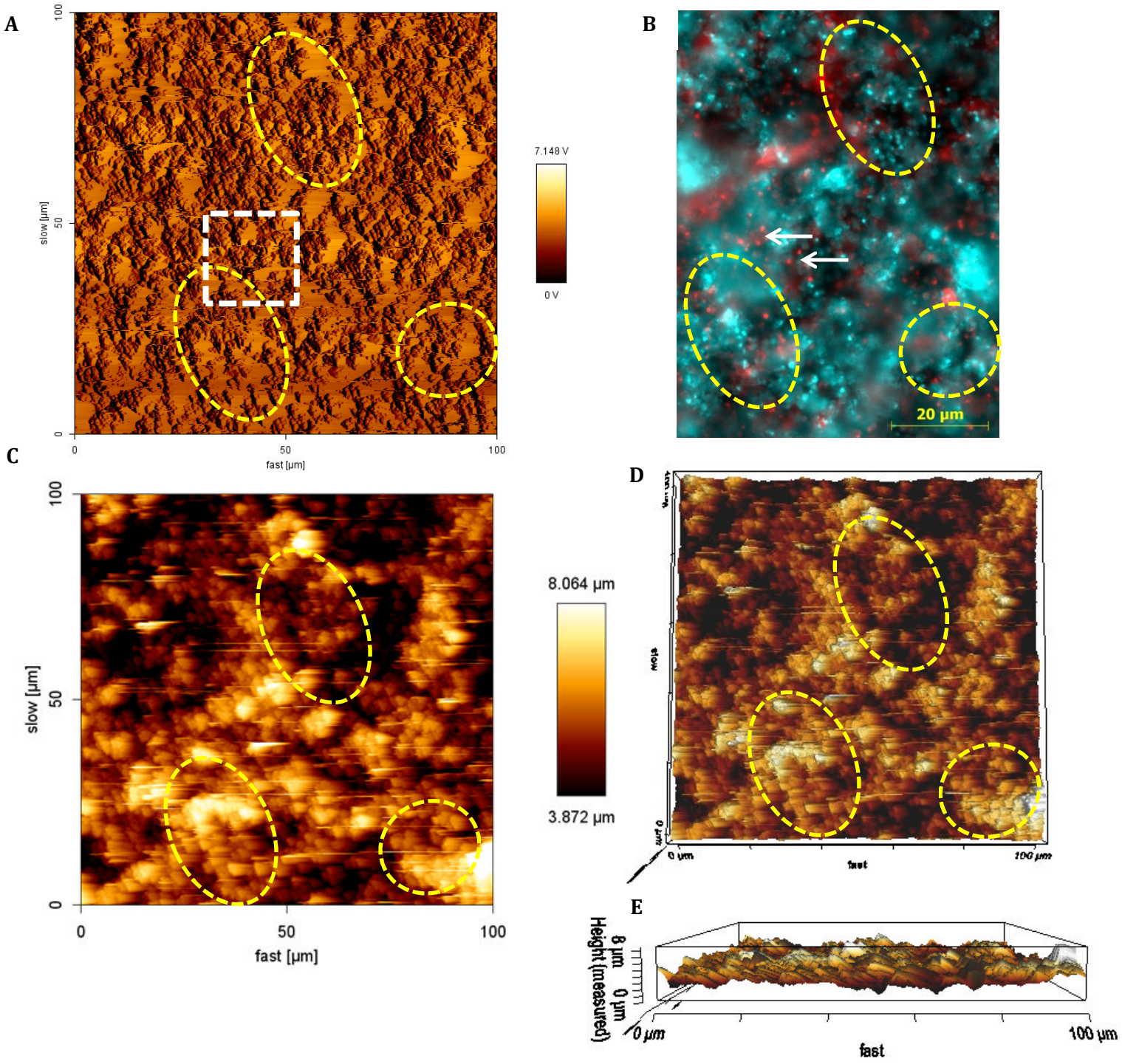

Figure 6.7: AFM micrograph of *M. hakonensis* colonising the surface of chalcopyrite after 4 days of incubation in the biofilm reactor at 65 ºC under conditions of continuous fluid flow with 0 K media (basal salts media). In (a), detail of the topography of the region is provided in the AFM micrograph. Micrograph (b) represents the same region seen in (a) but visualised using EFM. DAPI fluorescence (cyan) and EPS fluorescence (red) can be seen. In (c), height information of the same region presented in (a), brighter areas are indicative of higher regions. Micrographs (d) and (e) are three dimensional representations of (c). The yellow circles outline the same regions of interest viewed with the AFM in (a), (c) and (d); and with the EFM in (b). The white arrows in (b) indicate individual attached cells which show positive fluorescence with both ConA and DAPI. The AFM was operated in intermittent contact mode in air using a CS37/8 silicon cantilever (Mirkomasch, Estonia).

In the micrograph presented in Figure 6.7 (a) and (b) represent the same region on the chalcopyrite mineral section, after 4 days incubation in the biofilm reactor, visualised using either AFM (a) or EFM (b). Clusters of *M. hakonensis* cells were positively stained using DAPI and were identified through visualisation of cyan fluorescence in micrograph (b). Colonisation appears extensive with dense aggregates of cells evident in (b). EPS was positively identified after staining with TRITC-labelled ConA and was visualised as red fluorescence in micrograph (b). The EPS fluorescence was observed to be localised to the cell surfaces, indicative of capsular EPS and is demarcated with a white arrows in micrograph (b). EPS fluorescence was also observed in close association with the mineral surface in micrograph (b).

The topography of the attached *M. hakonensis* cells in this region was investigated using AFM and is presented in Figure 6.7 (a). The presence of biomass on the chalcopyrite surface was evident with the surface appearing textured by aggregates of biomass disseminated across it. The positive identification of both EPS and attached cells EFM micrograph 6.7 (b) confirms that the topographical features observed in 6.7 (a) are due to the presence of colonising *M. hakonensis* cells and the presence of EPS. Furthermore, certain features on the textured chalcopyrite surface are consistent with patterns of attachment visualised through fluorescing DAPI stained cells in this region and are demarcated by yellow ellipses in Figures 6.7 (a) and (b). The surface of the chalcopyrite mineral section was scanned using AFM prior to inoculation. The resulting surface topography features are presented in Figure 6.8.

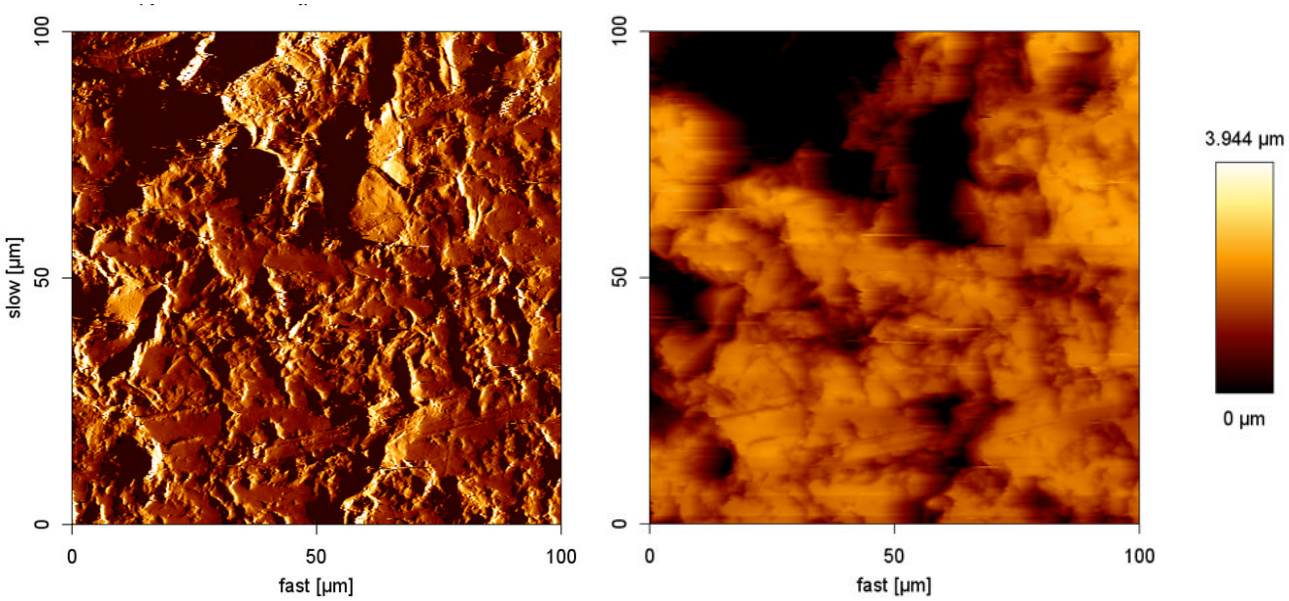

Figure 6.8: AFM micrographs depict the surface of the chalcopyrite mineral section prior to inoculation and incubation in the biofilm reactor. Micrograph (A) presents vertical deflection topographical features, and in (B) height information of the same region is presented.

Results depict only ridges and holes on the unpolished surface with smooth, relatively even surfaces. The textured clusters observed on the colonised surface in Figure 6.7 are not present.

At the resolution presented in Figure 6.7 (a) the shape and size of individual cells are difficult to detect. Increased resolution of the area demarcated with a white square in Figure 6.7 (a) is presented in Figure (6.9 b and c).

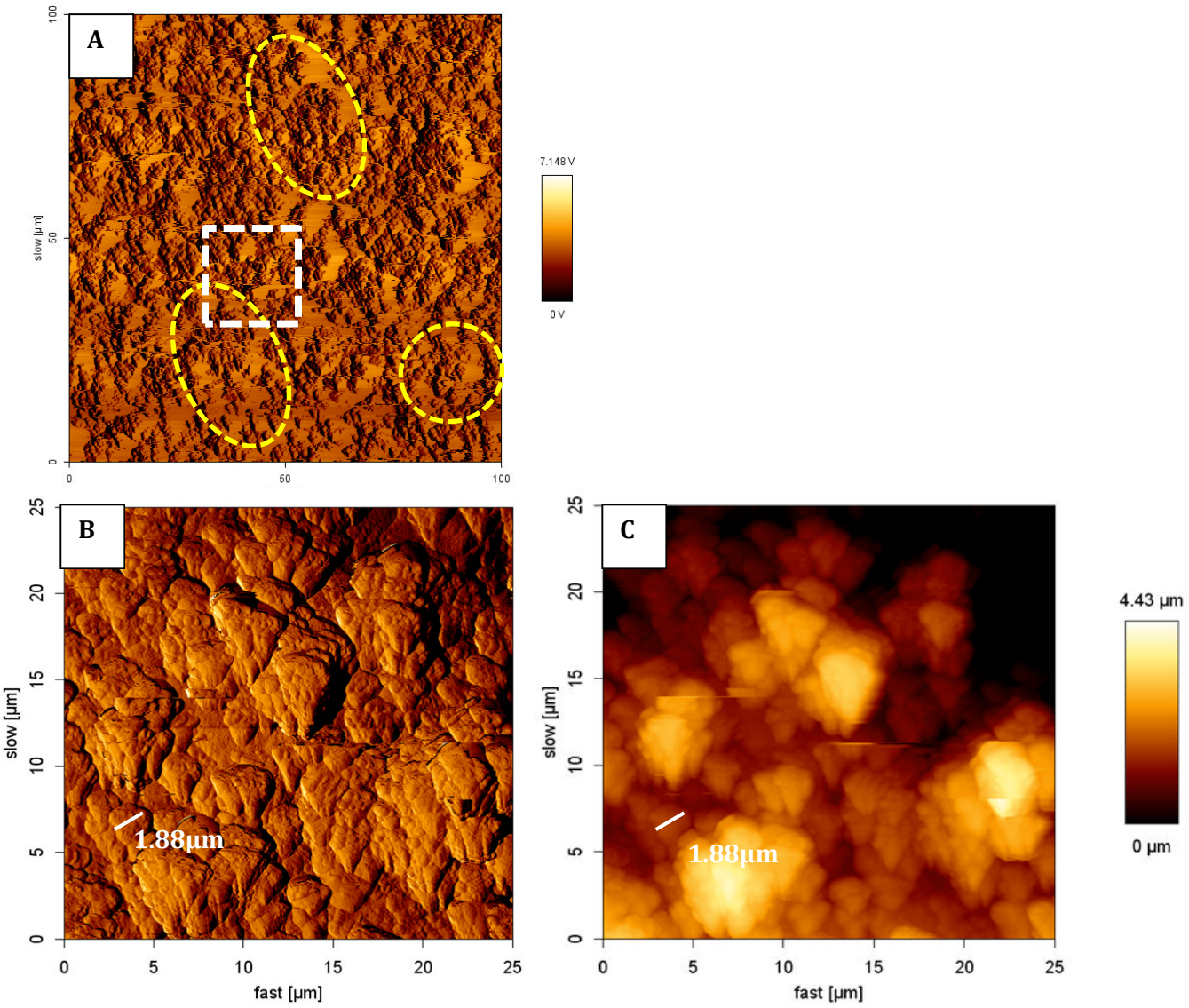

Figure 6.9: AFM micrographs depict the colonisation of *M. hakonensis* on the surface of a massive chalcopyrite mineral section after incubation in a biofilm reactor for 4 days. Micrograph (b) and (c) depict greater magnification of the region demarcated by the white square in (a) which is the same region presented in Figure 6.7 (a). Topographical features are visualised in the vertical deflection image in (b) with the height information of the same region provided in (c).

Where singles cells could be easily identified, the typical width was measured to be between 1.88 µm – 2.10 µm, demarcated with a white line in Figure 6.9 (b) and (c). However, from the magnified micrograph, cells appear to be layered upon one another. Furthermore, the presence of a smooth substance, likely EPS as confirmed using positive binding with TRITC-labelled ConA and EFM, increases the width and height of the attached cells observed in the micrograph.

The height across the sample region presented in Figure 6.7 was profiled and is presented in Figure 6.10. The heights observed range between 3.5 to 8.5 µm (Figure 6.10 (B)). Roughness of the surface after the cell attachment and biofilm formation reduced from an average surface roughness (Ra[1]) of 1.325 µm to and Ra of 858 nm (Ra measured using JPK imaging software). The reduction in smoothness is likely due to the presence of the organic EPS matter on the surface, the presence of which was also confirmed through positive staining with Con-A and visualisation through epifluorescent microscopy.

Further AFM results of *M. hakonensis* attaching to chalcopyrite after 4 days, acquired in contact mode in air are presented in Figure 6.11 (A1) and (A2). The EFM results of DAPI staining for this same region are presented in Figure 6.11 (B1), with TRITC-labelled ConA results presented in (B2) and the merged overlay of these two channels presented in (B3). Individual cells were clearly identifiable in both vertical deflection and height AFM micrographs. The DAPI and TRITC results confirm the presence of *M. hakonensis* and EPS produced by this microorganism. The TRITC-ConA signal is localised to the immediate cell surface (capsular EPS) as well as the immediate mineral surface. In both AFM and EFM micrographs, it is clear that cells are distributed across the entire surface. Dense aggregates of cells appear at ridges in the surface, demarcated with arrows. Defining features are demarcated by ellipses. These represent holes or ridges within the surface which are clearly identifiable under both AFM and EFM.

[1] *Ra is the arithmetic average of the absolute values of the surface height deviations measured from the mean plane. Roughness is often closely related to the friction and wear properties of a surface. A surface with a large value, will usually have high friction and wear quickly. (http://www.olympus-ims.com/en/knowledge/metrology/roughness/2d_parameter)*

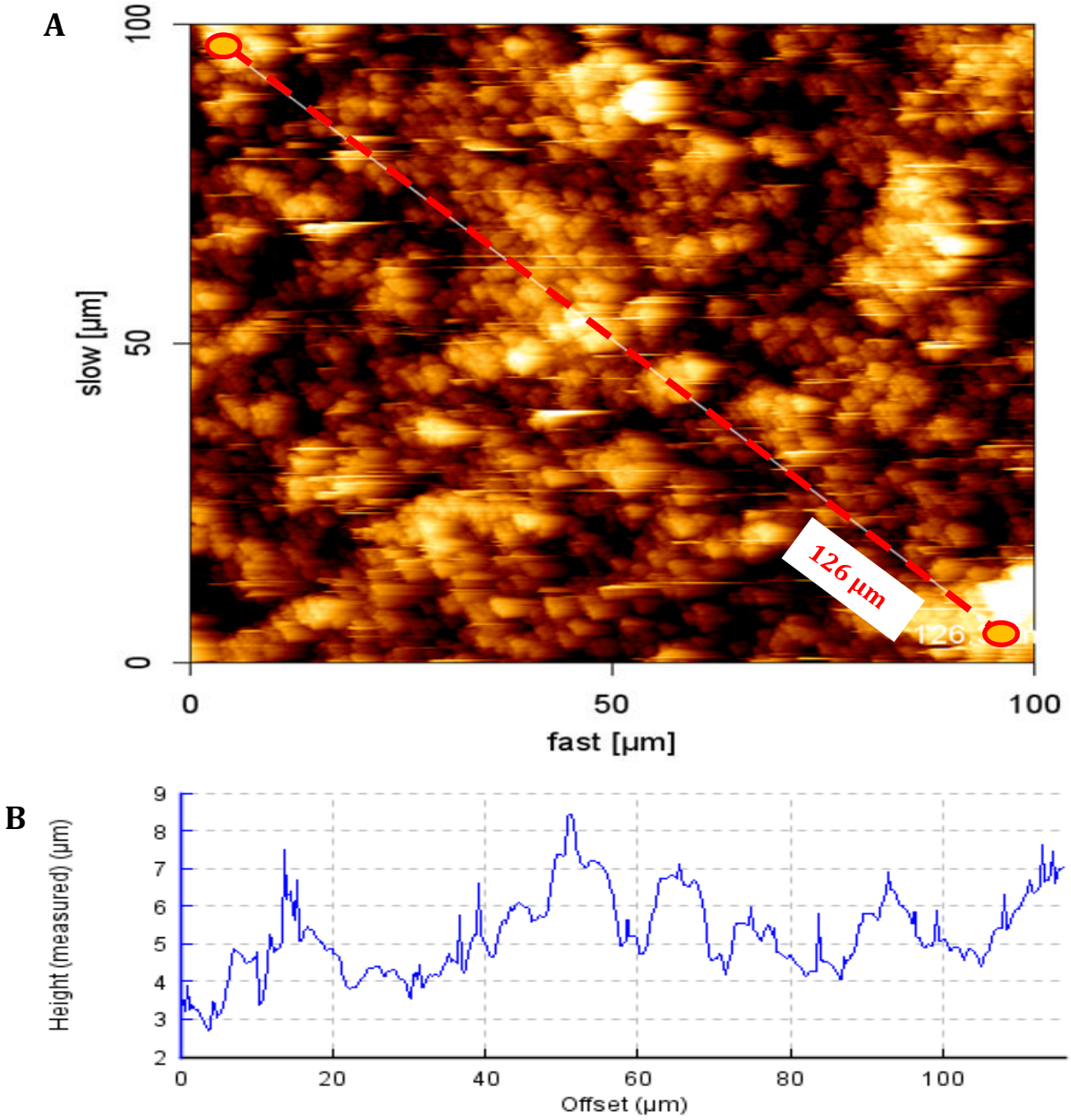

Figure 6.10: (A) Micrograph depicting the height information of a chalcopyrite mineral surface colonised by *M. hakonensis* after 4 days incubation in the biofilm reactor under conditions of continuous fluid flow. (B) Height profile of a cross-section of this area.

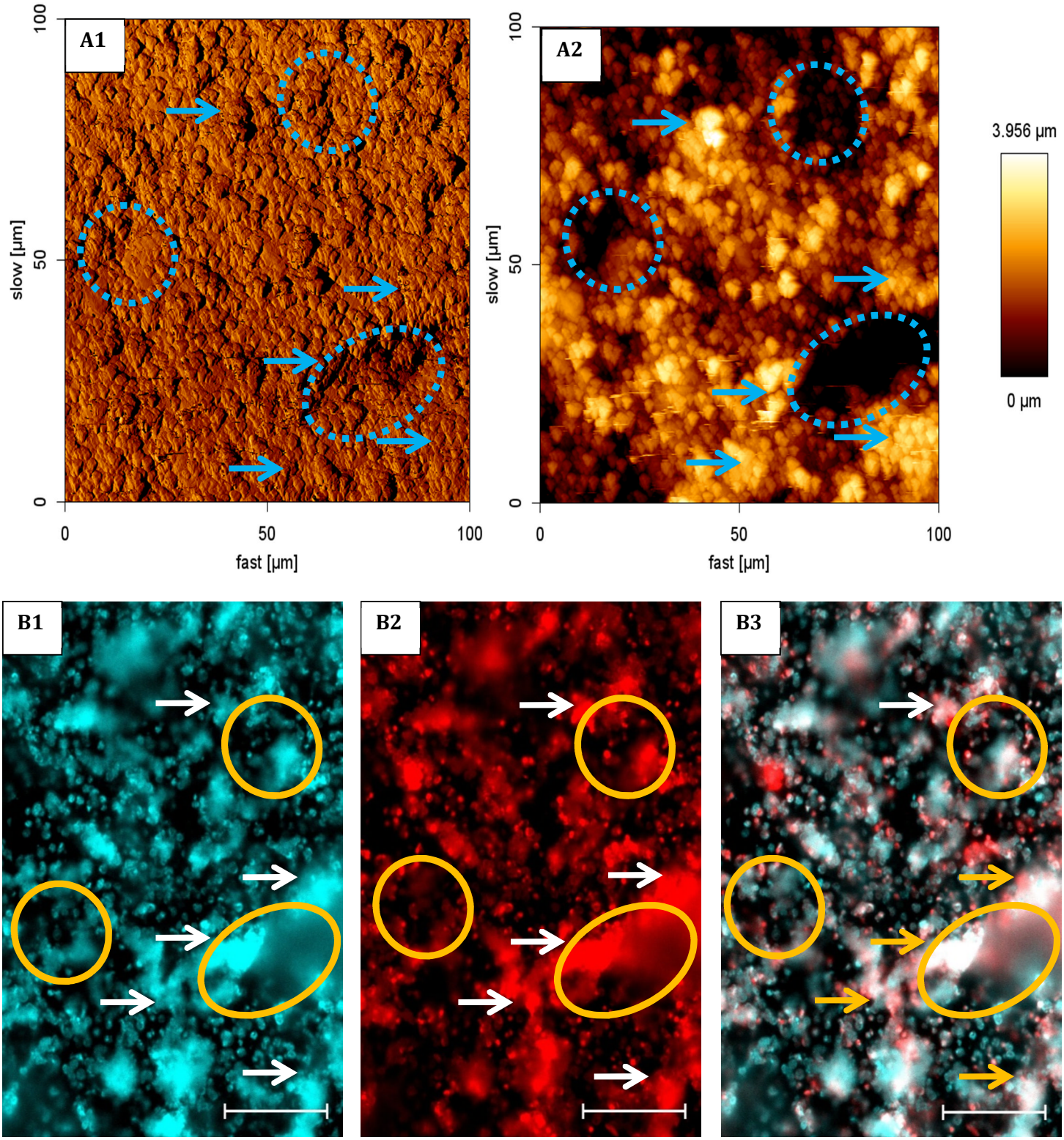

Figure 6.11: Micrographs depicting the colonised surface of a chalcopyrite mineral section inoculated with *M. hakonensis* and incubated for 4 days in the biofilm reactor under conditions of continuous fluid flow. (A1) and (A2) depict the vertical deflection topographical and height information for this particular region respectively. (B1) DAPI fluorescence of attached cells, (B2) TRITC-labelled ConA fluorescence indicative of EPS present and (B3) overlay of the DAPI and TRITC-ConA fluorescence. White bars in (B1 – B3) represent a scale of 20 µm. The yellow and blue circles outline the same regions of interest viewed with the AFM (A1 –A2), and with the EFM in (B1-B3) and demarcate fixed features in the ore. The white arrows indicate attached cells which show positive fluorescence with both ConA and DAPI in (B1 – B3). The position of these attached cells is demarcated with blue arrows in (A1 and A2) on the AFM micrographs.

Results for the colonisation of *M. hakonensis* on a chalcopyrite mineral section after 8 days are presented in Figure 6.12. Again Figure 6.12 (A1) and (A2) represent AFM results. EFM results of DAPI staining for this same region are presented in Figure 6.12 (B1), with TRITC-labelled ConA results presented in Figure 6.12 (B2) and the merged overlay of these two channels presented in Figure 6.12 (B3). From the results presented in Figure 6.12 (A1) and (A2), a densely populated, textured surface, similar to that observed after 4 days, was evident. Again, individual cells were clearly identifiable in both vertical deflection and height AFM micrographs. The DAPI and TRITC results presented in Figure 6.12 (B1) and (B2) confirm the presence of *M. hakonensis* and EPS produced by this microorganism. There is a consistent trend of the TRITC-ConA signal being localised to the immediate cells surface (capsular EPS) as well as the immediate mineral surface, as was observed after 4 days. The attached cells are clearly disseminated across this region of interest, which is evident in both AFM and EFM micrographs. The attached colonies also appear more densely aggregated in this region of interest. Dense aggregates of cells, demarcated with arrows, appear at ridges in the surface which are demarcated by ellipses.

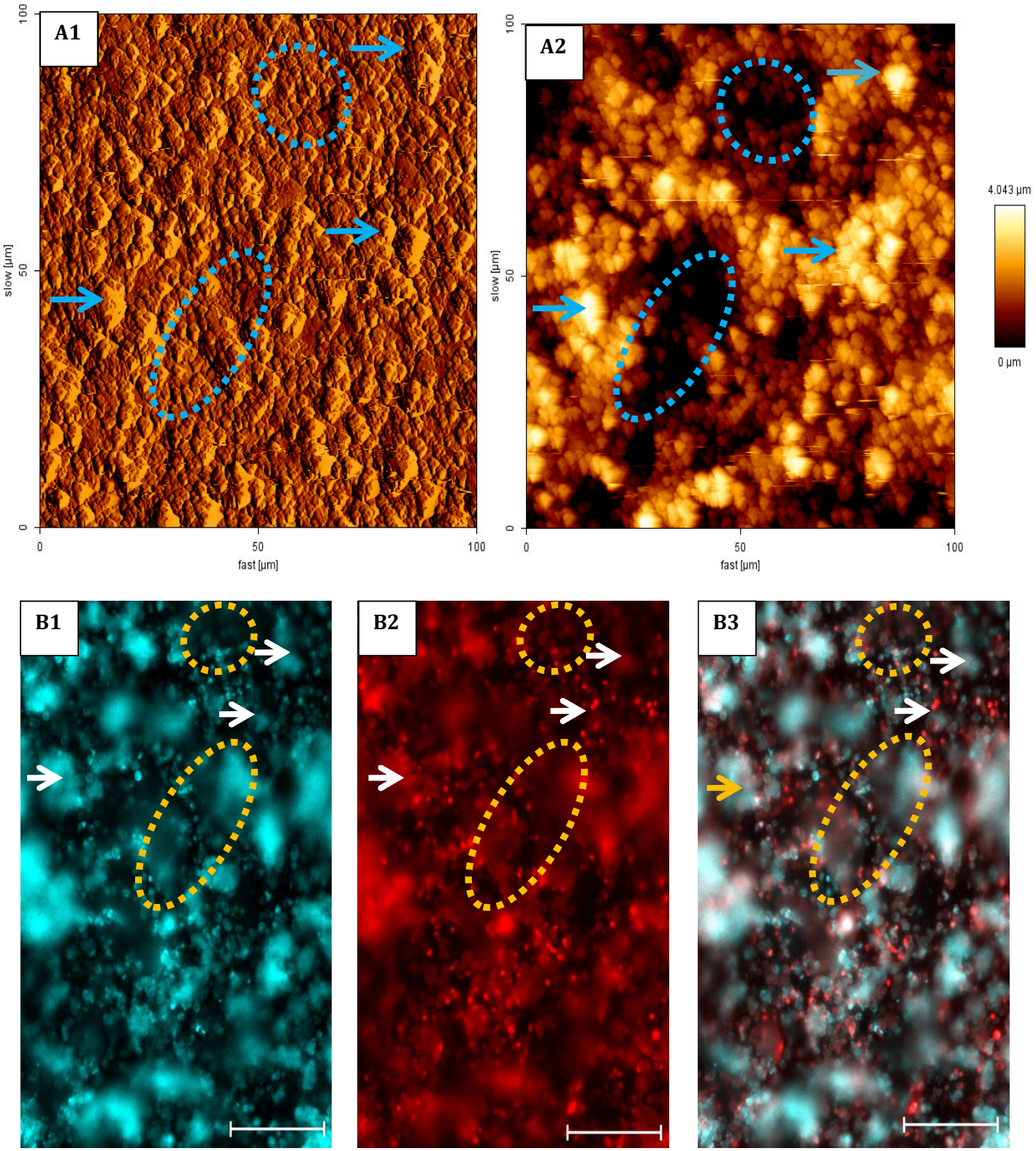

Figure 6.12: Micrographs depicting the colonised surface of a chalcopyrite mineral section inoculated with *M. hakonensis* and incubated for 8 days in the biofilm reactor under conditions of continuous fluid flow. (A1) and (A2) depict the vertical deflection topographical and height information for this particular region respectively. (B1) DAPI fluorescence of attached cells, (B2) TRITC-labelled ConA fluorescence indicative of EPS present and (B3) overlay of the DAPI and TRITC-ConA fluorescence. Scale bar represents 20 µm. The yellow and blue circles outline the same regions of interest viewed with the AFM (A1 –A2), and with the EFM in (B1-B3) and demarcate fixed features in the ore.

6.2.3 Biofilm establishment on pyrite surfaces

The colonisation of a pyrite mineral section by *M. hakonensis* after 4 days at 65 ºC was successfully captured using CLSM. These results are presented in Figure 6.13; with SYTO9™ stain results in column (A); and TRITC-labelled ConA results in (B). The overlay of the channels in (A) and (B) are presented in Figure 6.13 (C). Attached cells are clearly evident with SYTO9™ stain. These cells are spread across the entire surface with the formation of micro colonies observed across the surface. EPS is observed to be present across most of the mineral surface as well in column (B). A branching motif of the EPS is evident in Figure 6.13 (B4). This is much like the results observed during lectin screening of chalcopyrite associated EPS in Chapter 4.3.1. However, in the other areas imaged on the pyrite mineral surface, the EPS appears to be more closely associated to the mineral surface. At 65 ºC, the optimal temperature for growth, one would expect good attachment to the pyrite mineral surface, as was demonstrated by Bromfield et al. (2011). Attachment and subsequent sustained colonisation and biofilm formation of the pyrite surface are demonstrated here through the formation of micro-colonies and the presence of EPS after 4 days incubation in the biofilm reactor.

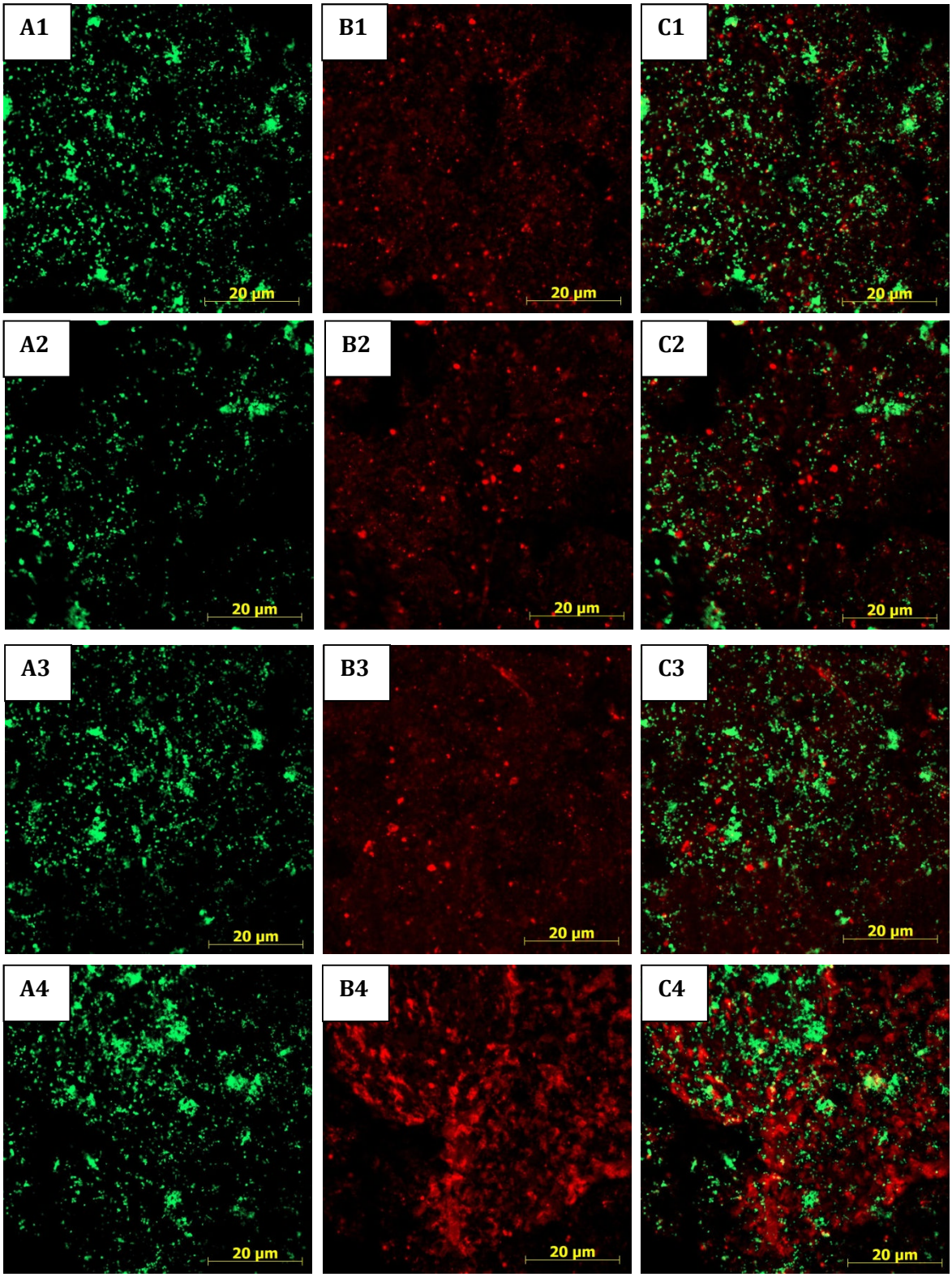

Figure 6.13: Micrographs depict colonisation of a pyrite mineral thin section by *M. hakonensis* after 4 days incubation in the biofilm reactor operated as a continuous flow through system at 65 ºC. Images represent different fields across the same mineral surface used in this experiment. Samples were stained with SYTO9™ (A) and TRITC-labelled ConA (B). Micrographs in (A) depict sessile cells on the surface exhibiting positive staining with SYTO9™, (B) depicts the same region showing the presence of EPS due to positive staining with ConA. Images in (C) depict overlays of the two channels in (A) and (B). A laser scanning module (LSM 510 Carl Zeiss® Jena) coupled to an inverted Axiovert 100 M BP microscope (Zeiss®) was used and operated using the ZEN LSM 510 Release 3.2 (Zeiss®) software. All micrographs were attained using a Plan-Neofluar® 100 x 1.3 oil objective.

The AFM micrograph for *M. hakonensis* colonising pyrite is shown in Figure 6.14 (A). The corresponding EFM micrograph showing DAPI fluorescence of colonising cells in the same region is provided in Figure 6.14 (B). Cells appear dispersed across the surface. A close up of the regions in (A), demarcated in yellow, is provided in Figure 6.14 (C) and (D) depicting topographical and height information respectively. From micrographs in Figure 6.14 (A) – (D), it becomes evident that, as with the colonisation to the chalcopyrite mineral surface, cell attachment and colonisation to pyrite is not limited to structural features visible at the detection limit of this scale.

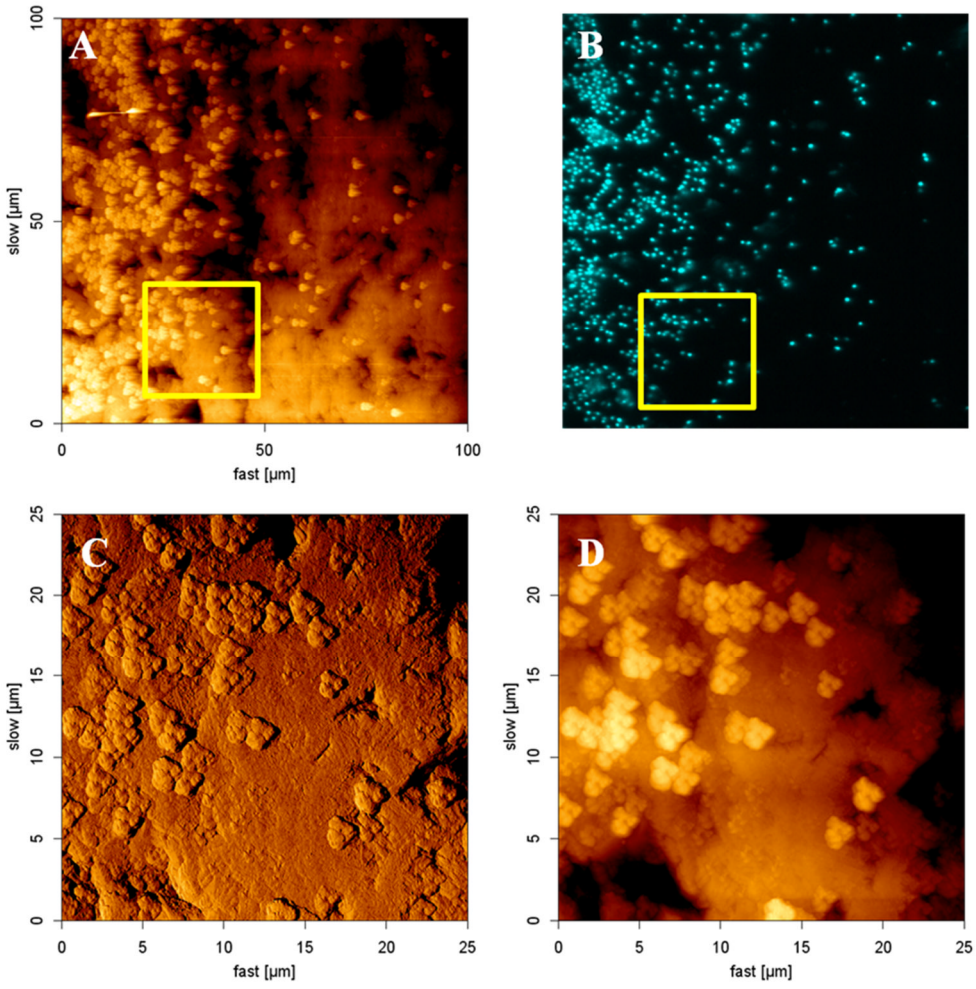

Figure 6.14: AFM micrograph for the attachment of *M. hakonensis* to a pyrite mineral surface after 4 days at 65 _C in a biofilm reactor operated under conditions of continuous fluid flow. In (a) the height image data is provided with brighter regions indicative of elevations on the surface, in (b) the EFM of this same region is depicted with attached cells visualised through the use of DAPI nucleic acid stain. In (c), a close up of the topography of the area demarcated by a yellow border in images (a) and (b) is depicted, with the height information of this same region depicted in (d).

The AFM micrograph in Figure 6.15 (A) depicts attachment of *M. hakonensis* to the glass control slide with DAPI fluorescence of colonising cells in the same region shown in Figure 6.15 (B). The overall surface area covered by cells was only 0.1% indicating low levels of non-specific colonisation.

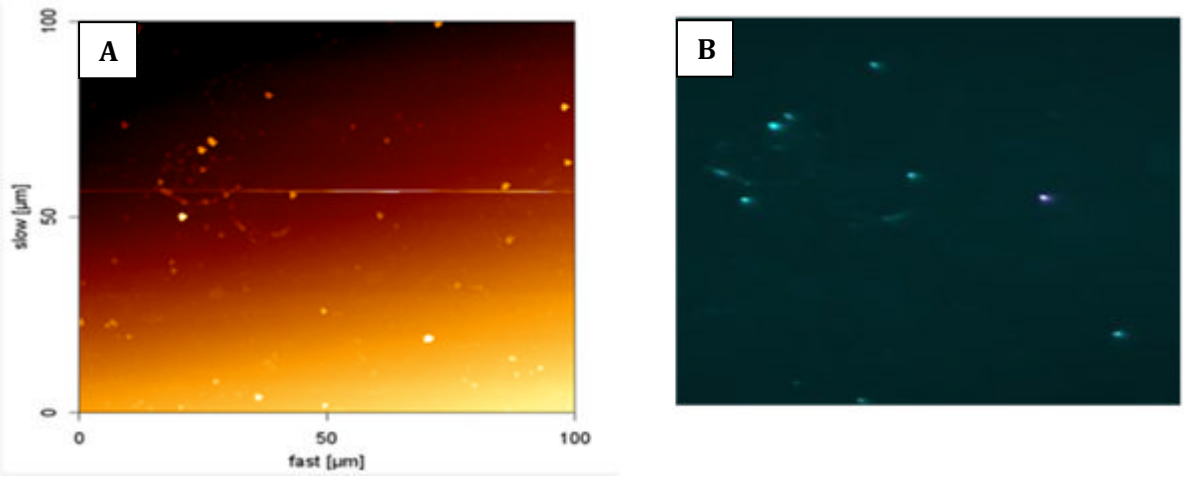

Figure 6.15: AFM micrograph for the attachment of *M. hakonensis* to a glass control after 4 days at 65 ºC in a biofilm reactor operated under conditions of continuous fluid flow. In (A) the height image data is provided with brighter regions indicative of elevations on the surface, in (B) the EFM of this same region is depicted with attached cells visualised through the use of DAPI nucleic acid stain.

A summary of the extent of attachment and colonisation of *M. hakonensis* to pyrite, chalcopyrite and the glass control at 65 ºC after 4 days incubation is provided in Table 6.2. The colonisation observed is expressed as a percentage surface area covered by the micro-organism. For the pyrite mineral system, the surface area covered by biomass was marginally lower relative to that observed for chalcopyrite (Table 6.2). Minimal surface area coverage was observed to the glass control slide, which is also depicted visually in Figure 6.15.

Table 6.2: Summary of the extent of attachment and colonisation of *M. hakonensis* to pyrite, chalcopyrite and the glass control at 65 ºC. Colonisation observed is expressed as a percentage surface area covered by the micro-organism.

Mineral system	Temperature (° C)	Age biofilm (days)	Surface area coverage (%)[a]
Chalcopyrite	65	2	2.0
	65	4	5.7
	65	8	4.2
Pyrite	65	4	4.3
Glass	65	4	0.1

6.2.3 Discussion of sulphide mineral colonisation

Attachment consists of a 4-stage sequence of events. These stages include: transport of the microorganism to the solid surface; an initial or primary adhesion stage involving electrostatic and hydrophobic interactions between the two surfaces; a firm or permanent adhesion stage; and a final stage involving colonisation and biofilm formation (van Loosdrecht *et al.* 1989, 1990). Biofilm formation is recognised to involve EPS and result in a more permanent attachment, with subsequent colonisation of the surface predicted. Colonisation and biofilm formation may be dependent on the organism type involved. The exact nature of this matrix may vary depending on the surrounding environment and the microorganisms involved (Harneit *et al.* 2006; Ghauri *et al.* 2007). Ohmura et al. (1993) reported that low coverage ratios of *Acidithiobacillus ferrooxidans* to pyrite may be indicative of cells adsorbing as a single layer. Harneit et al. (2006) reported the development of micro-colonies of *A. ferrooxidans*, covered in EPS, on the surface of pyrite. The micro-colonies subsequently developed into mono-layered biofilms, as observed using atomic force microscopy. In this study, at optimal temperature for growth, the ConA signal was highest after 4 days of incubation in the biofilm reactor. The EPS was localised to the mineral surface and also encapsulated individual cells.

in this study, the thickness of the biofilm varied across the mineral surface within one sample and typically ranged between 4 and 8 µm, with a maximum of 10 µm observed after 4 days. Interestingly, the film thickness did not vary greatly temporally under the conditions of this experiment, with similar film thicknesses observed after 8 days relative to that observed after 4 days. Koerdt et al. (2010) investigated biofilm development of *Sulfolobus* spp. at temperature ranges between 65 and 80 °C and pH between 2 and 3 under static growth conditions where growth medium was exchanged once every 24 h. They report a film thickness between 20 and 30 µm with a high density of cells exhibiting a 'carpet-like' like appearance across the surface interspersed with cell aggregates after 3 days when visualised using CFM and fluorescent lectins ConA and GS-II. Continuous fluid-flow operation and the use of 0 K media in the present study may have resulted in the lower attached cell densities observed relative to those reported by Koerdt et al. Furthermore, this study represents the first report of colonisation in flow through systems representative of a heap bioleach conditions.

The observation of bioleach micro-organisms exhibiting an ''affinity'' for attachment to visible defects and dislocation sites has been reported by Rojas-Chapana et al. (1998), Gehrke et al. (1998, 2001) and Harneit et al. (2005). It was postulated that sulphur atoms concentrate at grain boundaries and surface imperfections making these locations more favourable as sites of

attachment (Andrews, 1988). Rojas-Chapana et al. (1998) proposed that nutrient concentration gradients were generated at pyrite fragmentation sites, which attracted the settlement of microorganisms at these specific sites over others. All of the aforementioned studies were conducted using mesophilic microorganisms in shake flasks. The results of this study, which makes use of a thermophile and a continuous flow-through system are consistent with the reports of Becker et al. (2011), that report dispersed attached cell arrangements for the colonisation of Sulfobacillus thermosulfidooxidans, a moderate thermophile, to pyrite surfaces at optimal temperature conditions and under continuous fluid-flow. In addition, *M. hakonensis* is non-motile, which may be the reason why initial attachment and colonisation was not driven toward regions where nutrient concentration gradients may be prevalent.

6.3 BIOFILM ESTABLISHMENT ON LOW-GRADE COPPER SULPHIDES

6.3.1 Mineralogical mapping of low-grade chalcopyrite containing ore

Low-grade chalcopyrite mineral containing ore samples were cut into 60 and 100 µm thin sections, and mounted onto glass slides using an epoxy resin (Department of Geology, University of Cape Town). The 60 µm thin sections were polished for the purposes of mineral identification and scanned to create an electronic photographic data base. The surface of the thin section is divided into various regions, in order to systematically generate a mineralogical map of the surface of the sample. Ore microscopy was used to map thin sections of low-grade ore from Escondida containing chalcopyrite (CH-32-Type B). A summary of the mineralogical information provided (courtesy of BHP Billiton), as well as a summary of the characteristic optical properties used for mineral identification under reflected and transmitted light was compiled and is presented in Table 6.3. Photographs of the various regions on the surface of the samples were taken and the identity of the predominating sulfide and gangue minerals present determined through comparison of characteristic optical properties under reflected and transmitted light as summarised in Table 6.3. The spatial locale of minerals identified was noted. A scanned image of such a sample, labelled E, together of how the minerals were identified and mapped is presented in Figure 6.16 and Figure 6.17. In figure 6.16, the same region on the surface of a low-grade chalcopyrite mineral thin section as viewed under reflected light (Bi and ii), plane-polarised transmitted light (Biii and iv), and cross-polarised transmitted light (Bv and vi).

Table 6.3: Summary of the predominating sulfide and gangue minerals present (wt %) in the Escondida CH-32-Type B ore (courtesy of BHP Billiton), as well as a summary of the optical properties used for minerals identification under reflected and transmitted light using ore microscopy (Rodgers 1937, Anthony *et al.* 1990 and Deer *et al.* 1992). The complete mineralogical composition of the Escondida CH-32-Type B ore is provided in Appendix C.

Mineral	**Composition**	**Wt%**	**Characteristic optical properties**		
Major sulphide minerals			**RL**	**TL**	
Pyrite	FeS_2	4.0	Cream to pale yellow	Black	
Chalcopyrite	$CuFeS_2$	0.5	Brassy yellow	Black	
Covellite	CuS	0.3	Green intergrowth on chalcopyrite surface	Black	
Chalcocite	Cu_2S	0.2	Pale grey	Black	
Major gangue minerals				**PPL**	**XPL**
Quartz	SiO_2	44.8	Dull brown grey (does not reflect light)	Colourless to milky in thin section	Isotropic, exhibits weak birefringence (0.009) with light to darker greys and white interference colours
Muscovite	$KAl_2(Si_2Al)O_{10}(OH;F)_2$	28.6	Dull brown grey (does not reflect light)	Colourless in thin sections, may appear tinted in hues of grey or brown	Anisotropic, exhibits high birefringence (0.035 – 0.042) with interference colours ranging from violet through to red spectrum

Reflected light (**RL**). Transmitted light (**TL**), Plane polarised light (**PPL**), Cross polarised light (**XPL**)

The different light sources were used for identification of the minerals present in areas of interest. A mineralogical map of these regions could then be established prior to colonisation experiments. The sulfide and gangue minerals present in the region of interest are marked with an "X" and "G" respectively. Under reflected light (RL), sulphide minerals will reflect light and appear a brassy yellow colour, as can be observed in Figure 6.16. Gangue minerals do not reflect light under RL and appear dull brown/grey. Under plane polarised transmitted light, the sulphide minerals appear black, with gangue minerals present being colourless to milky with hues of grey or brown, observed in B (iii and iv). When the mineral section is observed under cross polarised transmitted light. The two main gangue minerals present can be distinguished. Muscovite exhibits high birefringence, indicated with the symbol "M" in B (v and vi), with quarts exhibiting weak birefringence with white and grey/brown interference, and designated "Q". Figure 6.17 represents similar mineralogical mapping with covellite intergrowth observed within the chalcopyrite mineral present, seen in Figure 6.17 (C).

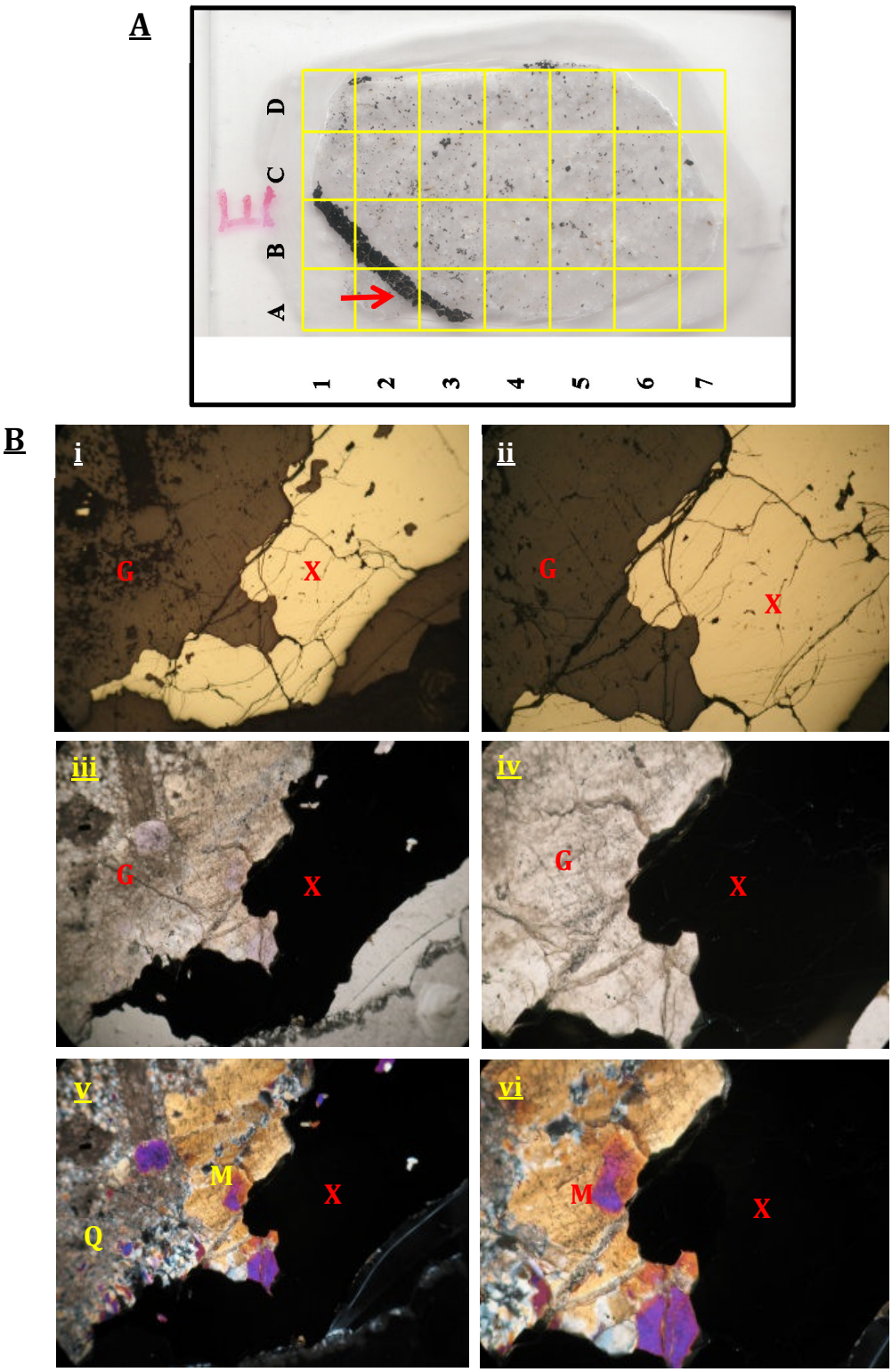

Figure 6.16: In micrograph A, the mineral surface of a low grade chalcopyrite thin section of ore is presented. The micrographs in Bi-vi refer to the same area in quadrant A2 on the mineral surface (indicated with a red arrow). In micrograph B, images in the left hand column (i, iii and v) were viewed using a 5 x objective, with the corresponding image in the right hand column (ii, iv, vi) viewed using the 10 x objective. Micrograph B i and ii, were viewed under reflected light (RL). Sulphide minerals will reflect light and appear a brassy yellow colour under RL; these minerals are indicated with the symbol "X". Gangue minerals do not reflect light under RL and appear dull brown/grey – indicated with "G". B iii and iv were viewed under plane polarised transmitted light. In these images, the sulphide minerals appear black, indicated with "X", with gangue minerals present being colourless – milky with hues of grey or brown, shown with the symbol "G". B v and vi were viewed using cross polarised transmitted light. The two main gangue minerals present can be identified under cross polarised light, with muscovite exhibiting high birefringence, indicated using "M", and quarts exhibiting weak birefringence with white and grey/brown interference, and designated "Q".

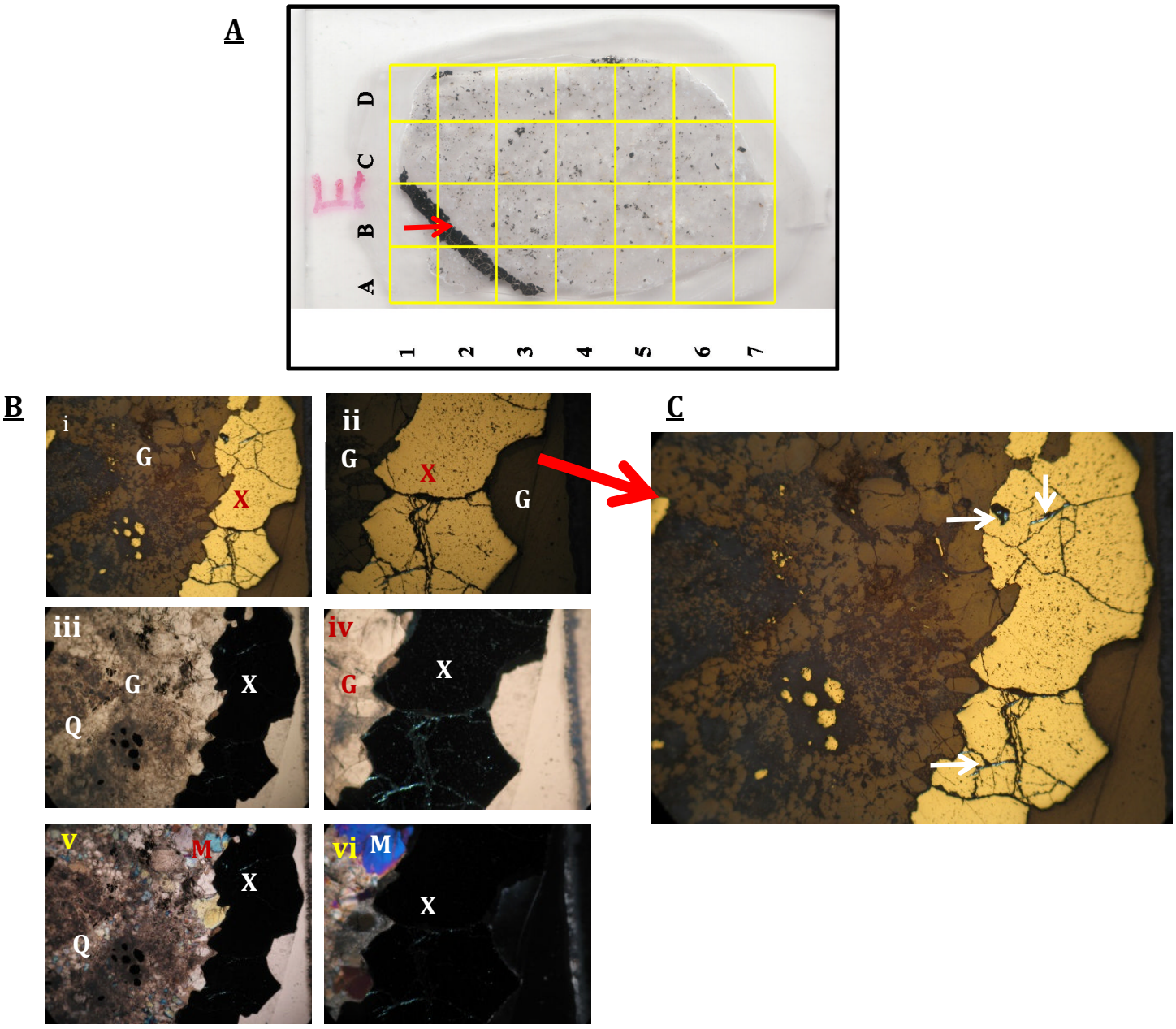

Figure 6.17: In micrograph A, the mineral surface of a low grade chalcopyrite thin section of ore is presented. The micrographs in Bi-vi refer to the same area in quadrant B2 on the mineral surface (indicated with a red arrow). In micrograph B, images in the left hand column (i, iii and v) were viewed using a 5 x objective, with the corresponding image in the right hand column (ii, iv, vi) viewed using the 10 x objective. Micrograph B i and ii, were viewed under reflected light (RL). Sulphide minerals will reflect light and appear a brassy yellow colour under RL; these minerals are indicated with the symbol "X". Gangue minerals do not reflect light under RL and appear dull brown/grey – indicated with "G". B iii and iv were viewed under plane polarised transmitted light. In these images, the sulphide minerals appear black, indicated with "X", with gangue minerals present being colourless – milky with hues of grey or brown, shown with the symbol "G". B v and vi were viewed using cross polarised transmitted light. The two main gangue minerals present can be identified under cross polarised light, with muscovite exhibiting high birefringence, indicated using "M", and quarts exhibiting weak birefringence with white and grey/brown interference, and designated "Q". Micrograph C is a magnified view of Bi and ii, viewed using a 50 x objective. Green covellite intergrowth on within the chalcopyrite can be seen in micrograph C, these are indicated with white arrows.

6.3.2 Colonisation and biofilm formation on low-grade chalcopyrite

The DAPI fluorescence resulting from the colonisation of a low-grade mineral ore surface by *M. hakonensis* at 65 °C in a biofilm reactor after 4 days of incubation is presented in Figures 6.18, 6.19 and 6.20.

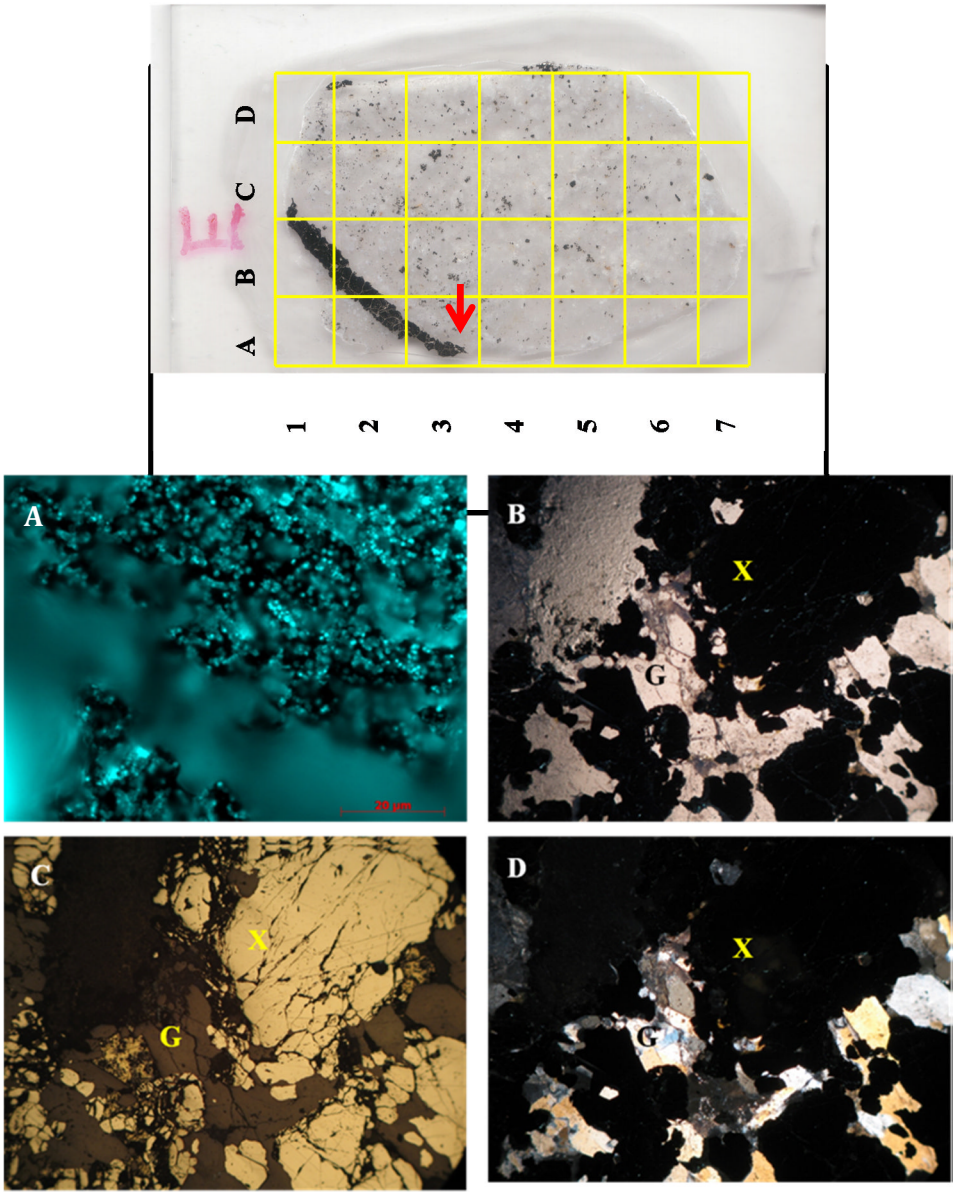

Figure 6.18: *M. hakonensis* attachment to LG chalcopyrite section "E" after 4 days incubation at 65 ° C. The mineral sample was mapped as depicted in the image on the far left. The EFM micrograph in (A) depicts DAPI fluorescence, visualised using a 100 x objective, of *M. hakonensis* colonising region "A2" on the low-grade sample on the far left. Figure 5 (B – D) depict the same regions on the surface of a low-grade chalcopyrite mineral thin section as viewed under plane-polarised transmitted light (B), reflected light (C) and transmitted cross-polarised light (D) used for mineralogical mapping, viewed using the 5 x objective, in order to distinguish between gangue and sulfide material in that region. The sulfide and gangue minerals present in the region of interest are marked with an "X" and "G" respectively in micrographs (B – D).

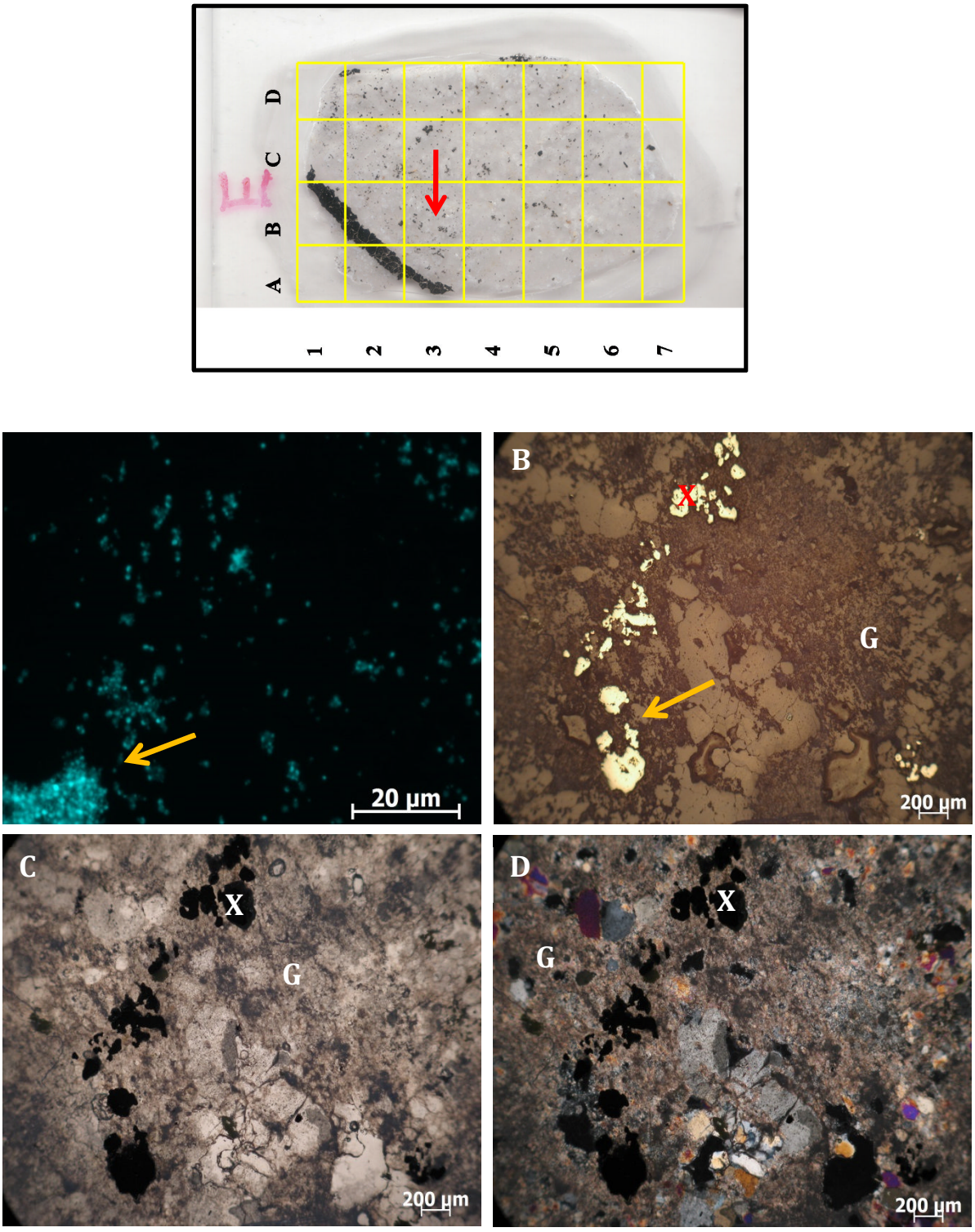

Figure 6.19: *M. hakonensis* attachment to LG chalcopyrite section E after 4 days incubation at 65 ° C. In particular, the results of colonisation to region B3, as indicated with the red arrow, on the mineral surface is shown in micrographs b to d. The EFM micrograph in (A) depicts DAPI fluorescence, visualised using a 100 x objective. Micrographs b to d depict the same regions on the surface of a low-grade chalcopyrite mineral thin section as viewed under reflected light (RL) in (B), plane-polarised transmitted light (PPL)in (C) and cross-polarised transmitted light (XPL) in (D) using the 5 x objective. Sulphide minerals are indicated with the symbol; "X", with gangue minerals present labelled "G".

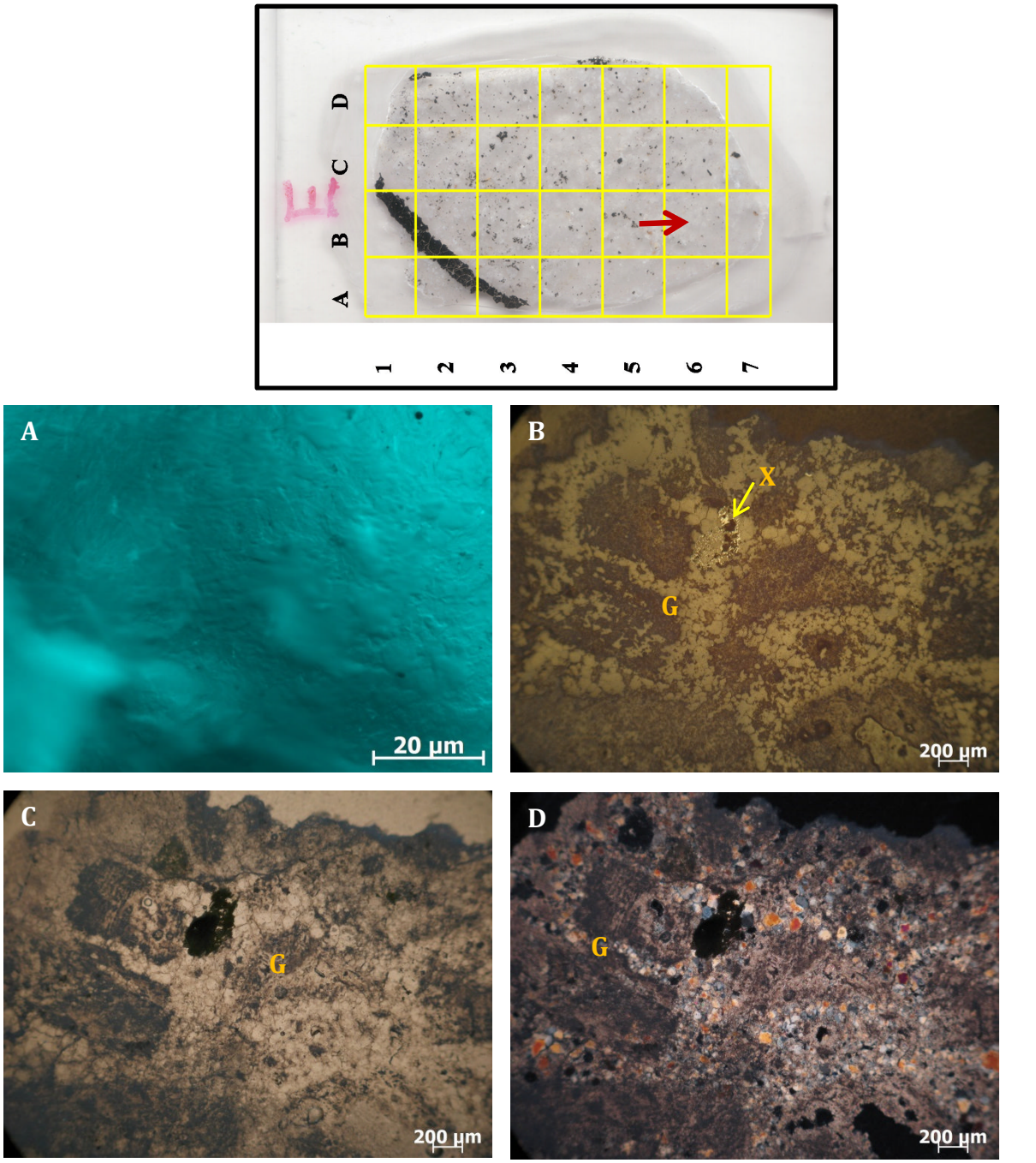

Figure 6.20: *M. hakonensis* attachment to LG chalcopyrite section E after 4 days incubation at 65 ° C. In particular, the results of colonisation to region B6, as indicated with the red arrow, on the mineral surface is shown in micrographs b to d. The EFM micrograph in (a) depicts DAPI fluorescence, visualised using a 100 x objective. Micrographs b to d depict the same regions on the surface of a low-grade chalcopyrite mineral thin section as viewed under reflected light (b), plane-polarised transmitted light (c) and cross-polarised transmitted light (d) using the 5 x objective. This region contains largely gangue minerals labelled "G". A small strip of chalcopyrite is present and labelled "X".

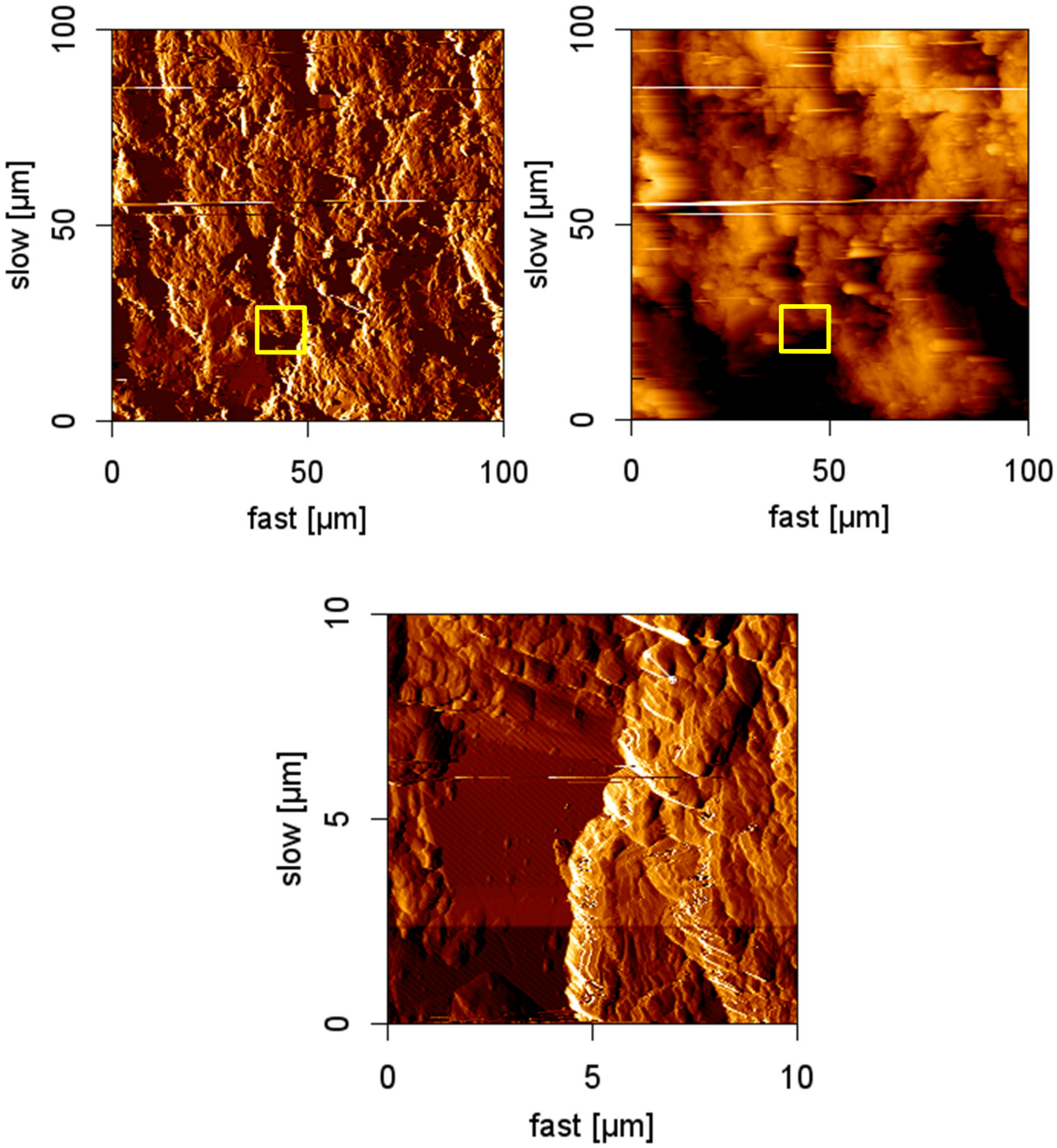

Figure 6.21: Micrograph depicts the AFM topography of the low-grade chalcopyrite mineral section "E" after 4 days incubation with *M. hakonensis* in a biofilm reactor at 65 ° C. No attached cells are visible on the scanned section.

Attachment of *M. hakonensis* to the low-grade ore mineral surface after 4 days is evident upon analysis of the results presented in Figures 6.18 and 6.19. In Figure 6.18, there is an abundance of sulphide mineral present in the regions under investigation. High densities of positive DAPI stained cells are evident in this region (Figure 6.18 a) after 4 days incubation in the biofilm reactor at optimal temperature for growth. In Figure 6.19, the density of positive DAPI fluorescence is less abundant but, clusters of cells are observed in the near of sulphide minerals present in the regions investigated. The prevalence of micro-colony formation by *M. hakonensis* in the near of and/or on sulphide mineral surfaces is evident on the low-grade chalcopyrite mineral sections after 4 days incubation at 65 ºC. The overall coverage of the low-grade mineral surface was sparse, and visibly less than that observed for massive sulphide mineral surfaces after 4 days incubation at 65 ºC. This is consistent with the findings of Bromfield et al. (2011), where preferential attachment of *M. hakonensis* to sulphide minerals over low-grade ore was demonstrated at optimal temperature conditions in a continuous flow-through column reactor.

6.4 THE EFFECT OF TEMPERATURE ON BIOFILM ESTABLISHMENT

The effect of varying temperature on the attachment and subsequent formation of *M. hakonensis* biofilms was investigated. The extent of biofilm formation after 4 days decreased as the temperature decreased. This trend was evident across all three mineral systems (Table 6.4). While firm attachment to all mineral surfaces (cells are not removed by continuous introduction of fresh basal salts medium into the reactor system) did occur after 4 days at room temperature (20 ± 1 ºC), the area covered by biofilm was substantially lower than that observed at higher temperatures. The extent of surface area coverage was only marginally higher for the pyrite and chalcopyrite relative to the low-grade ore (1.7%, 1.4% and 1.0% respectively) at room temperature. Similarly, at 45 ºC, the degree of mineral surface area covered by cells for the sulphide mineral systems was comparable (2.0% and 1.8% for chalcopyrite and pyrite respectively), with the extent of surface area covered for the low-grade ore system being marginally higher (2.8%) relative to the sulphide mineral systems. The extent of biofilm development, in terms of surface area covered, on the low-grade mineral surface (3.0%) is lower than that observed for the massive sulphide minerals (Table 1a). The trend of increased colonisation of sulphide mineral surfaces was expected as *M. hakonensis* utilises both pyrite and chalcopyrite as an energy source.

Table 6.4: Summary of the extent of attachment and colonisation of bioleach microorganisms to various sulfide mineral systems, investigated at three temperatures, expressed as a percentage surface area covered.

Mineral system	Temperature (° C)	Age biofilm (days)	Surface area coverage (%)[a]
Chalcopyrite	RT[b]	4	1.4
	45	4	2.0
	65	4	5.7
	65	2	2.0
	65	8	4.2
Pyrite	RT	4	1.7
	45		1.8
	65		4.3
Low-grade ore	RT	4	1.0
	45		2.8
	65		3.0
Glass	65	4	0.1

[a]Extent of surface attachment given as the % surface area covered by attached cells, [b]RT (room temperature) was measured at 20 ± 1°C

Micrographs depicting the results of the extent of *M. hakonensis* to low-grade chalcopyritic ore, pyrite and chalcopyrite at ambient temperature (Figure 6.22), at 45 ºC (Figure 6.23) and at 65 ºC (Figure 6.24) follow on the next few pages. From the results in Figure 6.22, attachment and colonisation at ambient temperatures is sparse. This trend is observed across all the mineral systems. Furthermore, there is no evidence of EPS being present after 4 days at ambient temperature for the pyrite and chalcopyrite systems. For colonisation to the different mineral systems at 45 ºC, presented in Figure 6.23, the density of the attached cells present is much higher. This is observed by positive fluorescence of DAPI and Syto 9 staining. In addition, positive staining with Con-A is observed for the sulphide mineral systems, depicting enhanced production of EPS by *M. hakonensis* during colonisation of pyrite and chalcopyrite at 45 ºC. The highest density of colonisation is observed at 65 ºC, presented in Figure 6.24. Attachment and colonisation increase across all mineral systems. Moreover, the presence of EPS is also observed to be greater at 65 ºC relative to the lower temperatures. This is observed through increased ConA fluorescence across the pyrite and chalcopyrite mineral surfaces (Figure 6.24).

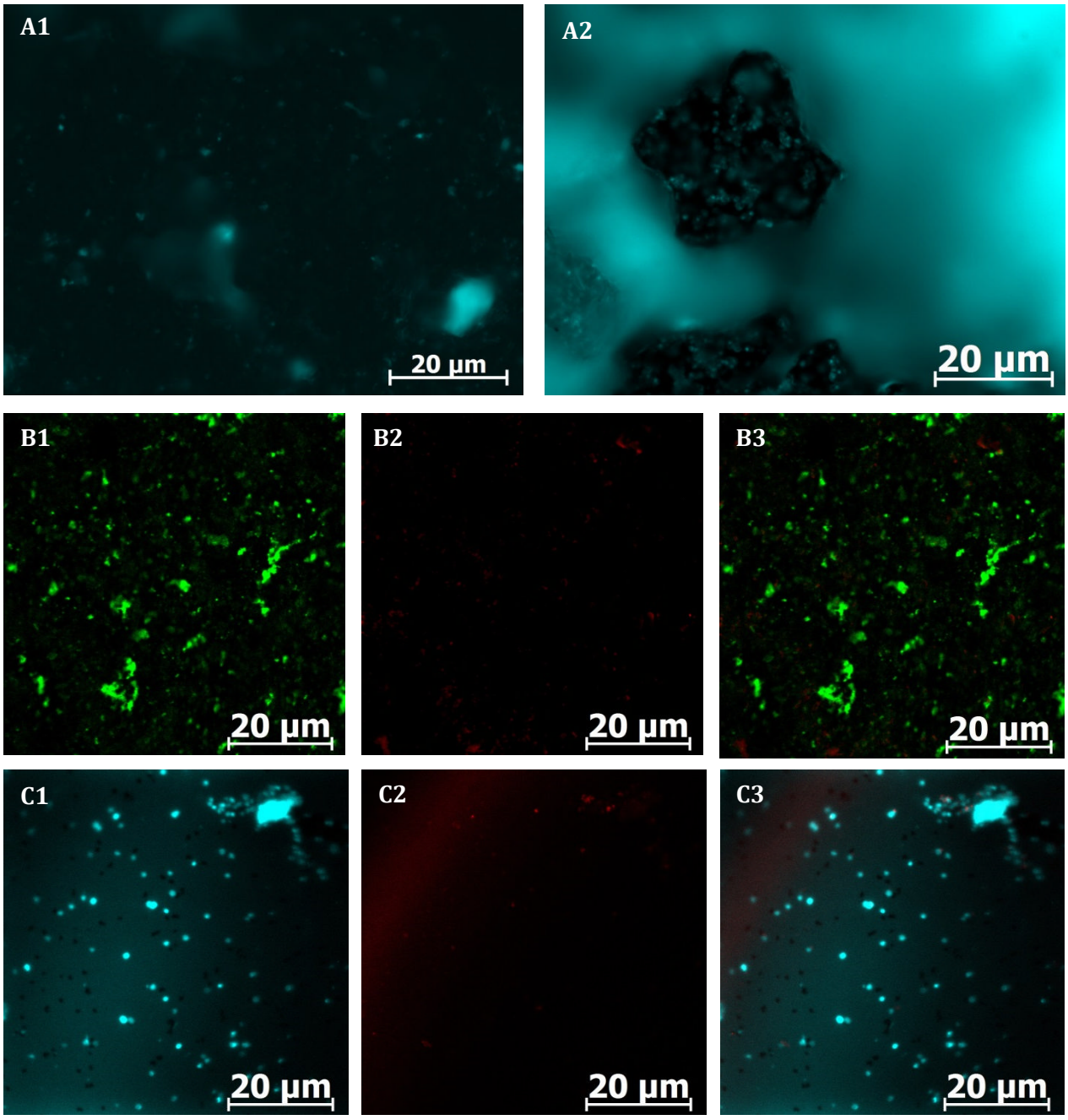

Figure 6.22: Micrographs depict colonisation of a low-grade ore section (A1 and A2), pyrite mineral thin section (B1 – B3) and chalcopyrite mineral section (C1 – C3) by *M. hakonensis* after 4 days incubation in the biofilm reactor operated as a continuous flow through system at ambient temperature (20 ±1 ºC). Samples were stained with DAPI (A1 and A2), SYTO9™ (B1 and C1) and TRITC-labelled ConA (B2 and C2). Micrographs in B3 and C3 depict the overlay of the SYTO9™ and TRITC-ConA. A laser scanning module (LSM 510 Carl Zeiss® Jena) coupled to an inverted Axiovert 100 M BP microscope (Zeiss®) was used and operated using the ZEN LSM 510 Release 3.2 (Zeiss®) software. All micrographs were attained using a Plan-Neofluar® 100 x 1.3 oil objective.

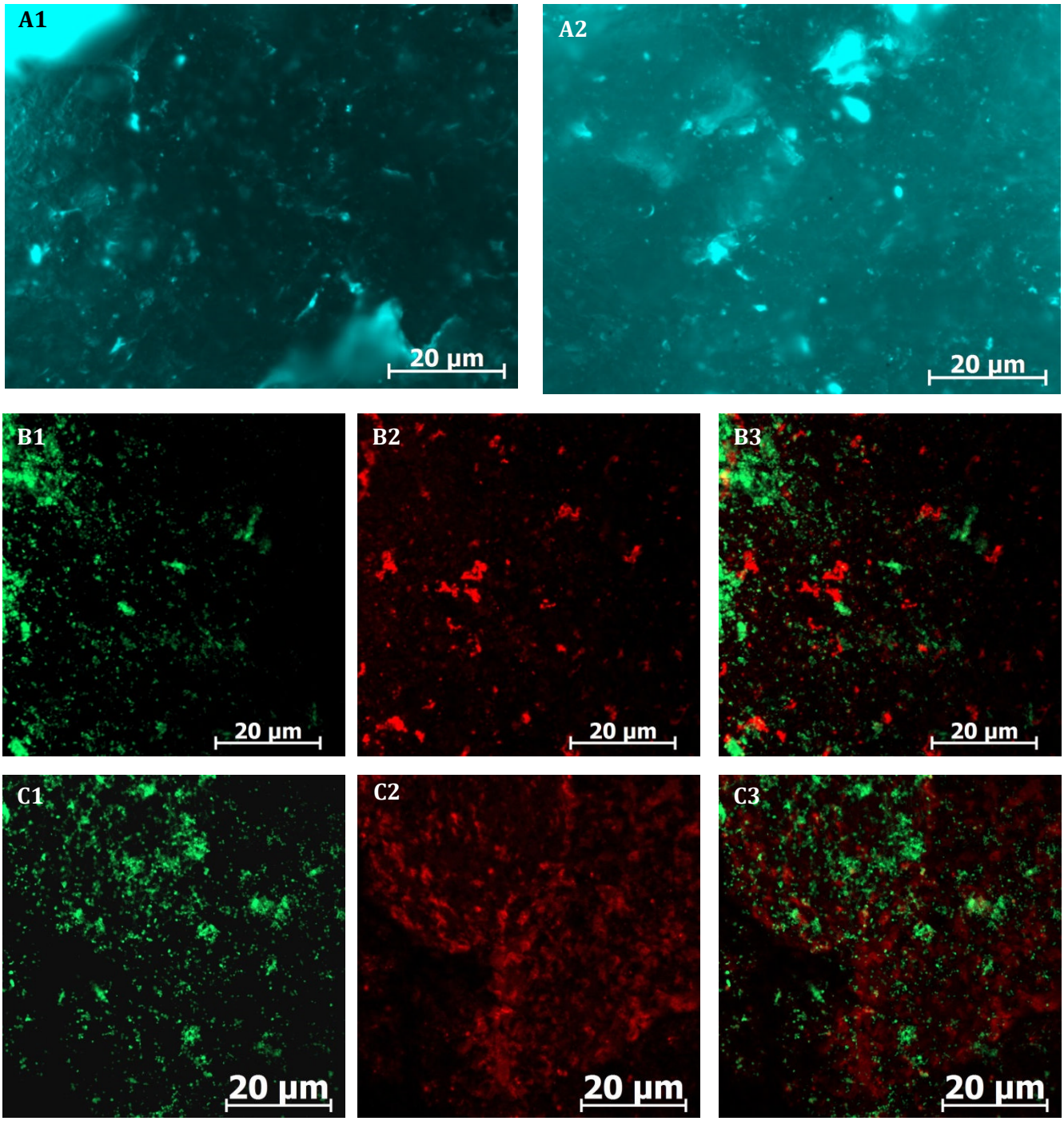

Figure 6.23: Micrographs depict colonisation of a low-grade ore section (A1 and A2), pyrite mineral thin section (B1 – B3) and chalcopyrite mineral section (C1 – C3) by *M. hakonensis* after 4 days incubation in the biofilm reactor operated as a continuous flow through system at 45 ºC. Samples were stained with DAPI (A1 and A2), SYTO9™ (B1 and C1) and TRITC-labelled ConA (B2 and C2). Micrographs in B3 and C3 depict the overlay of the SYTO9™ and TRITC-ConA. A laser scanning module (LSM 510 Carl Zeiss® Jena) coupled to an inverted Axiovert 100 M BP microscope (Zeiss®) was used and operated using the ZEN LSM 510 Release 3.2 (Zeiss®) software. All micrographs were attained using a Plan-Neofluar® 100 x 1.3 oil objective.

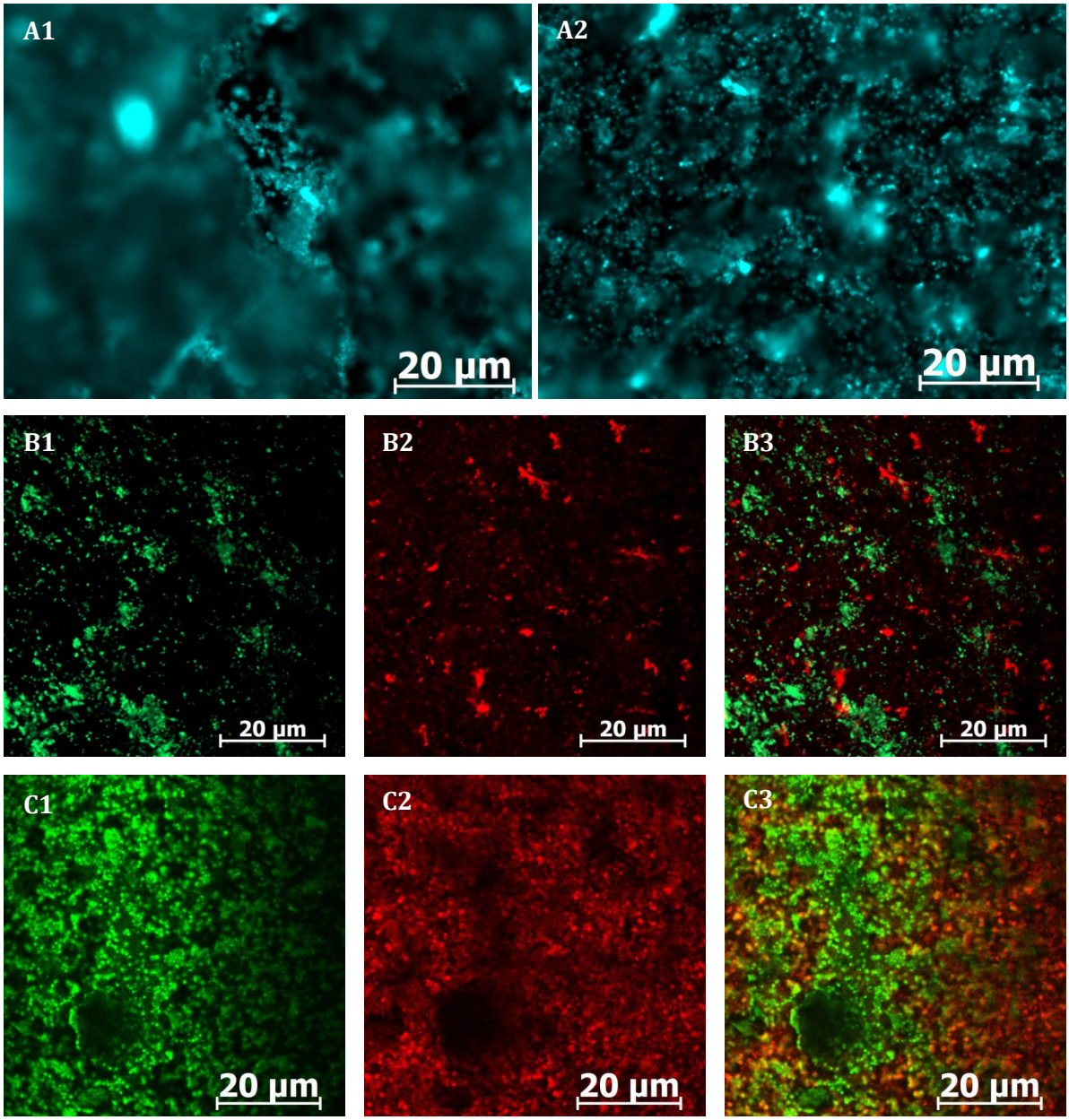

Figure 6.24: Micrographs depict colonisation of a low-grade ore section (A1 and A2), pyrite mineral thin section (B1 – B3) and chalcopyrite mineral section (C1 – C3) by *M. hakonensis* after 4 days incubation in the biofilm reactor operated as a continuous flow through system at 65 ºC. Samples were stained with DAPI (A1 and A2), SYTO9™ (B1 and C1) and TRITC-labelled ConA (B2 and C2). Micrographs in B3 and C3 depict the overlay of the SYTO9™ and TRITC-ConA. A laser scanning module (LSM 510 Carl Zeiss® Jena) coupled to an inverted Axiovert 100 M BP microscope (Zeiss®) was used and operated using the ZEN LSM 510 Release 3.2 (Zeiss®) software. All micrographs were attained using a Plan-Neofluar® 100 x 1.3 oil objective.

The trend of low levels of surface area colonised at decreased temperatures may be due to a decrease in metabolic activity at suboptimal temperatures. Franzmann et al. (2005) investigate the effects of temperature on growth and activity by extrapolating cardinal temperatures for iron and sulphur oxidation using the Ratkowsky and Arrhenius equations. This group reports an optimal temperature (where fastest rates of oxidation occurred) of 71 °C for *Sulfolobus metallicus* oxidation of sulphur, with an extrapolated minimum of 26.3 ± 1.6 °C and a maximum of 76.0 ± 0.1 °C. Thus, *S. metallicus* is still metabolically active at a minimum temperature of 26.3 ± 1.6 °C; however, the activity decreased as the temperature decreased. The optimal temperature range for growth for this microorganism is reported between 65 and 70 °C (Huber and Stetter, 1991 in Franzmann *et al.* 2005). The optimal temperature for growth for *M. hakonensis* occurs between 50 and 80 °C (Takayanagi *et al.* 1996; Kurosawa *et al.* 2003). The minimum temperature at which *M. hakonensis* remains metabolically active is not known. However, if we lend from what is known regarding the activity behaviour of *S. metallicus*, *M. hakonensis* may be metabolically active at 45 °C and 20 °C, albeit below its optimal activity. This may have had an impact on the extent of colonisation at suboptimal temperatures, as colonisation requires metabolic processes in the production of EPS and the formation of an effective biofilm. The work of Plumb et al. (2008) further corroborates this reasoning. They assessed growth activity of pure and mixed bioleach microorganisms on low-grade chalcopyrite ore at a temperature range between 28 and 65 °C. The fastest iron and sulphur oxidation rates were observed at 65 °C. Thermophilic archaea were detected growing on low-grade chalcopyrite ore at ''near-ideal'' temperatures (45–55 °C). However, growth rates were slow, indicative of impeded metabolic activity at suboptimal temperature regimes. This is consistent with the low extents of colonisation evident for low-grade ore at 65 °C relative to the massive sulphide mineral sections, and the decrease in the extent of colonisation with temperature irrespective of mineral system investigated observed in this study.

6.5 SUMMARY AND CONCLUSIONS

The formation and development of *M. hakonensis* biofilms on two massive sulphide mineral surfaces (chalcopyrite and pyrite) and a low-grade chalcopyrite bearing ore was assessed, with a borosilicate (glass) surface serving as control surface. These mono-species biofilms were grown in a specialised biofilm reactor under conditions of continuous fluid flow, mimicking fluid flow conditions found in a bioheap. The mature films were analysed through the use of fluorescent lectin and nucleic acid stains and visualised using CLSM and a combination of AFM–EFM. This provided valuable insight into biofilm architecture, allowing assessment of spatial distribution of microbial cells and EPS across the mineral surface, their variation with mineral type, temporally and in response to temperature. For attachment and biofilm formation on chalcopyrite surfaces at optimal temperatures for growth, micro-colony formation was evident after 2 days with the cell density increasing from 2.0% to 5.7% coverage of the surface after 4 days. This then decreased marginally to 4.7% after 8 days of incubation. The most prominent EPS signal was evident after 4 days of incubation at optimal temperature for growth. The greatest cell densities and extents of biofilm development, in terms of surface coverage, were observed on massive chalcopyrite at the optimal temperature for growth (5.7% coverage). The surface coverage decreased with a decrease in incubation temperature irrespective of mineral system (Table 6.2). The mineral surface was colonised after 2 days, with cells forming a monolayer and EPS not abundantly present. Attachment was improved after 4 days incubation at room temperature, irrespective of mineral system under investigation, with EPS becoming more significant. This study provides first known insights into biofilm development of *M. hakonensis* on massive sulphide mineral surfaces, demonstrating monolayer coverage and dependence on colonisation temperature. It also provides the first study on low-grade mineral ore surfaces investigated in situ under film flow. These results suggest that introduction of high temperature organisms into the heap under conditions sub-optimal for their growth may result in their retention on the ore surface, albeit at a lower loading. Hence re-inoculation at high temperatures may not be essential. Further, the short time frame required for colonisation under ideal contacting conditions (<4 days) highlights the importance of contacting in the heap environment. As non-specific attachment is negligible, the exposure of the sulphide mineral grains on the ore surface is required both for leaching and for colonisation.

References

Andrews, G. F. (1988). The selective adsorption of *Thiobacilli* to dislocation sites on pyrite sufaces. *Biotechnology and Bioengineering , 31*, 278-381.

Afzal Ghauri, M., Okibe, N. & Barrie Johnson, D., 2007. Attachment of acidophilic bacteria to solid surfaces: The significance of species and strain variations. *Hydrometallurgy*, 85(2-4), pp.72–80.

Becker, T. et al., 2011. In situ imaging of *Sulfobacillus thermosulfidooxidans* on pyrite under conditions of variable pH using tapping mode atomic force microscopy. *Process Biochemistry*, 46(4), pp.966–976.

Bromfield, L., Africa, C., Harrison, S. T. L., & Hille, R. P. Van. (2011). The effect of temperature and culture history on the attachment of *Metallosphaera hakonensis* to mineral sulfides with application to heap bioleaching. *Minerals Engineering*, *24*(11), 1157–1165.

Chazotte, B., 2011. Labelling Membrane Glycoproteins of Glycolipids with Fluorescent Wheat Germ Agglutinin. *Cold Spring Harbor Protocols*,

Flores S. M. and Toca-Herrera J. L. (2009) The new future of scanning probe microscopy: Combining atomic force microscopy with other surface-sensitive techniques, optical microscopy and fluorescent techniques. A review. *Nanoscale*, **1**,40-49.

Franzmann, P.D., Haddad, C.M., Hawkes, R.B., Robertson, W.J., Plumb, J.J., 2005. Effects of temperature on the rates of iron and sulfur oxidation by selected bioleaching bacteria and archae: application of the Ratkowsky equation. *Minerals Engineering* 18, 1304–1314

Gehrke, T. et al., 1998. Importance of Extracellular Polymeric Substances from *Thiobacillus ferrooxidans* for Bioleaching. , *Appl Environ Microbiol*. 64(7), pp.2743–2747.

Gehrke, T. et al., 2001. The EPS of *Acidithiobacillus ferrooxidans*-a model for structure-function relationships of attached bacteria and their physiology. *Water science and technology : a journal of the International Association on Water Pollution Research*, 43(6), pp.159–67.

Harneit, K. et al., 2006. Adhesion to metal sulfide surfaces by cells of *Acidithiobacillus ferrooxidans, Acidithiobacillus thiooxidans* and *Leptospirillum ferrooxidans. Hydrometallurgy*, 83(1-4), pp.245–254.

Huber H. and Stetter K. O., 1991 *Sulfolobus metallicus sp. nov.*, a novel strictly chemolithotrophic thermophilic archael species of metal-mobilizers, *Syst Appl Microbiol* 14:372-378

Koerdt, A. et al., 2010. Crenarchaeal biofilm formation under extreme conditions. *PloS one*, 5(11), p.e14104.

Kurosawa, N., Itoh, Y.H. & Itoh, T., 2003. Reclassification of *Sulfolobus hakonensis* Takayanagi et al. 1996 as *Metallosphaera hakonensis* comb. nov. based on phylogenetic evidence and DNA G+C content. *International Journal of Systematic and Evolutionary Microbiology*, 53(5), pp.1607–1608.

Mangold, S., Laxander, M., Harneit, K., Rohwerder, T., Claus, G., & Sand, W. (2008). Visualization of *Acidithiobacillus ferrooxidans* biofilms on pyrite by atomic force and epi fluorescence microscopy under various experimental conditions, *Hydrometallurgy* 94, 127–132.

Ohmura, N., Kitamura, K. & Saiki, H., 1993. Selective Adhesion of *Thiobacillus ferrooxidans* to Pyrite. , *Applied Environmental Microbiology.* 59(12), pp.4044–4050.

Olympus Corporation, June 2015,

http://www.olympusims.com/en/knowledge/metrology/roughness/2d_parameter

Plumb, J.J., Muddle, R. & Franzmann, P.D., 2008. Effect of pH on rates of iron and sulfur oxidation by bioleaching organisms. *Minerals Engineering*, 21(1), pp.76–82.

Rojas-Chapana, A., Bartels, C. C., Pohlmann, L., & Tributsch, H. (1998). Co-operative leaching and chemotaxis of thiobacilli studied with spherical sulphur. *Process Biochemistry , 31*, 239-248.

Takayanagi, S. et al., 1996. Sulfolobus hakonensis sp. nov., a novel species of acidothermophilic archaeon. *International journal of systematic bacteriology*, 46(2), pp.377–82.

van Loosdrecht, M. C., Lyklema, J., Norde, W., Schraa, G., & Zehnder, A. J. (1987). Electrophoteric Mobility and Hydrophobicity as a Measure To Predict the Inittial Steps of Bacterial Adhesion. *Applied and Environmental Microbiology , 53*, 1898-1901.

van Loosdrecht, M. C., Lyklema, J., Norde, W., Schraa, G., & Zehnder, A. J. (1990). Influence of Interfaces on Microbial Activity. *Microbiological reviews , 54*, 75-87

Chapter 7:
Conclusions and recommendations

In the context of bioleaching, microbial EPS components are thought to complex chemical oxidants and extend the chemical reaction space available for mineral dissolution reactions, making the microbial-mineral-EPS interface the dominant active zone in terms of microbial oxidation and mineral dissolution. There is a limited understanding of microbial biofilm formation within a bioleach heap. Monitoring the microbiology in industrial bioheaps has predominantly been carried out by sampling PLS and raffinate, or through the use of indirect methods (oxygen uptake) as obtaining samples from solid particles within the heap is challenging and often unreliable (Brierley 2001). The implication of various microorganisms having a set of defined or optimal conditions under which they colonise and proliferate is quite substantial. Understanding what creates favourable interfacial microenvironments enabling a sessile population to flourish (and thereby decrease lag time) has great implications for minimising costs and maximising productivity. Furthermore, limited work has been conducted on thermophilic microorganisms relevant to bioleaching. The aim of this research is to provide a thorough investigation into microbial-metal sulfide interfacial environments *in situ*, using a thermophilic archaeon *M. hakonensis*, low-grade metal-sulfide ores, a range of temperature regimes, heap-simulating conditions and an in depth extraction and analysis of the EPS produced under varied culturing conditions.

In the first part of this study, EPS was successfully visualised. The effect of varying culture growth substrate on the extent of EPS present, as well as on the resulting EPS architecture, and spatial distribution was assessed. For planktonic cells cultured on chalcopyrite mineral grains and sulfur, glucose and mannose specific lectin ConA resulted in positive binding, the locale of which was restricted to the area immediately around the cell surface. This is indicative of the presence of capsular EPS. Growth on chalcopyrite was correlated to an enhanced presence of cells which exhibited positive binding with the ConA lectin relative to sulphur grown cells, with 37 % of chalcopyrite grown cells observed to possess EPS, relative to only 16 % of sulfur grown cells. To further this investigation, a more robust lectin screening process was incorporated with a focus on EPS produced by sessile cells cultured on chalcopyrite surfaces. Cells were either cultured in batch agitated flasks on chalcopyrite mineral grains, and the mineral grains containing attached cells assessed; or cultured in the biofilm reactor with the flat chalcopyrite mineral slide assessed using the lectin staining. Thus, the effect of varying culture growth conditions, in terms of mineral-microbe contacting and fluid flow, could also be investigated. For sessile *M. hakonensis* on

chalcopyrite mineral grains cultured in shake flasks, three EPS architectural motifs were evident, namely; the confluent matt of EPS along the mineral surface, capsular EPS binding, and the diffuse cauliflower motif which branched outward from the mineral surface. The EPS assayed was found to contain fucose, rhamnose, glucose, mannose, galactose, sialic acids as well as N-acetyl-glucosamine (GlcNac) and N-acetyl-galactosamine (GalNac) containing residues. The aforementioned glycoconjugates were present in all three binding motifs. Cells were observed to be attached to the mineral surface and were also evident within the EPS milieu around the chalcopyrite mineral grains. The EPS architecture observed under these conditions support the hypothesis proposed by both Tribusch et al. (2001) and by Sand and Gehrke (2006); namely, that EPS extends the reaction space available for dissolution reactions. The cloud-like cauliflower formations of EPS which branch outward from the mineral surface, and the creation of a confluent EPS matt across the surface, serve the sessile microbial population well in extending the surface area coverage available for entrapment of ions and increasing dissolution reaction space. Further investigation on the chemical composition of *M. hakonensis* EPS is required to uncover the potential contribution of thermophiles in creation and proliferation of the microbial-mineral-EPS interfacial environment in the context of bioleaching.

Stemming from this, an investigation which involved extraction and characterisation of EPS from *M. hakonensis* was carried out. An extraction method was developed to allow the recovery of colloidal EPS, EPS associated loosely to the cell and capsular EPS from the thermophilic system. The extraction of these fractions allowed quantification of the material and analysis of its composition. These approaches were used in the study of the formation and location of EPS by *M. hakonensis* grown on three substrates and represent the first detailed description of EPS in thermophilic mineral leaching environments. The effect of varying culture growth history on the resulting EPS yield and composition was assessed. EPS yield varied with energy source for growth. Thus cells are able to adapt and adjust their interfacial environment through changing the chemical composition and abundance of their EPS. Following extraction using crown ether, the preferred method, EPS extracted from the chalcopyrite system yielded the most EPS, followed by sulphur and then the ferrous sulphate systems. Unlike the EPS in mesophilic leaching systems which are mainly comprised on neutral sugars and lipids, protein was the major component of the EPS extracted from *M. hakonensis*. Sugars, uronic acids, nucleic acid and iron were also present in the EPS in proportions varying with both the locale or EPS fraction and culture conditions. Sugar monomers identified in the extracted EPS by GC-MS included rhamnose, glucose, galactose, fucose and mannose. This was consistent with results obtained using lectin screening where positive binding was observed for lectins specific for mannose, glucose, fucose and galactose. A portion of the EPS could not be successfully identified using the methods employed, it was

inferred that this mass likely constituted lipid material. Although NMR was conducted on the EPS samples in order to assay for the presence of lipid material in the EPS, these results were inconclusive. It is recommended that any future EPS work include a more conclusive lipid analysis to verify the presence or absence of this component. It is to be noted that this study presents the first work where a thorough mass balance was conducted to account for the composition identified and identify any unknowns. Based on the hypothesis that the EPS-mediated reaction environment allows the creation of niche reaction conditions at the mineral-microbe interface, favourable to bioleaching, this work expanded knowledge of factors affecting EPS formation, its location and composition.

In the final study of this investigation, the formation and development of *M. hakonensis* biofilms on two massive sulphide mineral surfaces (chalcopyrite and pyrite) and a low-grade chalcopyrite bearing ore was assessed, with a borosilicate (glass) surface serving as control surface. These mono-species biofilms were grown in a specialised biofilm reactor under conditions of continuous fluid flow, mimicking fluid flow conditions found in a bioheap. The mature films were analysed through the use of fluorescent lectin and nucleic acid stains and visualised using CLSM and a combination of AFM–EFM. This provided valuable insight into biofilm architecture, allowing assessment of spatial distribution of microbial cells and EPS across the mineral surface, their variation with mineral type, temporally and in response to temperature. For attachment and biofilm formation on chalcopyrite surfaces at optimal temperatures for growth, micro-colony formation was evident after 2 days with the cell density increasing from 2.0% to 5.7% coverage of the surface after 4 days. This then decreased marginally to 4.7% after 8 days of incubation. The most prominent EPS signal was evident after 4 days of incubation at optimal temperature for growth. The greatest cell densities and extents of biofilm development, in terms of surface coverage, were observed on massive chalcopyrite at the optimal temperature for growth (5.7% coverage). The surface coverage decreased with a decrease in incubation temperature irrespective of mineral system (Table 6.2). The mineral surface was colonised after 2 days, with cells forming a monolayer and EPS not abundantly present. Attachment was improved after 4 days incubation at room temperature, irrespective of mineral system under investigation, with EPS becoming more significant. This study provides first known insights into biofilm development of *M. hakonensis* on massive sulphide mineral surfaces, demonstrating monolayer coverage and dependence on colonisation temperature. It also provides the first study on low-grade mineral ore surfaces investigated in situ under film flow. These results suggest that introduction of high temperature organisms into the heap under conditions sub-optimal for their growth may result in their retention on the ore surface, albeit at a lower loading. Hence re-

inoculation at high temperatures may not be essential. Further, the short time frame required for colonisation under ideal contacting conditions (<4 days) highlights the importance of contacting in the heap environment. As non-specific attachment is negligible, the exposure of the sulphide mineral grains on the ore surface is required both for leaching and for colonisation. The attachment of microorganisms plays an important role in the bioleach process explained via the "indirect contact mechanism" (Crundwell 2003). Furthermore, successful attachment, colonisation and biofilm formation enables the proliferation of microbial life and improved heap leach efficiency. Industrial bio-heap operations are carried out using complex, low-grade (gangue containing) copper ores. An appreciation of mineralogy, microorganisms which proliferate in thermophilic temperature ranges and the interfacial environments created is fundamental to overall understanding of the bioleach process in both heap and tank scenarios. Furthermore, understanding how these dynamics change as the leach progresses and parameters change e.g. temperature fluctuations, inoculation preparation will also better inform behaviour of microbial ecology *In situ.*

The findings of this study provide valuable knowledge to bio-heap interfacial environments through simulation of bio-heap conditions by considering low grade ore mineralogy, varying temperature ranges, thermophilic microorganisms and temperature ranges, fluid flow and integrated *in situ* investigations. The consideration of gangue mineralogy, thermophilic microorganisms, thermophilic temperature ranges, as well as *in situ* studies provides novel contributions to knowledge in a bioleach context. This increases the understanding of the role and importance of interfacial micro-environments created between microbes and minerals in the bioleach process as explained via the "indirect contact mechanism", and contributes to the mitigation of challenges currently faced by industry (Chapter 1). The findings of this study provide insight into: the proliferation of thermophilic archaea *M. hakonensis* when stressed with varying temperature ranges while colonising massive and low grade sulphide minerals; microbial colonisation and EPS production in the formation of active biofilms, bulk trends in microbial colonisation, spatial attachment, site specific and preferential microbe-mineral association under conditions representative of a bio-heap; bulk trends in EPS yield, composition and characterisation; the effect of varying culture growth conditions on the EPS composition; characterisation of the microbial-mineral sulphide interfacial environment *in situ* through lectin staining in combination with AFM, CFM and EFM microscopy techniques; as well as insight into the dynamics and three dimensional architecture of the interfacial environments created by colonisation of *M. hakonensis* on massive and low grade sulfide mineral surfaces.

Appendix A:
Media and buffer composition

Growth media used for *M. hakonensis*:

***M. hakonensis* growth medium (DMSZ 88)**	
Chemical	**Mass (g)**
$(NH_4)_2SO_4$	1.30
K_2HPO_4	0.28
$MgSO_4.7H_2O$	0.25
$CaCl_2.2H_2O$	0.07
Yeast extract	1.00
Elemental Sulphur	0.05 g
	0.062
Trace element solution	
$MnCl_2.2H_2O$	0.068
$ZnCl_2$	0.064
$CoCl_2.6H_2O$	0.031
H_3BO_3	0.01
Na_2MoO_4	0.067
$CuCl_2.2H_2O$	0.068

The ingredients were dissolved in 1L distilled water (except yeast extract or other substrates), pH adjusted temperature to 2.5 using 10 N H_2SO_4 and then autoclaved. Yeast extract and other organic substrates were sterilized separately by autoclaving of a 10% (w/v) stock solution at neutral pH.

Basal salts medium:

Chemical	**Mass (g)**
$(NH_4)_2SO_4$	1.5
KCl	0.05
$MgSO_4.7H_2O$	0.25
K_2HPO_4	0.25
Na_2SO_4	0.73

1 x Phosphate Buffered Saline (PBS):

Chemical	**Mass (g)**
NaCl	8
KCl	0.2
Na_2HPO_4	1.44
KH_2PO_4	0.24

The PBS media was dissolved in 0.8 L distilled water. The pH of the medium adjusted to pH 7.0 using hydrochloric acid (HCl). The volume was then made up to 1 L with distilled water and then autoclaved for 20 minutes at 120˚ C.

Appendix B:
Quantification of attachment per unit surface area

Calculation of the attachment was carried out as follows and by making the following assumptions:

- Repulsive forces between cells and minerals were ignored
- Attachment was monolayered with cells orientated such that the major axis was parallel to the surface of the mineral coated bead as depicted below

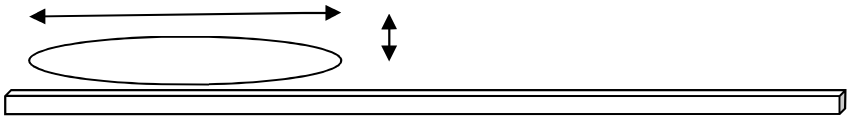

- Dimensions of the *M. hakonensis* used: 1.0 x 0.9 µm (Kurosawa *et al.* 2003)

Particle counting analysis was performed using ImageJ software as per Abramhoff 2001, and is outlined below. A minimum of 40 fields of view were used in order to calculate the % surface area covered by attached *M. hakonensis* cells. Micrographs in Figure B1 show cells positively stained with SYTO9 (a). The image is then converted to 8 bit grey scale, as seen in (b). This image is then Thresholded by selecting the "process tab" and selecting the "Binary" and then "Make binary" tabs. The program is capable of automating this step, thus all images in a folder will be automatically converted to grey scale and then thresholded. Once in this threshold format, the particles in the images can be analysed. The "Analyse particles" tab must be selected and then desired dimensions entered. The program then counts the number of particles or objects which match the defined size criteria. The resulting images will display an outline of cells counted with their count number overlaid onto the image, with a report stating the number of objects counted which match the defined dimensions, as well as the average size or area taken up by individual objects counted, the total area taken up by of all objects counted, and the % area taken up by all objects counted relative to the area in the field of view.

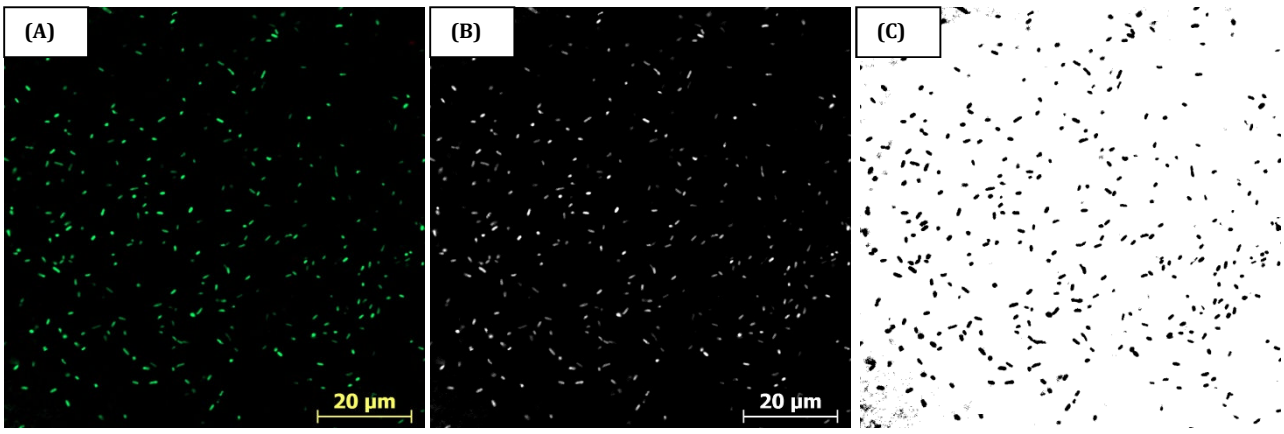

Figure B1: Fluorescing cells stained with SYTO9 (a), same image in grey scale (b),the same image as a threshold image ready for analysis by the Image J software program (c).

Appendix C:
Mineralogical information of substrata used

Below, the results of the size analysis showing the particle size distributions of the chalcopyrite (Andina mine) and pyrite (Agnes mine) mineral concentrate samples are presented.

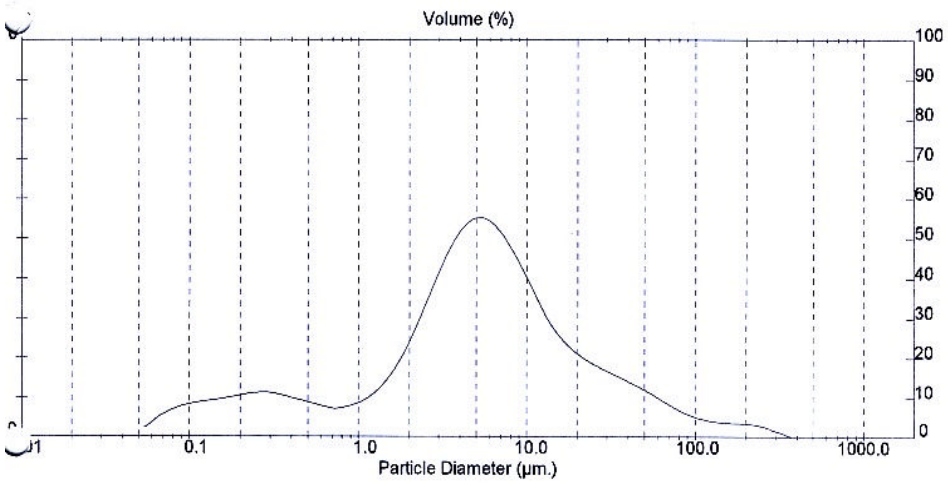

Figure E1: Chalcopyrite mineral concentrate (Andina mine) size analysis results.

Table C1: Summary of the particle size distribution information for the pyrite and chalcopyrite mineral samples used.

Mineral Sample	d10 (µm)	d50 (µm)	d90 (µm)
Chalcopyrite	0.31	5.25	33.10

Table C2: The mineralogical composition of low chalcopyrite containing mineral ore (Escondida, CH32-Type B) used in this study is presented below, with predominating sulfide minerals highlighted in gold, and predominating gangue minerals highlighted in green.

Minerals	CH32-Type B
Chalcocite	0.2
Chalcopyrite	0.5
Covellite	0.3
Bornite	0.1
Atacamite	0.0
Brochantite	0.0
Chrysocolla	0.0
Cuprite	0.0
Native_Copper	0.0
Tenorite	0.0
Turquoise	0.0
Enargite	0.1
Pyrite	4.0
Sphalerite	0.0
Molybdenite	0.0
Galena	0.0
Ilmenite	0.0
Monazite	0.0
Rutile	0.2
Thorite	0.0
Zircon	0.0
Muscovite	28.6
Biotite	0.5
Chlorite	0.7
Kaolinite	7.4
Calcite	0.0
Goethite	0.1
Hematite	0.2
Magnetite	0.0
Albite	5.7
Na_orthoclase	2.9
Plagioclase	1.7
Alunite	0.5
Jarosite	0.2
Gypsum	0.0
Barite	0.0
Svanbergite	0.6
Apatite	0.1
Hornblende	0.2
Iron	0.0
Chromite	0.0
Corundum	0.0
Aluminium_Phosphate	0.0
Quartz	44.8

Michel-Levy Interference Colour Chart

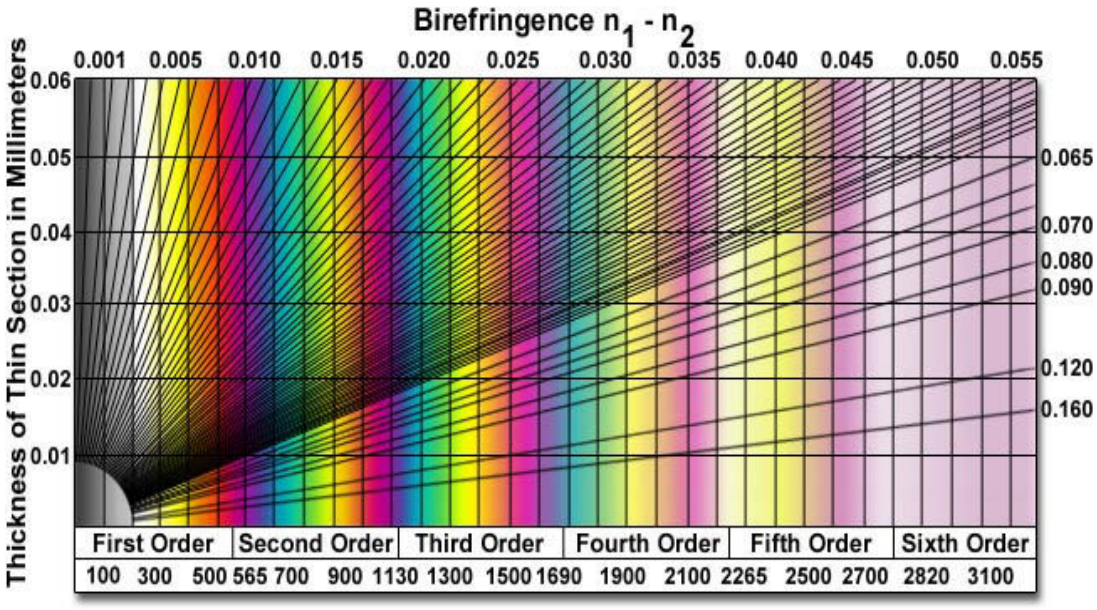

Table C.3: Summary of the predominating sulphide and gangue minerals present (wt %) in th Escondida CH-32-Type B ore (courtesy of BHP Billiton), as well as a summary of the optical properties used for mineral identification under reflected and transmitted light using ore microscopy (Rodgers 1937, Anthony *et al.* 1990 and Deer *et al.* 1992).

Mineral	Chemical composition	wt%	Characteristic optical properties		
			Reflected Light	Transmitted Light	
Major sulphide minerals					
Pyrite	FeS_2	4.0	Cream to pale yellow	Black	
Chalcopyrite	$CuFeS_2$	0.5	Brassy yellow	Black	
Covellite	CuS	0.3	Green intergrowth on chalcopyrite surface	Black	
Chalcocite	Cu_2S	0.2	Pale grey	Black	
Major gangue minerals				**PPL**	**XPL**
Quartz	SiO_2	44.8	Dull brown grey (does not reflect light)	Colourless to milky in thin sections	Isotropic Exhibits weak birefringence (0.009) with light to darker greys and white interference colours
Muscovite	$KAl2(Si_3Al)O_{10}(OH;F)_2$	28.6	Dull brown grey (does not reflect light)	Colourless in thin section, may appear tinted in hues of grey or brown	Anisotropic Exhibits high birefringence (0.035 - 0.042) with interference colours ranging from the violet through to red spectrum

Table C.4: The major sulfide and gangue minerals present in the Kennecott ore sample, and the associated characteristic optical properties used for their identification is presented.

Sulfide minerals

Mineral	Mineral formulae	Characteristic optical properties	
		Reflected light	Transmitted light
Chalcopyrite	$CuFeS_2$	Brassy yellow	Black
Pyrite	FeS_2	Pale yellow	Black
Molybdenite	MoS_2	Light grey	Black

Gangue minerals

Mineral	Mineral formulae	Reflected light	Transmitted light	
			PPL	XPL
Quartz	SiO_2	Dull brown to grey (does not reflect light)	Colourless to milky or white in thin sections	Exhibits weak birefringence (0.009) Isotropic Light to darker greys and white interference colours
Plagioclase	(Na,Ca) Al(Al,Si) Si_2O_8	Dull brown to grey (does not reflect light)	White to light-grey and colourless, may display lamellar twinning	Exhibits weak birefringence (0.007- 0.013)
Orthoclase	$KAlSi_2O_8$	Dull brown to grey (does not reflect light)	Colours may vary from white to colourless, cream to tan, may display cross hashed twinning May exhibit cross hash twinning	Exhibits weak birefringence (0.006-0.010) Extinction angle occurs between 5 to 19º
Biotite	$K(Mg,Fe,Al)_3$ $AlSi_3O_{10}(OH)_8$	Dull brown to grey (does not reflect light)	Black or dark brown	Strong birefringence (0.028-0.08) Exhibits pleochroism
Chlorite	$(Cl, Mg,Fe,Al)_6$ $AlSi_3O_{10}(OH)_2$	Dull brown to grey (does not reflect light)	Green of various tints, varying from almost white to almost black.	Exhibits weak to moderate birefringence (0.007-0.015) With yellow to green to very dark interference colours.
Calcite	$CaCO_3$	Dull brown to grey (does not reflect light)	Clear or white, to tan or grey. May display lamellar twinning.	May be tinted many colours and is anisotropic. Displays rainbow pleochroism. Exhibits strong birefringence 0.172-(0.190).
Amphibole (Hornblend)	$mCa(Mg,Fe)_3(SiO_3)_4$ + $n(Al,Fe)(F,OH)$ SiO_3	Dull brown to grey (does not reflect light)	Green to brown	Exhibits birefringence (0.022 – 0.027) With moderate to strong, white and/or yellow interference colours. Extinction at 10 to 20˚

Appendix D:

Biofilm reactor residence time calculation and flow rate rationale

biofilm specs		
diameter reactor (mm)	100.00	100.00
flow rate (µl min^{-1})	60.00	300.00
glass slide:		
length (mm)	75.00	75.00
width (mm)	26.00	26.00
film thickness (mm)	0.50	0.50
volume fluid on glass slide (mm^3)	975.00	975.00
volume fluid on glass slide (ml)	0.98	0.98
volume fluid on glass slide (µl)	975.00	975.00
volume fluid passing through the reactor (µl)	20000.00	20000.00
surface area film (height film*width slide) (mm^2)	13.00	13.00
residence time (hours)	5.56	1.11
linear velocity (m s^{-1}) [calculated using volumetric flow rate/surface area]	7.69E-05	3.85E-04
linear velocity (m s^{-1})	7.81E-05	1.88E-05

Flow rate used for Column attachment studies were based on Column studies previously conducted at the Centre for Bioprocess Engineering Research (CeBER), which in turn were based in industrial heap bioleach operation specifications. The specifications for the Column work are summarized in Table F1. Industrial heaps flow rate = 5 L m^{-2} hr^{-1}

Table F1: CeBER column reactor specifications

Column diameter (cm)	10
Working length (cm)	32
Surface area column (cm^2)	78
Volume cylinder (cm^3)	2513
Ore loading (kg)	4
Residence time (hours)	42
Flow rate (ml min^{-1})	0.7
Flow rate (ml $hour^{-1}$)	40
Linear velocity (m sec^{-1})	1.41E-06

Appendix E:
NMR Results

NMR results inconclusive due to presence of unknown contaminant.

^{1}H NMR spectrum of EPS at 400 MHz (303K)-1

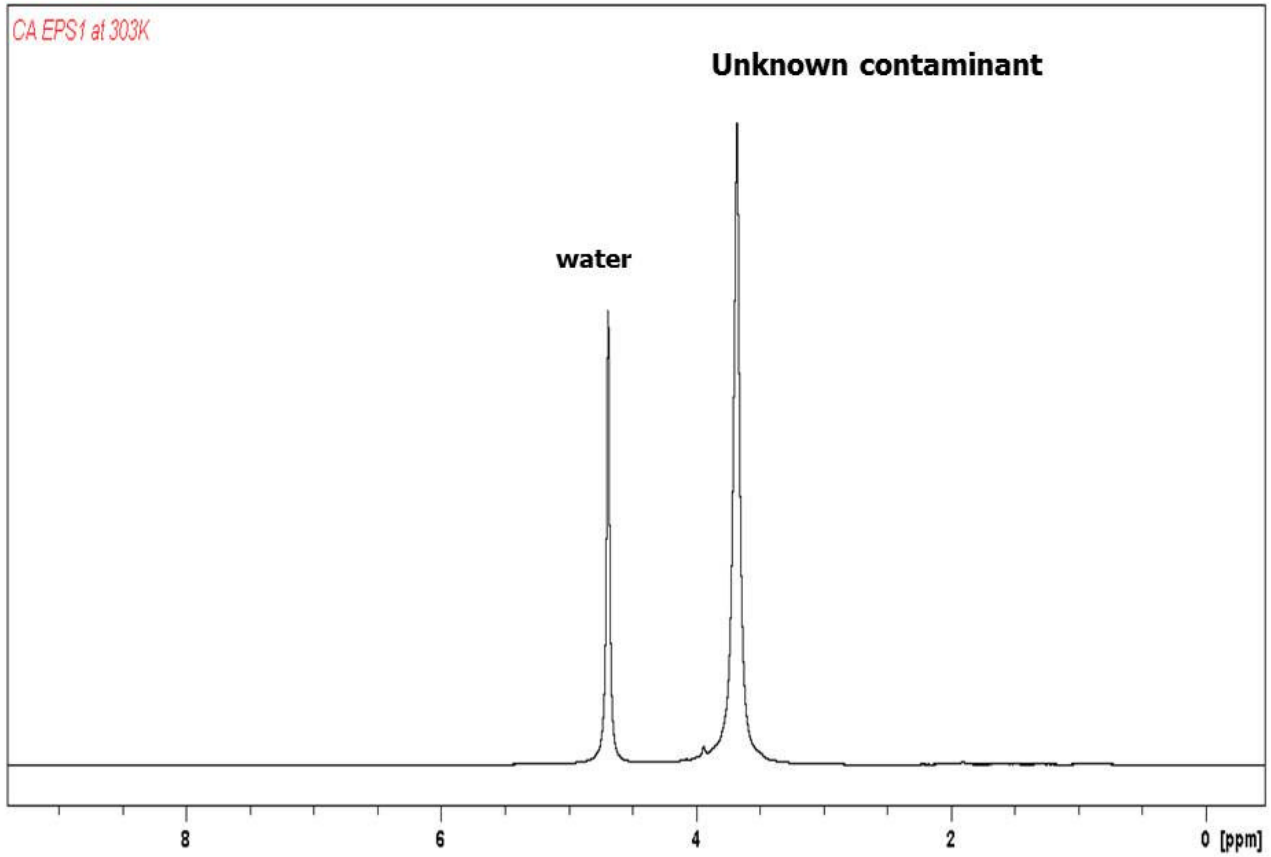

^{1}H NMR spectrum of EPS at 400 MHz (303K, pre-sat)-1

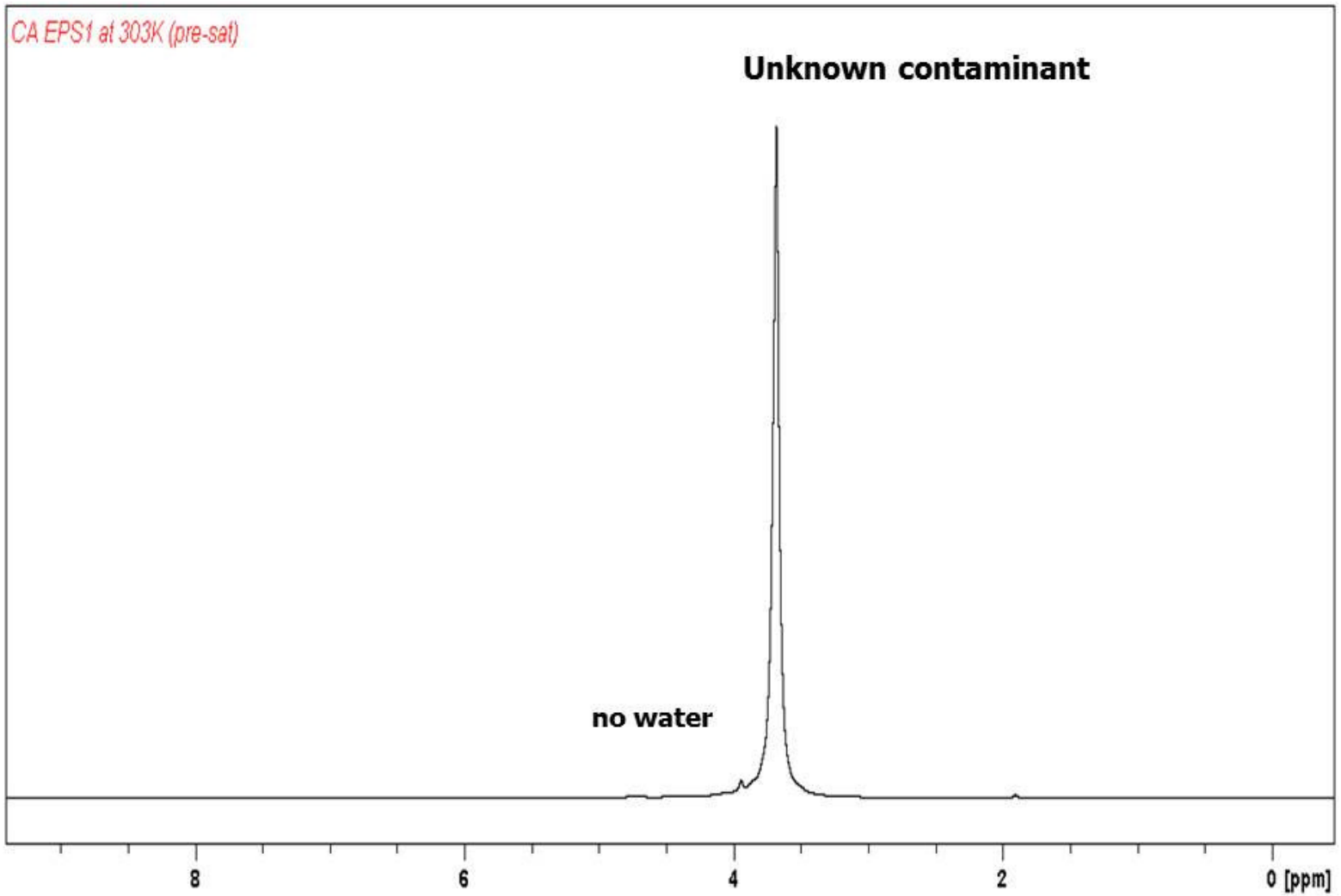

^{1}H NMR spectrum of EPS at 400 MHz (303K)-2

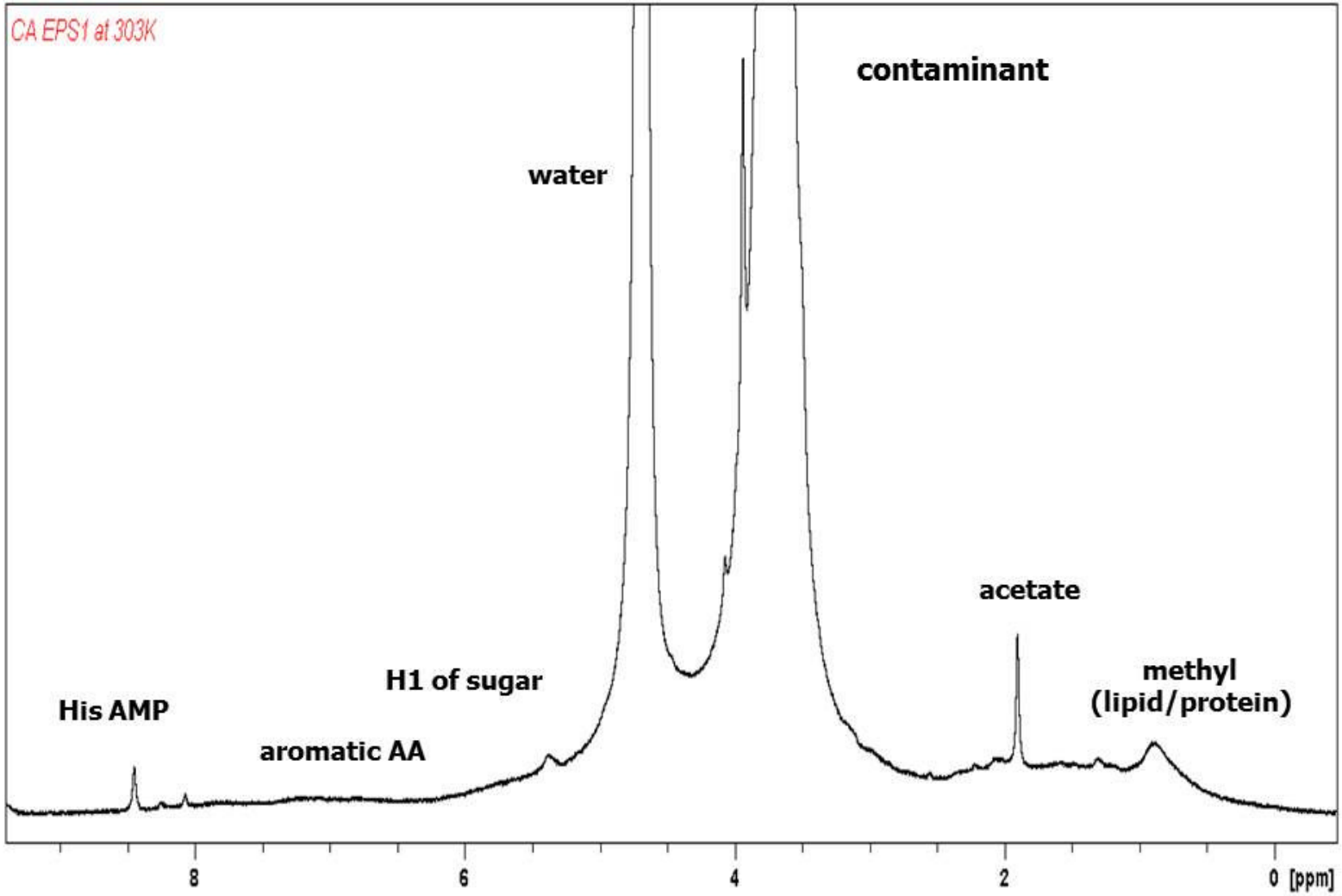

^{1}H NMR spectrum of EPS at 400 MHz (303K, pre-sat)-2